

# **Evolution of gonad transcriptomes and gamete- recognition genes in sea stars**

**by  
Vanessa Guerra**

MSc, San Francisco State University, 2014

BSc, Humboldt State University, 2010

Thesis Submitted in Partial Fulfillment of the  
Requirements for the Degree of  
Doctor of Philosophy

in the  
Department of Biological Sciences  
Faculty of Science

© Vanessa I. Guerra 2020  
SIMON FRASER UNIVERSITY  
Fall 2020

Copyright in this work rests with the author. Please ensure that any reproduction or re-use is done in accordance with the relevant national copyright legislation.

## Declaration of Committee

**Name:** Vanessa Guerra

**Degree:** Doctor of Philosophy

**Thesis title:** Evolution of gonad transcriptomes and gamete-recognition genes in sea stars

**Committee:** **Chair:** John Reynolds  
Professor, Biological Sciences

**Michael Hart**  
Supervisor  
Professor, Biological Sciences

**Bernard Crespi**  
Committee Member  
Professor, Biological Sciences

**Julian Christians**  
Examiner  
Professor, Biological Sciences

**Judith Mank**  
External Examiner  
Professor, Zoology  
University British Columbia

## Abstract

Evolved differences in life history traits, including fertilization ecology and mating systems, are expected to affect the strength of sexual selection acting on gamete-recognition genes (GRGs) responsible for gamete compatibility and fertilization success. The evolution of life history traits such as internal fertilization of eggs and mating system traits such as self-fertilization is expected to weaken the effects of sexual selection (due to the resolution of sperm competition among males and sexual conflicts between males and females). To assess these expectations, I compared the responses to selection of GRGs and other genes expressed in the gonads from multiple species of sea stars with different life histories. I first developed a bioinformatic protocol to reconstruct the transcriptomes of gonads from RNA-seq libraries using the data from the crown-of-thorns sea star *Acanthaster cf. solaris* and used that protocol to characterize GRGs and gene expression. I then compared GRGs in two recently diverged species with contrasting mating systems. I found little evidence of positive selection in the GRGs of the outcrossing species (*Cryptasterina pentagona*). Instead, I found evidence of relaxed selection in the self-fertilizing and hermaphroditic species (*Cryptasterina hystera*). I also found evidence of selection in non-GRG-genes linked to abiotic stressors, DNA regulation, polyspermy, and egg retention. In the last chapter, I compared the selection on female GRGs and other ovary genes using a phylogenetically broad sample of sea star species with two modes of reproduction. I found evidence of rapid evolution acting on female GRGs and of a stronger response to selection on female GRGs from sea stars with expected stronger sexual selection (gonochoric, broadcast spawning, planktonic fertilization) compared to species with derived life history traits associated with weaker sexual selection (hermaphroditic, benthic fertilization, brood protection). In summary, these results support the expectation of rapid evolution and strong selection on GRGs compared to other parts of animal genomes. GRG evolution likely contributes to the speciation process as a mechanism of reproductive incompatibility. And when selection targets GRG, life history traits can affect the response to selection.

**Keywords:** Sexual selection; gamete-recognition genes; fertilization; mating systems

## **Dedication**

I dedicate this thesis to the people that have helped me remain curious. In particular, I dedicate this thesis to my parents, Eduardo Guerra and Isabel Canedo; their hard work and sacrifice allowed me to delve into new worlds.

## Acknowledgements

I would like to acknowledge my collaborators, mentors, and colleagues who helped make this thesis possible. The dataset used in this thesis was the result of a large international collaboration. I thank Nina Yasuda, Souta Adachi, Masako Nakamura, and Shu Nakachi for the collection of sea star tissues from Japan and for their histological work to support the findings of chapter 2.

I would like to acknowledge Maria Byrne for her input on all of the chapters of this thesis and for her efforts (with Demian Koop) to collect samples for chapter 3.

I would like to acknowledge Katie Dobkowski and Siobhan Lane for the collection of the sea stars for chapter 4.

I would also like to thank Klaus Koepfli and Ellen Strong for welcoming me as a visitor to their research groups.

I would like to thank Carrie Craig for the collections of sea stars for chapter 4 and for proofreading.

I would also like to acknowledge the Crawford Lab. The input from Felix Breden, Bernard Crespi, Arne Mooers and Mark Collard has been invaluable. And the help and support from the rest of the Crawford Lab was essential for this work.

Lastly, I would like to acknowledge the mentorship of my senior supervisor, Mike Hart, for his continuous support and guidance.

# Table of Contents

Declaration of Committee .....	ii
Abstract .....	iii
Dedication .....	iv
Acknowledgements .....	v
Table of Contents .....	vi
List of Tables .....	xi
List of Figures .....	xii
<b>Chapter 1. Introduction .....</b>	<b>1</b>
1.1. Thesis Overview .....	5
1.2. References .....	10
<b>Chapter 2. Nonspecific expression of fertilization genes in the crown of thorns <i>Acanthaster cf. solaris</i>: Unexpected evidence of hermaphroditism in a coral reef predator (Guerra et al., 2020) .....</b>	<b>17</b>
Abstract .....	17
2.1. Introduction .....	19
2.2. Methods .....	21
2.2.1. RNA-seq and genome-guided assembly .....	21
2.2.2. Functional annotation of transcripts .....	23
2.2.3. Annotation of gamete-recognition genes .....	24
2.2.4. Differential expression analyses .....	25
2.2.5. Gonad histology .....	26
2.2.6. Confirmation of species identity .....	26
2.3. Results .....	27
2.3.1. Genome-guided assembly .....	27
2.3.2. Functional annotation .....	28
2.3.3. Annotation and structure of gamete-recognition gene orthologs .....	31
2.3.4. Differential gene expression between ovary and testis .....	36
2.3.5. Histological evidence for hermaphroditic individuals .....	39
2.3.6. Barcode identification of <i>Acanthaster cf. solaris</i> .....	42
2.4. Discussion .....	42
2.4.1. Gamete-recognition genes .....	42
2.4.2. Evidence of non-sex-specific gene expression .....	45
2.4.3. Ecological and evolutionary significance of hermaphrodites .....	47
2.5. References .....	50
<b>Chapter 3. Selection on genes associated with the evolution of divergent life histories: Gamete recognition or something else? .....</b>	<b>60</b>
Abstract .....	60
3.1. Introduction .....	61
3.2. Methods .....	64

3.2.1.	Sample collection and RNA-seq library construction .....	64
3.2.2.	Transcriptome assembly .....	64
3.2.3.	Quality assessment and functional annotation .....	65
3.2.4.	Differential expression analyses.....	66
3.2.5.	Orthologous gene identification and alignment.....	66
3.2.6.	Selection analyses .....	67
3.3.	Results .....	67
3.3.1.	Transcriptome assemblies, annotations, and expression .....	67
3.3.2.	Episodic diversifying selection on gamete-recognition genes .....	70
3.3.3.	Episodic diversifying selection on other genes in the transcriptome .....	72
3.3.4.	Genes with alignment-wide evidence of selection .....	74
3.4.	Discussion.....	78
3.4.1.	Gamete-recognition genes are not the targets of selection in <i>Cryptasterina</i> speciation.....	79
3.4.2.	Possible targets of selection in <i>Cryptasterina</i> speciation .....	81
3.5.	References.....	86

**Chapter 4. Multispecies comparison of response differences to selection in reproductive genes .....92**

Abstract.....	92
4.1. Introduction.....	93
4.2. Methods .....	95
4.2.1. Sample collection and RNA-seq library construction .....	95
4.2.2. Transcriptome assembly .....	95
4.2.3. Orthologous gene identification .....	99
4.2.4. Annotation of gamete-recognition genes .....	100
4.2.5. Selection analyses .....	101
4.3. Results .....	103
4.3.1. Transcriptome assemblies .....	103
4.3.2. Gamete recognition genes .....	104
4.3.3. Episodic diversifying selection on female gamete-recognition genes....	107
4.3.4. Episodic diversifying selection on other genes in the female gene set..	110
4.3.5. Tests of two hypotheses: more episodes of diversifying selection on GRGs? More episodes of diversifying selection among broadcast spawners?.....	112
4.4. Discussion.....	116
4.4.1. Selection on gamete-recognition genes .....	117
4.4.2. Evolution of mating systems.....	118
4.4.3. Hermaphroditism.....	119
4.5. References.....	119

**Chapter 5. Synthesis .....123**

Introduction .....	123
Non-sex specific expression of gamete-recognition genes .....	123
Gamete-recognition genes, reproductive isolation, and speciation .....	124

Mating system and gamete-recognition gene evolution .....	125
References.....	126
<b>Appendices .....</b>	<b>129</b>
Appendix A. Frequency distribution of coverage. Numbers of transcripts and percent coverage in BLAST comparisons to the UniProt database, <i>Acanthaster planci</i> protein reference database, and the <i>Strongylocentrotus purpuratus</i> database ..	130
Appendix B. List of gamete-recognition genes used as a reference database for pairwise analysis .....	132
Appendix C. Quality check step for samples and biological replicates. (A) Sum of mapped fragments for individual male and female samples. (B) Correlation matrix of the four samples. (C) Principal component analysis (PCA) with percent variation for each of the male and female samples. ....	133
Appendix D. Gamete-recognition genes of <i>Acanthaster cf. solaris</i> . Coding sequences for eight gamete-recognition genes from testis and ovary transcriptomes.....	136
Appendix E. Annotations and gene ontology results. Summary of GO, annotation terms for genes expressed in COTS gonads and percentage distribution of the top annotations with the NCBI invertebrate database .....	140
Appendix F. <i>Guanylate cyclase</i> alignment of <i>Acanthaster cf. solaris</i> and <i>Asterias amurensis</i> . The alignment shows amino acid sequence differences for the sperm receptor for asterosap .....	142
Appendix G. Characteristics of bindin of <i>Acanthaster cf. solaris</i> . Includes a schematic diagram of repetitive domains and a translated bindin sequence with domains highlighted.....	143
Appendix H. Bindin alignment of male and female sequences. The alignment shows amino acid sequence differences between the full-length coding sequence expressed in males versus four partial coding sequences expressed in one female	144
Appendix I. ARIS alignments. (A) <i>ARIS1</i> from <i>Asterias amurensis</i> and <i>Acanthaster cf. solaris</i> , (B) <i>ARIS2</i> from <i>Asterias amurensis</i> and <i>Acanthaster cf. solaris</i> , (C) <i>ARIS3</i> from <i>Asterias amurensis</i> and <i>Acanthaster cf. solaris</i> . ....	145
Appendix J. COTS gamete-recognition genes reassembled from the RNA-seq data of Stewart et al. 2015. Coding sequences for six gamete-recognition genes from pooled testis transcriptome samples, including genes expected to be expressed in ovaries of females ( <i>ARIS1</i> , <i>ARIS2</i> , <i>ARIS3</i> , <i>EBR1</i> ) .....	146
Appendix K. Domain architecture comparison among eleven predicted receptor for egg jelly (REJ) genes from the <i>Acanthaster cf. solaris</i> genome. Domains of each predicted gene were acquired from the programs SMART and Pfam. Predicted genes oki.62.230 and oki.62.231 were concatenated together for the diagram..	148
Appendix L. Reference sequences of gamete-recognition genes of echinoderms used to search for GRGs in <i>Cryptasterina</i> transcriptomes (Guerra et al., 2020; Hart & Foster, 2013; Matsumoto et al., 2003; Mengerink et al., 2002; Moy et al., 1996; Nakachi et al., 2008; Patiño et al., 2016; Popovic et al., 2014) .....	149
Appendix M. Summary statistics for the reference transcriptome assembled from all <i>Cryptasterina hystera</i> and <i>C. pentagona</i> individuals .....	159
Appendix N. Transcript length of reference transcriptome and annotated transcripts (y-axis = number of transcripts, x-axis = length of transcripts.....	161



Appendix O.	Counts of sequence length coverage (“count in bin”) and counts of transcripts that have at least the sequence percentage length coverage at each level (“> bin below”; e.g. 11,446 transcripts have a hit percentage cover of 90% or higher) for the reference transcriptome with the <i>Acanthaster planci</i> reference database and the UniProt reference database.....	162
Appendix P	List of the most expressed annotated DE transcripts from each comparison.....	163
Appendix Q.	Heatmap of the top 1000 most expressed genes (from left to right: male (blue), hermaphrodite (yellow), female (brown)).....	171
Appendix R.	Sample correlation matrix heatmap of all nine <i>Cryptasterina</i> individuals (from left to right: hermaphrodite (light brown), male (blue), female (brown)).....	173
Appendix S.	Volcano and MA plots of transcriptome comparisons. A) <i>C. hystera</i> vs male individuals of <i>C. pentagona</i> , B) <i>C. hystera</i> vs female individuals of <i>C. pentagona</i> , and C) male vs female individuals of <i>C. pentagona</i> . Volcano plot display the fold change (FC) and false discovery change (FDR). MA plot displays the fold change (log2 in y-axis) of each comparison vs the average expression (log counts). Red dots are differentially expressed transcripts and black dots are transcripts that did not meet the threshold.....	174
Appendix T.	Top 1000 most expressed genes. ....	176
Appendix U.	SNPs of individual <i>C. pentagona</i> females, <i>C. pentagona</i> males, and <i>C. hystera</i> . A) Scatter plots of SNPs of each <i>Cryptasterina</i> spp. individual for transcripts longer than 1000 bp. Green = <i>C. pentagona</i> female, Blue = <i>C. pentagona</i> male, Orange = <i>C. hystera</i> ; B) Violin plot of the ratio of SNPs of each transcript divided by the length of the transcript. Orange = <i>C. hystera</i> , Green = <i>C. pentagona</i> female, Blue = <i>C. pentagona</i> male, Red dots = Gamete recognition genes	178
Appendix V.	Alignments of GRGs. A) <i>EBR1 Cryptasterina</i> alignment of individuals, B) <i>EBR1 Cryptasterina</i> reference alignment with <i>Acanthaster cf solaris</i> , C) <i>OBi1 Cryptasterina</i> alignment of individuals, D) <i>OBi1 Cryptasterina</i> reference alignment with <i>Patiria miniata</i> , E) <i>Guanylate cyclase Cryptasterina</i> alignment of individuals, F) <i>Guanylate cyclase Cryptasterina</i> reference alignment with <i>Acanthaster cf solaris</i> , G) <i>REJ1 Cryptasterina</i> alignment of individuals, H) <i>REJ3 Cryptasterina</i> alignment of individuals, I) <i>Bindin Cryptasterina</i> alignment of individuals.....	180
Appendix W.	Schematic diagram of coding sequences of the gamete-recognition genes of <i>Cryptasterina</i> . Red triangles show locations of codons under selection. Domain abbreviations: collagen-like domains of bindin (KRG), bindin domain, polycystic kidney disease 1 (PKD), receptor for egg jelly (REJ), G-protein-coupled receptor proteolytic site (GPS), lipoxygenase homology 2 domain (LH2), eel-fucolectin fuchylectin-4 pentaxrin-1 (FTP), immunoglobulin (IG), ARIS N-terminus (ANF), serine/threonine protein kinases (TK), guanylyl cyclase (GC), 70 kilodalton heat shock protein domain (HSP70), M12B-type propeptide (MBM), zinc-dependent metalloprotease (ZM), CUB domain (CUB).....	208
Appendix X.	<i>OBi1</i> A) TCS of alleles of <i>C. pentagona</i> females, B) protein structure of <i>OBi1 Cryptasterina</i> reference protein and of <i>Patiria miniata</i> from (Hart et al., 2014). Red sections represent the codon regions under selection. Blue sections are the substrate-binding region, C) Amino acid alignment of region under selection in <i>Cryptasterina</i> individuals (Ch = <i>C. hystera</i> , Cp = <i>C. pentagona</i> ).....	210

Appendix Y. Gene ontology of genes with evidence of episodic diversifying selection in aBSREL. Left = female comparison ( <i>C. pentagona</i> female vs <i>C. hystera</i> ), right = male comparison ( <i>C. pentagona</i> male vs <i>C. hystera</i> ) .....	211
Appendix Z. Selection results of group comparison <i>C. hystera</i> vs <i>C. pentagona</i> A) male comparison and B) female comparison .....	213
Appendix AA. Orthogroups with evidence of selection in both branch site models (aBSREL) and in alignment-wide tests (MK) in the female and the male gene set. Gene acronyms and annotation from Blast with reference databases. The best hit to a reference gene in the NCBI <i>Acanthaster planci</i> database is also shown. Type of selection detected in the McDonald & Kreitman test. Branches under selection in aBSREL. Four orthogroups did not show evidence of individual codons under selection in MEME .....	221
Appendix AB. Schematics of potential role of <i>Udx1</i> as an intracellular calcium influx extender in the egg. Successful contact between sperm and egg (mediated by gamete-recognition genes) initiates three intracellular calcium influx pathways activated by cyclic ADP ribose ( <i>cADPR</i> ), nicotinic acid adenine dinucleotide-phosphate ( <i>NAADP</i> ), and the 1,4,5-triphosphate ( <i>IP3</i> ) production in sea stars. <i>cADPR</i> and <i>IP3</i> binds to receptor ( <i>RyR</i> ) and <i>IP3</i> receptor respectably to release calcium from the endoplasmic reticulum. And <i>NAADP</i> induces the release of calcium through the two-pore channel ( <i>TPC1</i> ). <i>IP3</i> is released from DAG through the H <sub>2</sub> O <sub>2</sub> sensitive Src family tyrosine kinase ( <i>SFK</i> ) and phospholipase C ( <i>PLC</i> ) activity. The H <sub>2</sub> O <sub>2</sub> product from the calcium sensitive <i>Udx1</i> interacts with cortical granules during the formation of the fertilization envelop after fertilization and it could also be acting as a secondary activator for the <i>SFK</i> and <i>PLC</i> activity. Other annotated signal molecules found in the reference transcriptome of <i>Cryptasterina</i> noted in this figure ( <i>TRPC4/5/6/7</i> , <i>ANO4/TMEM16</i> , <i>HVCN1</i> and <i>KCNKA / KCNH2</i> ) could be activated through plasma membrane deactivation or <i>DAG</i> activation (Ramos et al., 2014; Wong et al., 2004; Wozniak & Carlson, 2020).....	223
Appendix AC. Potential localization of expression of three genes under selection ( <i>FERR1</i> , <i>MIC60</i> , and <i>ABCB7</i> ) likely linked to oxidative stress and iron metabolism. The iron reductase (FE <sup>3+</sup> to FE <sup>2+</sup> ) <i>FERR1</i> gene could either be expressed internally in the mitochondrion or in the plasma membrane of the cell along with an ion transporter. <i>MIC60</i> is likely expressed in the cristae junctions of the mitochondrion along with other interacting MICO molecules to provide structure. The mitochondrial transmembrane protein <i>ABCB7</i> is likely expressed in the crista of the mitochondrion. ....	224
Appendix AD. Reference for Supplemental Material of Chapter 3 .....	225

## List of Tables

Table 2.1	Summary statistics for the <i>Acanthaster cf. solaris</i> reference transcriptome. ....	24
Table 2.2	Summary statistics for the <i>Acanthaster cf. solaris</i> reference transcriptome. ....	29
Table 4.1	List of transcriptomes and transcript counts. The new RNA-seq libraries collected from this study are deposited in the unpublished NCBI BioProject no. PRJNA667548. An asterisk indicates the RNA-seq libraries or the transcriptome shotgun assembly sequences downloaded from NCBI projects: Reich et al., 2015 (NCBI BioProject no. PRJNA236087), Musacchia et al., 2017 (NCBI BioProject no. PRJEB20544), Hall et al., 2017 (NCBI BioProject no. PRJDB3175), PRJNA612126, Unpublished (NCBI BioProject no PRJNA612126), Guerra et al., 2020 (NCBI BioProject no PRJNA412251), Hart et al., 2020 in review (NCBI BioProject no PRJNA544828), Bates et al. 2019 (NCBI BioProject no PRJNA398668), and Hart et al., 2013 (NCBI BioProject no PRJNA175319). F = ovary, M = testis, H = ovotestis, P = planktonic, B = benthic .....	99
Table 4.2	Summary of evidence of selection in the female gamete-recognition genes .....	108
Table 4.3.	Summary of evidence of selection in the female gamete-recognition genes divided into partitions between recombination breakpoints identified by GARD.....	109
Table 4.4.	Table of total branches under selection in aBSREL.....	114
Table 4.5.	Summary of the number of partitions of GRGs based on recombination breakpoints found by GARD. The partitions with significant evidence of episodic diversifying selection of sites or branches identified with BUSTED were presented as yes or no results. The corresponding p-values were provided for the BUSTED results. ....	116

## List of Figures

- Figure 2.1 Frequency distribution of transcript lengths in the genome-guided transcriptome assembly from gonads of COTS. Five distributions representing all transcripts in the reference transcriptome and transcripts with annotations from one of the four reference databases: SwissProt database, NCBI invertebrate database, *Strongylocentrotus purpuratus* database, and the *Acanthaster planci* database .....30
- Figure 2.2 Protein domain architecture for eight gamete-recognition genes in COTS. Each line and diagram shows the order and approximate length of protein domain types predicted for a gamete-recognition gene from *Acanthaster* cf. *solaris*, along with the orthologous gene structure for a closely related species of sea star (*Patiria miniata*), or a more distantly related species of sea star (*Asterias amurensis*). For genes that have not been previously characterized in sea stars, the ortholog from a sea urchin (*Strongylocentrotus purpuratus*) is shown. Protein domain predictions were based on sequence comparisons to the SMART and Pfam databases. Protein domain types: adenylyl/ guanylyl cyclase (GC), ARIS C-terminus (AC), ARIS N-terminus (AN), bindin (B), coagulation factor 5/8 C-terminal (FA58C), coiled coil (CC), CUB domain (CUB), eel-fucolectin fachylectin-4 pentaxrin-1 (FTP), epidermal growth factor-like (EGF), G-protein-coupled receptor proteolytic site (GPS), immunoglobulin (IG), kringle (K), lectin C (L), lipoxygenase homology 2 domain (LH2), low complexity (LC), M12B-type propeptide (MB), polycystic kidney disease 1 (PKD), receptor for egg jelly (REJ), serine/threonine protein kinases (TK), transmembrane (TR), thrombospondin type 1 repeats (TSP1), zinc-dependent metalloprotease (ZM). .....33
- Figure 2.3 Differential expression of 672 male- and female-specific transcripts in COTS. Columns in the heat map represent biological repeats of ovary and testis tissues from six individual sea stars, including four from our study (Female 1, 2; Male 1, 2) and two from Hall et al. (2017) (Female 3; Male 3). Coloured lines in each column represent individual transcripts. Colour differences indicate expression variation among genes within and between tissue types. The clustering diagram shows grouping of transcripts into sets with similar expression patterns across samples, including one large set that is more strongly expressed in females (yellow) than in males (purple), and a smaller set that is more strongly expressed in males than in females .....38
- Figure 2.4 Histological sections showing development of male and female gametes in hermaphrodites (a, b) and in male (c) or female (d) individuals. Hermaphrodites included individuals with male gametes developing in an ovary (a) and others with female gametes developing in a testis (b). Samples were collected in June and July 2018 at Nishidomari, Otsuki, Kochi Prefecture. Histology and micrographs by S. Adachi and M. Nakamura. oc, oocyte; se, spermatogenic epithelium; sp, spermatozoa 40
- Figure 2.5 Histological sections showing details of hermaphroditic gamete expression in an otherwise mostly “female” individual (a) in which most of the lobes of the ovary contained only oocytes, but some were

hermaphroditic structures containing both oocytes and spermatozoa. Hermaphroditic gonad lobes (b) included both oocytes and spermatozoa. Individual spermatozoa had spherical heads each ~ 2 µm in diameter (c). Boxes in (a) and (b) show areas of detail illustrated at higher magnification in (b) and (c). Sample was collected in June 2018 at Nishidomari, Otsuki, Kochi Prefecture. Histology and micrographs by S. Adachi and M. Nakamura. h, hermaphroditic gonad lobe; oc, oocyte; ov, ovarian lobe; sp, spermatozoa .....41

Figure 2.6	Summary of sex-specific expression patterns for eight gamete-recognition genes in COTS. Bar graphs show expression profiles for ovary- or testis-specific genes in gonad tissue samples from our study (Female 1, 2; Male 1, 2) and from Hall et al. (2017) (Female 3; Male 3). The height of each bar shows expression (as TPM) for each of the genes in each gonad sample. The dashed line shows TPM = 4. Note the nonspecific, low level of expression for several testis or ovary genes in most samples of the other sex, plus the high level of expression for two testis-specific genes ( <i>bindin</i> , <i>guanylate cyclase</i> ) in one female.....46
Figure 3.1	<i>Cryptasterina</i> habitat including (A) a coral rubble bank on One Tree Island, Great Barrier Reef, Australia, (B) <i>Cryptasterina hystera</i> on the underside of coral rubble, and (C) <i>Cryptasterina pentagona</i> on the underside of rock cobble .....64
Figure 3.2	(A) Principal component analysis (PCA) of all nine <i>Cryptasterina</i> individuals. The yellow circles represent the four <i>C. hystera</i> hermaphrodites, the blue circles represent the two <i>C. pentagona</i> males, and the brown circles represents the three <i>C. pentagona</i> females. (B) Venn diagrams of orthologous genes present in each individual or shared among individuals in each gene set. <i>Left</i> Female gene set showing the number of genes from four <i>C. hystera</i> individuals (yellow leaf), three <i>C. pentagona</i> females (brown leaf), shared orthologous genes (large orange circle), shared orthologous genes with evidence of episodic diversifying selection (medium orange circle), and genes under selection in the McDonald–Kreitman test (small dark orange circle). <i>Right</i> Male gene set showing the number of genes from four <i>C. hystera</i> (yellow leaf), two <i>C. pentagona</i> males (blue leaf), shared orthologous genes (large green circle), shared orthologous genes with evidence of episodic diversifying selection (medium green circle), and genes under selection in the McDonald–Kreitman test (small dark green circle) .....69
Figure 3.3	Number of genes in the male gene set and the female gene set with codons (MEME) and branches (aBSREL) under positive selection. The size of the circles represents the number of genes in the category; the color of each symbol shows which species ( <i>C. hystera</i> , <i>C. pentagona</i> , or both) included lineages under selection in aBSREL analyses (e.g., one gene in the male set that had 9 sites under selection and one <i>C. hystera</i> lineage under selection; more than 40 genes in the female set that had 1 site under selection and 1 <i>C. pentagona</i> lineage under selection). Three violet symbols show the number of sites and lineages ( <i>in C. pentagona</i> ) under positive selection for three gamete-recognition genes ( <i>OBI1</i> , <i>REJ1</i> , <i>REJ3</i> ).....73

Figure 3.4	Schematic diagrams of coding sequence domains in 11 annotated genes under selection in both codon models and MK tests. Domain abbreviations: ABC membrane (ABC), ATPase domain (AAA), low complexity (L), MICOS complex, helix loop helix domain (HLH), orange domain (OR), condensin multi-subunit 1 (Cnd1_N or Cnd1), Vps4 C terminal oligomerization domain (VC), domon domain (DOMON), cytochrome b-561 or ferric transmembrane domain (B561), transmembrane region (TP), protein kinase C conserved region 2 (C2), munc13 (SWH B), kinesin motor and catalytic domain (KISc), epsin N-terminal homology domain (ENTH), coiled coil domain (C), von Willebrand factor type A domain (vWA), I/LWEQ domain (ILWEQ). Black triangles show locations of codons under selection ..... 75
Figure 4.1	List of gamete-recognition genes assembled in each species ..... 104
Figure 4.2.	Bubble plot of total number of episodes of diversifying selection across orthogroups in the female gene set (orange, cyan) and gamete-recognition genes (red, blue). Pairs of symbols for some GRGs show the number of positively selected branches with planktonic (red) or benthic (blue) fertilization. Symbols for single genes in different categories were jittered to make both symbols visible. .... 111
Figure 4.3.	Plot of average number of MEME codons (left) and aBSREL lineages (right) under selection in GRG (white circles) and nonGRG (gray circles). .... 112
Figure 4.4.	Plot of average aBSREL lineages under selection in planktonic (yellow = non GRG and orange = GRG) and benthic (dark blue = nonGRG and light blue = GRG) fertilizers..... 115

# Chapter 1.

## Introduction

An important goal of evolutionary biology is to understand the evolution of life history differences and their consequences. One significant component of life histories is the genes that encode proteins involved in recognition between gametes and regulate their successful fusion and therefore the reproductive success of the adult individuals (Palumbi, 1994). Gamete-recognition genes are often highly polymorphic, with high rates of molecular evolution, a result in part due to a response to sexual selection (such as sperm competition among males, or sexual conflict between males and females) associated with life history and mating system traits (Burgarella et al. 2015; Metz, 1998, Palumbi et al., 1991; Patiño et al., 2016; Sunday et al., 2013). Differences in life history traits, such as those differences found between marine invertebrate species with broadcast spawning of gametes and planktonic fertilization, and other species with benthic fertilization of eggs in egg masses or within the female (i.e., internal fertilizers), are expected to impact the strength of sexual selection acting on gamete-recognition genes and affect the molecular evolution of gamete traits (Charlesworth, 2006; LaMunyon & Ward, 1995; Patiño et al., 2016). However, little evidence exists of such effects. In this thesis, I test that hypothesis about the effect of mating system differences on the molecular evolution of gamete traits, specifically the gamete-recognition genes (GRGs) that regulate the fertilization process. I characterize and compare gonad transcriptomes across species that have evolved different modes of reproduction and different mating systems that are expected to differ in the strength of sexual selection, and test the expectation that those differences lead to variation in the strength of selection on GRGs.

Arguably, one of the most well-characterized gamete-recognition systems in animals are found in the sea stars, sea urchins, and other Echinodermata (Palumbi, 2009). In this thesis, I use sea star variation in life history traits as a system to test the association between life history evolution and the molecular evolution of genes under selection. In addition to an improved understanding of the ecology of reproduction in echinoderms, the study of echinoderm GRGs has led to insights into the general features of sperm-egg interactions in chordates and other organisms, including human

gamete interactions and the possible causes of human fertility variation (or different forms of infertility). Studies in sea urchin (*Strongylocentrotus purpuratus*, *Arbacia punctulata*, and *Lytechinus variegatus*) and sea star (*Asterias amurensis*, *Patiria miniata*) fertilization systems have provided us with protein structures, gene sequences, and functional analyses of proteins expressed in both gametes that are associated with stages of fertilization that include sperm motility, the acrosome reaction, and the binding and fusion of gametes (Dan, 1952; Dan, 1954; Glabe & Vacquier, 1977; Hart et al., 2002; Hart et al., 2014; Lillie, 1919; Nakachi et al., 2006; Palumbi et al., 2009; Vacquier et al., 1977). Echinoderm and chordate gametes share some general features of anatomy, function, and localization of proteins that mediate gamete interactions. For example, gamete interactions in sea stars (Asteroidea) are thought to start with the attraction of the sperm to the egg through chemotaxis. Sperm attraction and activation is induced by the egg protein asterosap and the sperm receptor guanylate cyclase (Nishigaki et al., 1996; Nishigaki et al., 2000). In parallel with echinoderms, known chordate sperm receptors for chemotaxis cluster in the sperm tail and share molecular pathways that initiate sperm motility (Gray & Drummond, 1976; Lishko et al., 2018, Miller et al., 2016; Ren et al., 2001; Seifert et al., 2015). In general, sperm chemotaxis remains poorly described among chordates; only recently were the sperm receptors for tunicates and humans characterized (Yoshida et al., 2018, Miller et al., 2016, Fitzpatrick et al., 2020). As expected, these receptors and ligands in sea stars diverge quickly (as little as 29% nucleotide similarities within sea stars), likely due to their co-evolution under selection (Nakachi et al. 2008). In comparisons among more distantly-related taxa, the similarity between these genes seems to be reflected mainly at the functional level (including types of protein domains), a potential result of convergent evolution or extreme divergence at the nucleotide and amino acid level.

After gamete contact in sea star fertilization, several egg coat proteins including the acrosome reaction-inducing substances (ARIS), co-ARIS, and asterosap interact with the lipid bilayer of sperm and the sperm receptor for egg jelly (REJ) to induce an exocytotic event in the sperm that results in morphological changes in both egg and sperm (Dan, 1960, Hoshi et al., 1993, Hoshi et al., 2012, Kawamura et al., 2002,). These changes include the acrosome reaction in which acrosome fuses with the sperm plasma membrane, and the formation of an acrosomal process that penetrates the egg jelly and is coated by the protein contents of the acrosome including bindin). Most chordates also have variations of sulfated glycoproteins expressed in the egg coat involved in



fertilization, and some of these zona pellucida (ZP) genes initiate the acrosome reaction (Bleil et al. 1980; Bleil et al., 1983; Hoshi et al., 1993; Litscher & Wassarman, 2007; Morgan & Hart, 2019). In rodents, ZP glycoproteins expressed in the egg coat also attach to a receptor in the sperm named ZP3r or sp56 related to the regulator of complement activation proteins (RCA) (Buffone et al., 2008; Wassarman, 2009). In humans, a member of the RCA group, *C4BPA*, is in linkage disequilibrium with ZP genes, and co-evolving with ZP genes under selection (Hart et al., 2018, Morgan & Hart, 2019). Further functional analysis is needed to confirm if C4BPA is a receptor for the zona pellucida proteins in humans.

The acrosome reaction exposes internal acrosomal contents on the cell surface, and leads to interaction between sperm acrosomal proteins and egg coat molecules. In sea urchins and sea stars, the single major component of the acrosome is the protein bindin, which interacts with the egg bindin receptor proteins EBR1 and OBi1 (Hart, 2013, Kamei & Glabe, 2003; Vacquier, 2012) leading to gamete binding. In primates and other mammals, the sperm acrosomal protein Izumo1 has similar adhesion functions to bindin (Grayson & Civetta, 2012, Inoue et al., 2005, Morgan & Hart, 2019), is exposed after exocytosis, and interacts with Juno in the egg coat for gamete binding (Inoue et al., 2005, Kaji et al., 2000, Le Naour et al., 2000, Miyado et al., 2000, Satouh, 2012).

The last step of fertilization is the plasma membrane fusion of the gametes. The highly conserved fusogenic motif B18 of bindin forms an alpha helix with affinity to sulfated egg proteins (Patiño et al., 2009; Rocha et al., 2008; Vacquier, 2012). The formation of the alpha helix is enhanced by presence of  $Zn^{2+}$  and additional proteins from the egg, and this interaction is dependent on the prior successful interaction between bindin and egg receptors.

Gamete-recognition genes have coding sequences under positive selection, evolving at high rates compared to other gamete genes, and protein models have shown that these codon regions under selection are often those parts of the protein that interact with a cognate molecule expressed in the other gamete type (Grayson et al., 2015; Hart et al., 2014; Palumbi, 2009; Vicens et al., 2014; Wilburn et al., 2016). A high rate of evolution of gamete-recognition genes is theorized to be driven in large part by sexual selection, including sperm competition among males (which can drive high rates of evolution in male-expressed genes) and sexual conflict between male and female mates (which can drive high rates of evolution in both male- and female-expressed genes)

(Gavrilets, 2000; Gavrilets & Hayashi, 2005). One specific form of sexual conflict that may affect the evolution of sperm-egg recognition genes is a conflict of interest over the rate or frequency of sperm-egg fusions. Selection on sperm genes that favours a high rate of sperm-egg fusions is beneficial for both gametes, but it may have a detrimental effect on eggs and females when sperm concentrations are high if high fertilization rates lead to multiple sperm entering single eggs. This polyspermy is fatal to all gametes involved in each polyspermy event, but the costs are greater for females than for males because individual sperm are smaller and much less costly to produce in comparison to eggs (Gavrilets, 2000; Gavrilets & Hayashi, 2005). Thus, high rates of sperm-egg fusions are theorized to lead to the selection for sperm alleles that promote success in competition with other sperm (to the detriment of eggs and females), and selection for egg alleles that lower the rate of sperm-egg fusion and reduce the risk of polyspermy.

Selection acting on GRGs can be detected by branch sites models of codon evolution. Branch sites models analyze alignments of protein-coding sequences to identify lineages in a gene tree or sites in an alignment that have high values of omega ( $w=dN/dS$ ), an estimate of the relative rate of nonsynonymous substitutions (dN) and synonymous substitutions (dS). Specific versions of these models can be used to identify codons at which some subset of lineages have high  $w$  values (Murrell et al., 2012); others can be used to identify lineages in the gene tree on which some subset of codons show high  $w$  values (Smith et al., 2015); and others can be used to test specific a priori hypotheses of site-specific differences among sets of branches in each gene tree that differ in some specific trait that is predicted to affect selection (e.g., lineages in which organisms have evolved mating systems with high versus low potential for selection associated with sperm competition and sexual conflicts of interest) (Murrell et al., 2015).

Studies that have compared GRGs using codon models in animals with relatively recent episodes of selection have identified sites under positive selection (Galindo et al., 2003; Hart et al., 2014; Levitan & Stapper, 2010; Metz et al., 1996; Patiño et al., 2016, Pujolar & Pogson, 2011). These studies found more evidence of positive selection on GRGs compared to other parts of the genome. Similar work on gamete recognition of plants and humans has found binding sites in male- and female-expressed genes to also be under selection and coevolving (Sato et. al., 2002, Hart et al., 2018). Additional studies that include a wider range of gamete-recognition genes from multiple sea star

species could bring insight into the evolution of mating system differences and their consequences.

In mating systems where sperm competition and sexual conflicts of interest are strong, sexual selection is expected to favour the evolution of novel male and female traits that confer advantages on males (in competition with sperm of other males for fertilization) and on females (in defense against male adaptations) (Chapman et al., 2003; Gavrillets, 2000, Parker, 2006). For sea stars and other broadcast-spawning marine invertebrates, specific gamete traits include male adaptations for sperm binding to eggs, and female countermeasures to avoid fatal polyspermy (Franke et al., 2002; Levitan, 2004). Because these sexual selection processes act on males and females within populations, responses to selection (coevolved combinations of sperm- and egg-expressed gamete-recognition genes) may differ between populations. For example, comparative analysis of *bindin* in sea urchins showed lineages with differing omega values: low omega values in some clades were attributed to neutral processes, and high values of omega in other sea urchin clades were thought to be the result of sexual selection and possibly sexual conflict over fertilization rate (Lessios, 2011; Palumbi, 2009; Wilburn et al., 2016). When sexual selection and conflicts of interest are strong, reproductive isolation between populations can evolve as a secondary outcome of sexual selection within each population (Palumbi, 1999, Levitan et al., 2006).

Parts of this model for the evolution of gamete traits, reproductive compatibility, population differences, and speciation by sexual selection can be tested by comparing patterns of molecular evolution among species or lineages with different mating system traits that are expected to be associated with strong or weak sexual selection and conflicts of interest, and by comparing GRGs to other parts of the genome that are not expected to evolve under the influence of sexual selection or conflicts of interest. I used those two comparative approaches in this thesis.

## **1.1. Thesis Overview**

In this thesis I carried out a comparison among sea stars (Asteroidea) in which different mating system traits have evolved in parallel in diverse species or lineages. Most sea star species are gonochoric (two separate sexes) broadcast spawners with large body size, large gonads, and high fecundity (including large testes in males and

high sperm production). In these species, adults release either eggs or sperm into the marine plankton, where males may often experience strong sperm competition (because individual males cannot monopolize or prevent access by other males to the eggs of females) and males and females may often be in intense sexual conflict over optimal rates of sperm-egg contact with high risk of polyspermy. This mating system and mode of reproduction is probably ancestral for sea stars (and is widely shared with many other species of echinoderms and other marine invertebrate phyla) (Hart et al., 1997; Puritz et al., 2012). However, several sea star lineages have evolved modified life-history and mating system traits that are expected to weaken the effects of sexual selection. These traits include small body size, reduced sperm production, and fertilization of small clutches of eggs in the benthic habitat where access to eggs and fertilizations may be limited to sperm of males immediately adjacent to females and egg masses, with reduced intensity of sperm competition. In the most highly derived life histories, benthic egg masses are self-fertilized by hermaphroditic adults in which sperm competition is reduced (because eggs are fertilized by sperm from one male), and sexual conflicts of interest may be fully resolved (because the reproductive interests of males and females are combined in a single self-fertilizing individual; Byrne et al., 2003; Strathmann et al., 1984). This pattern of ancestral broadcast spawning and derived benthic fertilization is not unique to sea stars, and is characteristic of life history evolution among other echinoderms and other phyla (Strathmann, 1987). A recent study of one gamete-recognition gene (encoding the sperm acrosomal protein *bindin*) showed greater evidence of a response to selection (positive selection and high values of  $w$  with high rates of amino acid change) in two genera of sea stars in which all species are gonochoric out-crossers in comparison to two genera with species that have evolved benthic fertilization and are capable of selfing (Patiño et al., 2016). This result indicates that sexual selection on *bindin* evolution may be weaker in species that have some combination of these derived life-history and mating system traits with reduced sexual selection. In this thesis, I extend that comparative method to other gamete-recognition genes (sex-specific gene expression only known from either sperm or eggs in sea stars), compare them to other genes not involved in gamete-recognition, and contrast those patterns among several lineages of sea stars with ancestral and derived life histories.

**Ch2:** Development of a de novo transcriptome pipeline using *Acanthaster cf solaris*. Here

I develop and describe the protocol for assembly and analysis of RNA-seq data to characterize sea star gonad transcriptomes and identify gamete-recognition genes, and then I apply this protocol to data for the crown-of-thorns sea star (COTS) from the western Pacific, *Acanthaster cf. solaris*. I focus on this single species for two reasons. First, COTS is an important keystone predator on corals and coral reefs in the Indo-Pacific. Populations of COTS undergo natural fluctuations in population size estimated to occur every decade (Uthicke et al., 2009). In the past few decades, high-density populations of COTS, known as outbreaks, have remained unusually dense for longer than expected in locations such as Japan and Australia (Birkeland & Lucas, 1990, Uthicke et al. 2009, Nakamura 2014). Outbreaks have contributed to coral reef decline and loss of biodiversity in the Indo-Pacific (Uthicke et al., 2009). The causes of the population fluctuations are still debated (Mendonça, 2010) and may include unexpectedly successful reproduction, high survival rates for the feeding planktonic larval stage associated with coastal eutrophication (Birkeland, 1982), and overfishing (Cowan et al., 2016, Cowan et al., 2017). Second, the available RNA-seq data for my analyses of this species are limited to a relatively small number of sequence reads (about 5 million reads for each of two male and two female individuals). As a result, this first analysis of data from COTS can be considered a difficult test (because small RNA-seq libraries reduce the coverage needed for the confident reconstruction of genes and estimation of their expression with de novo approaches) of the assembly and analysis protocol: if gamete-recognition genes can be successfully assembled and analyzed from limited data for this species, then the same protocol is expected to successfully assemble such genes from other species for which many more data are available. My analyses of two male and two female gonad transcriptomes have revealed unexpected evidence for male gene expression (including the GRG *bindin*) in one of the ovary samples, including odd patterns of expression assessed with PCA, a correlation matrix or heatmap of gene expression patterns, and the expression of sex-specific GRGs. This is consistent with previously described (but unexplained) expression of some egg-specific genes in testis RNA-seq data (Stewart et al., 2015), and with anecdotal reports of embryonic development in laboratory spawning of eggs without addition of sperm. My collaborators and I interpreted these gene expression results, plus the documentation of ovotestes (individuals with gonads that produced both sperm and eggs) in a separate study, as evidence of frequent but previously unrecognized hermaphroditism in COTS individuals. Documenting unexpected hermaphroditism in this species may help to

account for population outbreaks in an important predator on coral reefs. Further study of the mating system of COTS could help us better understand the sex-determination systems of these and other sea stars.

**Ch3:** Divergence of gamete-recognition genes in *Cryptasterina* species with contrasting mating systems.

Here I applied the assembly and analysis protocol to a comparison between two closely related sister species from northeastern Australia with different mating systems. I used the same methods to identify gamete-recognition genes (and other genes expressed in sperm and eggs), and apply codon models of positive selection to ask whether the two species differ in the response to selection on gamete-recognition genes (but not other genes) in the expected direction due to their mating system differences. I focused on this two-species comparison for two reasons. First, *Cryptasterina hystera* and *C. pentagona* have striking mating system differences but are otherwise similar in their morphology and natural history (so similar that they were not recognized as distinct species until their mating system differences were discovered (Dartnall et al., 2003). *C. pentagona* individuals are gonochoric broadcast spawners with planktonic fertilization and the potential for strong sexual selection; *C. hystera* individuals are simultaneous hermaphrodites with internal self-fertilization and limited potential for sperm competition (because they lack adaptations for sperm transfer between individuals) or sexual conflict (because outcrossing appears to be rare). Second, the two species diverged very recently (<10,000 years ago; Hart & Puritz, 2020; Puritz et al., 2012). As a result, this two-species comparison can be considered a difficult test (because the power to assess selection on an alignment of gene copies from recently diverged species could be reduced by a limited number of substitutions in the alignment; Smith et al. 2015) of my method of analysis: if a difference in the response to selection on gamete-recognition genes can be detected in this pair of species (after a recent speciation event), then the same approach is expected to successfully test the effect of mating system differences on other sea star species or lineages that have much longer divergence times over which mating system differences could lead to changes in the strength of sexual selection and evidence of a response to those differences in selection among lineages. I found little evidence of a stronger response to sexual selection in the gamete-recognition genes of the outcrossing sea star *C. pentagona*: GRGs did not show stronger evidence of positive selection (high values of  $w$ ) in comparison to other genes expressed in the

gonads, and GRGs in *C. pentagona* did not show stronger evidence of positive selection in comparison to GRGs in *C. hystera*. Instead, I found evidence of relaxed selection on some GRGs of the self-fertilizing *C. hystera* and evidence of selection in non-GRGs linked to abiotic stress.

**Ch4:** Comparative analysis of gamete-recognition genes among many species with contrasting mating systems.

Here I applied the same RNA-seq methods and comparative approach to a multispecies comparative analysis of gamete transcriptomes and selection acting on GRGs of sea star species with different modes of fertilization and mating systems. I analyzed previously sequenced and new RNA-seq data from sea stars from five taxonomic orders. These analyses included data from a large sample of gonochoric broadcast spawners, including *Acanthaster cf. solaris* (Chapter 1) and *Cryptasterina pentagona* (Chapter 2), plus 21 others in the Orders Velatida (*Pteraster militaris*), Forcipulatida (*Asterias amurensis*, *Asterias forbesi*, *Asterias rubens*, *Evasterias troschellii*, *Marthasterias glacialis*), Paxillosida (*Astropecten aranciacus*, *Luidia clathrate*), Spinulosida (*Echinaster spinulosus*, *Henricia leviuscula*), and Valvatida (*Crossaster papposus*, *Dermasterias imbricata*, *Mediaster aequalis*, *Patiria miniata*, *Pisaster brevispinus*, *Pisaster giganteus*, *Pisaster ochraceus*, *Pycnopodia helianthoides*, *Solaster dawsoni*, *Solaster endeca*, and *Solaster stimpsoni*) with the potential for strong sperm competition, sexual selection, and sexual conflict. I compared them to four species in three orders that have evolved derived life history traits including small body size, benthic fertilization, and brood protection. These included three gonochoric species with external fertilization of eggs in benthic egg masses (*Leptasterias hexactis*; *Henricia pumila* and *Henricia sanguinolenta*), as well as the hermaphroditic *Cryptasterina hystera* (with internal self-fertilization of eggs, internal brooding of embryos and live birth of juvenile sea stars) that are expected to have reduced potential for sperm competition and weaker sexual selection. I found evidence of a stronger responses to selection, in the form of a high number of codons under selection and more lineages under selection, among GRGs than other genes in the ovary transcriptomes. And the response to selection among GRGs was stronger in planktonic fertilizer than in benthic fertilizers.

## 1.2. References

- Birkeland, C. (1982). Terrestrial runoff as a cause of outbreaks of *Acanthaster planci* (Echinodermata: Asteroidea). *Marine Biology*, 69(2), 175-185.
- Birkeland, C., & Lucas, J. (1990). *Acanthaster planci: major management problem of coral reefs*. CRC press.
- Bleil, J. D., & Wassarman, P. M. (1980). Structure and function of the zona pellucida: identification and characterization of the proteins of the mouse oocyte's zona pellucida. *Developmental Biology*, 76(1), 185-202
- Bleil, J. D., & Wassarman, P. M. (1983). Sperm-egg interactions in the mouse: sequence of events and induction of the acrosome reaction by a zona pellucida glycoprotein. *Developmental Biology*, 95(2), 317-324
- Buffone, M. G., Zhuang, T., Ord, T. S., Hui, L., Moss, S. B., & Gerton, G. L. (2008). Recombinant mouse sperm ZP3-binding protein (ZP3R/sp56) forms a high order oligomer that binds eggs and inhibits mouse fertilization in vitro. *Journal of Biological Chemistry*, 283(18), 12438-12445
- Burgarella, C., Gayral, P., Ballenghien, M., Bernard, A., David, P., Jarne, P., ... & Glémin, S. (2015). Molecular evolution of freshwater snails with contrasting mating systems. *Molecular Biology and Evolution*, 32(9), 2403-2416
- Byrne, M., Hart, M. W., Cerra, A., & Cisternas, P. (2003). Reproduction and larval morphology of broadcasting and viviparous species in the *Cryptasterina* species complex. *The Biological Bulletin*, 205(3), 285-294
- Charlesworth, D. (2006). Evolution of plant breeding systems. *Current Biology*, 16(17), R726-R735.
- Cowan, Z. L., Dworjanyan, S. A., Caballes, C. F., & Pratchett, M. S. (2016). Predation on crown-of-thorns starfish larvae by damselfishes. *Coral Reefs*, 35(4), 1253-1262
- Cowan, Z. L., Pratchett, M., Messmer, V., & Ling, S. (2017). Known predators of crown-of-thorns starfish (*Acanthaster* spp.) and their role in mitigating, if not preventing, population outbreaks. *Diversity*, 9(1), 7
- Dan, J. C. (1952). Studies on the acrosome. I. Reaction to egg-water and other stimuli. *The Biological Bulletin*, 103(1), 54-66
- Dan, J. C., Kitahara, A., & Kohri, T. (1954). Studies on the acrosome. II. Acrosome reaction in starfish spermatozoa. *The Biological Bulletin*, 107(2), 203-218
- Dan, J. C. (1960). Studies on the acrosome: VI. Fine structure of the starfish acrosome. *Experimental Cell Research*, 19(1), 13-28.



- Dartnall, A. J., Byrne, M., Collins, J., & Hart, M. W. (2003). A new viviparous species of asterinid (Echinodermata, Asteroidea, Asterinidae) and a new genus to accommodate the species of pantropical exiguoid sea stars. *Zootaxa*, 359, 1-14
- Fitzpatrick, J. L., Willis, C., Devigili, A., Young, A., Carroll, M., Hunter, H. R., & Brison, D. R. (2020). Chemical signals from eggs facilitate cryptic female choice in humans. *Proceedings of the Royal Society B*, 287(1928), 20200805
- Galindo, B. E., Vacquier, V. D., & Swanson, W. J. (2003). Positive selection in the egg receptor for abalone sperm lysin. *Proceedings of the National Academy of Sciences*, 100(8), 4639-4643
- Gavrilets, S. (2000). Rapid evolution of reproductive barriers driven by sexual conflict. *Nature*, 403(6772), 886-889
- Gavrilets, S., & Hayashi, T. I. (2005). Speciation and sexual conflict. *Evolutionary Ecology*, 19(2), 167-198
- Glabe, C. G., & Vacquier, V. D. (1977). Species specific agglutination of eggs by bindin isolated from sea urchin sperm. *Nature*, 267(5614), 836-838
- Gray, J. P., & Drummond, G. I. (1976). Guanylate cyclase of sea urchin sperm: subcellular localization. *Archives of Biochemistry and Biophysics*, 172(1), 31-38
- Grayson, P., & Civetta, A. (2012). Positive selection and the evolution of *izumo* genes in mammals. *International Journal of Evolutionary Biology*, 2012
- Grayson, P. (2015). Izumo1 and Juno: the evolutionary origins and coevolution of essential sperm–egg binding partners. *Royal Society Open Science*, 2(12), 150296
- Hart, M. W., Byrne, M., & Smith, M. J. (1997). Molecular phylogenetic analysis of life-history evolution in asterinid starfish. *Evolution*, 51(6), 1848-1861.
- Hart, M. W. (2002). Life history evolution and comparative developmental biology of echinoderms. *Evolution & Development*, 4(1), 62-71
- Hart, M. W. (2013). Structure and evolution of the sea star egg receptor for sperm bindin. *Molecular Ecology*, 22(8), 2143-2156
- Hart, M. W., Sunday, J. M., Popovic, I., Learning, K. J., & Konrad, C. M. (2014). Incipient speciation of sea star populations by adaptive gamete-recognition coevolution. *Evolution*, 68(5), 1294-1305
- Hart, M. W., Stover, D. A., Guerra, V., Mozaffari, S. V., Ober, C., Mugal, C. F., & Kaj, I. (2018). Positive selection on human gamete-recognition genes. *PeerJ*, 6, e4259

- Hart, M. W., & Puritz, J. B. (2020). Correction to 'Extraordinarily rapid life-history divergence between *Cryptasterina* sea star species'. *Proceedings of the Royal Society B*, 287(1930), 20201325
- Hoshi, K., Sugano, T., Endo, C., Yoshimatsu, N., Yanagida, K., & Sato, A. (1993). Induction of the acrosome reaction in human spermatozoa by human zona pellucida and effect of cervical mucus on zona-induced acrosome reaction. *Fertility and Sterility*, 60(1), 149-153
- Hoshi, M., Moriyama, H., & Matsumoto, M. (2012). Structure of acrosome reaction-inducing substance in the jelly coat of starfish eggs: A mini review. *Biochemical and Biophysical Research Communications*, 425(3), 595-598
- Inoue, N., Ikawa, M., Isotani, A., & Okabe, M. (2005). The immunoglobulin superfamily protein Izumo is required for sperm to fuse with eggs. *Nature*, 434(7030), 234-238
- Jean, C., Haghhighirad, F., Zhu, Y., Chalbi, M., Ziyat, A., Rubinstein, E., ... & Boucheix, C. (2019). JUNO, the receptor of sperm IZUMO1, is expressed by the human oocyte and is essential for human fertilisation. *Human Reproduction*, 34(1), 118-126
- Kaji, K., Oda, S., Shikano, T., Ohnuki, T., Uematsu, Y., Sakagami, J., ... & Kudo, A. (2000). The gamete fusion process is defective in eggs of Cd9-deficient mice. *Nature Genetics*, 24(3), 279-282
- Kamei, N., & Glabe, C. G. (2003). The species-specific egg receptor for sea urchin sperm adhesion is EBR1, a novel ADAMTS protein. *Genes & Development*, 17(20), 2502-2507
- Kawamura, M., Matsumoto, M., & Hoshi, M. (2002). Characterization of the sperm receptor for acrosome reaction-inducing substance of the starfish, *Asterias amurensis*. *Zoological Science*, 19(4), 435-442
- Kosakovsky Pond, S. L., Murrell, B., Fourment, M., Frost, S. D., Delport, W., & Scheffler, K. (2011). A random effects branch-site model for detecting episodic diversifying selection. *Molecular Biology and Evolution*, 28(11), 3033-3043
- LaMunyon, C. W., & Ward, S. (1995). Sperm precedence in a hermaphroditic nematode (*Caenorhabditis elegans*) is due to competitive superiority of male sperm. *Experientia*, 51(8), 817-823
- Le Naour, F., Rubinstein, E., Jasmin, C., Prenant, M., & Boucheix, C. (2000). Severely reduced female fertility in CD9-deficient mice. *Science*, 287(5451), 319-321
- Lessios, H. A. (2011). Speciation genes in free-spawning marine invertebrates. *Integrative and Comparative Biology*, 51(3), 456-465

- Levitan, D. R. (2004). Density-dependent sexual selection in external fertilizers: variances in male and female fertilization success along the continuum from sperm limitation to sexual conflict in the sea urchin *Strongylocentrotus franciscanus*. *The American Naturalist*, 164(3), 298-309
- Levitan, D. R., & Ferrell, D. L. (2006). Selection on gamete-recognition proteins depends on sex, density, and genotype frequency. *Science*, 312(5771), 267-269
- Levitan, D. R., & Stapper, A. P. (2010). Simultaneous positive and negative frequency-dependent selection on sperm bindin, a gamete-recognition protein in the sea urchin *Strongylocentrotus purpuratus*. *Evolution: International Journal of Organic Evolution*, 64(3), 785-797
- Lillie, F. R. (1919). *Problems of fertilization*. University of Chicago Press
- Lishko, P. V., & Mannowetz, N. (2018). CatSper: a unique calcium channel of the sperm flagellum. *Current Opinion in Physiology*, 2, 109-113
- Litscher, E. S., & Wassarman, P. M. (2007). Egg extracellular coat proteins: from fish to mammals. *Histology and Histopathology*
- Mendonça, V. M., Al Jabri, M. M., Al Ajmi, I., Al Muharrami, M., Al Areimi, M., & Al Aghbari, H. A. (2010). Persistent and expanding population outbreaks of the corallivorous starfish *Acanthaster planci* in the northwestern Indian Ocean: are they really a consequence of unsustainable starfish predator removal through overfishing in coral reefs, or a response to a changing environment. *Zoological Studies*, 49(1), 108-123
- Metz, E. C., & Palumbi, S. R. (1996). Positive selection and sequence rearrangements generate extensive polymorphism in the gamete-recognition protein bindin. *Molecular Biology and Evolution*, 13(2), 397-406
- Metz, E. C., Gómez-Gutiérrez, G., & Vacquier, V. D. (1998). Mitochondrial DNA and bindin gene sequence evolution among allopatric species of the sea urchin genus *Arbacia*. *Molecular Biology and Evolution*, 15(2), 185-195
- Miki, K., & Clapham, D. E. (2013). Rheotaxis guides mammalian sperm. *Current Biology*, 23(6), 443-452
- Miller, M. R., Mannowetz, N., Iavarone, A. T., Safavi, R., Gracheva, E. O., Smith, J. F., ... & Lishko, P. V. (2016). Unconventional endocannabinoid signaling governs sperm activation via the sex hormone progesterone. *Science*, 352(6285), 555-559
- Miyado, K., Yamada, G., Yamada, S., Hasuwa, H., Nakamura, Y., Ryu, F., ... & Okabe, M. (2000). Requirement of CD9 on the egg plasma membrane for fertilization. *Science*, 287(5451), 321-324

- Murrell, B., Wertheim, J. O., Moola, S., Weighill, T., Scheffler, K., & Pond, S. L. K. (2012). Detecting individual sites subject to episodic diversifying selection. *PLoS Genet*, 8(7), e1002764
- Murrell, B., Weaver, S., Smith, M. D., Wertheim, J. O., Murrell, S., Aylward, A., ... & Scheffler, K. (2015). Gene-wide identification of episodic selection. *Molecular Biology and Evolution*, 32(5), 1365-1371
- Morgan, C. C., & Hart, M. W. (2019). Molecular evolution of mammalian genes with epistatic interactions in fertilization. *BMC Evolutionary Biology*, 19(1), 154
- Nakachi, M., Moriyama, H., Hoshi, M., & Matsumoto, M. (2006). Acrosome reaction is subfamily specific in sea star fertilization. *Developmental Biology*, 298(2), 597-604
- Nakachi, M., Hoshi, M., Matsumoto, M., & Moriyama, H. (2008). Conserved sequences of sperm-activating peptide and its receptor throughout evolution, despite speciation in the sea star *Asterias amurensis* and closely related species. *Zygote*, 16(3), 229-237
- Nakamura, M., Okaji, K., Higa, Y., Yamakawa, E., & Mitarai, S. (2014). Spatial and temporal population dynamics of the crown-of-thorns starfish, *Acanthaster planci*, over a 24-year period along the central west coast of Okinawa Island, Japan. *Marine Biology*, 161(11), 2521-2530
- Nishigaki, T., Chiba, K., Miki, W., & Hoshi, M. (1996). Structure and function of asterosaps, sperm-activating peptides from the jelly coat of starfish eggs. *Zygote*, 4(3), 237-245
- Nishigaki, T., Chiba, K., & Hoshi, M. (2000). A 130-kDa membrane protein of sperm flagella is the receptor for asterosaps, sperm-activating peptides of starfish *Asterias amurensis*. *Developmental Biology*, 219(1), 154-162
- Palumbi, S. R., & Metz, E. C. (1991). Strong reproductive isolation between closely related tropical sea urchins (genus *Echinometra*). *Molecular Biology and Evolution*, 8(2), 227-239
- Palumbi, S. R. (1994). Genetic divergence, reproductive isolation, and marine speciation. *Annual Review of Ecology and Systematics*, 25(1), 547-572
- Palumbi, S. R. (1999). All males are not created equal: fertility differences depend on gamete-recognition polymorphisms in sea urchins. *Proceedings of the National Academy of Sciences*, 96(22), 12632-12637
- Palumbi, S. R. (2009). Speciation and the evolution of gamete-recognition genes: pattern and process. *Heredity*, 102(1), 66-76

- Parker, G. A. (2006). Sexual conflict over mating and fertilization: an overview. *Philosophical Transactions of the Royal Society B: Biological Sciences*, 361(1466), 235-259
- Patiño, S., Aagaard, J. E., MacCoss, M. J., Swanson, W. J., & Hart, M. W. (2009). Bindin from a sea star. *Evolution & Development*, 11(4), 376-381
- Patiño, S., Keever, C. C., Sunday, J. M., Popovic, I., Byrne, M., & Hart, M. W. (2016). Sperm bindin divergence under sexual selection and concerted evolution in sea stars. *Molecular Biology and Evolution*, 33(8), 1988-2001
- Pujolar, J. M., & Pogson, G. H. (2011). Positive Darwinian selection in gamete-recognition proteins of Strongylocentrotus sea urchins. *Molecular Ecology*, 20(23), 4968-4982
- Puritz, J. B., Keever, C. C., Addison, J. A., Byrne, M., Hart, M. W., Grosberg, R. K., & Toonen, R. J. (2012). Extraordinarily rapid life-history divergence between *Cryptasterina* sea star species. *Proceedings of the Royal Society B: Biological Sciences*, 279(1744), 3914-3922
- Ren, D., Navarro, B., Perez, G., Jackson, A. C., Hsu, S., Shi, Q., ... & Clapham, D. E. (2001). A sperm ion channel required for sperm motility and male fertility. *Nature*, 413(6856), 603-609.
- Rocha, S., Lúcio, M., Pereira, M. C., Reis, S., & Brezesinski, G. (2008). The conformation of fusogenic B18 peptide in surfactant solutions. *Journal of Peptide Science: An Official Publication of the European Peptide Society*, 14(4), 436-441
- Sato, K., Nishio, T., Kimura, R., Kusaba, M., Suzuki, T., Hatakeyama, K., ... & Satta, Y. (2002). Coevolution of the S-locus genes SRK, SLG and SP11/SCR in *Brassica oleracea* and *B. rapa*. *Genetics*, 162(2), 931-940
- Satouh, Y., Inoue, N., Ikawa, M., & Okabe, M. (2012). Visualization of the moment of mouse sperm-egg fusion and dynamic localization of IZUMO1. *Journal of Cell Science*, 125(21), 4985-4990
- Seifert, R., Flick, M., Bönigk, W., Alvarez, L., Trötschel, C., Poetsch, A., ... & Kremmer, E. (2015). The C at S per channel controls chemosensation in sea urchin sperm. *The EMBO Journal*, 34(3), 379-392
- Smith, M. D., Wertheim, J. O., Weaver, S., Murrell, B., Scheffler, K., & Kosakovsky Pond, S. L. (2015). Less is more: an adaptive branch-site random effects model for efficient detection of episodic diversifying selection. *Molecular Biology and Evolution*, 32(5), 1342-1353
- Strathmann, M. F. (2017). Reproduction and development of marine invertebrates of the northern Pacific coast: data and methods for the study of eggs, embryos, and larvae. University of Washington Press

- Strathmann, R. R., Strathmann, M. F., & Emson, R. H. (1984). Does limited brood capacity link adult size, brooding, and simultaneous hermaphroditism? A test with the starfish *Asterina phylactica*. *The American Naturalist*, 123(6), 796-818
- Sunday, J. M., & Hart, M. W. (2013). Sea star populations diverge by positive selection at a sperm-egg compatibility locus. *Ecology and Evolution*, 3(3), 640-654
- Stewart, M. J., Stewart, P., & Rivera-Posada, J. (2015). De novo assembly of the transcriptome of *Acanthaster planci* testes. *Molecular Ecology Resources*, 15(4), 953-966
- Uthicke, S., Schaffelke, B., & Byrne, M. (2009). A boom–bust phylum? Ecological and evolutionary consequences of density variations in echinoderms. *Ecological Monographs*, 79(1), 3-24
- Vacquier, V. D., & Moy, G. W. (1977). Isolation of bindin: the protein responsible for adhesion of sperm to sea urchin eggs. *Proceedings of the National Academy of Sciences*, 74(6), 2456-2460
- Vacquier, V. D. (2012). The quest for the sea urchin egg receptor for sperm. *Biochemical and Biophysical Research Communications*, 425(3), 583-587
- Vicens, A., & Roldan, E. R. (2014). Coevolution of positively selected IZUMO1 and CD9 in rodents: evidence of interaction between gamete fusion proteins?. *Biology of Reproduction*, 90(5), 113-1
- Wassarman, P. M. (2009). Mammalian fertilization: the strange case of sperm protein 56. *Bioessays*, 31(2), 153-158
- Wilburn, D. B., & Swanson, W. J. (2016). From molecules to mating: Rapid evolution and biochemical studies of reproductive proteins. *Journal of Proteomics*, 135, 12-25
- Yoshida, K., Shiba, K., Sakamoto, A., Ikenaga, J., Matsunaga, S., Inaba, K., & Yoshida, M. (2018). Ca<sup>2+</sup> efflux via plasma membrane Ca<sup>2+</sup>-ATPase mediates chemotaxis in ascidian sperm. *Scientific Reports*, 8(1), 1-16

## Chapter 2.

### **Nonspecific expression of fertilization genes in the crown of thorns *Acanthaster cf. solaris*: Unexpected evidence of hermaphroditism in a coral reef predator (Guerra et al., 2020)**

This chapter was adapted from Guerra, V., Haynes, G., Byrne, M., Yasuda, N., Adachi, S., Nakamura, M., ... & Hart, M. W. (2020). Nonspecific expression of fertilization genes in the crown-of-thorns *Acanthaster cf. solaris*: Unexpected evidence of hermaphroditism in a coral reef predator. *Molecular Ecology*, 29(2), 363-379

#### **Abstract**

The characterization of gene expression in gametes has advanced our understanding of the molecular basis for ecological variation in reproductive success and the evolution of reproductive isolation. These advances are especially significant for ecologically important keystone predators such as the coral-eating crown-of-thorns sea stars (COTS, *Acanthaster*) which are the most influential predator species in Indo-Pacific coral reef ecosystems and the focus of intensive management efforts. I used RNA-seq and transcriptome assemblies to characterize the expression of genes in mature COTS gonads from a population in southern Japan. I described the sequence and domain organization of eight genes with sex-specific expression and well known functions in fertilization in other echinoderms. I found unexpected expression of genes in one ovary transcriptome that are characteristic of males and sperm, including genes that encode the sperm-specific guanylate cyclase receptor for an egg pheromone, and the sperm acrosomal protein bindin. In a reassembly of previously published RNA-seq data from COTS testes, I found a complementary pattern: strong expression of four genes that are otherwise well known to encode egg-specific fertilization proteins, including the egg receptor for bindin (EBR1) and the acrosome reaction-inducing substance in the egg coat (ARIS1, ARIS2, ARIS3). In collaboration with colleagues in Japan, we also found histological evidence of both eggs and sperm developing in the same gonad in several COTS individuals from a parallel study. These results suggest the occurrence of hermaphrodites, and the potential for reproductive assurance via self-fertilization. These

findings have implications for management of COTS populations, especially in consideration of the large size and massive fecundity of these sea stars.

**Keywords:**

*Acanthaster*, reproductive assurance, outbreaks, bindin, RNA-seq



## 2.1. Introduction

Echinoderms are model organisms for investigation of fertilization biology from gamete behavior and recognition molecules (Hirohashi et al., 2008; Podolsky & Strathmann, 1996; Swanson & Vacquier, 2002) to sexual selection in populations (Levitan, 2004) and population connectivity (Puritz et al., 2017). At the level of gamete interactions, the events of echinoderm fertilization are regulated by the products of gamete-recognition genes that are localized in organelles, plasma membranes, or the extracellular coats of sperm and eggs (Patiño et al., 2016; Wilburn & Swanson, 2016). Original characterization of echinoderm gamete-recognition genes was largely based on analyses of proteins and gene transcripts from species for which extensive genomic resources are available (especially the sea urchin *Strongylocentrotus purpuratus*; Lessios, 2007; Swanson & Vacquier, 2002; Wilburn & Swanson, 2016). Recent studies have assembled gonad and gamete transcriptomes of several echinoderm species from short-read RNA-seq data to characterize gamete-recognition genes and their products (Hall et al., 2017; Hart, 2012; Hart & Foster, 2013; Stewart, Stewart, & Rivera-Posada, 2015; Weber et al., 2017). Knowledge of the organization, sequence, and diversity of gamete-recognition genes has led to an improved understanding of variation in reproductive success, biochemical interactions between gametes, the mechanisms underlying reproductive isolation between species, and the drivers of speciation (Lessios, 2011; Palumbi, 2009; Wilburn & Swanson, 2016).

On coral reefs, crown-of-thorns sea stars (COTS) in the genus *Acanthaster* are keystone coral predators and are among the most ecologically influential species in tropical marine ecosystems. Periodic population outbreaks of COTS can decimate reefs and reduce coral cover by up to 90% (Birkeland, 1982; Colgan, 1987; Pratchett & Caballes, 2014) with cascading negative consequences for reef communities (Haywood et al., 2019; Kayal et al., 2012; Timmers et al., 2011; Timmers, Bird, Skillings, Smouse, & Toonen, 2012). Across the Great Barrier Reef, predation by COTS is responsible for ~40% of coral loss over 30 years (De'ath et al., 2012). Although the causes of COTS outbreaks remain uncertain, the enormous fecundity of individual females (up to 200 million eggs) is considered key to rapid increase in population size and the initiation of outbreaks (Babcock, Milton, & Pratchett, 2016; Uthicke, Schaffelke, & Byrne, 2009). This species is the most fecund echinoderm, with clutch sizes for individual females much

higher than those reported for any other sea stars (Babcock et al., 2016). High fecundity and fertilization success are used in simulation models of source-sink dynamics among COTS populations for reef management applications (Hock, Wolff, Condie, Anthony, & Mumby, 2014; Rogers, Pláganyi, & Babcock, 2017). Although the terrestrial nutrient run-off hypothesis, in which larval growth and survival are increased by blooms of phytoplankton, presently has the greatest scope for explaining outbreaks (Birkeland, 1982; Uthicke et al., 2018), key gaps remain in our understanding of the life history of COTS, especially its fertilization biology and the role of gamete-recognition genes in fertility. These important knowledge gaps are addressed here.

Numerous genes involved in sperm chemoattraction toward the egg, sperm capacitance and the acrosome reaction, and sperm–egg binding have been identified in echinoderms (Hirohashi et al., 2008). Sea star eggs release asterosap, a small peptide pheromone, from the extracellular coat (egg jelly). This peptide diffuses into seawater and binds to a membrane-bound guanylate cyclase receptor in the sperm tail, and this binding activates sperm metabolism and chemoattraction towards the egg (Hoshi, 2002; Hoshi, Moriyama, & Matsumoto, 2012; Kawamura et al., 2002; Wilburn & Swanson, 2016; Nishigaki et al., 2000). Sea star oocytes also express an acrosome reaction-inducing substance composed of three glycoprotein subunits (ARIS1, ARIS2, ARIS3) that form part of the egg coat and interact with a sperm receptor for egg jelly (REJ; Naruse et al., 2011). The egg vitelline envelope has a receptor for the sperm acrosomal protein bindin (EBR1; Hart & Foster, 2013; Patiño et al., 2009). The interaction between bindin and EBR1 is required for gamete binding and fusion (Kamei & Glabe, 2003).

Despite the ecological importance of COTS, little is known about the genes that mediate fertilization in this species and their influence on fertility, a fundamental driver of outbreaks. Thus far, one partial coding sequence for each of the three *Acanthaster* ARIS genes is available (Naruse et al., 2011), as well as a partial *EBR1* transcript from a testis transcriptome (Stewart et al., 2015). The draft genome assembly for COTS (Hall et al., 2017) includes a predicted *bindin* gene, but the coding sequence organization and repetitive structure have not been analyzed or compared to that of other sea stars. There is intense interest in COTS pheromones and the overall COTS secretome, particularly with respect to the use of genomic information for the design of biocontrol applications (Hall et al., 2017). This secretome research has focused on the adults and their behavior (Hall et al., 2017). Here I focus on the genes that influence gamete behavior and

ultimately COTS fertility. I sequenced and analyzed highly expressed genes of the gonads of four reproductively mature male and female individuals from southern Japan, analyzed data from a testis transcriptome (Stewart et al., 2015) and obtained genomic sequences for gamete-recognition molecules from the draft COTS genome (Hall et al., 2017). By characterizing new sea star orthologs of echinoderm gamete-recognition and binding genes I provide a clearer view of the fertilization biology of this important marine predator.

I found unexpected evidence of nonsex-specific expression of some gamete-recognition genes in our study and in data from a previous study (Stewart et al., 2015). One interpretation of that evidence is that some COTS of one sex may be facultative hermaphrodites in which a small portion of the gonad is allocated to developing gametes of the other sex. I collaborated with colleagues in Japan to find confirmation of that interpretation in histological sections showing that some COTS individuals have oocytes and spermatozoa in the same gonad. The occurrence of hermaphrodites in COTS has important implications for understanding the reproduction and demography of these coral predators, and for application of models of population fertility and source-sink propagule dynamics currently being used to inform management of COTS populations on the Great Barrier Reef (Hock et al., 2014; Rogers et al., 2017).

## **2.2. Methods**

### **2.2.1. RNA-seq and genome-guided assembly**

Sea stars were collected from two localities in Japan where COTS were previously classified as *Acanthaster planci*. That name is now known to represent a species complex, but the taxonomy of the Pacific species of COTS is uncertain. One available name for COTS from the western Pacific is suggested to be *Acanthaster cf. solaris* (Haszprunar et al. 2017; Schreber, 1793).

Ovary and testis tissues were carefully isolated from a reproductively mature male and female from Kekubo (31°22'55.61"N, 131°18'47.25"E), and a male and a female from Kushima (31°21'59.29"N, 131°19'10.93"E), in the field or at the University of Miyazaki in August 2013. Each tissue sample was preserved in RNAlater and stored at -70°C. The samples were shipped cold to the Hawai'i Institute of Marine Biology (HIMB)

at the University of Hawai'i. Extraction of RNA, construction of indexed cDNA libraries, and 75-base paired-end sequencing on a MiSeq instrument (Illumina, Inc.) were carried out in the HIMB Genetics Core Facility using proprietary library preparation methods and standard Illumina sequencing kits.

In preparation for the genome-guided transcriptome assembly, I combined the paired-end raw reads of the four libraries collected for this study with the reads from three additional libraries (two testes, one ovary) that were created as part of the analysis and annotation of the COTS genome (Hall et al., 2017). The reads were filtered with trimmomatic v. 0.32 (Bolger et al., 2014) using the default settings in Trinity v. 2.6.5 (Grabherr et al., 2011). Trimmomatic implements several filtering steps that improve overall library quality: removal of adapter sequences; trimming of bases at the leading and trailing ends of each sequence read that have average quality score of five or less (using a sliding window of four bases in width); removal of individual bases with a quality score of five or less from the sequence ends; and deletion of sequences shorter than 25 bases. I used the default program settings in the fastqc tool v. 0.11.3 (<http://www.bioinformatics.babraham.ac.uk/projects/fastqc/>) to evaluate the overall quality of the trimmed sequences and to detect data biases due to sequencing or amplification errors. The cleaned RNA-seq reads from this study were deposited in the Sequence Read Archive of the National Centre for Biotechnology Information under the BioProject PRJNA412251.

A genome-guided reference transcriptome was assembled in Trinity using a coordinate-sorted bam file created with GSNAP (Wu & Watanabe, 2005) made from trimmed sequences that were pooled from all seven samples from the two gonadal tissues (three ovaries and four testes). To identify and analyze the expression of sex-specific genes, I used the same genome-guided approach to assemble individual libraries for each of the seven gonad samples. I also used the genome-guided approach to reassemble reads from a previous study (Stewart et al., 2015) in which gonad RNA from multiple COTS males from an Australian population was pooled and sequenced to characterize genes and gene expression patterns.

The quality of the reference transcriptome was assessed by the representation of full-length known proteins, contig length, and contig composition. I did not initially use expression filters for the reference transcriptomes; this approach was suggested in the Trinity documentation to conserve biological information. I used BLASTX (Altschul et al.,

1990) to compare predicted protein sequences for transcripts in our assembled reference transcriptome to proteins in the UniProt 90 reference database (Apweiler et al., 2012), the NCBI *Acanthaster planci* protein reference database (annotation release ID 100), and the NCBI *Strongylocentrotus purpuratus* protein reference database (annotation release ID 101); I used expectation scores with a cutoff value of  $e = 1 \times 10^{-20}$  or lower to identify orthologs. I calculated percentage length coverage of the protein hits using the perl script “analyze\_blastPlus\_topHit\_coverage.pl” from Trinity v. 2.6.5 (Grabherr et al., 2011) toolkit (see Appendix A for frequency distribution of coverage); I used a cutoff value of 80% or higher coverage. Summary statistics that characterize the dimensions and composition of the reference transcriptome were calculated with the perl script “TrinityStats.pl” from the Trinity v. 2.6.5 (Grabherr et al., 2011) toolkit (Table 1).

### **2.2.2. Functional annotation of transcripts**

Functional annotation of the reference transcriptome used Trinotate v. 3.0 (<https://trinotate.github.io/>) (Haas et al., 2013). First, coding regions of the transcripts were predicted with the default settings using the TransDecoder method in Trinotate. The reference transcriptome and the output of TransDecoder (Haas et al., 2013) were then searched for matches using blast+ (Altschul et al., 1990) against a custom UniProt database (Apweiler et al., 2012), the NCBI Invertebrate reference database, the NCBI *Strongylocentrotus purpuratus* reference database, and the NCBI *Acanthaster planci* reference database. The UniProt database was populated with information from Gene Ontology (GO; Ashburner et al., 2000), Clusters of Orthologous Groups (COG; Tatusov et al., 2000), and pathways from the Kyoto Encyclopedia of Genes and Genomes (KEGG; Kanehisa & Goto, 2000). The output of TransDecoder was also used to search for several functional features: protein domains were identified using the method in HMMER (Finn et al., 2011) and the PFAM protein domain database (Punta et al., 2012); signal peptide predictions were found using the program SignalP (Petersen et al., 2011); and transmembrane regions were identified using TMHMM (Krogh et al., 2001).

Summary statistic	Value	Individual
<b>Cleaned Illumina reads</b>	104,679,122	
<b>ovary</b>	4,523,681	female 1
	5,065,063	female 2
	4,472,748	male 1
	4,708,152	male 2
<b>ovary &amp; testis</b>	85,909,478	female 3, male 3 <sup>a</sup>
<b>Total transcripts</b>	312,554	
<b>Total genes</b>	243,681	
<b>GC content (%)</b>	42.4	
<b>Median transcript length (nt)</b>	441	
<b>Average transcript length (nt)</b>	1121	
<b>Transcript contig N50 (nt)</b>	2853	

<sup>a</sup> Data from Hall et al. (2017)

**Table 2.1 Summary statistics for the *Acanthaster cf. solaris* reference transcriptome.**

### 2.2.3. Annotation of gamete-recognition genes

I compared transcripts in the reference transcriptome to sequences in a custom database that was compiled from previously published gamete-recognition gene sequences (Hart, 2013; Hart & Foster, 2013; Matsumoto et al., 2003; Mengerink et al., 2002; Moy et al., 1996; Nakachi et al., 2008; Patiño et al., 2016; Popovic et al., 2014; see Appendix B for a list of gamete-recognition genes). I used blast+ (Altschul et al., 1990) with a minimum expectation score of  $e = 1 \times 10^{-5}$ . To confirm the identification of orthologs, I translated the top hits for each search and compared their protein domain organization using Smart (Schultz et al., 1998).

In cases where the reference transcriptome included a partial coding sequence for a gamete-recognition gene, I used those partial coding sequences to find complete coding sequences by searching the genome. I used blast+ to search for the orthologous sequence in the recently published COTS draft genome assembly (Hall et al., 2017). If the gene of interest was identified, I then manually assembled the complete coding sequence using data from the scaffolds of the draft genome that had been assembled from a COTS individual collected from Motobu, Okinawa (called the OKI genome in Hall et al., 2017). I assembled complete coding sequences by conceptual translation of the scaffold sequence to identify splice sites and introns. I confirmed the identity of exons by examining the coverage of cDNA reads mapped to the scaffold sequence, and by

comparing the exons to the incomplete predicted transcriptomes from the assemblies. I used GMAP (Wu & Watanabe, 2005) and GSNAP (Wu & Nacu, 2010) with default settings to map trimmed cDNA sequences to each single scaffold of interest. The GSNAP outputs were processed in Samtools (Li et al., 2009) with default settings, and visualized with IGV (Robinson et al., 2011).

## **2.2.4. Differential expression analyses**

### **Comparison of biological replicates**

To identify possible batch effects or unexpected biological differences between replicates within each biological group (males or females), I used the alignment-based method of the RNA-seq pipeline in Trinity v. 2.6.5 (Grabherr et al., 2011). This pipeline aligns the trimmed sequence reads from each of the individuals to the reference transcriptome using the perl script “align\_and\_estimate-abundance.pl”. This script calls on the program bowtie2 version 2.2.1 (Langmead & Salzberg, 2012) for alignment, and the program Rsem v. 1.2.7 (Li & Dewey, 2011) to estimate transcript abundance. I used the TPM metric (number of reads mapped to the transcript, standardized for gene length and total number of reads; Li & Dewey, 2011) as my measure of standardized expression level for each of the assembled transcripts for each individual sea star. I used a cutoff value of 4 TPM to define the presence of gamete-recognition genes. In this work flow, the gene and transcript matrices containing the sequence abundance information for each of the individuals are built with the perl script “abundance\_estimates\_to\_matrix.pl”. The matrices are used to assess the similarity or difference between pairs of biological replicates relative to differential expression between the sexes. The perl script “PtR.pl” uses the matrices to plot the distribution of mapped sequences for comparisons of individuals and groups based on a correlation matrix and a principal component analysis (PCA; see Appendix C for quality check results). This quality check indicated that one of the samples from the study by Hall et al. (2017) (the male from an Australian population) that I included in the data used to create the reference gonad transcriptome had an unexpected low gene expression similarity to the other male samples. This single male sample was collected out of breeding season (M. Hall, personal communication). Because gene expression in that nonreproductive gonad may not reflect typical patterns of gene expression in testes, I deleted that sample from subsequent analysis. This quality check also indicated that one of the female

samples in the study had an unusually low number of unique sequences compared to the second female, and expressed some genes that were also expressed in the two males in the study as well as in males from previous studies (Hall et al., 2017; Stewart et al., 2015; see Appendix C for quality check results).

### **Differential expression**

I used the differential expression (DE) method in the RNA-seq pipeline of Trinity v. 2.6.5 (Grabherr et al., 2011). The DE analysis with biological replicates uses the perl script “run\_DE\_analysis.pl” from the Trinity v. 2.6.5 toolkit that calls on the edger (Robinson, McCarthy, & Smyth, 2009) program to annotate the transcripts that are differentially expressed. The most differentially expressed transcripts are then extracted using the perl script “analyze\_diff\_expr.pl” in the Trinity toolkit (Grabherr et al., 2011); I used cutoff values of  $p = .01$  for control of the false discovery rate (FDR) and eight-fold or greater difference to identify differentially expressed transcripts.

### **2.2.5. Gonad histology**

In a parallel study of COTS reproduction in southern Japan, my colleagues (S. Adachi and M. Nakamura), collected gonad samples in June and July 2018 from populations in Kochi Prefecture and used standard histological methods to fix, section, mount, stain, and photograph these samples in order to document the gamete type(s) present in each sample; these methods have previously been used for histological analysis of gonads in COTS and other sea stars (Byrne, 1992; Lucas, 1973; Yamazato & Kiyon, 1973; see Birkeland & Lucas, 1990). The tissue samples were dehydrated through a graded series of ethanol, cleared in xylene, and embedded in paraffin. The sections (4  $\mu\text{m}$  thick) were stained with hematoxylin and eosin and photographed under bright field illumination (see Guerra et al., 2020).

### **2.2.6. Confirmation of species identity**

I followed the advice of Haszprunar et al. (2017) to use mitochondrial *COI* barcodes for species identification. I downloaded the available barcode sequences for *Acanthaster* ( $n = 249$ ) from the Barcode of Life Data System (Ratnasingham & Hebert, 2007). I did not have tissue samples as vouchers for the four individuals in my study to use in amplification of the *COI* barcode sequence; instead, I found the individual



transcript that was annotated as mitochondrial *COI* in each of the individual transcriptome assemblies, and I added each of those *COI* coding sequences to the barcode data. From GenBank I obtained and added the *COI* coding sequence from the complete mitochondrial genome for *Acanthaster 'planci'* from a Japanese population (AB231475.1; Yasuda et al., 2006) as an additional reference sequence. The translated coding sequences could be readily aligned by eye without gaps. I trimmed that alignment to the length of the shortest sequence in the barcode database (582 bp), and converted the alignment to nexus format.

I used TCS 1.2.1 (Clement et al., 2000) to estimate genealogical relationships among those *COI* haplotypes by the statistical parsimony method. I used the 95% parsimony connection limit, and forced haplotypes that differed by more than the connection limit (10 steps or nucleotide differences) into separate networks. This approach is widely used to identify provisional species differences using *COI* barcodes (Hart & Sunday, 2007).

## **2.3. Results**

### **2.3.1. Genome-guided assembly**

I assembled 104,679,122 paired-end trimmed sequences from seven RNA-seq libraries, including libraries made from the gonads of two male and two female COTS collected for this study and libraries made from the gonads of two males and one female from a prior study (Hall et al., 2017), with a per-base quality score in Fastqc of 33 or higher (Table 1). The genome-guided assembly had 312,554 transcripts of which 243,681 were identified as genes (much larger than the likely number of unique genes, Table 1). These estimates reflect the occurrence of multiple alternatively spliced isoforms within genes, multiple paralogous genes within gene families, and multiple partial sequences from different parts of the same unigenes. The average contig length of the reference transcriptome was 1,121 bp with a contig N50 length of 2,853 bp (Table 1). I aligned transcripts to the UniProt database (including Swiss-Prot sequences) using cutoff values of  $e = 10^{-20}$  and 80% query coverage, and found 5,441 transcripts annotated by reference proteins (see Appendix D for gamete-recognition genes). The COTS genome has an estimated 24,500 coding genes (Hall et al., 2017), suggesting

that ~22% (5,441 reference proteins) of the expected genes were successfully annotated in spite of the limited representation of transcripts for the class Asteroidea in the reference database.

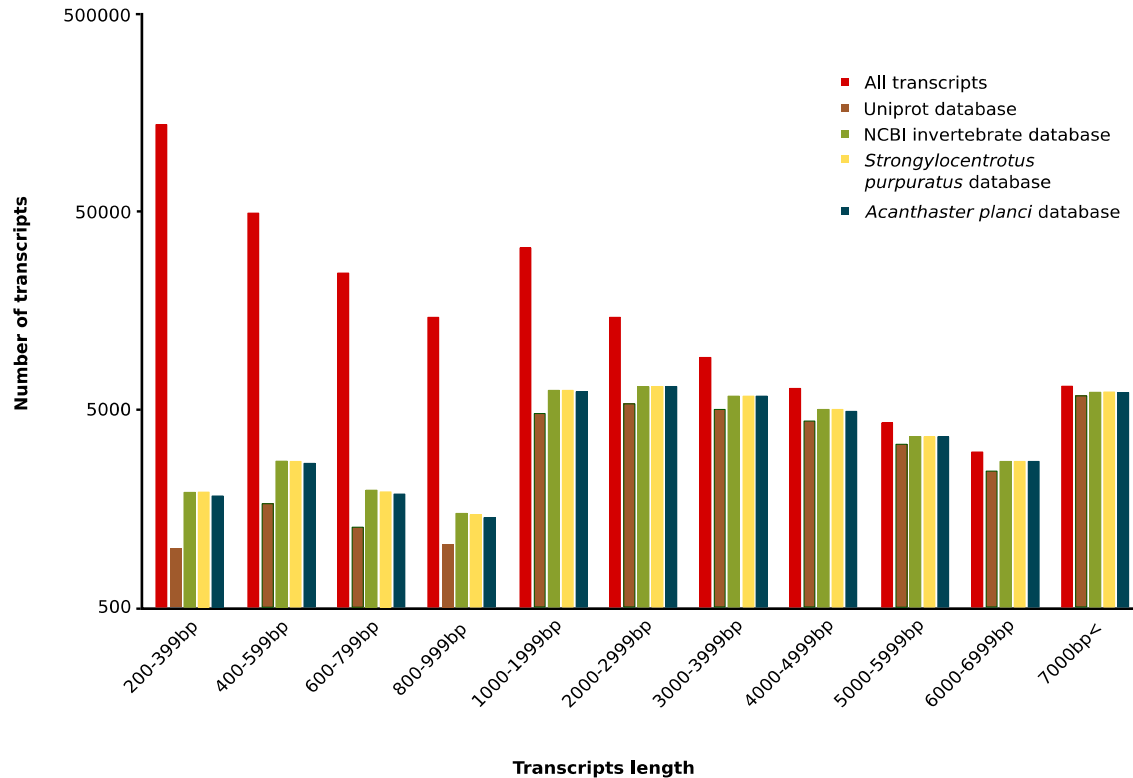
### 2.3.2. Functional annotation

In order to obtain plausible functional annotations for many transcripts, I repeated the comparison of transcripts to the UniProt database (made of Swiss-Prot sequences curated for Trinotate V3.0), the NCBI *Acanthaster planci* reference database (annotation release ID 100), the NCBI *Strongylocentrotus purpuratus* reference database (annotation release ID 101), and the NCBI invertebrate reference database (RefSeq Release 74), but with less stringent comparison criteria based on expectation scores alone ( $e = 10^{-5}$ ). I found 63,057 annotations in total (20% of all transcripts in the reference transcriptome; Table 2) including 12,492 transcripts with transmembrane regions (TMHMM), 39,595 transcripts with orthology in the EggNOG database; and 40,670 transcripts with identifiable protein domains (HMMER-Pfam). Most of the transcripts that were successfully annotated with the NCBI invertebrate database matched proteins from *Acanthaster planci* (94.6%) (see Appendix E for annotation and gene ontology results). About half (141,863) of the transcripts in the reference transcriptome were relatively short sequences (200–399 bp) that may include incompletely assembled splice isoforms or partial coding sequences from hard-to-assemble transcripts (e.g., repetitive genes; see Góngora-Castillo & Buell, 2013; Haas et al., 2013), and few were annotated in the NCBI invertebrate database (3.6%). By contrast, over three quarters (83%) of transcripts longer than 2,000 bp were successfully annotated (Figure 2-1). Like the high proportion of expected genes that were annotated, the large proportion of long transcripts that were successfully annotated suggests that the reference transcriptome is a reasonably accurate reflection of gene expression in these two tissues.

Annotation approaches	Number of hits
BLASTX - SwissProt	43,943
BLASTP - SwissProt	44,170
BLASTP - NCBI invertebrate database	55,137
BLASTP – <i>A. planci</i> database	54,249
BLASTP – <i>S. purpuratus</i> database	49,408
eggNOG	39,595
HMMER - Pfam	40,670
TMHMM	12,492
Unique transcripts from all BLAST searches	63,057

**Table 2.2** Summary statistics for the *Acanthaster cf. solaris* reference transcriptome.

**Figure 2.1** Frequency distribution of transcript lengths in the genome-guided transcriptome assembly from gonads of COTS. Five distributions representing all transcripts in the reference transcriptome and transcripts with annotations from one of the four reference databases: SwissProt database, NCBI invertebrate database, *Strongylocentrotus purpuratus* database, and the *Acanthaster planci* database



The transcriptome assemblies included many putative alternatively spliced transcripts (68,873 unconfirmed isoforms), but there is little context to understand the extent of their representation in the COTS transcriptome (Grabowski & Black, 2001; Mistry et al., 2003). Counting isoforms in an assembly is difficult because some apparent isoform differences (including the many transcripts <400 bp in our assemblies) are likely to represent assembly errors, especially partial assembly of full-length transcripts. However, the large number of possible isoforms indicates the potential importance of alternatively spliced transcripts in the creation of diverse protein sequences in mature COTS gonads, similar to other echinoderm transcriptomes (Elphick et al., 2015; Fuess et al., 2015; Pérez-Portela et al., 2016; Yang et al., 2016; see also Modrek & Lee, 2002).

### 2.3.3. Annotation and structure of gamete-recognition gene orthologs

Eight transcripts were strongly similar to echinoderm genes involved in the acrosome reaction or in processes that regulate the adhesion and fusion of sperm and egg (see Appendix D for gamete-recognition genes sequences; Figure 2-2). These genes were found in both the reference assembly and in the individual assemblies of testes (*guanylate cyclase*, *bindin*, *REJ1*, *REJ3*) and ovaries (*EBR1*, *ARIS1*, *ARIS2*, *ARIS3*), respectively. Two of those genes usually only expressed in sea star testes (*guanylate cyclase*, *bindin*; > 1000 TPM) were also unexpectedly strongly expressed (>100 TPM) in the ovary of one of the three females (Figure 2-6).

The membrane-bound guanylate cyclase in echinoderm sperm is a cell-surface receptor: it interacts with the peptide pheromone called asterosap that is released by the egg and functions to attract sperm (Matsumoto et al., 2003; Nishigaki et al., 2000). The membrane-bound guanylate cyclase is the only guanylate cyclase that has been confirmed to interact and coevolve directly with asterosap. One transcript (TRINITY\_DN32538\_c1\_g1\_i2, length 3,219 bp) was the top match for *guanylate cyclase* when compared to *Asterias amurensis* (AB070354.1) (see Appendix F for *guanylate cyclase* alignment). Similar to the *guanylate cyclase* of *A. amurensis*, the COTS gene encoded a tyrosine kinase catalytic domain (TK) and a guanylyl cyclase catalytic domain (GC; Figure 2-2) that were separated from the extracellular asterosap-binding domain by a transmembrane sequence. I found this transcript in the reference transcriptome, the two male assemblies, and in the female 1 assembly.

*Bindin* is expressed in the acrosomal vesicle of echinoderm sperm, and the bindin protein is exposed on the outer surface of the sperm head following the acrosome reaction; bindin interaction with the egg bindin receptor EBR1 and the other bindin receptor OBi1 influences both gamete adhesion and plasma membrane fusion (Foltz et al., 1993; Hart, 2013; Kamei & Glabe, 2003; Vacquier, 2012). Two transcripts were found as potential matches to different parts of the *bindin* gene (TRINITY\_GG\_38156\_c12\_g2\_i2, TRINITY\_GG\_38156\_c6\_g1\_i1), but the transcripts appeared to be missing part of the repetitive sections of the expected *bindin* sequence (Patiño et al., 2009, 2016), possibly due to errors in assembling repetitive coding sequences. I found the complete *bindin* coding sequence by searching the OKI genome, in which most of the *bindin* gene (Bindin\_oki.118.25.t1) had previously been predicted by the AUGUSTUS method (Hall et al., 2017). I noted some differences between the gene

prediction for *bindin* (from the genome) and the transcripts from our study, which were resolved in favor of features directly observed in the transcripts (over features that were inferred by the gene prediction algorithm; see Appendix G for characteristics of *bindin* sequence). The *bindin* coding sequence includes a conserved signal sequence followed by a preprobindin motif and an RXRR motif that encodes an enzymatic cleavage site similar to previously described *bindin* sequences from other sea star species (Patiño et al., 2009, 2016). The mature *bindin* sequence of COTS is composed of repetitive domains that include collagen-like sequences of many lysine-arginine-glycine-rich triplets, as in many sea stars, and two types of longer repetitive domains including eight tandem-repeated copies of a distinctive and long motif ~80 codons in length (type q), and ten tandem-repeated copies of a shorter motif of 12-14 codons (type r; see Patiño et al., 2016) (see Appendix G for characteristics of *bindin*). The mature *bindin* coding sequence ends with the highly conserved motif that is strongly similar to the *bindin* core domain of sea urchins and other sea stars and is known to encode the peptide that mediates the fusion of gamete plasma membranes (Glabe, 1985; Ulrich et al., 1998).



Similar to *guanylate cyclase*, I found *bindin* transcripts assembled from the ovary sample of female 1 in addition of the three testis samples from males. Two transcripts (TRINITY\_GG\_18363\_c5\_g1\_i1, TRINITY\_GG\_18363\_c2\_g1\_i1) from the transcriptome of female 1 were strongly similar or identical to *bindin* transcripts from the testis transcriptomes (see Appendix H for *bindin* alignment of male and female sequences). The expression of *guanylate cyclase* and *bindin* in female 1 was surprising because these genes are only known to be expressed in sperm and have well-characterized functions in fertilization but not in other cellular processes, and because we positively identified that tissue sample as ovary (containing only oocytes) and did not observe testis tissue or sperm in that tissue sample.

I identified two sperm-specific gamete-recognition genes (*REJ1*, *REJ3*) that are orthologs of sea urchin genes encoding the receptors for egg jelly (*suREJ1* and *suREJ3*), along with nine additional predicted genes that contain a conserved REJ-type protein domain (total of eleven) in the COTS genome (Figure 2; Figure S4). Previous studies have not reported sequences and protein domain organization of REJ genes from sea stars. The acrosome reaction in sea urchins is initiated by the interaction between a sperm receptor (*suREJ1*, expressed in the acrosome membrane of the sperm) and a fucose sulphate glycoprotein polymer in the egg jelly coat (Vacquier & Moy, 1997).

The *REJ1* (TRINITY\_GG\_18482\_c15\_g1\_i1) gene structure included two eel-fucolectin tachylectin-4 pentaxrin-1 domains (FTP) at the amino end of the predicted protein, followed by an immunoglobulin (IG) domain and three epidermal growth factor-like domains (EGF), similar to the lectin C and EGF domains in the amino end of the sea urchin coding sequence (Figure 2). The largest single part of the coding sequence of the *REJ1* transcript was a REJ domain for which the amino acid sequence is highly conserved across genes and organisms but for which the function is not known. The carboxyl end of the gene structure included a G protein-coupled receptor proteolytic site (GPS) and a lipoxygenase homology 2 (beta barrel) domain (LH2) surrounded by transmembrane helix regions, which are proposed to encode part of an ion channel in sea urchin and human REJ-containing genes (Gunaratne et al., 2007). The *REJ1* gene structure in COTS is considerably longer (3,134 codons) than the sea urchin gene (1,464 codons) due to additional coding sequence domains in both ends of the gene. In spite of those differences in comparison to sea urchin *REJ* genes, I am reasonably



confident that this REJ-containing transcript represents the *suREJ1* ortholog because it was the only transcript that included both a REJ domain and an EGF domain similar to *suREJ1* out of the eleven REJ-containing transcripts in our COTS reference assembly that had significant blast matches to known sea urchin genes.

The *REJ3* gene structure (TRINITY\_GG\_11119\_c8\_g1\_i1) (2,916 codons) included a GPS and an LH2 domain plus ten transmembrane regions, and was strongly similar in length (2,916 codons) and arrangement to the sea urchin gene (2,694 codons). The COTS gene differed from the sea urchin gene in the presence at the amino end of a lectin C-type domain and two polycystic kidney disease (PKD) repeats not found in *suREJ3*.

I found four gamete-recognition gene orthologs in all ovary samples and the reference transcriptome: *ARIS1*, *ARIS2*, *ARIS3*, and *EBR1*. The ARIS proteins form a complex of glycoproteins expressed in the egg coat that participate in the acrosome reaction after the sperm contacts the egg (Naruse et al., 2011). I found full-length coding sequences that were strongly similar to each of the ARIS paralogs of *Asterias amurensis* and to the partial coding sequences previously described for COTS (Naruse et al., 2011). The alignments of each of the ARIS genes to those of *A. amurensis* (see Appendix I for *ARIS* alignments) showed strong conservation of amino acids in most of the alignment, with larger differences in the carboxyl end of the predicted protein. The *ARIS1* gene structure (TRINITY\_GG\_10398\_c12\_g1\_i1) included FA58C and kringle domains that separated ARIS-N and ARIS-C domains like those of *A. amurensis*. Similarly, the *ARIS2* and *ARIS3* gene structures (TRINITY\_GG\_31908\_c1\_g1\_i1, TRINITY\_GG\_32225\_c25\_g1\_i2) included ARIS-N and ARIS-C domains like those of *A. amurensis* (Figure 2). The only notable difference was that the transmembrane domains predicted for the carboxyl ends of ARIS sequences for *A. amurensis* (Naruse et al., 2011) were not predicted in the ARIS sequences of COTS by the TMHMM algorithm.

I found the *egg bindin receptor 1 (EBR1)* expressed in each of the ovary transcriptomes and the reference transcriptome. *EBR1* is a receptor for *bindin* composed of repetitive domains that are highly variable (Hart, 2013; Kamei & Glabe, 2003). The transcript (TRINITY\_GG\_22397\_c47\_g3\_i2) accounts for 3,296 amino acids of EBR1 covering the complete length of the *EBR1* gene from *Patiria miniata*. I used this transcript to find the *EBR1* gene in the OKI genome. The predicted gene oki.23.112.t1 (length 3,201 amino acids) was nearly identical to the transcripts from this study and had

the same characteristic predicted protein domains as *EBR1* from *P. miniata*: signal peptide, M12B propeptide, zinc-dependent metalloprotease domain (ZnMc), epidermal growth factor-like domain, a series of Thrombospondin type 1 repeats (TSP1), and a series of paired TSP1-CUB (bone morphogenetic protein) domains. Similar to *P. miniata*, the repetitive CUB domains and the TSP1 domains in the COTS gene are highly variable among repeat copies (Figure 2).

These results suggest that COTS gonads that are visually identified as one sex may express some genes that are characteristic of the other sex (and have well defined functions in the gamete of the other sex). To further explore that possibility, I reassembled the testis RNA-seq data of Stewart et al. (2015) to search for gamete-recognition genes. I found the expected male-specific gamete-recognition gene transcripts (*bindin*, *guanylate cyclase*), as well as unexpected female-specific genes (*ARIS1*, *ARIS2*, *ARIS3*, and *EBR1*; see Appendix J for COTS gamete-recognition genes reassembled from the RNA-seq data of Stewart et al., 2015). Notably, the three *ARIS* transcripts assembled from these testis samples included full-length coding sequences that were unambiguously identified as orthologs of ARIS genes expressed in ovaries of COTS and in other sea stars (Naruse et al., 2011). Thus, two independent data sources indicate nonsex-specific expression of gamete-recognition genes in COTS gonad transcriptomes (see Appendix H for *bindin* alignment of male and female sequences).

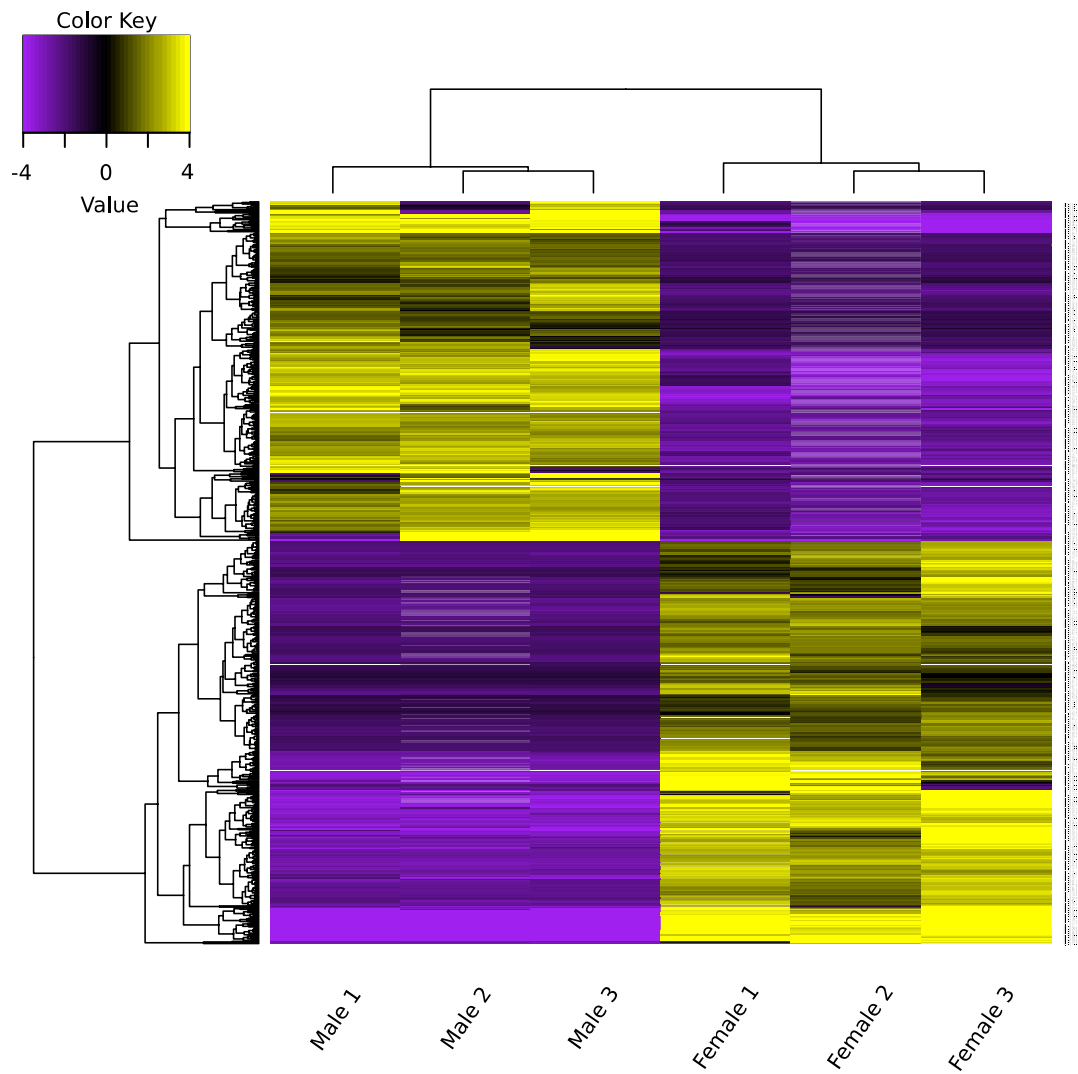
I was not able to assemble and annotate the gamete-recognition genes *OBi1* and *asterosap*. The absence of these genes may be due to assembly problems (associated with the complexity of repetitive genes like *asterosap*), similarity to paralogs in large gene families (such as the heat shock proteins related to *OBi1*), or the small size of some genes (*asterosap*). *OBi1* is part of a large gene subfamily (*hsp70*) with many similar paralogs (Foltz et al., 1993).

#### **2.3.4. Differential gene expression between ovary and testis**

Differential expression (DE) analysis between testis and ovary tissues grouped by biological repeats showed a total of 672 differentiated transcripts with a minimum *p*-value cutoff for FDR of 0.01 and a minimum fold change of 8, including 365 transcripts that were upregulated in females and 307 that were upregulated in males (see supplemental information in Guerra et al., 2020). These are unexpectedly small numbers of differentially expressed transcripts in comparison to other similar studies of male and

female gonad gene expression in echinoderms (e.g., almost 20,000 differentially expressed transcripts; Pérez-Portela et al., 2016). Relaxing one of the criteria for differential expression (e.g., increasing the  $p$ -value to .1) increased the number of transcripts (15,985) that might be differentially expressed but at the cost of reduced confidence in each identified gene (Figure 2-3). Of the upregulated ovary transcripts, 231 were annotated; and of the upregulated testis transcripts, 248 were annotated. In upregulated ovary transcripts, several differentially-expressed transcripts with TPM expression of 1,000 or higher had only hits to uncharacterized COTS genes.

**Figure 2.3** Differential expression of 672 male- and female-specific transcripts in COTS. Columns in the heat map represent biological repeats of ovary and testis tissues from six individual sea stars, including four from our study (Female 1, 2; Male 1, 2) and two from Hall et al. (2017) (Female 3; Male 3). Coloured lines in each column represent individual transcripts. Colour differences indicate expression variation among genes within and between tissue types. The clustering diagram shows grouping of transcripts into sets with similar expression patterns across samples, including one large set that is more strongly expressed in females (yellow) than in males (purple), and a smaller set that is more strongly expressed in males than in females



The annotations of the most differentially expressed ovary transcripts were linked to the microtubule cytoskeleton structure and nucleosome function, and extracellular space (including *ARIS1*, *ARIS2*, and *ARIS3*; Appendix D). The most differentially expressed testis transcripts were linked to ATP binding and cytoskeleton structure. *Bindin* and *guanylate cyclase* were highly expressed (above 2,500 TPM), but these genes were not differentially expressed due to the high expression of these genes in one female. *REJ1* and *REJ3* were expressed in males at rates 5- to 10-fold higher than in females, but TPM values for these genes were relatively lower (TPM ~ 20 in males vs. TPM ~ 3 in females) than the high TPM values observed for *bindin* and *guanylate cyclase*.

### **2.3.5. Histological evidence for hermaphroditic individuals**

My Japanese colleagues found three COTS individuals that were histologically hermaphroditic, with both male and female gametes in the same gonad (Figures 2-4, 2-5). In an individual identified morphologically as a female due to the presence of large mature ovaries filled with oocytes, we also found areas of spermatogenic epithelium and spermatozoa in the lumen beside the oocytes (Figure 2-4a). In another individual that was identified morphologically as a male due to the presence of large testes filled with spermatozoa, we found oocytes scattered in the gonad lumen among sperm (Figure 4b). In such individuals, most of the lobes of the gonad were devoted to one sex, but a small proportion of gonad lobes (Figure 5a) also contained gametes of both sexes. The size of oocytes (100–150  $\mu\text{m}$  diameter; Figure 5b), similar to that previously reported for female COTS from southern Japan, and the morphological appearance of sperm (including round sperm heads ~2  $\mu\text{m}$  in diameter; Figure 5c), were both consistent with the interpretation that hermaphrodites were capable of ovulating full-sized functional oocytes and were capable of spawning functional spermatozoa. The relatively small portion of male or female gametogenic tissue in gonad sections of the hermaphrodites was consistent with the two instances I identified of testis-specific gene expression in an individual with morphological ovaries (female 1 in my study) and of ovary-specific gene expression in at least one individual with morphological testes (in the pooled testis library by Stewart et al., 2015).

**Figure 2.4** Histological sections showing development of male and female gametes in hermaphrodites (a, b) and in male (c) or female (d) individuals. Hermaphrodites included individuals with male gametes developing in an ovary (a) and others with female gametes developing in a testis (b). Samples were collected in June and July 2018 at Nishidomari, Otsuki, Kochi Prefecture. Histology and micrographs by S. Adachi and M. Nakamura. oc, oocyte; se, spermatogenic epithelium; sp, spermatozoa

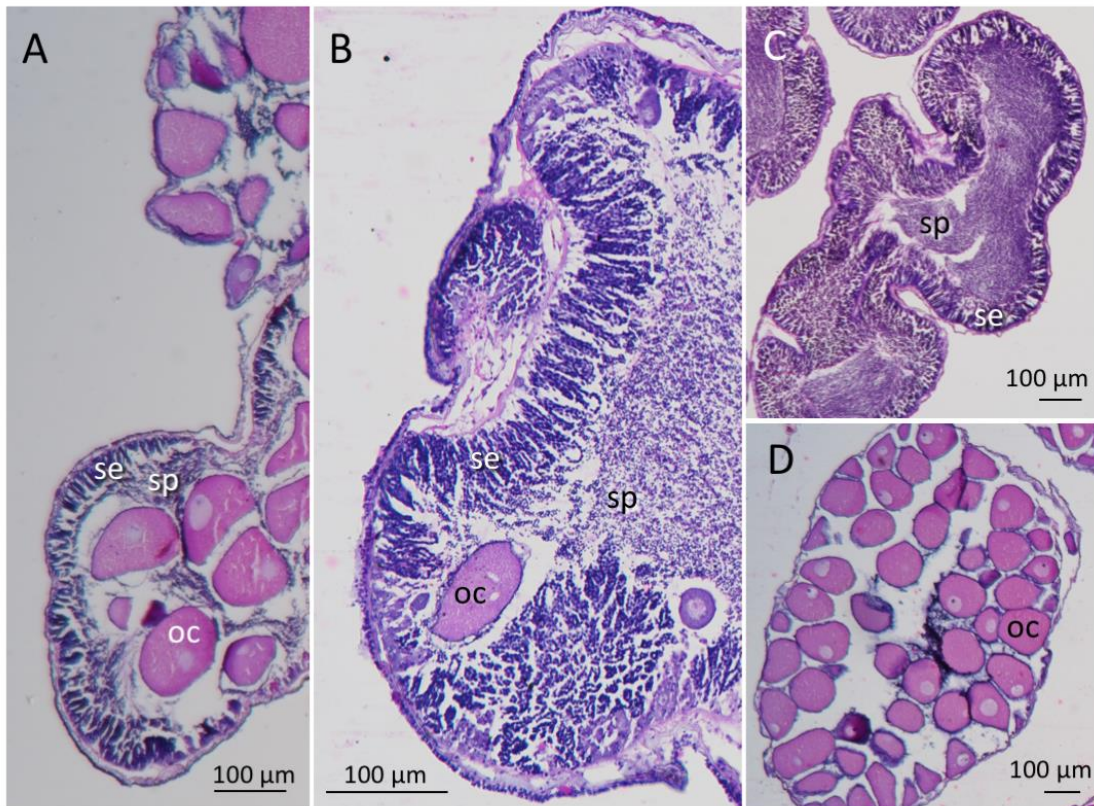
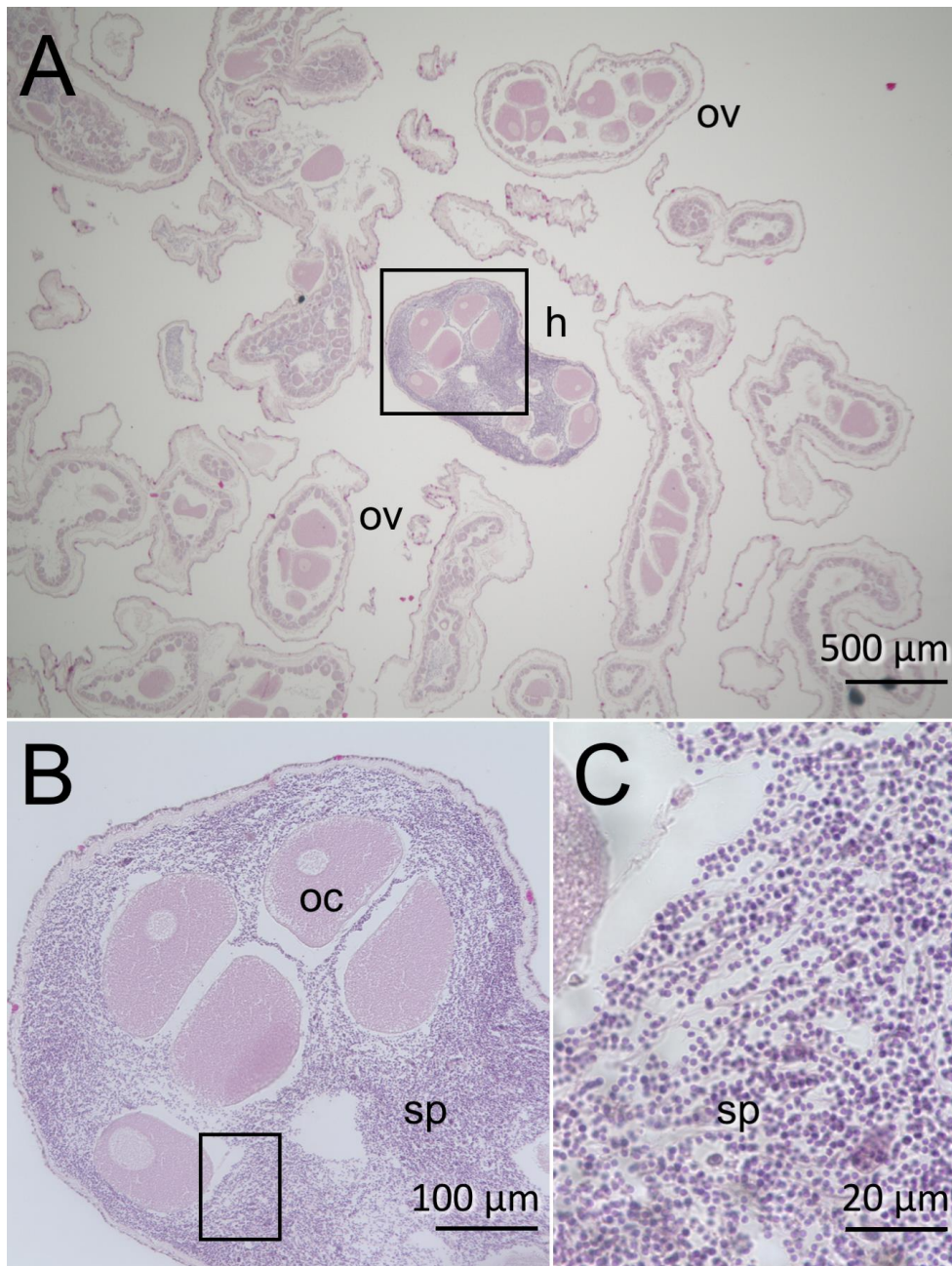




**Figure 2.5** Histological sections showing details of hermaphroditic gamete expression in an otherwise mostly “female” individual (a) in which most of the lobes of the ovary contained only oocytes, but some were hermaphroditic structures containing both oocytes and spermatozoa. Hermaphroditic gonad lobes (b) included both oocytes and spermatozoa. Individual spermatozoa had spherical heads each ~ 2  $\mu\text{m}$  in diameter (c). Boxes in (a) and (b) show areas of detail illustrated at higher magnification in (b) and (c). Sample was collected in June 2018 at Nishidomari, Otsuki, Kochi Prefecture. Histology and micrographs by S. Adachi and M. Nakamura. h, hermaphroditic gonad lobe; oc, oocyte; ov, ovarian lobe; sp, spermatozoa



### 2.3.6. Barcode identification of *Acanthaster cf. solaris*

The genealogical analysis found four haplotype networks separated from each other by genetic distances greater than the 95% parsimony connection limit (10 steps; see supplemental information in Guerra et al., 2020). Those four networks corresponded to the four provisional species (and the four Biological Index Numbers or BINs) reviewed by Haszprunar et al. (2017). The *COI* coding sequences from the four individuals in my study were grouped with the coding sequence from the complete mitochondrial genome in a large and diverse network that included 28 haplotypes. The most common of those haplotypes ( $n = 34$  individuals) occurred in three of the four individuals in my study, and in a geographically diverse group of individuals from other sites in the western Pacific; the fourth individual in my study differed from the others by a single C-to-T transition. Individuals in that network were grouped in the same BIN (AA1630) corresponding to the provisional name *Acanthaster cf. solaris* (see Haszprunar et al. (2017)).

## 2.4. Discussion

I identified a suite of sex-specific gamete-recognition genes in the ovary and testis transcriptomes of COTS, enriching the catalog of sequences for these genes in sea stars including two genes (*REJ1* and *REJ3*) not been previously described in Asteroidea. For *A. cf. solaris*, I characterized genes that encode proteins involved in sperm-egg interaction mediated by sperm chemoattraction, activation, and binding to the egg coat

### 2.4.1. Gamete-recognition genes

*Guanylate cyclase* is expressed in the sea star sperm tail and binds to asterosap, a sperm chemoattractant peptide released by the egg coat (Matsumoto et al., 2003; Nishigaki et al., 2000). The *guanylate cyclase* of COTS has a coding sequence organization similar to that of the sea star *Asterias amurensis*. However, there are amino acid differences between this gene in these two species, including substitutions in the extracellular domain that encodes the asterosap binding site (see Appendix F for *guanylate cyclase* alignment). The extracellular domain (but not the intracellular domain)



of guanylate cyclase is also highly divergent between closely related sister species of *Ophioderma* brittlestars (Weber et al., 2017).

I did not isolate *asterosap* from ovary transcripts, although its presence was expected. *Asterosap* is a short peptide encoded by a series of repetitive motifs that are transcribed and translated together, then post-translationally cleaved into small functional peptide units that are secreted into the egg coat (Nishigaki et al., 1996). If *asterosap* evolves under concerted evolution of repeats, similar to that seen for repetitive regions in *bindin* (Patiño et al., 2016), then among-species differences in gene structure may limit the ability to identify *asterosap* in COTS by comparison to genes from distantly related species.

Sperm capacitation and the acrosome reaction in sea stars are mediated by the interaction between REJ proteins on the sperm head and ARIS glycoproteins in the egg coat (Hoshi et al., 2012). In sea urchins, *suREJ1* expressed in the sperm head interacts with a fucose sulphate polymer (FSP) in the egg coat that induces the acrosome reaction (Vacquier & Moy, 1997). A second member of this gene family, *suREJ3* expressed in the sperm plasma membrane, also appears to be involved in the acrosome reaction (Neill et al., 2004; Neill & Vacquier, 2004). Positive selection on codons in the N-terminus region of *suREJ1* and *suREJ3* is an important mechanism underlying species divergence in sea urchins and may play a role in the origin or maintenance of reproductive isolation (Mah et al., 2005; Pujolar & Pogson, 2011). The localization of positive selection to the N-terminus of REJ proteins is functionally significant because that domain encodes the FSP-binding site (Vacquier & Moy, 1997).

The COTS testis transcriptome included an ortholog for *suREJ1*, the first *REJ* gene to be characterized in sea stars. It is notable that COTS *REJ1* differs in both gene architecture and amino acid sequence from *suREJ1*, including differences in the type (but not the number) of lectin domains (see also Weber et al., 2017). Selection acting on the functional properties of that N-terminus region may be responsible for these protein domain differences and warrants further study among sea star species, especially across the clade of closely-related *Acanthaster* species.

The COTS ovary transcriptome included three homologous *ARIS* genes that encode the acrosome reaction-inducing substance. These were similar to the *ARIS* genes of *Asterias amurensis* (Naruse et al., 2011), including conserved ARIS N-terminus and ARIS C-terminus domains. The *ARIS1* gene of COTS encoded two additional

conserved domains, FA58C and KD, suggested to be involved in the interaction of ARIS1 with other ARIS proteins in several other species (Naruse et al., 2011). Although ARIS1 alone can initiate the acrosome reaction in sea stars in the laboratory, this reaction normally occurs only when ARIS1 is expressed together with ARIS2 and ARIS3 (Hoshi et al., 1994; Naruse et al., 2011). Glycosylated sites on ARIS proteins may play a role in the acrosome reaction of sea star sperm similar to the role of FSP in sea urchins.

Although the ARIS receptor has not been identified for sea star sperm, it seems likely that this is a role for COTS *REJ1* and *REJ3* identified from the testis transcriptome. At least nine additional genes with REJ domains are present in the OKI genome (see Appendix K for domain architecture comparison among eleven predicted receptors for egg jelly genes). Each of these genes is found in a different scaffold. All 11 genes share part of their protein architecture with the 10 *REJ* genes of sea urchins and the *PKD* genes of humans (Gunaratne et al., 2007).

The architecture of COTS *bindin*, including distinctive repeat motifs flanked by a conserved nonrepetitive region at each of the predicted N- and C-terminus regions, was similar to other echinoderms in which *bindin* functions in sperm binding to receptors on the egg (Patiño et al., 2009, 2016; Vacquier & Moy, 1977). Although the organization of the COTS *bindin* coding sequence was similar to that of other sea stars, the repeat motifs were species-specific. These differences probably arise by concerted evolution (Patiño et al., 2016; Vacquier, 1998). This gene in COTS is the longest *bindin* coding sequence reported from a sea star due to the length of the q repeat motifs, and the number of copies of the q and r repeats. Unlike other sea stars, in which the *bindin* coding sequences include alternating collagen-like repeats interspersed with one or more copies of longer repeat types, COTS *bindin* was organized into a single collagen-like domain of many KRG-like triplets followed by a single long domain of many q- and r-type repeats. In this respect, this gene was more similar to *bindin* in *Evasterias troschelii* (Order Forcipulatida) than to asterinids or other members of the Order Valvatida (see Patiño et al., 2016) to which COTS are more closely related.

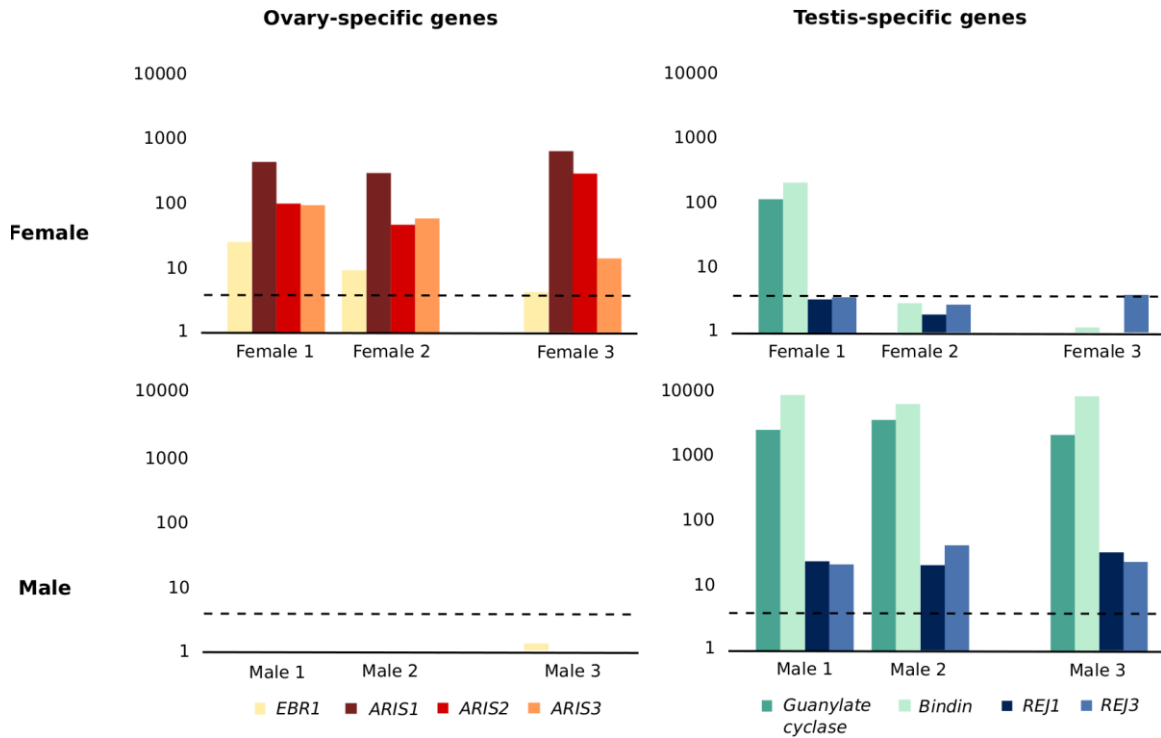
The homolog for the egg *bindin* receptor *EBR1* in COTS has a coding sequence organization similar to *EBR1* of the sea star *Patiria miniata* and that of sea urchins. This includes several nonrepetitive domains in the 5' end of the coding sequence, a series of TSP1 repeats, and a series of paired TSP1-CUB domains (known as core EBR repeats; Kamei & Glabe, 2003) that make up the 3' end of the gene. Unlike *P. miniata*, there is no

predicted EGF domain in the nonrepetitive region upstream of the TSP1 repeats in COTS *EBR1*. In sea urchins, most of the *EBR1* coding sequence consists of TSP1 and core EBR repeats in *Mesocentrotus franciscanus*, but the 3' end of *EBR1* in *Strongylocentrotus purpuratus* consists of several HYR-like domain repeats. This major difference in *EBR1* between sea urchins is linked to species-specificity of sperm binding (Kamei & Glabe, 2003). More *EBR1* sequence data from other sea star species are needed to understand the possible functional or evolutionary significance of these differences and potential for species-specific features. This is a good candidate to investigate the divergence among *Acanthaster* species, an important problem that remains unresolved.

#### **2.4.2. Evidence of non-sex-specific gene expression**

I found evidence of nonspecific expression of some gamete-recognition genes, including expression of *bindin* and *guanylate cyclase* in one of the ovary transcriptomes (Figure 2-6). This result is surprising because these genes are only known to be expressed in testes, and because they have well-understood functions in male reproduction in echinoderms (Hirohashi et al., 2008). Similarly, I found four female-specific gamete-recognition genes (*ARIS1*, *ARIS2*, *ARIS3*, *EBR1*) in the pooled testis transcriptome generated by Stewart et al. (2015). These authors also reported a partial coding sequence similar to *EBR1* in that transcriptome.

**Figure 2.6 Summary of sex-specific expression patterns for eight gamete-recognition genes in COTS. Bar graphs show expression profiles for ovary- or testis-specific genes in gonad tissue samples from our study (Female 1, 2; Male 1, 2) and from Hall et al. (2017) (Female 3; Male 3). The height of each bar shows expression (as TPM) for each of the genes in each gonad sample. The dashed line shows TPM = 4. Note the nonspecific, low level of expression for several testis or ovary genes in most samples of the other sex, plus the high level of expression for two testis-specific genes (*bindin*, *guanylate cyclase*) in one female**



The expression of sex-specific gamete-recognition genes in the gonads of the opposite sex suggest that COTS individuals may occasionally develop as hermaphrodites in which a gonad that appears to be morphologically of one sex (and expresses genes that are characteristic of one gamete type), like the individuals in our study, also includes gametes of the other sex (and expresses genes that are characteristic of the other gamete type). My colleagues and I confirmed this interpretation by finding multiple individuals identified as one sex based on overall gonad anatomy were actually hermaphrodites as revealed by gonad histology. Hermaphroditism is a fixed trait in some asterinid sea stars in which each gonad is an ovotestis, but the extent of hermaphroditism can be variable: some gonads with both sexes expressed can be predominantly male or predominantly female, including the

presence of microhermaphrodites with 'ovaries' containing a minute amount of sperm (Byrne, 1996, 2005; Byrne & Cerra, 1996) that can generate progeny by self-fertilization (Barbosa, Klanten, Jones, & Byrne, 2012). Similarly, in normally gonochoric asterinids each gonad can appear to be uniformly one sex but with small patches of tissue consisting of the other sex (Byrne, 1992). Hermaphroditic individuals are well known to occur in other echinoderm species that are typically gonochoric (Byrne, Hart, Cerra, & Cisternas, 2003; Komatsu, Kano, Yoshizawa, Akabane, & Oguro, 1979; Komatsu & Oguro, 1972; Lawrence, 1987; Moore, 1932, 1935; Yamaguchi & Lucas, 1984).

Although it is not known whether COTS hermaphrodites are self-fertile, selfing is common in hermaphroditic echinoderms (Barbosa et al., 2012), and eggs surrounded by a fertilization envelope are occasionally released by COTS ovaries (M. Byrne, personal observation). If ovotestes are predominantly one sex, hermaphroditism would be difficult to detect on visual inspection of massive gonads such as those produced by COTS. The hermaphroditic region of the COTS gonads we observed in histological sections was small, but consistent with the possibility that facultative hermaphrodites may self-fertilize eggs. Ovotestes may be more likely to be discovered using molecular screening because the examination of serial histological sections would be impractical for such massive gonads.

My results show hermaphroditic expression of gamete-recognition genes in two of the three published analyses of COTS gonad transcriptomes (Stewart et al., 2015, and this study; but not Hall et al., 2017). Although previous histological studies have not reported ovotestes in COTS, a re-examination of histological sections from previous studies might reveal additional cases of hermaphrodites, and could be used to estimate the prevalence of hermaphrodites in other population samples.

### **2.4.3. Ecological and evolutionary significance of hermaphrodites**

The unexpected finding of hermaphrodites among COTS has implications with respect to our understanding of the reproductive biology of these ecologically important predators and for the application of simulation models of reproductive success and source-sink connectivity networks to the understanding of population outbreaks (Hock et al., 2014; Rogers et al., 2017). The presence of hermaphrodites and the observation of eggs released by isolated females with a fertilization envelope (M. Byrne, personal observation) may explain some cases of apparent long-distance fertilization of COTS

eggs released up to 100 m downstream of a spawning male (Babcock, Mundy, & Whitehead, 1994). Such cases run counter to the paradigm of variable fertilization rates in the sea, in which low fertilization rates for eggs released more than ~ 1 m from sperm are caused by low sperm density and decreased sperm-egg contacts (Levitan, Sewell, & Chia, 1992; Pennington, 1985). Isolated females of the sea star *Patiria miniata* also occasionally release eggs with a fertilization envelope and these develop into functional larvae and juveniles (Sunday, Raeburn, Stewart & Hart, 2009). As in COTS, gross examination of the gonads of these “female” *P. miniata* did not reveal evidence of testis tissue. The molecular and histological evidence for hermaphroditism in COTS suggests that facultative hermaphrodites may be more common in normally gonochoric sea stars than has been previously appreciated, and points toward potential for phenotypic plasticity in sex determination in some sea star species. Comparable discoveries involving reproductive traits and potential for flexible propagation in the absence of a mate are important in our understanding of the population dynamics, ecology and conservation of other top predators including snakes (Booth & Schuett, 2016) and sharks (Chapman et al., 2007).

If hermaphrodites are more common than expected and if such individuals are self-fertile, then reproductive assurance through self-fertilization (Jarne & Auld, 2006) in COTS could be added to the growing list of life history traits (e.g., larval cloning; Allen et al., 2019) that are likely to facilitate high reproductive success, and the boom-and-bust nature of the population outbreaks that decimate coral reefs. The interpretation of facultative hermaphroditism in COTS as a potential adaptation depends on the phylogenetic context: in taxa such as sea stars in which most species are gonochoric outcrossers, the occurrence of facultative hermaphrodites is evolutionarily derived and might be considered an adaptation. But in other gonochoric species (e.g., the pelagic tunicate *Oikopleura dioica*) that occur in taxa (Appendicularia) that are typically hermaphrodites (Deibel & Lowen, 2012), the occurrence of facultative hermaphrodites in some individuals might be interpreted as an atavism rather than an adaptation. I do not know of cases of this second type of facultative hermaphroditism.

Given the high fecundity of individual COTS, self-fertilization of even a small proportion of eggs might contribute to maintenance and buildup of preoutbreak populations. Reproductive assurance might be especially important if the tendency to develop as a hermaphrodite is associated with local scarcity of COTS under

nonoutbreak conditions. The adult secretome of COTS includes peptide pheromones that diffuse in seawater and affect movement and aggregation behaviour by conspecific individuals (Hall et al., 2017). I speculate that the absence of such pheromone signals (for isolated individuals) also conveys important ecological information (that no spawning partners are nearby), and could promote the development of hermaphroditic gonads and self-fertilization. Such a capacity for facultative reproductive assurance would greatly enhance the reproductive potential of COTS populations at low spatial density. Field surveys (perhaps combined with re-examination of histological sections from previous studies) are needed to document and quantify the geographic extent and frequency of hermaphrodites; those new surveys could use a combination of spawning assays, histology, or molecular methods such as qPCR or protein mass spectrometry to detect gene expression products. New experimental work is also needed to test the hypothesis that local conditions (especially population abundance) influence sex ratio and the tendency to develop as a hermaphrodite.

## 2.5. References

- Allen, J. D., Richardson, E. L., Deaker, D., Aguera, A., & Byrne, M. (2019). Larval cloning in the crown-of-thorns sea star, a keystone coral predator. *Marine Ecology Progress Series*, 609, 271–276. <https://doi.org/10.3354/meps12843>
- Altschul, S. F., Gish, W., Miller, W., Myers, E. W., & Lipman, D. J. (1990). Basic local alignment search tool. *Journal of Molecular Biology*, 215, 403–410. [https://doi.org/10.1016/S0022-2836\(05\)80360-2](https://doi.org/10.1016/S0022-2836(05)80360-2)
- Apweiler, R., Martin, M. J., O'Donovan, C., Magrane, M., Alam-Faruque, Y., Antunes, R., ... Zhang, J. (2012). Reorganizing the protein space at the Universal Protein Resource (UniProt). *Nucleic Acids Research*, 40, D71–D75. <https://doi.org/10.1093/nar/gkr981>
- Ashburner, M., Ball, C. A., Blake, J. A., Botstein, D., Butler, H., Cherry, J. M., ... Sherlock, G. (2000). Gene ontology: Tool for the unification of biology. *Nature Genetics*, 25, 25–29. <https://doi.org/10.1038/75556>
- Babcock, R. C., Mundy, C. N., & Whitehead, D. (1994). Sperm diffusion models and *in situ* confirmation of long-distance fertilization in the free-spawning asteroid *Acanthaster planci*. *Biological Bulletin*, 186, 17–28.
- Babcock, R. C., Milton, D. A., & Pratchett, M. S. (2016). Relationships between size and reproductive output in the crown-of-thorns starfish. *Marine Biology*, 163, 234. <https://doi.org/10.1007/s00227-016-3009-5>
- Barbosa, S. S., Klanten, O. S., Jones, H., & Byrne, M. (2012). Selfing in *Parvulastra exigua*, an asterinid sea star with benthic development. *Marine Biology*, 159, 1071–1077. <https://doi.org/10.1007/s00227-012-1887-8>
- Birkeland, C. (1982). Terrestrial runoff as a cause of outbreaks of *Acanthaster planci* (Echinodermata: Asteroidea). *Marine Biology*, 69, 175–185. <https://doi.org/10.1007/BF00396897>
- Birkeland, C., & Lucas, J. S. (1990). *Acanthaster planci: Major management problem of coral reefs*. Boca Raton, FL: CRC Press.
- Bolger, A. M., Lohse, M., & Usadel, B. (2014). Trimmomatic: A flexible trimmer for Illumina sequence data. *Bioinformatics*, 30, 2114–2120. <https://doi.org/10.1093/bioinformatics/btu170>
- Booth, W., & Schuett, G. W. (2016). The emerging phylogenetic pattern of parthenogenesis in snakes. *Biological Journal of the Linnean Society*, 118, 172–186. <https://doi.org/doi/10.1111/bij.12744>



- Byrne, M. (1992). Reproduction of sympatric populations of *Patiriella gunnii*, *P. calcar* and *P. exigua* in New South Wales, asterinid seastars with direct development. *Marine Biology*, 114, 297–316.
- Byrne, M. (1996). Viviparity and intragonadal cannibalism in the diminutive sea stars *Patiriella vivipara* and *P. parvivipara* (family Asterinidae). *Marine Biology*, 125, 551–567. <https://doi.org/10.1007/BF00353268>
- Byrne, M., & Cerra, A. (1996). Evolution of intragonadal development in the diminutive asterinid sea stars *Patiriella vivipara* and *P. parvivipara* with an overview of development in the Asterinidae. *Biological Bulletin*, 191, 17–26. <https://doi.org/10.2307/1543057>
- Byrne, M., Hart, M. W., Cerra, A., & Cisternas, P. (2003). Reproduction and larval morphology of broadcasting and viviparous species in the *Cryptasterina* species complex. *Biological Bulletin*, 205, 285–294.
- Byrne, M. (2005). Viviparity in the sea star *Cryptasterina hystera* (Asterinidae) - Conserved and modified features in reproduction and development. *Biological Bulletin*, 208, 81–91.
- Chapman, D. D., Shivji, M. S., Louis, E., Sommer, J., Fletcher, H., & Prodohl, P. A. (2007). Virgin birth in a hammerhead shark. *Biology Letters*, 3, 425–427. <https://doi.org/10.1098/rsbl.2007.0189>
- Clement, M., Posada, D., & Crandall, K. A. (2000). TCS: A computer program to estimate gene genealogies. *Molecular Ecology*, 9, 1657–1660. <https://doi.org/10.1046/j.1365-294x.2000.01020.x>
- Colgan, M. W. (1987). Coral reef recovery on Guam (Micronesia) after catastrophic predation by *Acanthaster planci*. *Ecology*, 68, 1592–1605. <https://doi.org/10.2307/1939851>
- De'ath, G., Fabricius, K. E., Sweatman, H., & Puotinen, M. (2012). The 27- year decline of coral cover on the Great Barrier Reef and its causes. *Proceedings of the National Academy of Sciences USA*, 109(44), 17995– 17999. <https://doi.org/10.1073/pnas.1208909109>
- Deibel, D., & Lowen, B. (2012). A review of the life cycles and life-history adaptations of pelagic tunicates to environmental conditions. *ICES Journal of Marine Science*, 69, 358–369. <https://doi.org/10.1093/icesjms/fsr159>
- Elphick, M. R., Semmens, D. C., Blowes, L. M., Levine, J., Lowe, C. J., Arnone, M. I., & Clark, M. S. (2015). Reconstructing SALMFamide neuropeptide precursor evolution in the phylum Echinodermata: Ophiuroid and crinoid sequence data provide new insights. *Frontiers in Endocrinology*, 6, 1–10. <https://doi.org/10.3389/fendo.2015.00002>

- Finn, R. D., Clements, J., & Eddy, S. R. (2011). HMMER web server: Interactive sequence similarity searching. *Nucleic Acids Research*, *39*, 29–37. <https://doi.org/10.1093/nar/gkr367>
- Finn, R. D., Mistry, J., Tate, J., Coghill, P., Heger, A., Pollington, J. E., ... Bateman, A. (2012). The Pfam protein families databases. *Nucleic Acids Research*, *30*, 1–12. <https://doi.org/10.1093/nar/gkp985>
- Foltz, K. R., Partin, J. S., & Lennarz, W. J. (1993). Sea urchin egg receptor for sperm: Sequence similarity of binding domain and hsp70. *Science*, *259*, 1421–1425. <https://doi.org/10.1126/science.8383878>
- Fuess, L. E., Eisenlord, M. E., Closek, C. J., Tracy, A. M., Mauntz, R., Gignoux-Wolfsohn, S., ... Roberts, S. B. (2015). Up in arms: Immune and nervous system response to sea star wasting disease. *PLoS ONE*, *10*, 1–16. <https://doi.org/10.1371/journal.pone.0133053>
- Glabe, C. G. (1985). Interaction of the sperm adhesive protein, bindin, with phospholipid vesicles. 2. Bindin induces the fusion of mixed-phase vesicles that contain phosphatidylcholine and phosphatidylserine in vitro. *Journal of Cell Biology*, *100*, 800–806. <https://doi.org/10.1083/jcb.100.3.800>
- Góngora-Castillo, E., & Buell, C. R. (2013). Bioinformatics challenges in *de novo* transcriptome assembly using short read sequences in the absence of a reference genome sequence. *Natural Product Reports*, *30*, 490. <https://doi.org/10.1039/c3np20099j>
- Grabherr, M. G., Haas, B. J., Yassour, M., Levin, J. Z., Thompson, D. A., Amit, I., ... Regev, A. (2011). Full-length transcriptome assembly from RNA-Seq data without a reference genome. *Nature Biotechnology*, *29*, 644–652. <https://doi.org/10.1038/nbt.1883>
- Grabowski, P. J., & Black, D. L. (2001). Alternative RNA splicing in the nervous system. *Progress in Neurobiology*, *65*, 289–308. [https://doi.org/10.1016/S0301-0082\(01\)00007-7](https://doi.org/10.1016/S0301-0082(01)00007-7)
- Guerra, V., Haynes, G., Byrne, M., Yasuda, N., Adachi, S., Nakamura, M., Nakachi, S., and Hart, M. W., (2020). Nonspecific expression of fertilization genes in the crown-of-thorns *Acanthaster cf. solaris*: Unexpected evidence of hermaphroditism in a coral reef predator. *Molecular Ecology*, *29*(2), 363–379. <https://doi.org/10.1111/mec.15332>
- Gunaratne, H. J., Moy, G. W., Kinukawa, M., Miyata, S., Mah, S. A., & Vacquier, V. D. (2007). The 10 sea urchin receptor for egg jelly proteins (SpREJ) are members of the polycystic kidney disease-1 (PKD1) family. *BMC Genomics*, *8*, 235. <https://doi.org/10.1186/1471-2164-8-235>

- Haas, B. J., Papanicolaou, A., Yassour, M., Grabherr, M., Blood, P. D., Bowden, J., ... Regev, A. (2013). *De novo* transcript sequence reconstruction from RNA-seq using the Trinity platform for reference generation and analysis. *Nature Protocols*, 8, 1494–1512. <https://doi.org/10.1038/nprot.2013.084>
- Hall, M. R., Kocot, K. M., Baughman, K. W., Fernandez-Valverde, S. L., Gauthier, M. E. A., Hatleberg, W. L., ... Degnan, B. M. (2017). The crown-of-thorns starfish genome as a guide for biocontrol of this coral reef pest. *Nature*, 544, 231–234. <https://doi.org/10.1038/nature22033>
- Hart, M. W., & Sunday, J. (2007). Things fall apart: biological species form unconnected parsimony networks. *Biology Letters*, 3, 509–512. <https://doi.org/10.1098/rsbl.2007.0307>
- Hart, M. W. (2012). Next-generation studies of mating system evolution. *Evolution*, 66, 1657–1680. <https://doi.org/10.1111/j.1558-5646.2012.01605.x>
- Hart, M. W. (2013). Structure and evolution of the sea star egg receptor for sperm binding. *Molecular Ecology*, 22, 2143–2156. <https://doi.org/10.1111/mec.12251>
- Hart, M. W., & Foster, A. (2013). Highly expressed genes in gonads of the bat star *Patiria miniata*: Gene ontology, expression differences, and gamete-recognition loci. *Invertebrate Biology*, 132, 241–250. <https://doi.org/10.1111/ivb.12029>
- Haszprunar, G., Vogler, C., & Wörheide, G. (2017). Persistent gaps of knowledge for naming and distinguishing multiple species of crown-of-thorns seastar in the *Acanthaster planci* species complex. *Diversity*, 9, 22. <https://doi.org/10.3390/d9020022>
- Haywood, M. D. E., Thomson, D. P., Babcock, R. C., Pillans, R. D., Keesing, J. K., Miller, M., ... Field, S. N. (2019). Crown-of-thorns starfish impeded the recovery potential of coral reefs following bleaching. *Marine Biology*, 166, 99. <https://doi.org/10.1007/s00227-019-3543-z>
- Hirohashi, N., Kamei, N., Kubo, H., Sawada, H., Matsumoto, M., & Hoshi, M. (2008). Egg and sperm recognition systems during fertilization. *Development Growth & Differentiation*, 50, S221–S238. <https://doi.org/10.1111/j.1440-169X.2008.01017.x>
- Hock, K., Wolff, N. H., Condie, S. A., Anthony, K. R. N., & Mumby, P. J. (2014). Connectivity networks reveal the risks of crown-of-thorns starfish outbreaks on the Great Barrier Reef. *Journal of Applied Ecology*, 51, 1188–1196. <https://doi.org/10.1111/1365-2664.12320>
- Hoshi, M., Nishigaki, T., Ushiyama, A., Okinaga, T., Chiba, K., & Matsumoto, M. (1994). Egg-jelly signal molecules for triggering the acrosome reaction in starfish spermatozoa. *International Journal of Developmental Biology*, 38, 167–174.

- Hoshi, M., Moriyama, H., & Matsumoto, M. (2012). Structure of acrosome reaction-inducing substance in the jelly coat of starfish eggs: A mini review. *Biochemical and Biophysical Research Communications*, 425, 595–598. <https://doi.org/10.1016/j.bbrc.2012.08.033>
- Jarne, P., & Auld, J. R. (2006). Animals mix it up too: The distribution of self-fertilization among hermaphroditic animals. *Evolution*, 60, 1816–1824. <https://doi.org/10.1554/06-246.1>
- Kamei, N., & Glabe, C. G. (2003). The species-specific egg receptor for sea urchin sperm adhesion is EBR1, a novel ADAMTS protein. *Genes & Development*, 17, 2502–2507. <https://doi.org/10.1101/gad.1133003>
- Kanehisa, M., & Goto, S. (2000). Kyoto encyclopedia of genes and genomes. *Nucleic Acids Research*, 28, 27–30. <https://doi.org/10.1093/nar/28.1.27>
- Kawamura, M., Matsumoto, M., & Hoshi, M. (2002). Characterization of the sperm receptor for acrosome reaction-inducing substance of the starfish, *Asterias amurensis*. *Zoological Science*, 19, 435–442. <https://doi.org/10.2108/zsj.19.435>
- Kayal, M., Vercelloni, J., Lison de Loma, T., Bosserelle, P., Chancerelle, Y., Geoffroy, S., ... Adjeroud, M. (2012). Predator crown-of-thorns starfish (*Acanthaster planci*) outbreak, mass mortality of corals, and cascading effects on reef fish and benthic communities. *PLoS ONE*, 7, e47363. <https://doi.org/10.1371/journal.pone.0047363>
- Komatsu, M., & Oguro, C. (1972). Notes on the hermaphroditic specimen of the sea-star, *Certonardoa semiregularis* (Muller et Troschel). *Proceedings of the Japanese Society of Systematic Zoology*, 8, 49–52.
- Komatsu, M., Kano, Y. T., Yoshizawa, H., Akabane, S., & Oguro, C. (1979). Reproduction and development of the hermaphroditic sea star, *Asterina minor* Hayashi. *Biological Bulletin*, 157, 258–274. <https://doi.org/10.2307/1541053>
- Krogh, A., Larsson, B., Von Heijne, G., & Sonnhammer, E. L. L. (2001). Predicting transmembrane protein topology with a hidden Markov model: Application to complete genomes. *Journal of Molecular Biology*, 305, 567–580. <https://doi.org/10.1006/jmbi.2000.4315>
- Langmead, B., & Salzberg, S. L. (2012). Fast gapped read alignment with bowtie2. *Nature Methods*, 9, 357–359. <https://doi.org/10.1038/nmeth.1923>
- Lawrence, J. (1987). *A functional biology of echinoderms*. London, UK: Croom Helm.
- Lessios, H. A. (2007). Reproductive isolation between species of sea urchins. *Bulletin of Marine Science*, 81, 191–208.

- Lessios, H. A. (2011). Speciation genes in free-spawning marine invertebrates. *Integrative and Comparative Biology*, 51, 456–465. <https://doi.org/10.1093/icb/icr039>
- Levitan, D. R., Sewell, M. A., & Chia, F.S. (1992). How distribution and abundance influence fertilization success in the sea urchin *Strongylocentrotus franciscanus*. *Ecology*, 73, 248–254.
- Levitan, D. R. (2004). Density-dependent sexual selection in external fertilizers: variances in male and female fertilization success along the continuum from sperm limitation to sexual conflict in the sea urchin *Strongylocentrotus franciscanus*. *American Naturalist*, 164, 298–309. <https://doi.org/10.1086/423150>
- Li, B., & Dewey, C. N. (2011). RSEM: Accurate transcript quantification from RNA-Seq data with or without a reference genome. *BMC Bioinformatics*, 12, 323. <https://doi.org/10.1186/1471-2105-12-323>
- Li, H., Handsaker, B., Wysoker, A., Fennell, T., Ruan, J., Homer, N., ... Durbin, R. (2009). The sequence Alignment/Map format and SAMtools. *Bioinformatics*, 25, 2078–2079. <https://doi.org/10.1093/bioinformatics/btp352>
- Lucas, J. S. (1973). Reproductive and larval biology of *Acanthaster planci* (L.) in Great Barrier Reef waters. *Micronesica*, 9, 197–203.
- Mah, S. A., Swanson, W. J., & Vacquier, V. D. (2005). Positive selection in the carbohydrate recognition domains of sea urchin sperm receptor for egg jelly (suREJ) proteins. *Molecular Biology and Evolution*, 22, 533–541. <https://doi.org/10.1093/molbev/msi037>
- Matsumoto, M., Solzin, J., Helbig, A., Hagen, V., Ueno, S.I., Kawase, O., ... Weyand, I. (2003). A sperm-activating peptide controls a cGMP-signaling pathway in starfish sperm. *Developmental Biology*, 260, 314–324. [https://doi.org/10.1016/S0012-1606\(03\)00236-7](https://doi.org/10.1016/S0012-1606(03)00236-7)
- Mengerink, K. J., Moy, G. W., & Vacquier, V. D. (2002). suREJ3, a poly-cystin-1 protein, is cleaved at the GPS domain and localizes to the acrosomal region of sea urchin sperm. *Journal of Biological Chemistry*, 277, 943–948. <https://doi.org/10.1074/jbc.M109673200>
- Mistry, N., Harrington, W., Lasda, E., & Wagner, E. J. (2003). Of urchins and men: evolution of an alternative splicing unit in fibroblast growth factor receptor genes. *RNA*, 9, 209–217. <https://doi.org/10.1261/rna.2470903.RNA>
- Modrek, B., & Lee, C. (2002). A genomic view of alternative splicing. *Nature Genetics*, 30, 13–19. <https://doi.org/10.1038/ng0102-13>
- Moore, H. B. (1932). A hermaphrodite sea urchin. *Nature*, 130, 59. <https://doi.org/10.1038/130059a0>

- Moore, H. B. (1935). A case of hermaphroditism and viviparity in *Echinocardium cordatum*. *Journal of the Marine Biological Association of the UK*, 20, 103–107.
- Moy, G. W., Mendoza, L. M., Schulz, J. R., Swanson, W. J., Glabe, C. G., & Vacquier, V. D. (1996). The sea urchin sperm receptor for egg jelly is a modular protein with extensive homology to the human polycystic kidney disease protein, PKD1. *Journal of Cell Biology*, 133, 809–817. <https://doi.org/10.1083/jcb.133.4.809>
- Nakachi, M., Hoshi, M., Matsumoto, M., & Moriyama, H. (2008). Conserved sequences of sperm-activating peptide and its receptor throughout evolution, despite speciation in the sea star *Asterias amurensis* and closely related species. *Zygote*, 16, 229–237. <https://doi.org/10.1017/S0967199408004759>
- Naruse, M., Ishikawa, R., Sakaya, H., Moriyama, H., Hoshi, M., & Matsumoto, M. (2011). Novel conserved structural domains of acrosome reaction-inducing substance are widespread in invertebrates. *Molecular Reproduction and Development*, 78, 57–66. <https://doi.org/10.1002/mrd.21274>
- Neill, A. T., Moy, G. W., & Vacquier, V. D. (2004). Polycystin-2 associates with the polycystin-1 homolog, suREJ3, and localizes to the acrosomal region of sea urchin spermatozoa. *Molecular Reproduction and Development*, 67, 472–477. <https://doi.org/10.1002/mrd.20033>
- Neill, A. T., & Vacquier, V. D. (2004). Ligands and receptors mediating signal transduction in sea urchin spermatozoa. *Reproduction*, 127, 141–149. <https://doi.org/10.1530/rep.1.00085>
- Nishigaki, T., Chiba, K., & Hoshi, M. (2000). A 130-kDa membrane protein of sperm flagella is the receptor for asterosaps, sperm-activating peptides of starfish *Asterias amurensis*. *Developmental Biology*, 219, 154–162. <https://doi.org/10.1006/dbio.1999.9598>
- Nishigaki, T., Chiba, K., Miki, W., & Hoshi, M. (1996). Structure and function of asterosaps, sperm-activating peptides from the jelly coat of starfish eggs. *Zygote*, 4, 237–245. <https://doi.org/10.1017/S0967199400003154>
- Palumbi, S. R. (2009). Speciation and the evolution of gamete recognition genes: Pattern and process. *Heredity*, 102, 66–76. <https://doi.org/10.1038/hdy.2008.104>
- Patiño, S., Aagaard, J. E., MacCoss, M. J., Swanson, W. J., & Hart, M. W. (2009). Bindin from a sea star. *Evolution and Development*, 11, 376–381. <https://doi.org/10.1111/j.1525-142X.2009.00344.x>
- Patiño, S., Keever, C. C., Sunday, J. M., Popovic, I., Byrne, M., & Hart, M. W. (2016). Sperm bindin divergence under sexual selection and concerted evolution in sea stars. *Molecular Biology and Evolution*, 33, 1988–2001. <https://doi.org/10.1093/molbev/msw081>

- Pennington, J. T. (1985). The ecology of fertilization of echinoid eggs: The consequences of sperm dilution, adult aggregation, and synchronous spawning. *Biological Bulletin*, 169, 417–430. <https://doi.org/10.2307/1541492>
- Pérez-Portela, R., Turon, X., & Riesgo, A. (2016). Characterization of the transcriptome and gene expression of four different tissues in the ecologically relevant sea urchin *Arbacia lixula* using RNA-seq. *Molecular Ecology Resources*, 16, 794–808. <https://doi.org/10.1111/1755-0998.12500>
- Petersen, T. N., Brunak, S., Von Heijne, G., & Nielsen, H. (2011). SignalP 4.0: Discriminating signal peptides from transmembrane regions. *Nature Methods*, 8, 785–786. <https://doi.org/10.1038/nmeth.1701>
- Podolsky, R. D., & Strathmann, R. R. (1996). Evolution of egg size in free spawners: Consequences of the fertilization-fecundity trade-off. *American Naturalist*, 148, 160–173. <https://doi.org/10.1086/285916>
- Popovic, I., Marko, P. B., Wares, J. P., & Hart, M. W. (2014). Selection and demographic history shape the molecular evolution of the gamete compatibility protein bindin in *Pisaster* sea stars. *Ecology and Evolution*, 4, 1567–1588. <https://doi.org/10.1002/ece3.1042>
- Pratchett, M. S., & Caballes, C. F. (2014). Limits to understanding and managing outbreaks of crown-of-thorns starfish (*Acanthaster* spp.). *Oceanography and Marine Biology Annual Review*, 52, 133–200. <https://doi.org/10.1201/b17143-4>
- Pujolar, J. M., & Pogson, G. H. (2011). Positive Darwinian selection in gamete-recognition proteins of *Strongylocentrotus* sea urchins. *Molecular Ecology*, 20, 4968–4982. <https://doi.org/10.1111/j.1365-294X.2011.05336.x>
- Puritz, J. B., Keever, C. C., Addison, J. A., Barbosa, S. S., Byrne, M., Hart, M. W., ... Toonen, R. J. (2017). Life history predicts past and present population connectivity in two sympatric sea stars. *Ecology and Evolution*, 7, 3916–3930. <https://doi.org/10.1002/ece3.2938>
- Ratnasingham, S., & Hebert, P. D. N. (2007). BOLD: The Barcode of Life Data System ([www.barcodinglife.org](http://www.barcodinglife.org)). *Molecular Ecology Notes*, 7, 355–364. <https://doi.org/10.1111/j.1471-8286.2006.01678.x>
- Revelli, A., Ghigo, D., Moffa, F., Massobrio, M., & Tur-Kaspa, I. (2002). Guanylate cyclase activity and sperm function. *Endocrine Reviews*, 23(4), 484–494.
- Robinson, J. T., Thorvaldsdóttir, H., Winckler, W., Guttman, M., Lander, E. S., Getz, G., & Mesirov, J. P. (2011). Integrative genomics viewer. *Nature Biotechnology*, 29, 24–26. <https://doi.org/10.1038/nbt.1754>. Integrative
- Robinson, M. D., McCarthy, D. J., & Smyth, G. K. (2009). edgeR: A Bioconductor package for differential expression analysis of digital gene expression data. *Bioinformatics*, 26, 139–140. <https://doi.org/10.1093/bioinformatics/btp616>

- Rogers, J. G. D., Pláganyi, É. E., & Babcock, R. C. (2017). Aggregation, Allee effects and critical thresholds for the management of the crown-of-thorns starfish *Acanthaster planci*. *Marine Ecology Progress Series*, 578, 99–114. <https://doi.org/10.3354/meps12252>
- Schultz, J., Milpetz, F., Bork, P., & Ponting, C. P. (1998). SMART, a simple modular architecture research tool: Identification of signaling domains. *Proceedings of the National Academy of Sciences USA*, 95, 5857– 5864. <https://doi.org/10.1073/pnas.95.11.5857>
- Stewart, M. J., Stewart, P., & Rivera-Posada, J. (2015). De novo assembly of the transcriptome of *Acanthaster planci* testes. *Molecular Ecology Resources*, 15, 953–966. <https://doi.org/10.1111/1755-0998.12360>
- Sunday, J., Raeburn, L., Stewart, H., & Hart, M. W. (2009). Allelic inheritance in naturally occurring parthenogenetic offspring of the gonochoric sea star *Patiria miniata*. *Invertebrate Biology*, 128, 276–282. <https://doi.org/10.1111/j.1744-7410.2008.00165.x>
- Swanson, W. J., & Vacquier, V. D. (2002). The rapid evolution of reproductive proteins. *Nature Reviews Genetics*, 3, 137–144. <https://doi.org/10.1038/nrg733>
- Tatusov, R. L., Galperin, M. Y., Natale, D. A., & Koonin, E. V. (2000). The COG database: A tool for genome-scale analysis of protein functions and evolution. *Nucleic Acids Research*, 28, 33–36. <https://doi.org/10.1093/nar/28.1.33>
- Timmers, M. A., Andrews, K. R., Bird, C. E., deMaintenton, M. J., Brainard, R. E., & Toonen, R. J. (2011). Widespread dispersal of the crown-of-thorns sea star, *Acanthaster planci*, across the Hawaiian Archipelago and Johnston Atoll. *Journal of Marine Biology*, 2011, 1–10. <https://doi.org/10.1155/2011/934269>
- Timmers, M. A., Bird, C. E., Skillings, D. J., Smouse, P. E., & Toonen, R. J. (2012). There's no place like home: crown-of-thorns outbreaks in the central Pacific are regionally derived and independent events. *PLoS ONE*, 7, e31159. <https://doi.org/10.1371/journal.pone.0031159>
- Ulrich, A. S., Otter, M., Glabe, C. G., & Hoekstra, D. (1998). Membrane fusion is induced by a distinct peptide sequence of the sea urchin fertilization protein bindin. *Journal of Biological Chemistry*, 273, 16748– 16755. <https://doi.org/10.1074/jbc.273.27.16748>
- Uthicke, S., Schaffelke, B., & Byrne, M. (2009). A boom–bust phylum? Ecological and evolutionary consequences of density variations in echinoderms. *Ecological Monographs*, 79, 3–24. <https://doi.org/10.1890/07-2136.1>
- Uthicke, S., Liddy, M., Patel, F., Logan, M., Johansson, C., & Lamare, M. (2018). Effects of larvae density and food concentration on Crown-of-Thorns seastar (*Acanthaster cf. solaris*) development in an automated flow-through system. *Scientific Reports*, 8, 642. <https://doi.org/10.1038/s41598-017-19132-w>



- Vacquier, V. D., & Moy, G. W. (1977). Isolation of bindin: The protein responsible for adhesion of sperm to sea urchin eggs. *Proceedings of the National Academy of Sciences USA*, *74*, 2456–2460. <https://doi.org/10.1073/pnas.74.6.2456>
- Vacquier, V. D., & Moy, G. W. (1997). The fucose sulfate polymer of egg jelly binds to sperm REJ and is the inducer of the sea urchin sperm acrosome reaction. *Developmental Biology*, *192*, 125–135. <https://doi.org/10.1006/dbio.1997.8729>
- Vacquier, V. D. (1998). Evolution of gamete-recognition proteins. *Science*, *281*, 1995–1998. <https://doi.org/10.1126/science.281.5385.1995>
- Vacquier, V.D. (2012). The quest for the sea urchin egg receptor for sperm. *Biochemical and Biophysical Research Communications*, *425*, 583–587. <https://doi.org/10.1016/j.bbrc.2012.07.132>
- Weber, A. A. T., Abi-Rached, L., Galtier, N., Bernard, A., Montoya- Burgos, J. I., & Chenuil, A. (2017). Positive selection on sperm ion channels in a brooding brittle star: Consequence of life-history traits evolution. *Molecular Ecology*, *27*, 3744–3759. <https://doi.org/10.1111/mec.14024>
- Wilburn, D. B., & Swanson, W. J. (2016). From molecules to mating: Rapid evolution and biochemical studies of reproductive proteins. *Journal of Proteomics*, *135*, 12–25. <https://doi.org/10.1016/j.jprot.2015.06.007>
- Wu, T. D., & Watanabe, C. K. (2005). GMAP: A genomic mapping and alignment program for mRNA and EST sequences. *Bioinformatics*, *21*, 1859–1875. <https://doi.org/10.1093/bioinformatics/bti310>
- Wu, T. D., & Nacu, S. (2010). Fast and SNP-tolerant detection of complex variants and splicing in short reads. *Bioinformatics*, *26*, 873–881. <https://doi.org/10.1093/bioinformatics/btq057>
- Yamaguchi, M., & Lucas, J. S. (1984). Natural parthenogenesis, larval and juvenile development, and geographical distribution of the coral reef asteroid *Ophidiaster granifer*. *Marine Biology*, *83*, 33–42. <https://doi.org/10.1007/BF00393083>
- Yamazato, K., & Kiyan, T. (1973). Reproduction of *Acanthaster planci* in Okinawa. *Micronesica*, *9*, 185–195.
- Yang, A., Zhou, Z., Pan, Y., Jiang, J., Dong, Y., Guan, X., ... Chen, Z. (2016). RNA sequencing analysis to capture the transcriptome landscape during skin ulceration syndrome progression in sea cucumber *Apostichopus japonicus*. *BMC Genomics*, *17*, 1–16. <https://doi.org/10.1186/s12864-016-2810-3>
- Yasuda, N., Hamaguchi, M., Sasaki, M., Nagai, S., Saba, M., & Nadaoka, K. (2006). Complete mitochondrial genome sequence for Crown-of-thorns starfish *Acanthaster planci* and *Acanthaster brevispinus*. *BMC Genomics*, *7*, 17. <https://doi.org/10.1186/1471-2164-7-17>

## Chapter 3.

# Selection on genes associated with the evolution of divergent life histories: Gamete recognition or something else?

### Abstract

Gamete compatibility, and fertilization success, is mediated by gamete-recognition genes (GRGs) that are expected to show genetic evidence of a response to sexual selection associated with mating system traits. To assess these expectations, I compared patterns of episodic diversifying selection among genes expressed in the gonads of *Cryptasterina pentagona* and *C. hystera* (found in the upper intertidal of the coast of Queensland and atolls of the Great Barrier Reef), which recently speciated (<10,000 years ago) and have evolved different life history traits including mating systems (gonochoric or hermaphroditic), modes of fertilization, and larval dispersal. I found some evidence for positive selection on a GRG in the outcrossing *C. pentagona*, and I found evidence of loss of gene function in a GRG of the self-fertilizing *C. hystera*. The modification or loss of gene functionality may be evidence of relaxed selection on some aspects of gamete interaction in *C. hystera*. In addition to GRGs, I also found genes under selection linked to abiotic stress, chromosomal regulation, polyspermy, and egg laying. I interpret those results as possible evidence that *Cryptasterina* spp. may have been adapting in divergent ways to oxidative stress or other factors associated with reproduction in the physiologically challenging environment of the high intertidal.

### KEYWORDS

*Cryptasterina hystera*, *Cryptasterina pentagona*, RNA-seq, selection, brooding

### 3.1. Introduction

Evolution of mating systems and other life history traits can impact the strength of sexual selection and the way in which reproductive genes diverge (Levitan, 2008; Patiño et al., 2016). Understanding these differences can help us better understand the evolutionary mechanisms leading to reproductive isolation and speciation. One response to strong sexual selection, driven by male competition and male-female conflicts, is the accumulation of amino acid differences in genes regulating sperm-egg interactions under positive selection (Frank, 2000; Hart, 2013). Over time, the accumulation of genetic differences in gamete-recognition genes is expected to lead to reproductive isolation (Gavrilets & Hayashi, 2005; Palumbi, 1999). Particularly good evidence for this effect comes from comparisons between species that have evolved different modes of reproduction, such as self-fertilization instead of outcrossing, in which the strength of sexual selection is expected to differ due to the resolution of male competition or male-female conflicts (Charlesworth, 2006; Patiño et al., 2016).

In mating systems in which sperm competition and sexual conflicts of interest are strong, sexual selection is expected to favor the evolution of novel male and female gamete traits that confer advantages on males (in competition with sperm of other males for fertilization) and on females (in defense against fatal polyspermy of eggs). Because these sexual selection processes act on males and females within populations, the response to selection (coevolved combinations of sperm- and egg-expressed gamete-recognition genes) may differ between populations. As a result, reproductive isolation between populations can evolve as a secondary outcome of sexual selection within each population (Levitan, 2006; Palumbi, 1999). Parts of this model of speciation by sexual selection can be tested by comparing patterns of molecular evolution among species or lineages with different mating systems (Weber et al., 2017). Species with mating system traits in which sexual selection is expected to be less intense (sperm competition is reduced, or sexual conflicts between the sexes are resolved due to shared interest; Palopoli et al., 2015, Patiño et al., 2016) should show a weaker response to selection on gamete-recognition genes (GRGs) involved in sperm-egg interactions in comparison to other species or lineages with mating system traits that are associated with intense sexual selection (strong sperm competition, unresolved sexual conflicts of interest over fertilization rates) (Palumbi, 1999; Patiño et al., 2016). If the effects of mating system

evolution are specific to gamete-recognition (and sexual selection), then the evidence for a response to selection on other types of genes not involved in sperm-egg interactions should be similar between species or lineages with different mating systems. Such effects should be clearest in comparisons between closely related lineages with few other phenotypic or ecological differences other than mating system traits.

Here I analyze evidence of selection acting on genes that mediate sperm–egg interactions in closely-related sister species of sea stars from Australia. *Cryptasterina hystera* recently diverged (<10,000 years ago) from *C. pentagona* through disruptive selection in peripatry (Puritz et al., 2012). *Cryptasterina hystera* rapidly evolved to be hermaphroditic, with internal self-fertilization, brooded development of offspring, and live birth of juveniles (Puritz et al., 2012), whereas *Cryptasterina pentagona* is gonochoric, with broadcast spawning, outcrossing, and planktonic dispersal of larvae (similar to most other asterinid sea stars). A recent sea star study that focused on one gamete-recognition gene (encoding the sperm acrosomal protein bindin) showed greater evidence of a response to selection (positive selection leading to high rates of amino acid change) in two genera of sea stars in which all species are gonochoric outcrossers in comparison to two genera (including *Cryptasterina*) with species capable of selfing (Patiño et al., 2016). This result indicates that selection may act differently on gamete-recognition genes of species that have mating systems with reduced sexual selection.

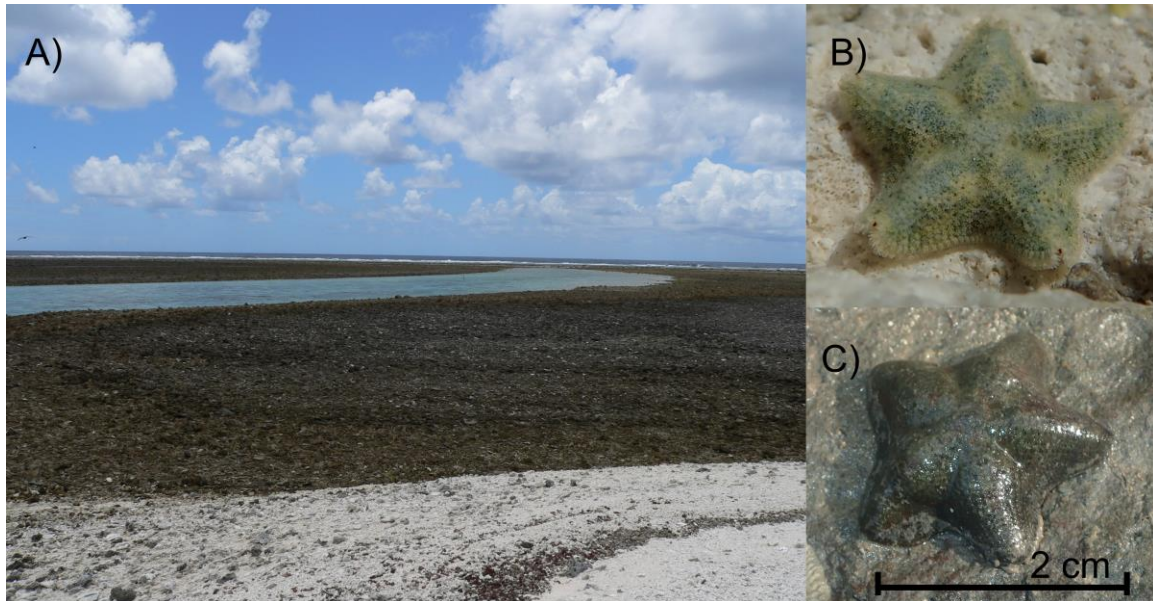
Gamete compatibility and specificity of fertilization in sea stars and other echinoderms are mediated by a suite of GRGs that encode proteins involved in a series of gamete interactions that include sperm activation and chemotaxis (mediated by the egg pheromone asterosap, a guanylate cyclase receptor in sperm), the acrosome reaction (ARIS proteins in the egg coat, and REJ proteins in sperm), sperm–egg binding mediated by bindin and its interactions with egg bindin receptors, and egg activation including the fast and slow blocks to polyspermy (Hirohashi et al., 2008). Although some of these key steps in fertilization shared across metazoans were discovered in echinoderms, not all of the signaling molecules involved in these key steps have been identified in echinoderms, and much of our knowledge of fertilization biology in echinoderms is restricted to a few well-studied species (Wozniak & Carlson, 2020). Consequently, studies of the molecular evolution of GRGs among echinoderm species have developed slowly by extending comparative studies from a few well-studied taxa to their close relatives. Those comparative studies, using population genetic and

phylogenetic methods (Harper & Hart, 2005; Hart et al., 2014; Patiño et al., 2016; Sunday & Hart, 2013; Zigler et al., 2005), suggest that changes to these signaling pathways can lead to the evolution of prezygotic reproductive isolation (Palumbi, 1999; Zigler et al., 2005).

Here I extend the comparison of GRGs from a single gene or set of coevolving genes to analysis of evidence for selection on any of the GRGs involved in multiple phases of the fertilization process in *Cryptasterina* species. I looked for evidence of a response to selection on GRGs and on other genes expressed in gonads and gametes, and use those results to explore other possible sources of selection on traits that may have been associated with the evolution of reproductive isolation between *Cryptasterina* species with different mating systems.

I found surprisingly little evidence for GRGs as an especially important target of selection in divergence between *Cryptasterina* species, so I explored other evidence for selection acting on other classes of genes also expressed in gametes and gonads. One alternative hypothesis to divergence of the *Cryptasterina* species by GRG evolution focuses on genes that might mediate interactions with the intertidal environment. Although the two species have few morphological differences, they live in different habitats: *Cryptasterina pentagona* is found in high-intertidal cobble habitats along the coast of Queensland; *Cryptasterina hystera* is found in high-intertidal cobble or coral rubble habitats of southernmost Queensland and some atolls of the Great Barrier Reef (Byrne & Walker, 2007) (Figure 3-1). *Cryptasterina hystera* likely diverged from *C. pentagona* after a range expansion event that left the ancestors of *C. hystera* geographically isolated in a new environment (Puritz et al., 2012). Life under cobble in the high intertidal zone may provide a suitable habitat in the form of protection from UV irradiation and sediment, but may also be associated with abiotic stressors such as hypoxia, dehydration, high temperatures, and salinity changes (Giraud-Billoud et al., 2019). I found some intriguing evidence for these other environmental interactions (rather than gamete interactions) as possible sources of selection acting on genes expressed in gonads that might be associated with divergence between *Cryptasterina* species, and discuss the possible ecological significance of those discoveries.

**Figure 3.1** *Cryptasterina* habitat including (A) a coral rubble bank on One Tree Island, Great Barrier Reef, Australia, (B) *Cryptasterina hystera* on the underside of coral rubble, and (C) *Cryptasterina pentagona* on the underside of rock cobble



## 3.2. Methods

### 3.2.1. Sample collection and RNA-seq library construction

Individuals of *Cryptasterina pentagona* were collected from an intertidal locality in northeastern Australia at Kissing Point (19°13'S, 146°48'E) on the coast of Queensland, and individuals of *C. hystera* from backreef habitats on One Tree Island (23°30'S, 152°05'E) on the Great Barrier Reef. Gonads from nine individuals (two male *C. pentagona*, three female *C. pentagona*, four *C. hystera*) were dissected in the laboratory, fixed in RNAlater, and shipped to ARQ Genetics (Bastrop, Texas, USA) for RNA extraction. Total RNA was then sent to the British Columbia Cancer Agency Genome Sciences Centre (Vancouver, British Columbia, Canada) for stranded RNA-seq library construction and 75-base paired-end sequencing on an Illumina HiSeq instrument.

### 3.2.2. Transcriptome assembly

The raw paired-end libraries were first filtered with Trimmomatic v. 0.32 (Bolger et al., 2014) using the default settings of Trinity v. 2.6.5 (Grabherr et al., 2011) to

remove low-quality bases and sequences. The overall quality of the reads was assessed with the default settings of FastQC tool v. 0.11.3

(<http://www.bioinformatics.babraham.ac.uk/projects/fastqc/>). There is no genome available for *Cryptasterina* spp., so a de novo reference transcriptome was built with the cleaned, pooled, and normalized reads from all RNA-seq libraries using the default parameters in Trinity v. 2.6.5 (Grabherr et al., 2011). In addition to the reference transcriptome, individual transcriptomes were assembled with Trinity for each of the nine libraries following the same steps.

### 3.2.3. Quality assessment and functional annotation

The quality of the de novo reference transcriptome was assessed by counting the number of transcripts with a reference match and by estimating the percent coverage of transcripts to matched reference sequences. Two comparisons were done using the *Acanthaster planci* reference transcriptome from NCBI and the UniProt reference database (Apweiler et al., 2012). Each comparison was done with blastx using a minimum expectation score of  $e = 1 \times 10^{-20}$  to capture the hits with the highest similarities. The percent coverage of the best hits was calculated using the perl program `analyze_blastPlus_topHit_coverage.pl` from the Trinity v.2.6.5 toolkit (Grabherr et al., 2011). Contig length and characteristics of the reference transcriptome were calculated using the perl program `TrinityStats.pl` from the Trinity v.2.6.5 toolkit (Grabherr et al., 2011). Functional annotation of the reference transcriptome followed the Trinotate v.3.0 annotation steps (<https://trinotate.github.io/>; Haas et al., 2013).

#### Annotation of gamete-recognition genes

In addition to these functional annotations, I identified orthologs of specific GRGs by searching the reference transcripts with BLAST+ (Altschul et al., 1990) against a custom database (see Appendix L for the reference sequences of gamete-recognition genes) populated with echinoderm GRGs using a cutoff value for expectation scores of  $e = 1 \times 10^{-5}$  or lower. The protein domains of the hits were then predicted with SMART (Schultz et al., 1998).

### 3.2.4. Differential expression analyses

To confirm the biological groups and perform a differential expression analysis (a step necessary to confirm that the tissues come from individuals in a similar biological state), I first quantified the transcript abundance. The Trinity v. 2.6.5 (Grabherr et al., 2011) perl program `align_and_estimate_abundance.pl` was used to perform an alignment-based quantification with the RSEM abundance estimation method, and a matrix count was built with the perl program `abundance_estimates_to_matrix.pl`. The results were then used to identify biological groups with the perl program PtR from Trinity that generates expression matrix comparisons and a principal components analysis (PCA). The identified biological groups were then compared to each other to find differentially expressed genes with the perl program `run_DE_analysis.pl` and `analyze_diff_expr.pl` in Trinity using the edgeR method and a false-discovery rate (FDR) of eight-fold or greater with a p-value less than 0.01. The differentially expressed (DE) genes were further divided into gene clusters using the perl program `define_clusters_by_cutting_tree.pl` in Trinity.

### 3.2.5. Orthologous gene identification and alignment

I first compiled a set of aligned orthologous genes each consisting of the two gene copies for a single gene from each of the nine *Cryptasterina* spp. individuals. The program OrthoFinder (Emms & Kelly, 2015) with the option for multiple sequence alignment was used to find orthogroups from each individual in two combinations: *C. hystera* individuals plus *C. pentagona* females (called the female gene set); and *C. hystera* individuals plus *C. pentagona* males (male gene set). Orthology analysis is sensitive to the presence of unresolved isoforms, and picking the incorrect isoform (perhaps because the correct isoform was not present in an individual or transcriptome) can result in inaccuracies in the selection analysis. For this reason, I modified the pairwise analysis of OrthoFinder to retain from the assemblies only candidate orthologs with a percentage length coverage of at least 90% and a minimum expectation score of  $e = 1 \times 10^{-60}$ .

Single-copy genes present in all nine *Cryptasterina* spp. individuals were used for downstream analysis. The final results were populated with phased data (for the two gene copies from each individual sea star) acquired by following the GATK best



practices workflow for RNAseq (<https://gatk.broadinstitute.org/hc/en-us>) and the default filtering settings of the perl program `run_variant_calling.py` from Trinity v. 2.6.5 (Grabherr et al., 2011). The phased haplotypes for each orthogroup (consisting of 8 *C. hystera* haplotypes and 6 *C. pentagona* haplotypes for each orthogroup in the female gene set, or 8 *C. hystera* haplotypes and 4 *C. pentagona* haplotypes in the male gene set) were then aligned with the perl program `translatorx_vLocal.pl` (Abascal et al., 2010) using the default MUSCLE option for protein alignments, and the stop codons were removed using the program PAL2NAL (Suyama et al., 2006). A neighbor-joining tree was then constructed with the program NINJA (Wheeler, 2009) for each alignment in preparation for positive selection analyses in HyPhy (Pond et al., 2005) that map sequence variation onto a gene tree.

### **3.2.6. Selection analyses**

The aligned orthogroups were then analyzed with three selection tests. I used MEME (Murrell et al. 2012) to identify signatures of positive selection events (episodic diversifying selection) in individual sites in each alignment. I used aBSREL (Smith et al. 2015) to identify signatures of positive selection in individual branches. These two branch-sites models provide complementary insight into selection acting on a coding sequence alignment, one focused on sites in the alignment and the other focused on lineages or branches in the gene tree. For the subset of genes with at least one lineage under episodic diversifying selection in aBSREL, I also characterized the alignment-wide evidence for selection on each gene using the McDonald–Kreitman (MK) test (Egea et al., 2008; McDonald & Kreitman, 1991).

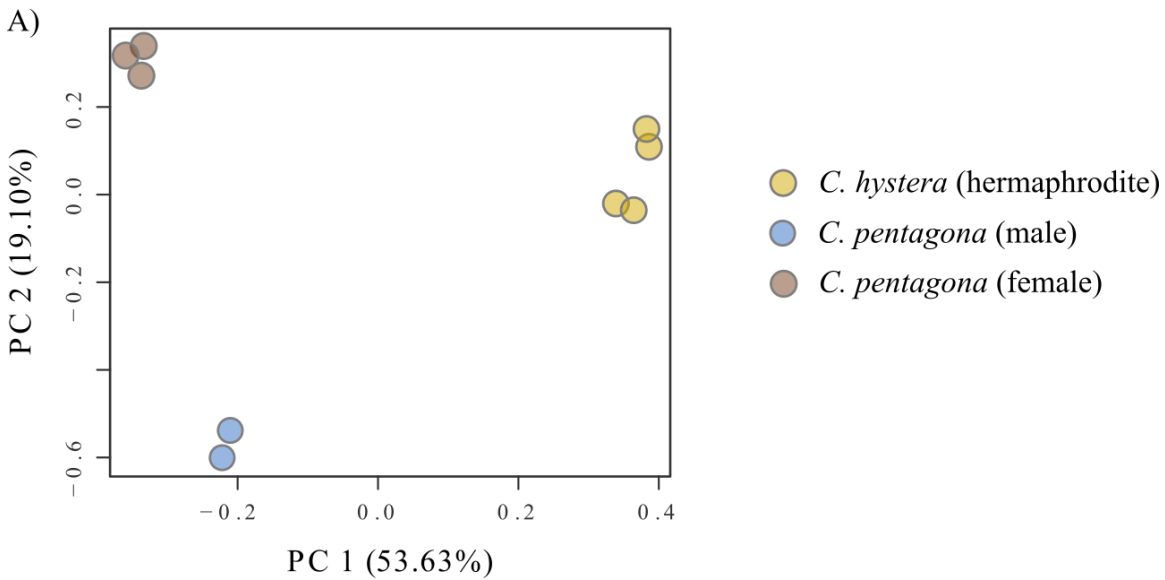
## **3.3. Results**

### **3.3.1. Transcriptome assemblies, annotations, and expression**

The reference assembly was composed of 525,005 transcripts (286,387 genes), of which 95,355 were annotated (see Appendix M for summary statistics for the reference transcriptomes and Appendix N for the transcript length of reference transcriptome and annotated transcripts). At 90%, 80%, and 70% query coverage, 11,446, 12,463, and 13,388 transcripts were found with the *A. planici* reference

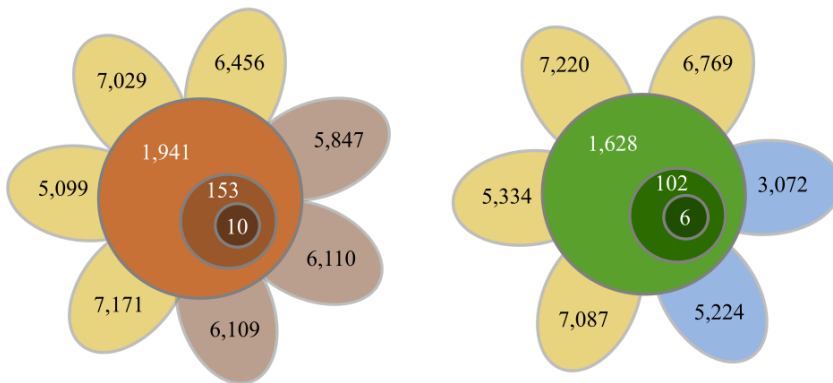
respectively (see Appendix O for counts of query coverage). Similarly, I found 5553, 6757, and 7834 transcripts with the UniProt reference respectively (see Appendix O for counts of query coverage). Annotated genes included novel signaling proteins for sea stars, such as *TIMP3*, *TRPC4-6*, *ANO4/TMEM16*, *CLCA1-2*, *KCNKA*, *HVCN1* in the oocyte and *TRPC2*, *OTOP*, *PIEZO1*, *NALCN*, *CatSper*, *CLCA*, *HCN1-4*, *KCNK2* or *TREK-1*, *KCMA1* in the sperm. A principal components analysis (PCA) confirmed that each individual clustered with their corresponding group, either the hermaphroditic *C. hystera*, or the gonochoric *C. pentagona* males or *C. pentagona* females (Figure 3-2). The expression of GRGs (see Appendix P with the list of the most expressed annotated DE transcripts) was consistent with that result and with the gonad types of each individual: hermaphroditic gonads of *C. hystera* showed expression of GRGs that are characteristic of both sperm and eggs; and the gonochoric testes or ovaries of *C. pentagona* showed expression of either sperm- or egg-specific GRGs but not both (see Guerra et al., 2020).

**Figure 3.2** (A) Principal component analysis (PCA) of all nine *Cryptasterina* individuals. The yellow circles represent the four *C. hystera* hermaphrodites, the blue circles represent the two *C. pentagona* males, and the brown circles represents the three *C. pentagona* females. (B) Venn diagrams of orthologous genes present in each individual or shared among individuals in each gene set. *Left* Female gene set showing the number of genes from four *C. hystera* individuals (yellow leaf), three *C. pentagona* females (brown leaf), shared orthologous genes (large orange circle), shared orthologous genes with evidence of episodic diversifying selection (medium orange circle), and genes under selection in the McDonald–Kreitman test (small dark orange circle). *Right* Male gene set showing the number of genes from four *C. hystera* (yellow leaf), two *C. pentagona* males (blue leaf), shared orthologous genes (large green circle), shared orthologous genes with evidence of episodic diversifying selection (medium green circle), and genes under selection in the McDonald–Kreitman test (small dark green circle)



B) Female gene set

Male gene set



Differential expression analysis of the gonadal tissues of the two *Cryptasterina* species showed a higher number of differentially expressed transcripts between *C. hystera* and either the male or female transcripts of *C. pentagona* than between male and female *C. pentagona* (see Appendix P-T for differential expression summary). A total of 41,581 transcripts were differentially expressed between *C. hystera* and female *C. pentagona*, and 28,337 transcripts were differentially expressed between *C. hystera* and male *C. pentagona*. A total of 2,286 transcripts were differentially expressed between the male and female tissues of *C. pentagona*. Additional information on the differential expression analysis and polymorphism is found in the supplement (see Appendix Q-U for differential expression analysis and SNPs of individuals summary).

OrthoFinder identified 1628 orthogroups that were expressed in both *C. pentagona* males and in all *C. hystera* (the male gene set), including some that were also expressed in females (Figure 3-2). Similarly, OrthoFinder found a set of 1941 female genes that were expressed in all *C. pentagona* females and in all *C. hystera* (the female gene set).

### 3.3.2. Episodic diversifying selection on gamete-recognition genes

I found two GRGs in the female gene set (the two *bindin* receptors *EBR1* and *OBi1*). Neither of these genes had branches in the gene trees with evidence of episodic diversifying selection in aBSREL, and neither showed evidence of alignment-wide selection in the MK test. The reference sequence for *EBR1* was 3310 amino acids in length (see Appendix V with alignments of GRGs and reference transcriptome deposited in the public Research Data Repository (RADAR)). *EBR1* from *C. hystera* had a stop codon at site 391 leading to a truncated predicted amino acid sequence; I found no *EBR1* nucleotide variation among *C. hystera* haplotypes from four individuals. By contrast, I found 9-88 pairwise nucleotide differences among *EBR1* gene copies from three individuals of *C. pentagona*.

The reference sequence for *OBi1* was 897 amino acids long. Similar to *EBR1*, I found no nucleotide variation in *C. hystera*, and 9-42 pairwise nucleotide differences among *C. pentagona* gene copies. MEME found one site under positive selection in *OBi1* (codon 430) within the predicted HSP70-like domain in Pfam and next to the beta barrel in the substrate-binding region (see Appendix W with schematic diagram of coding sequences of the gamete-recognition genes of *Cryptasterina*). I did not find any of the

*ARIS* genes (*ARIS1*, *ARIS2*, or *ARIS3*) with the targeted blast searches using previously annotated *ARIS* genes. This was surprising because the *ARIS* genes are highly expressed in eggs (Guerra et al., 2020; Hart & Foster, 2013). The absence of all three *ARIS* genes could indicate a pseudogenization event.

Four other GRGs were identified by BLAST comparison of the reference transcriptome to my custom database of echinoderm GRGs (*guanylate cyclase* or *GC*, which encodes the sperm receptor for the egg chemoattractant asterosap; *REJ1* and *REJ3*, which encode the sperm receptors for the ARIS complex in the egg jelly coat; and *bindin*), and all had close resemblance to gamete-recognition genes from *Acanthaster planci* or *Patiria miniata*. Only one had evidence of episodic diversification with aBSREL (*REJ1*), and none showed evidence of alignment-wide selection in the MK test.

*Guanylate cyclase* had a conserved domain architecture strongly similar to the *Acanthaster* gene, but 23% of the 1016 amino acids were different between the reference sequence of *Cryptasterina* and *Acanthaster*. Between *C. pentagona* and *C. hystera* there were three amino acid differences, but no sites were detected to be under selection. I found no nucleotide differences among *C. hystera* haplotypes, and much more variation (4-30 pairwise nucleotide differences) among *C. pentagona* haplotypes.

Only a partial *REJ1* coding sequence was recovered; the first 900 amino acids present in the *REJ1* gene of *Acanthaster* were missing (the targeted search was unsuccessful, so the absence of the complete gene is possibly due to an assembly error). The missing region encodes the FTP domains that, if similar to the CRD modules of sea urchin *REJ1*, could impact the interaction of *REJ1* with the egg jelly (Moy et al., 1996). The reference *REJ1* gene for *Cryptasterina* was 1875 amino acids long. There were no nucleotide differences among *C. hystera* gene copies, and only 2-9 nucleotides differed between pairs of gene copies in the alignment of *C. pentagona* haplotypes. I found evidence of episodic diversifying selection on an internal branch of the gene tree leading to two *C. pentagona* haplotypes in aBSREL. I was not able to confirm that the signature of selection found in *REJ1* is the result of adaptive evolution because the MK test failed on this gene due to the absence of intraspecific variation.

Unlike *REJ1*, I found a complete coding sequence for *REJ3* with a length of 2877 amino acids. The *REJ3* alignment in *C. pentagona* showed 5-69 pairwise nucleotide differences, and no variation in *C. hystera*. I found no branches under selection in *REJ3*

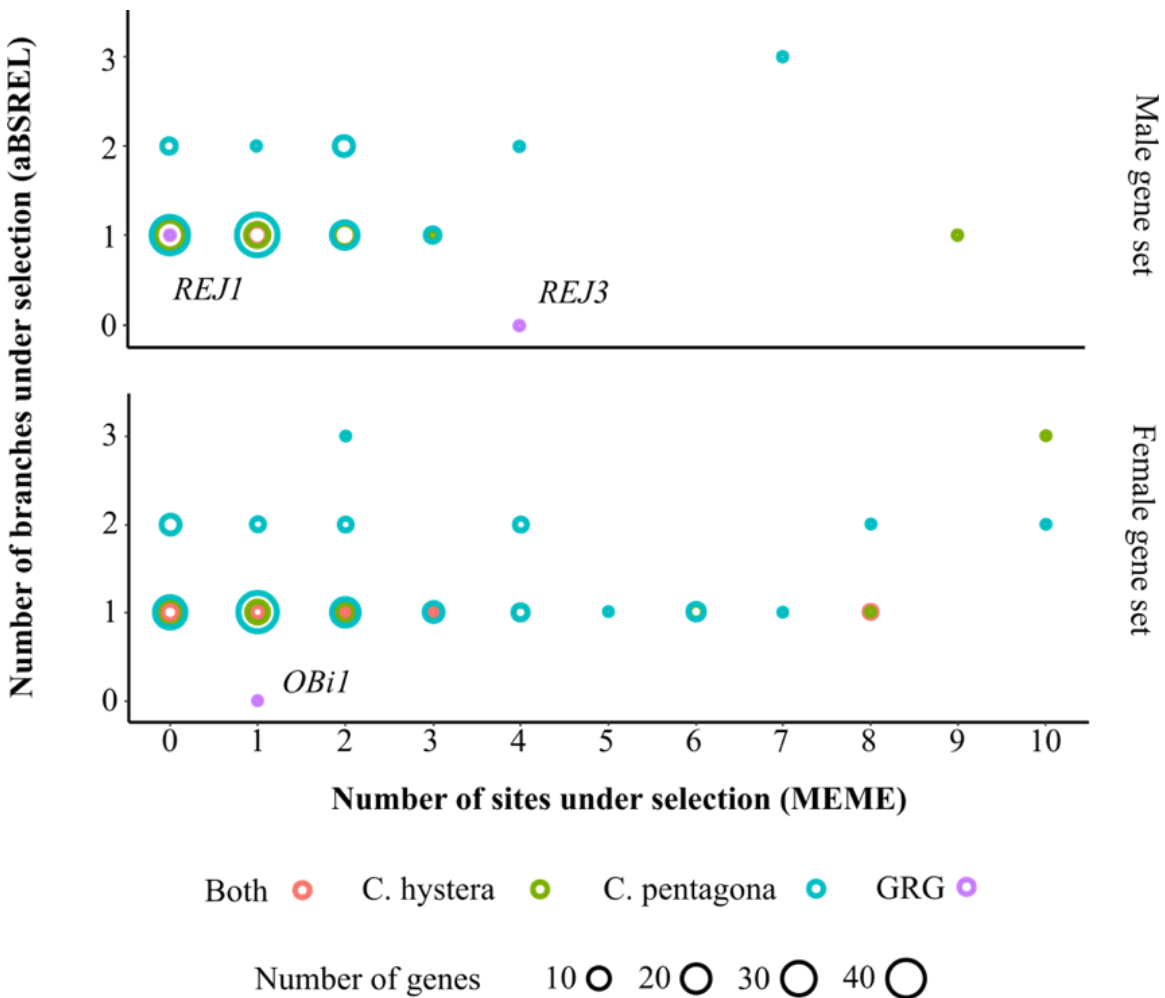
and no alignment-wide selection in the MK test, but I found four codons under selection near the transmembrane regions (codon positions 175, 224, 287, 2617).

The assembly of *bindin* resulted in multiple contigs containing segments of the gene (TRINITY\_DN51054\_c1\_g1\_i2, DN51054\_c1\_g1\_i3, DN64324\_c1\_g1\_i4). Because Trinity was not able to assemble all parts of the complex *bindin* coding sequence (Patiño et al., 2016) from every individual, I focused on the most complete section of *bindin* represented by the reference sequence TRINITY\_DN64324\_c1\_g1\_i4 (561 nucleotides). I found no evidence of episodic diversifying selection in *bindin*.

### **3.3.3. Episodic diversifying selection on other genes in the transcriptome**

A total of 153 orthogroups in the female gene set (7.9%) and 102 orthogroups in the male gene set (6.3%) had evidence of episodic diversifying selection (and only 14 in both groups with alignment-wide evidence of selection in the MK test described in the next section). Of these genes, MEME found evidence of at least one codon (and up to 10 codons) under episodic diversifying selection in 108 orthogroups in the female gene set and 64 in the male gene set. For both gene sets, all of the orthogroups with a significant result in the MEME analysis (one or more codons under positive selection) also gave a significant result in the aBSREL analysis (one or more branches under positive selection in the gene tree) (Figure 3-3). The majority of those genes with a positive result (124 of 153 in the female gene set, and 78 of 102 in the male gene set) had 1–3 branches leading to one or more *C. pentagona* haplotypes that were under selection in aBSREL, whereas fewer of the genes had a branch under selection leading to one or more *C. hystera* haplotypes (51 of 153 in the female comparison, and 35 of 102 in the male comparison).

**Figure 3.3** Number of genes in the male gene set and the female gene set with codons (MEME) and branches (aBSREL) under positive selection. The size of the circles represents the number of genes in the category; the color of each symbol shows which species (*C. hystera*, *C. pentagona*, or both) included lineages under selection in aBSREL analyses (e.g., one gene in the male set that had 9 sites under selection and one *C. hystera* lineage under selection; more than 40 genes in the female set that had 1 site under selection and 1 *C. pentagona* lineage under selection). Three violet symbols show the number of sites and lineages (*in C. pentagona*) under positive selection for three gamete-recognition genes (*OBi1*, *REJ1*, *REJ3*)



Comparison to the number of codons and branches under selection in gamete-recognition genes did not suggest that the evidence of positive selection is stronger among GRGs. Although I found a larger proportion of GRGs (3 of 6, or 50%) with some codons or branches under positive selection in comparison to other genes in the

transcriptome (<10%), I found few codons or branches under selection in GRGs in comparison to many other genes under positive selection in the transcriptome that had up to 10 codons under selection, and up to 3 branches under selection (Figure 3-3). Furthermore, the number of variable sites in GRG alignments was similar to the number in other genes in the transcriptome, which suggests that the smaller number of sites and lineages under selection in GRGs was not an artifact of fewer overall polymorphisms or substitutions.

In particular, I did not find any indication of more lineages under positive selection in GRGs from *C. pentagona* (with outcrossing and potential for sperm competition among males and sexual conflicts of interest between males and females) than in GRGs from *C. hystera* (in which sperm competition and sexual conflicts of interest have been resolved by the evolution of selfing). In non-GRGs from both the female and male gene sets, I found about twice as many lineages under selection in *C. pentagona* compared to *C. hystera*; by contrast, I found just one lineage under positive selection in a GRG (a single branch leading to two *REJ1* haplotypes from *C. pentagona*). That comparison argues against the expectation that stronger sexual selection on GRGs in *C. pentagona* or the resolution of sexual selection in *C. hystera* has had a particularly important role in the rapid evolution of reproductive isolation between those species.

Genes with evidence of episodic diversifying selection (153 orthogroups in the female gene set and 102 in the male gene set) had diverse gene ontology categories, but the most representative GO categories were shared between the two gene sets (see Appendix Y with gene ontology of genes with evidence of episodic diversifying selection in aBSREL). The list of genes with evidence of episodic diversifying selection included genes expected to function in the slow block to polyspermy, chromosome structure, the plasma membrane, and the mitochondrion (see Appendix Z for selection results). Notable genes (and functions) in this list include *Udx1* (hardening of the fertilization envelope), *TRPM3* (sperm activation), and F-box genes (E3 ubiquitin protein ligase function).

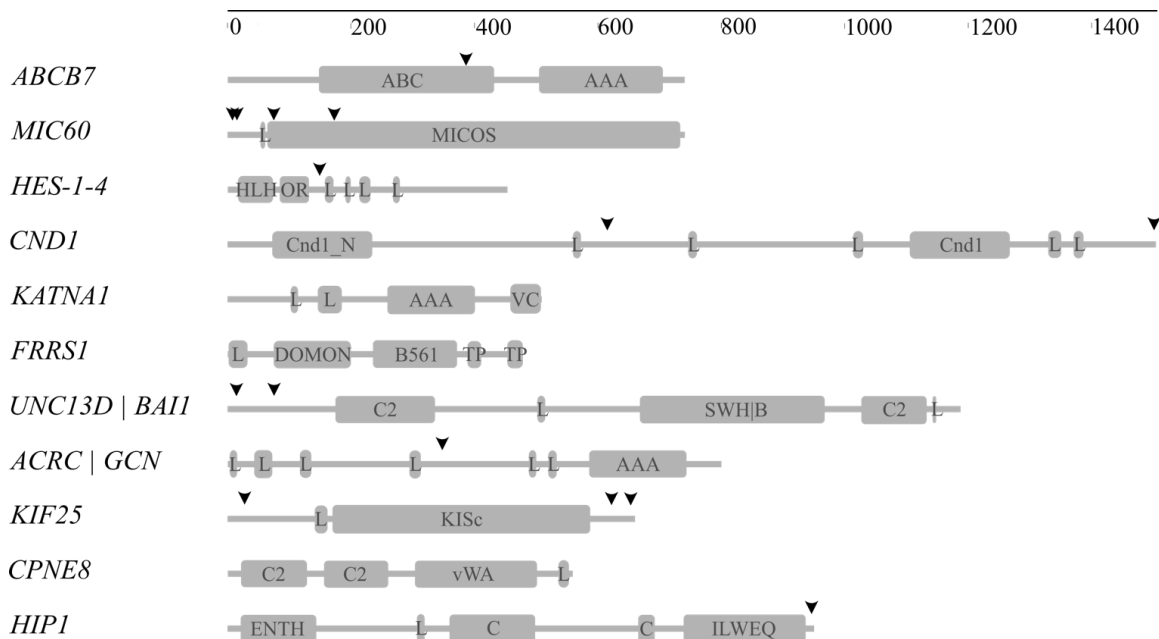
#### **3.3.4. Genes with alignment-wide evidence of selection**

Among the genes with evidence of episodic diversifying selection, I found 14 with alignment-wide evidence of selection in the MK test including both the male and female gene set (see Appendix AA for orthogroups with evidence of selection in both branch



site models (aBSREL) and in alignment-wide test (MK), Figure 3-4): *ABCB7*, *MIC60*, *HES4B*, *CND1*, *KATNA1*, *FRRS1*, *UNC13D*, and an unannotated gene (TRINITY\_DN63448\_c1\_g2\_i3) were under alignment-wide selection in the female gene set; *ACRC*, *KIF25*, and two unannotated genes (TRINITY\_DN56009\_c3\_g1\_i1 and TRINITY\_DN61873\_c2\_g1\_i8) in the male gene set; and *HIP1* and *CPNE8* under alignment-wide selection in both the male and the female gene sets.

**Figure 3.4 Schematic diagrams of coding sequence domains in 11 annotated genes under selection in both codon models and MK tests. Domain abbreviations: ABC membrane (ABC), ATPase domain (AAA), low complexity (L), MICOS complex, helix loop helix domain (HLH), orange domain (OR), condensin multi-subunit 1 (Cnd1\_N or Cnd1), Vps4 C terminal oligomerization domain (VC), domon domain (DOMON), cytochrome b-561 or ferric transmembrane domain (B561), transmembrane region (TP), protein kinase C conserved region 2 (C2), munc13 (SWH|B), kinesin motor and catalytic domain (KISc), epsin N-terminal homology domain (ENTH), coiled coil domain (C), von Willebrand factor type A domain (vWA), I/LWEQ domain (ILWEQ). Black triangles show locations of codons under selection**



In the female gene set, I found eight genes under selection. Two of these genes were involved in mitochondrial function (*ABCB7* and *MIC60*). *ATP-binding cassette subfamily B member 7 (ABCB7)* is an inner mitochondrial gene linked to iron transport in

humans (Kim et al., 2020). Similar to *ABCB7* of the sea urchin *Strongylocentrotus purpuratus* (Accession number SPU\_003241), the coding sequence of *ABCB7* (740 amino acids) included an adenosine triphosphate (ATP-)binding cassette (*ABC*) membrane domain and an ATPase domain (*AAA*). A terminal branch of *C. pentagona* was under selection and one codon of the *ABC* domain (366) was under selection. The *ABC* domain anchors the protein to the mitochondrial membrane in humans. *ABCB7* was expressed in all individuals of *Cryptasterina*, with a slightly lower expression in males of *C. pentagona*. The second mitochondrial gene under selection was the *MICOS complex subunit 60* (*MIC60*), also called the inner membrane mitochondrial protein (*IMMT*). *MIC60* helps maintain the structure of mitochondrial cristae (Glytsou et al., 2016). The *MIC60* coding sequence (742 amino acids) was composed of one large *MICOS* complex. *MIC60* was under selection in a *C. hystera* branch, and included four codons under selection. Isoforms of *MIC60* were expressed in all *Cryptasterina* individuals.

Two other genes in the female gene set under selection may be localized to or have a role with functions in the nucleus (*HES4B*, *CND1*). *Transcription factor 4 B-like* (*HES4B*) has a similar domain organization to *HES1*, so it is difficult to assess which transcription factor we analyzed. The *HES1/4*-like coding sequence in *Cryptasterina* (455 amino acids) included a helix loop domain (*HLH*) and an orange domain. Both of these domains are expected to interact with other proteins, but their functions are still not well understood (Sun et al., 2007). The *Cryptasterina* gene did not have any close matches with marine invertebrate or chordate genes outside the sea star *Acanthaster planci*. MEME found one codon under selection (149) near the orange domain and aBSREL detected two selection events in a terminal and an ancestral branch leading to *C. pentagona*. Isoforms of *HES1/4* were up-regulated in the female samples of *C. pentagona* relative to expression in the male samples of *C. pentagona*, and also expressed in *C. hystera*. *Nuclear condensin complex subunit 1* (*CND1*) has a role in chromosome regulation and segregation (Hirano, 2016). The *CND1* coding sequence (1504 amino acids) included two *Cnd1\_N* domains. I found one lineage in *C. pentagona* under selection in aBSREL, and two codon sites under selection (not in the *Cnd1\_N* domains) in MEME. Although the expression of this gene was low in both species, isoforms of this gene were expressed in all *Cryptasterina* individuals.

Four other genes under selection in the female gene set were involved in the cytoskeleton, plasma membrane, and lysosome/endosome functions. *Katanin p60 ATPase-containing subunit A1-like (KATNA1)* encodes an enzyme that severs microtubules (Roll-Mecak & McNally, 2010). The *Cryptasterina* coding sequence (510 amino acids) included an AAA domain and a Vps4\_C domain. *KATNA1* was under selection along an internal branch leading to *C. hystera*, and it was expressed in all *Cryptasterina* individuals. *Ferric chelate reductase 1-like (FRRS1 or SDR2)* is a neurological gene in humans linked to plasma membrane function and iron regulation (Waters et al., 2002). The *Cryptasterina* coding sequence (478 amino acids) included a DOMON and a B561 domain. The aBSREL analysis detected selection in an ancestral lineage of *C. pentagona*. *FRRS1* was expressed in *C. hystera* and the females of *C. pentagona*. The last two genes are not well characterized in echinoderms: one (TRINITY\_DN62906\_c0\_g3\_i4) is similar to the *brain-specific angiogenesis inhibitor 1-like (BAI1)* associated protein 3 gene and to *unc-13 homolog D*; the other (TRINITY\_DN63448\_c1\_g2\_i3) is an unknown gene. TRINITY\_DN62906\_c0\_g3\_i4 was under selection in an internal lineage of *C. pentagona* and had two codons under selection in the N terminus. The uncharacterized gene TRINITY\_DN63448\_c1\_g2\_i3 was under selection on an internal *C. pentagona* branch and in one codon.

In the male gene set, I found four genes under selection in MK tests (*ACRC*, *KIF25*, TRINITY\_DN56009\_c3\_g1\_i1, and TRINITY\_DN61873\_c2\_g1\_i8). *Acidic repeat-containing protein (GCNA/ACRC)* is expressed in the nucleus of germ cells of the testis in humans (Bhargava et al., 2020). The *ACRC* coding sequence (799 amino acids) included a single SprT domain and multiple low complexity regions. MEME found one codon (site 276) under selection. Isoforms of *ACRC* were expressed in all individuals of *Cryptasterina*. *Kinesin family member 25 (KIF25)* and other kinesin genes encode molecular motors that orchestrate the separation of chromosomes during replication (Decarreau et al., 2017). The *Cryptasterina* coding sequence (662 amino acids) included a large kinesin motor catalytic domain (KISc) and a short coiled-coil domain. MEME detected three sites under selection (codons 21, 628, and 647), and aBSREL detected evidence of episodic diversifying selection in an internal branch in *C. hystera*. This gene was up-regulated in the male and female individuals of *C. pentagona*.

The last two genes under selection in the male gene set did not have annotations. TRINITY\_DN56009\_c3\_g1\_i1 (M-OG0001402, 220 amino acids) encoded

a series of low-complexity regions. Evidence of episodic diversifying selection was found in a terminal branch of *C. pentagona*. Isoforms of this gene were present in all individuals of *C. pentagona*. The uncharacterized gene TRINITY\_DN61873\_c2\_g1\_8 (M-OG0000313, 711 amino acids) encoded a DDE transposase sub-family (DDE\_Tnp\_1\_7) domain. I found evidence of episodic diversifying selection in a terminal and internal *C. pentagona* branches, and two codons (401, 559) under selection near the DDE\_Tnp\_1\_7 domain. Isoforms of this gene were expressed in all *Cryptasterina* individuals.

I found two genes that were under selection in both male and female gene sets, and in both cases the aBSREL test indicated positive selection in one or more *C. hystera* lineages. Human *Copine 8 (CPNE8)* is a Ca<sup>2+</sup>-dependent phospholipid-binding protein (Maitra et al., 2003). The coding sequence of *CPNE8* in *Cryptasterina* (559 amino acids) was composed of two protein kinase C conserved regions (C2) and a von Willebrand factor type A domain (vWA). vWA domains in the extracellular region regulate adhesion events have also been identified in the vitellogenin protein (AFH56436.1) that is present in diverse metazoans (coral, nematodes, abalone, and chicken) and expressed in the gonads of both sexes (Prowse & Byrne, 2012). Evidence of episodic diversifying selection was found in an internal branch of *C. hystera* in both male and female gene sets. Isoforms of this gene were expressed in all the *Cryptasterina* individuals.

*Huntingtin interacting protein 1-like (HIP1)* in *C. elegans* and humans encodes an Epsin N-terminal homology (ENTH) domain, made of 122 codons, which occurs within a larger AP180 N-terminal homology (ANTH) domain, made of 269 codons (Parker, 2001). In the human gene these nested domains are followed by 2 predicted coiled coil domains, and an F-actin domain called the ILWEQ domain (the coiled coil domains are located in a different region of the *C. elegans* gene). MEME identified positive selection on codon 949 in the *Cryptasterina* alignments from both gene sets, and evidence of episodic diversifying selection was found in an internal *C. hystera* branch in both the female and male gene sets.

### 3.4. Discussion

The recent speciation and rapid life-history divergence between *Cryptasterina hystera* and *C. pentagona* was unlikely the result of strong selection acting on gamete-

recognition genes (GRGs) annotated in this study. I identified GRGs from three known steps in gamete interaction leading to fertilization, but did not find strong evidence for divergence of those GRGs under selection in comparison to other genes in the gonadal transcriptome. Instead, my results point toward selection on genes linked to interactions with the intertidal environment.

### **3.4.1. Gamete-recognition genes are not the targets of selection in *Cryptasterina* speciation**

I compared patterns of selection on GRGs to other genes in the same transcriptomes, but found no strong evidence for a greater response to selection among GRGs: the numbers of sites under selection (0–1) and lineages under selection (0–1) among GRGs were lower than the numbers of sites (up to 10) and lineages (up to 3) under selection among other orthogroups in the female and male gene sets. The most important result is that I did not find many *C. pentagona* lineages under positive selection in GRGs (just one, in *REJ1*), in spite of the expectation that *C. pentagona* (with broadcast spawning and outcrossing) should experience stronger sexual selection associated with sperm competition among males and sexual conflicts of interest between males and females over fertilization rates (and the risk of polyspermy) in comparison to *C. hystera*. These findings argue against gamete-recognition genes as important targets of selection in the divergence of *C. hystera* from *C. pentagona*. However, not all GRGs were assessed and some of the identified GRGs showed signs of pseudogenization. It remains possible that new GRGs not previously described and not analyzed in this study, including GRGs created through the process of neofunctionalization, may have participated in that speciation event. In particular, the binding region of *REJ1* is expected to interact with the *ARIS* protein complex in the egg coat, but *ARIS1*, *ARIS2*, and *ARIS3* (which are abundantly expressed in other sea star oocytes; Guerra et al., 2020; Hart & Foster, 2013) are not expressed in *Cryptasterina* ovaries. This gap in evidence suggests that *ARIS* genes in *Cryptasterina* have diverged so strongly from other sea stars that they cannot be recognized by sequence-similarity searches using BLAST, or that the function of the *ARIS* proteins in the egg coat has been replaced by neofunctionalization of other genes. That gap also prevented me from finding possible evidence of positive selection acting on the genes that encode *ARIS*-like molecules in the egg coat.

I found other evidence of possible pseudogenization and potential loss of gene function in the acrosome initiation and in gamete fusion. *REJ1* was missing the binding site for the *ARIS* complex in both species, an evolutionary feature that may indicate a coevolutionary change between the receptor (missing its ligand-binding site) and its ligands (not expressed in the egg coat). *REJ1* was also under selection in *C. pentagona*. I found other evidence of selection acting on parts of the *REJ3* coding sequence that are not predicted to interact with the egg coat. This could indicate a change in the function of *REJ3* in the plasma membrane of the sperm. The function of *ARIS* genes in sea stars may be analogous to the family of *ZP* genes that encode the glycoproteins that make up the thick fibrous egg coat or zona pellucida in chordates. Diverse chordate *ZP* genes show signatures of neofunctionalization and pseudogenization that have resulted in the evolution of at least six subfamilies of *ZP* genes and extensive variation in *ZP* gene expression among species (Goudet et al., 2008). These parallel results suggest that neofunctionalization may be a common feature of the evolution of egg coat proteins. Finally, I found evidence of truncated coding sequence organization (and possible loss of gene function) in the egg binding receptor *EBR1*, but unlike *REJ1* these features were limited to *C. hystera*. Positive selection is not a general feature of the evolution of *bindin* in *Cryptasterina* (Patiño et al., 2016), so this change in *EBR1* could indicate a species-specific change in gamete binding in the self-fertilizing species. The truncation and possible loss of function of *EBR1* may be the result of a fixed deleterious mutation associated with the relaxation of selection for effective gamete binding after the evolution of internal self-fertilization (where selfing may not depend on efficient sperm–egg binding in the close confines of the hermaphroditic gonad). This change in the structure and possible function of *EBR1* in *C. hystera* may have affected the specificity of fertilization, as the gametes of the two species are compatible with each other and can generate viable F1 hybrids (M. Byrne, unpublished observations). It is notable that the apparent truncation of the 3' end of the *EBR1* coding sequence in *C. hystera* includes the C-terminal repetitive region of *EBR1* that has been shown to confer species specificity of sperm binding in sea urchins (Kamei & Glabe, 2003). Observational and experimental studies of spawning and fertilization in *Cryptasterina* would be helpful in understanding the functional significance of these unusual features of GRGs in *C. hystera*.

I found evidence of selection in *OBi1*, and this is the second case of positive selection on *OBi1* in sea stars (Hart et al., 2014; Sunday & Hart, 2013). Hart et al. (2014) found evidence of positive selection in *OBi1* from *Patiria miniata* at two codons in the

alpha helix of the substrate-binding region that is predicted to interact with *bindin*. Because the codon detected to be under selection in *Cryptasterina* falls outside the substrate-binding region, unlike the codons under selection in *P. miniata*, it is unlikely that this selection is the result of co-evolution between *bindin* and *OBI1* (see Appendix X schematics of *OBI1*).

I found no evidence in codon models for more sites or lineages under selection among GRGs compared to other expressed gonad genes in either *C. hystera* or *C. pentagona*. Similarly, among the genes for which I found a significant result in codon models, I found evidence of alignment-wide selection in MK tests only in other genes in the transcriptome (and not in GRGs). One unexpected pattern in those results for nonGRGs was a larger number of genes with evidence of positive selection along lineages leading to the gonochoric species *C. pentagona* in comparison to the hermaphroditic *C. hystera* in both the male gene set and the female gene set. This apparent difference in the response to selection between the two mating systems could be caused by the much smaller effective population size in *C. hystera* that has been ascribed to extensive self-fertilization (Puritz et al., 2012) and the expected reduced effectiveness of selection in small populations. That interpretation also supports the conclusion that the response to selection on GRGs was not obviously stronger in lineages leading to *C. pentagona*, because the difference in effective population size and the difference in mode of fertilization are both expected to contribute to stronger signals of positive selection in *C. pentagona* compared to *C. hystera*, which we did not observe.

### **3.4.2. Possible targets of selection in *Cryptasterina* speciation**

My codon model analyses identified a large suite of other male- and female-expressed genes under positive selection that have gene annotations linked to polyspermy, gamete physiology, chromosome regulation, oxidative stress, and egg laying. Although I did not develop or test predictions about these genes and their possible adaptive evolution in the divergence of *Cryptasterina* species (and some of them did not show evidence of alignment-wide selection in MK tests), I review some of them here as a contribution to possible development of hypotheses for future study and analysis.

## The slow block to polyspermy

In sea urchins, *Udx1* is involved in the formation of the fertilization envelope as part of the slow block to polyspermy (Wong et al., 2004). Specifically, *Udx1* synthesizes the hydrogen peroxide ( $H_2O_2$ ) which chemically hardens the fertilization envelope through the activation of ovoperoxidase (Wong et al., 2004). The role of *Udx1* expression (Hart & Foster, 2013) and hydrogen peroxide in sea star oocytes is unclear: sea stars do not have a hydrogen peroxide burst during the fertilization process as is observed in sea urchins (Schomer & Epel, 1998), and ovoperoxidase is present at low concentrations in *Cryptasterina* species and other sea stars (Oulhen et al., 2013). In frogs, hydrogen peroxide released from *Udx1* extends the calcium influx of the slow block to polyspermy and it activates the egg (Sato et al., 2001). The hydrogen peroxide produced by *Udx1* in sea stars may interact with ovoperoxidase at lower concentrations to induce the hardening of the fertilization envelope (see Appendix AB with schematics of potential role of *Udx1*), or may aid in the calcium influx extension and egg activation, or *Udx1* may have some other role in larval development (Miller & Heyland, 2013) that is associated with adaptation of a larval trait and with the difference between larval development in the plankton (in *C. pentagona*) or in the gonad of the parent (in *C. hystera*).

## Ion channels

Mammalian *TRPM3* encodes a calcium channel that mediates calcium influx after sperm activation by changes of hypo-osmolarity or by sphingosine. Other members of the TRPM family of cation channels include the thermosensitive channel TRPM8 expressed in the sperm of humans, which is thought to be involved in thermotaxis (Martínez-López et al., 2011). I did not find a TRPM8 ortholog in *Cryptasterina*. Similar to TRPM8, TRPM3 in *Cryptasterina* could play a role in sperm activation or modification of sperm swimming behavior. Sea star sperm are immotile in seminal plasma, but activate in sea water.

## Chromosomal regulation

I also detected selection on several genes (*KATNA1*, *KIF*, *ACRC*) with annotations involving chromosomal regulation and cell division. This class of genes is especially interesting in speciation studies because changes to chromosomal regulatory genes can result in genomic incompatibility between diverging populations due to compensatory evolution of chromosome-associated proteins (Beck & Llopart, 2015;



Peyregne et al., 2017). *Katanin catalytic subunit A1 (KATNA1)* was under positive selection in the female gene set. In microalgae, KATNA1 breaks down the cytoskeleton during desiccation events and is a key to the evolution of tolerance to low salinity (Liang et al., 2019). Small changes to katanins are thought to create postzygotic incompatibility between species due to changes to the meiotic spindle length (Kozak et al., 2014).

### **Adaptations to the high intertidal**

*Cryptasterina* spp. are expected to have evolved metabolic adaptations to oxidative stress and other features of the high intertidal (Christensen et al., 2011). In particular, the evolution of viviparity in *C. hystera* may have been facilitated by the evolution of physiological traits that permitted life in the high intertidal away from the typical aquatic environment for broadcast spawning and planktonic larval development that are characteristic of *C. pentagona* and most other sea stars. Several studies have documented adaptations of mitochondrial function in intertidal animals linked to oxidative stress (Sokolova, 2018). Similarly, the switch to internal brooding and viviparity is expected to come with physiological adaptations to reduce oxidative stress due to oxygen limitations on the development of brooded embryos (Strathmann et al., 1984). I found evidence of selection acting on several genes (*ABCB7*, *FRRS1*, *Mic60*) linked to the mitochondrion and its reactive oxygen species (ROS) in *Cryptasterina* (see Appendix AC with potential localization of expression of three genes under selection). *ABCB7* mitigates the ROS pathway by inducing the hypoxia-inducible factor 1 alpha in humans (Kim et al., 2020). *ABCB7*, also known as *Abtm-1*, encodes an ATP-binding transmembrane protein that regulates iron homeostasis of the mitochondria. The iron regulator *ferric chelate reductase 1 (FRRS1 or SDR2)* reduces  $Fe^{3+}$  to  $Fe^{2+}$  to promote iron uptake in plant tissues (Waters et al., 2002). *FRRS1*, similar to *ABCB7*, may be evolving to reduce oxidative stress in *Cryptasterina*. *Mic60* encodes a structural protein that, in combination with other mitochondrial proteins, maintains the width of cristae junctions (Glytsou et al., 2016). The cristae junctions are the regions where the mitochondrial respiration-component complexes are located. The adaptive evolution of *MIC60* may represent a response to selection for modified mitochondrial function in the intertidal that may have coincided with or facilitated the evolution of brooding in *C. hystera*.

## Egg retention and the evolution of live bearing

Huntingtin interacting protein 1 (HIP1) is generally associated with clathrin-mediated endocytosis (Gottfried et al., 2010), the process of moving proteins through the plasma membrane by invagination. However, RNAi inhibition of *HIP1* expression in *C. elegans* causes delayed egg laying and retention of embryos in the female reproductive tract; normal HIP1 expression in *C. elegans* is localized to muscle cells of the vulva or gonopore (Parker et al., 2007; Parker, 2001).

Evidence for selection on *HIP1* in *Cryptasterina* was stronger and more consistent across analyses than for most other genes in this study. I found positive selection in both MEME and aBSREL analyses of *HIP1* haplotypes expressed in males (1 codon under selection, 1 lineage under selection) and in both codon model analyses of *HIP1* expressed in females (1 codon, 1 lineage), and I detected alignment-wide evidence of selection on *HIP1* in both MK tests. Notably, in both aBSREL models (for male- expressed and for female-expressed haplotypes) I detected positive selection specifically on an internal lineage leading to two *C. hystera* haplotypes. In those two haplotypes the 3' end of the coding sequences encodes an amino acid motif (GWDEEDIPLQ) that is similar to the last ten codons of *HIP1* from other sea stars including *Acanthaster planci* (XM\_022253800, GWDEEDPAEGFLDLPIPQ) and *Asterias rubens* (XM\_033772280, GWDEEDPEGFYNEPITPQ); by contrast, the other 16 haplotypes expressed in other *C. hystera* and in both male and female *C. pentagona* ended in a highly derived amino acid motif (GWDEENIAHS) that was the source of the signal of positive selection in both MEME and aBSREL models and in MK tests.

These intriguing parallels between the function of HIP1 (in egg retention in *C. elegans*) and the adaptive evolution of *HIP1* (in *Cryptasterina*) suggest a role for that gene in the evolution of modified spawning behavior, internal fertilization, and live bearing. The observation that *HIP1* was expressed in both male and female *C. pentagona* argues for its possible role in spawning (or retention) of both eggs and sperm, and indicates that *HIP1* could be involved in the evolutionary switch from gonochoric broadcast spawning to retention of gametes, internal self-fertilization, and brooding of offspring. Those comparisons suggest that a taxonomically broad analysis of *HIP1* molecular evolution across echinoderm lineages with different mating systems and modes of reproduction could be especially useful and interesting.

In addition to *HIP1*, I also found a set of F-box genes with signatures of selection in aBSREL models; F-box genes have E3 ubiquitin protein ligase functions and have been linked to the independent evolution of hermaphroditism in several nematode lineages (Guo et al., 2009). I found numerous genes with E3 ubiquitin protein ligase functions in *Cryptasterina* that included *F-box 42* and *46*, *RFFL*, *RNF8*, *PPIL2*, *UHRF1*, *E3D*, *RNF8*, and *RNF13*. In nematodes, RNA interference experiments show that hermaphroditism can be induced by changes in the expression of as few as two genes, one of which regulates E3 ubiquitin protein ligase function (Baldi et al., 2009). These comparisons suggest that evolutionary changes in the mating system of *Cryptasterina* spp. could be linked to similar pathways involving F-box gene expression.

### 3.5. References

- Abascal, F., Zardoya, R., & Telford, M. J. (2010). TranslatorX: Multiple alignment of nucleotide sequences guided by amino acid translations. *Nucleic Acids Research*, *38*(suppl\_2), W7-13. <https://doi.org/10.1093/nar/gkq291>
- Altschul, S. F., Gish, W., Miller, W., Myers, E. W., & Lipman, D. J. (1990). Basic local alignment search tool. *Journal of Molecular Biology*, *215*(3), 403–410. [https://doi.org/10.1016/S0022-2836\(05\)80360-2](https://doi.org/10.1016/S0022-2836(05)80360-2)
- Apweiler, R., Martin, M. J., O'Donovan, C., Magrane, M., Alam-Faruque, Y., Antunes, R., Casanova, E. B., Bely, B., Bingley, M., Bower, L., Bursteinas, B., Chan, W. M., Chavali, G., Da Silva, A., Dimmer, E., Eberhardt, R., Fazzini, F., Fedotov, A., Garavelli, J., ... Zhang, J. (2012). UniProt Consortium. Reorganizing the protein space at the Universal Protein Resource (UniProt). *Nucleic Acids Research*, *40*(D1), D71-75. <https://doi.org/10.1093/nar/gkr981>
- Baldi, C., Cho, S., & Ellis, R. E. (2009). Mutations in two independent pathways are sufficient to create hermaphroditic nematodes. *Science*, *326*(5955), 1002–1005. <https://doi.org/10.1126/science.1176013>
- Beck, E. A., & Llopart, A. (2015). Widespread positive selection drives differentiation of centromeric proteins in the *Drosophila melanogaster* subgroup. *Scientific Reports*, *5*(July), 1–8. <https://doi.org/10.1038/srep17197>
- Bhargava, V., Goldstein, C. D., Russell, L., Xu, L., Ahmed, M., Li, W., Casey, A., Servage, K., Kollipara, R., Picciarelli, Z., Kittler, R., Yatsenko, A., Carmell, M., Orth, K., Amatruda, J. F., Yanowitz, J. L., & Buszczak, M. (2020). GCNA Preserves Genome Integrity and Fertility Across Species. *Developmental Cell*, *52*(1), 38-52.e10. <https://doi.org/10.1016/j.devcel.2019.11.007>
- Bolger, A. M., Lohse, M., & Usadel, B. (2014). Trimmomatic: A flexible trimmer for Illumina sequence data. *Bioinformatics*, *30*(15), 2114–2120. <https://doi.org/10.1093/bioinformatics/btu170>
- Byrne, M., & Walker, S. J. (2007). Distribution and reproduction of intertidal species of *Aquilonastra* and *Cryptasterina* (Asterinidae) from one tree reef, southern Great Barrier Reef. *Bulletin of Marine Science*, *81*(2), 209–218.
- Charlesworth, D. (2006). Evolution of Plant Breeding Systems. *Current Biology*, *16*(17), 726–735. <https://doi.org/10.1016/j.cub.2006.07.068>
- Christensen, A. B., Nguyen, H. D., & Byrne, M. (2011). Thermotolerance and the effects of hypercapnia on the metabolic rate of the ophiuroid *Ophionereis schayeri*: inferences for survivorship in a changing ocean. *Journal of Experimental Marine Biology and Ecology*, *403*(1–2), 31–38. <https://doi.org/10.1016/j.jembe.2011.04.002>

- Decarreau, J., Wagenbach, M., Lynch, E., Halpern, A. R., Vaughan, J. C., Kollman, J., & Wordeman, L. (2017). The tetrameric kinesin Kif25 suppresses pre-mitotic centrosome separation to establish proper spindle orientation. *Nature Cell Biology*, 19(4), 384–390. <https://doi.org/10.1038/ncb3486>
- Egea, R., Casillas, S., & Barbadilla, A. (2008). Standard and generalized McDonald–Kreitman test: a website to detect selection by comparing different classes of DNA sites. *Nucleic Acids Research*, 36(suppl\_2), W157–W162.
- Emms, D. M., & Kelly, S. (2015). OrthoFinder: solving fundamental biases in whole genome comparisons dramatically improves orthogroup inference accuracy. *Genome Biology*, 16(1), 157. <https://doi.org/10.1186/s13059-015-0721-2>
- Frank, S. A. (2000). Sperm competition and female avoidance of polyspermy mediated by sperm-egg biochemistry. *Evolutionary Ecology Research*, 2(5), 613–625.
- Gavrilets, S., & Hayashi, T. I. (2005). Speciation and sexual conflict. *Evolutionary Ecology*, 19(2), 167–198. <https://doi.org/10.1007/s10682-004-7916-4>
- Giraud-Billoud, M., Rivera-Ingraham, G. A., Moreira, D. C., Burmester, T., Castro-Vazquez, A., Carvajalino-Fernández, J. M., Dafre, A., Niu, C., Tremblay, N., Paital, B., Rosa, R., Storey, J. M., Vega, I. A., Zhang, W., Yepiz-Plascencia, G., Zenteno-Savin, T., Storey, K. B., & Hermes-Lima, M. (2019). Twenty years of the ‘preparation for oxidative stress’ (POS) theory: ecophysiological advantages and molecular strategies. *Comparative Biochemistry and Physiology -Part A : Molecular and Integrative Physiology*, 234, 36–49. <https://doi.org/10.1016/j.cbpa.2019.04.004>
- Glytsou, C., Calvo, E., Cogliati, S., Mehrotra, A., Anastasia, I., Rigoni, G., Raimondi, A., Shintani, N., Loureiro, M., Vazquez, J., Pellegrini, L., Enriquez, J. A., Scorrano, L., & Soriano, M. E. (2016). Optic Atrophy 1 Is Epistatic to the Core MICOS Component MIC60 in Mitochondrial Cristae Shape Control. *Cell Reports*, 17(11), 3024–3034. <https://doi.org/10.1016/j.celrep.2016.11.049>
- Gottfried, I., Ehrlich, M., & Ashery, U. (2010). The Sla2p/HIP1/HIP1R family: Similar structure, similar function in endocytosis? In *Biochemical Society Transactions* (pp. 187–191). <https://doi.org/10.1042/BST0380187>
- Goudet, G., Mugnier, S., Callebaut, I., & Monget, P. (2008). Phylogenetic analysis and identification of pseudogenes reveal a progressive loss of zona pellucida genes during evolution of vertebrates. *Biology of Reproduction*, 78(5), 796–806. <https://doi.org/10.1095/biolreprod.107.064568>
- Grabherr, M. G., Haas, B. J., Yassour, M., Levin, J. Z., Thompson, D. A., Amit, I., Adiconis, X., Fan, L., Raychowdhury, R., Zeng, Q., Chen, Z., Mauceli, E., Hacohen, N., Gnirke, A., Rhind, N., di Palma, F., Birren, B. W., Nusbaum, C., Lindblad-Toh, K., ... Regev, A. (2011). Full-length transcriptome assembly from RNA-Seq data without a reference genome. *Nature Biotechnology*, 29(7), 644–652. <https://doi.org/10.1038/nbt.1883>

- Guerra, V., Haynes, G., Byrne, M., Yasuda, N., Adachi, S., Nakamura, M., Nakachi, S., and Hart, M.W., (2020). Nonspecific expression of fertilization genes in the crown-of-thorns *Acanthaster cf. solaris*: Unexpected evidence of hermaphroditism in a coral reef predator. *Molecular Ecology*, 29(2), 363–379. <https://doi.org/10.1111/mec.15332>
- Guo, Y., Lang, S., & Ellis, R. E. (2009). Independent Recruitment of F Box Genes to Regulate Hermaphrodite Development during Nematode Evolution. *Current Biology*, 19(21), 1853–1860. <https://doi.org/10.1016/j.cub.2009.09.042>
- Harper, F. M., & Hart, M. W. (2005). Gamete compatibility and sperm competition affect paternity and hybridization between sympatric *Asterias* sea stars. *Biological Bulletin*, 209(2), 113–126. <https://doi.org/10.2307/3593129>
- Hart, M. W. (2013). Structure and evolution of the sea star egg receptor for sperm bindin. *Molecular Ecology*, 22(8), 2143–2156. <https://doi.org/10.1111/mec.12251>
- Hart, M. W., & Foster, A. (2013). Highly expressed genes in gonads of the bat star *Patiria miniata*: gene ontology, expression differences, and gamete-recognition loci. *Invertebrate Biology*, 132(3), 241–250. <https://doi.org/10.1111/ivb.12029>
- Hart, M. W., Sunday, J. M., Popovic, I., Learning, K. J., & Konrad, C. M. (2014). Incipient speciation of sea star populations by adaptive gamete-recognition coevolution. *Evolution*, 68(5), 1294–1305. <https://doi.org/10.1111/evo.12352>
- Hirano, T. (2016). Condensin-Based Chromosome Organization from Bacteria to Vertebrates. *Cell*, 164(5), 847–857. <https://doi.org/10.1016/j.cell.2016.01.033>
- Hirohashi, N., Harada, K., & Chiba, K. (2008). Hormone-induced cortical maturation ensures the slow block to polyspermy and does not couple with meiotic maturation in starfish. *Developmental Biology*, 318(1), 194–202. <https://doi.org/10.1016/j.ydbio.2008.03.029>
- Kamei, N., & Glabe, C. G. (2003). The species-specific egg receptor for sea urchin sperm adhesion is EBR1, a novel ADAMTS protein. *Genes and Development*, 17(20), 2502–2507. <https://doi.org/10.1101/gad.1133003>
- Kim, J. Y., Kim, J. K., & Kim, H. (2020). ABCB7 simultaneously regulates apoptotic and non-apoptotic cell death by modulating mitochondrial ROS and HIF1 $\alpha$ -driven NF $\kappa$ B signaling. *Oncogene*, 1–14. <https://doi.org/10.1038/s41388-019-1118-6>
- Kozak, G. M., Brennan, R. S., Berdan, E. L., Fuller, R. C., & Whitehead, A. (2014). Functional and population genomic divergence within and between two species of killifish adapted to different osmotic niches. *Evolution*, 68(1), 63–80. <https://doi.org/10.1111/evo.12265>
- Levitan, D. R. (2006). Selection on Gamete Recognition Proteins Depends on Sex, Density, and Genotype Frequency. *Science*, 312(5771), 267–269. <https://doi.org/10.1126/science.1122183>

- Levitan, Don R. (2008). Gamete traits influence the variance in reproductive success, the intensity of sexual selection, and the outcome of sexual conflict among congeneric sea urchins. *Evolution*, 62(6), 1305–1316. <https://doi.org/10.1111/j.1558-5646.2008.00378.x>
- Liang, S., Zhang, Z., Liu, H., Guo, L., Sun, S., & Yang, G. (2019). Digging out molecular markers associated with low salinity tolerance of *Nannochloropsis oceanica* through bulked mutant analysis. *Journal of Oceanology and Limnology*, 1–13. <https://doi.org/10.1007/s00343-019-9189-3>
- Maitra, R., Grigoryev, D. N., Bera, T. K., Pastan, I. H., & Lee, B. (2003). Cloning, molecular characterization, and expression analysis of Copine 8. *Biochemical and Biophysical Research Communications*, 303(3), 842–847. [https://doi.org/10.1016/S0006-291X\(03\)00445-5](https://doi.org/10.1016/S0006-291X(03)00445-5)
- Martínez-López, P., Treviño, C. L., de la Vega-Beltrán, J. L., De Blas, G., Monroy, E., Beltrán, C., Orta, G., Gibbs, G. M., O'Bryan, M. K., & Darszon, A. (2011). TRPM8 in mouse sperm detects temperature changes and may influence the acrosome reaction. *Journal of Cellular Physiology*, 226(6), 1620–1631. <https://doi.org/10.1002/jcp.22493>
- McDonald, J. H., & Kreitman, M. (1991). Adaptive protein evolution at the Adh locus in *Drosophila*. *Nature*, 351, 652–654. <https://doi.org/10.1038/351652a0>
- Miller, A. E. M., & Heyland, A. (2013). Iodine accumulation in sea urchin larvae is dependent on peroxide. *Journal of Experimental Biology*, 216(5), 915–926. <https://doi.org/10.1242/jeb.077958>
- Moy, G. W., Mendoza, L. M., Schulz, J. R., Swanson, W. J., Glabe, C. G., & Vacquier, V. D. (1996). The sea urchin sperm receptor for egg jelly is a modular protein with extensive homology to the human polycystic kidney disease protein, PKD1. *Journal of Cell Biology*, 133(4), 809–817. <https://doi.org/10.1083/jcb.133.4.809>
- Oulhen, N., Reich, A., Wong, J. L., Ramos, I., & Wessel, G. M. (2013). Diversity in the fertilization envelopes of echinoderms. *Evolution and Development*, 15(1), 28–40. <https://doi.org/10.1111/ede.12012>
- Palopoli, M. F., Peden, C., Woo, C., Akiha, K., Ary, M., Cruze, L., ... & Phillips, P. C. (2015). Natural and experimental evolution of sexual conflict within *Caenorhabditis* nematodes. *BMC evolutionary biology*, 15(1), 1-13
- Palumbi, S. R. (1999). All males are not created equal: fertility differences depend on gamete-recognition polymorphisms in sea urchins. *Proceedings of the National Academy of Sciences*, 96(22), 12632–12637. <https://doi.org/10.1073/pnas.96.22.12632>
- Parker, J. A. (2001). *The Caenorhabditis elegans homologue of huntingtin interacting protein 1 has multiple roles in development* (Doctoral dissertation, University of British Columbia).

- Parker, J. Alex, Metzler, M., Georgiou, J., Mage, M., Roder, J. C., Rose, A. M., Hayden, M. R., & Néri, C. (2007). Huntingtin-interacting protein 1 influences worm and mouse presynaptic function and protects *Caenorhabditis elegans* neurons against mutant polyglutamine toxicity. *Journal of Neuroscience*, *27*(41), 11056–11064. <https://doi.org/10.1523/JNEUROSCI.1941-07.2007>
- Patiño, S., Keever, C. C., Sunday, J. M., Popovic, I., Byrne, M., & Hart, M. W. (2016). Sperm Bindin Divergence under Sexual Selection and Concerted Evolution in Sea Stars. *Molecular Biology and Evolution*, *33*(8), 1988–2001. <https://doi.org/10.1093/molbev/msw081>
- Peyregne, S., Boyle, M. J., Dannemann, M., & Prufer, K. (2017). Detecting ancient positive selection in humans using extended lineage sorting. *Genome Research*, *27*(9), 1563–1572. <https://doi.org/10.1101/gr.219493.116>
- Pond, S. L. K., Frost, S. D. W., & Muse, S. V. (2005). HyPhy: Hypothesis testing using phylogenies. *Bioinformatics*, *21*(5), 676–679. <https://doi.org/10.1093/bioinformatics/bti079>
- Prowse, T. A., & Byrne, M. (2012). Evolution of yolk protein genes in the Echinodermata. *Evolution and Development*, *14*(2), 139–151. <https://doi.org/10.1111/j.1525-142X.2012.00531.x>
- Puritz, J. B., Keever, C. C., Addison, J. A., Byrne, M., Hart, M. W., Grosberg, R. K., & Toonen, R. J. (2012). Extraordinarily rapid life-history divergence between *Cryptasterina* sea star species. *Proceedings of the Royal Society B: Biological Sciences*, *279*(1744), 3914–3922. <https://doi.org/10.1098/rspb.2012.1343>
- Roll-Mecak, A., & McNally, F. J. (2010). Microtubule-severing enzymes. *Current Opinion in Cell Biology*, *22*(1), 96–103. <https://doi.org/10.1016/j.ceb.2009.11.001>
- Sato, K. I., Ogawa, K., Tokmakov, A. A., Iwasaki, T., & Fukami, Y. (2001). Hydrogen peroxide induces Src family tyrosine kinase-dependent activation of *Xenopus* eggs. *Development Growth and Differentiation*, *43*(1), 55–72. <https://doi.org/10.1046/j.1440-169X.2001.00554.x>
- Schomer, B., & Epel, D. (1998). Redox changes during fertilization and maturation of marine invertebrate eggs. *Developmental Biology*, *203*(1), 1–11. <https://doi.org/10.1006/dbio.1998.9044>
- Sokolova, I. (2018). Mitochondrial adaptations to variable environments and their role in animals' stress tolerance. *Integrative and Comparative Biology*, *58*(3), 519–531. <https://doi.org/10.1093/icb/icy017>
- Strathmann, R. R., Strathmann, M. F., & Emson, R. H. (1984). Does limited brood capacity link adult size, brooding, and simultaneous hermaphroditism? A test with the starfish *Asterina phylactica*. *The American Naturalist*, *123*(6), 796–818. <https://doi.org/10.1086/284240>



- Sun, H., Ghaffari, S., & Taneja, R. (2007). bHLH-Orange Transcription Factors in Development and Cancer. *Translational Oncogenomics*, 2, 107–120. <https://doi.org/10.4137/tog.s436>
- Sunday, J. M., & Hart, M. W. (2013). Sea star populations diverge by positive selection at a sperm-egg compatibility locus. *Ecology and Evolution*, 3(3), 640–654. <https://doi.org/10.1002/ece3.487>
- Suyama, M., Torrents, D., & Bork, P. (2006). PAL2NAL: Robust conversion of protein sequence alignments into the corresponding codon alignments. *Nucleic Acids Research*, 34(suppl\_2), w609-612. <https://doi.org/10.1093/nar/gkl315>
- Waters, B. M., Blevins, D. G., & Eide, D. J. (2002). Characterization of FRO1, a pea ferric-chelate reductase involved in root iron acquisition. *Plant Physiology*, 129(1), 85–94. <https://doi.org/10.1104/pp.010829>
- Weber, A. A.-T. T., Abi-Rached, L., Galtier, N., Bernard, A., Montoya-Burgos, J. I., & Chenuil, A. (2017). Positive selection on sperm ion channels in a brooding brittle star: consequence of life-history traits evolution. *Molecular Ecology*, 26(14), 3744–3759. <https://doi.org/10.1111/mec.14024>
- Wheeler, T. J. (2009). Large-scale neighbor-joining with NINJA. *Lecture Notes in Computer Science (Including Subseries Lecture Notes in Artificial Intelligence and Lecture Notes in Bioinformatics)*, 375–389. [https://doi.org/10.1007/978-3-642-04241-6\\_31](https://doi.org/10.1007/978-3-642-04241-6_31)
- Wong, J. L., Créton, R., & Wessel, G. M. (2004). The oxidative burst at fertilization is dependent upon activation of the dual oxidase udx1. *Developmental Cell*, 7(6), 801–814. <https://doi.org/10.1016/j.devcel.2004.10.014>
- Wozniak, K. L., & Carlson, A. E. (2020). Ion channels and signaling pathways used in the fast polyspermy block. *Molecular Reproduction and Development*, 87(3), 350–357. <https://doi.org/10.1002/mrd.23168>
- Zigler, K. S., McCartney, M. A., Levitan, D. R., & Lessios, H. A. (2005). Sea urchin binding divergence predicts gamete compatibility. *Evolution*, 59(11), 2399–2404. <https://doi.org/10.1111/j.0014-3820.2005.tb00949.x>

See Appendix S for references quoted in the Appendix material of Chapter 3

## **Chapter 4.**

# **Multispecies comparison of response differences to selection in reproductive genes**

### **Abstract**

Gamete-recognition genes that mediate fertilization success are expected to show evidence of a response to sexual selection on gamete traits, and sea star species with diverse fertilization characteristics are expected to differ in their evolutionary response to the strength of sexual selection. These assumptions have not been thoroughly tested. Using 53 female gonad transcriptomes from 26 species, I compare the differences in the response to selection on gamete-recognition genes and other genes in the transcriptomes in four orders of sea stars, including species with planktonic fertilization (and expected strong sexual selection) and species with benthic fertilization (and expected weaker sexual selection). The results from the two comparisons indicate that gamete-recognition genes are under significant positive selection in comparison to other genes not involved in gamete interactions. And when GRG were the targets of selection, the response to selection was stronger in sea stars with planktonic fertilization than in sea stars with benthic fertilization.

## 4.1. Introduction

Genetic divergence in reproductive genes, caused by selection on fertilization, can contribute to the process of reproductive isolation and speciation (Galindo et al., 2003, Pujolar & Pogson, 2011, Sunday & Hart 2013). The rate of accumulation of genetic differences between populations and species due to selection may depend on life history characteristics such as modes of reproduction (Charlesworth, 2006; Patiño et al., 2016). However, because other evolutionary mechanisms (e.g., ecological speciation) also contribute to reproductive isolation, the assessment of that expected covariation between modes of reproduction and the response to selection on gamete-recognition genes (GRGs) can produce inconclusive results if based on few species and lineages (Chapter 3, Patino et al., 2016). In this study, I use a large dataset composed of multiple species of sea stars with contrasting life history characteristics to assess two predictions: that gamete-recognition genes show stronger evidence of a response to selection; and that GRGs show greater evidence of a response to selection in lineages or species with broadcast spawning and planktonic fertilization than in lineages or species with benthic fertilization.

Reproductive genes with highly divergent nucleotide or amino acid sequences among species are common among animals, plants, and fungi (Begun et al., 2000; Charlesworth & Guttman, 1997; Charlesworth & Awadalla, 1998; Clark & Swanson, 2005; Galindo et al., 2003; Metz & Palumbi, 1996). The mechanisms that can cause high rates of among-species divergence in GRGs are as diverse as the genes themselves. A model group of organisms to study the differences in selective pressure associated with life history characteristics and potential differences in the rapid evolution of reproductive genes are sea stars (Hart, 2012). The ancestral mode of reproduction of sea stars is broadcast spawning by large-bodied adults with large gonads and high fecundity, including large numbers of sperm (Hart et al., 1997). Broadcast-spawning echinoderms release their gametes into the water where gamete-recognition genes (GRGs) expressed in organelles, plasma membranes, or the extracellular matrix of their gametes regulate fertilization. In such species, males are expected to compete for fertilization of eggs, and sperm from many males may have access to the planktonic eggs of each female, leading to potentially high rates of sperm competition, high frequency of sperm-egg contact, and potential for polyspermy and sexual conflicts of interest over fertilization

rates (Palumbi et al., 2009; Vacquier & Swanson et al., 2011). Derived modes of reproduction and fertilization in sea stars have independently evolved multiple times, always in association with the evolution of small adult body size and reduced fecundity (including smaller numbers of sperm and reduced potential for sperm competition). Some species in the sea star genera *Leptasterias* and *Henricia* have evolved benthic fertilization in which females spawn smaller numbers of eggs in benthic egg masses that are fertilized only by sperm spawned by nearby males. Species in other genera (e.g., *Cryptasterina*, *Parvulastra*) have evolved highly derived modes of fertilization in which hermaphroditic individuals ovulate small clutches of eggs that are self-fertilized by a few sperm. In both of these forms of benthic fertilization (external egg masses fertilized by outcrossing with one or a few males, or internal selfing), sperm competition and sexual conflict are expected to be reduced due to the smaller body size and reduced number of sperm spawned by males, the limited access to eggs by multiple males, and the shared interests of male and female genomes in self-fertilization (e.g. self-sperm is mainly expected to compete with self-sperm) (Byrne et al., 2003; Chia, 1966; Mercier, 2008). Selection on GRGs involved in these processes is expected to lead to high relative rates of amino acid evolution among species (in comparison to other genes not involved in fertilization). And the life history differences between sea stars with different modes of fertilization are expected to leave signatures of stronger sexual selection in the form of codon sites and lineages under selection in lineages or species with broadcast spawning and planktonic fertilization.

In this final chapter I used the bioinformatic pipeline developed in Chapter 2 and Chapter 3 to assess differences in the response to selection acting on female GRGs compared to other genes from 53 transcriptomes (newly generated and from previously published studies). In this study I found i) evidence of a stronger response to selection including a higher number sites under selection in GRGs when compared to non-GRGs; and ii) evidence of a stronger response to selection in the number of lineages under selection in GRGs from sea stars with planktonic fertilization when compared to the GRGs from sea stars with benthic fertilization. These findings provide further evidence of rapid evolution in GRGs caused by sexual selection, and support the hypothesis that differences in selection responses are caused by differences in life history traits.

## 4.2. Methods

### 4.2.1. Sample collection and RNA-seq library construction

Adult sea stars belonging to four taxonomic orders of the class Asteroidea were collected from intertidal and subtidal sites near the University of Washington Friday Harbor Laboratories, Washington State, USA, and the Bamfield Marine Sciences Centre, British Columbia, Canada, during the breeding season for individual species in between April and July of 2015 and 2016. The ovary or testis of each sea star was dissected and fixed in RNAlater and preserved at -80°C. RNA extracts were prepared from tissue samples at a commercial facility (ARQ Genetics, Bastrop, TX, USA). Stranded RNAseq libraries were prepared and sequenced at Genome British Columbia on Illumina instruments using standard protocols. The paired-end 75-base sequence data were submitted to the SRA database under the project number PRJNA667548. Previously published RNA-seq data were downloaded from NCBI (Table 1). Here in section 4.2 I describe the collection of samples and data from both male and female individuals, but in sections 4.3 and 4.4 I present the results only for analyses of female-expressed genes from ovary samples. The sequence data for males have been more challenging to assemble and analyze, and will be presented and published later.

### 4.2.2. Transcriptome assembly

The quality of the new RNA-seq data were assessed with the program FastQC v. 0.11.3 (<http://www.bioinformatics.babraham.ac.uk/projects/fastqc/>). Low-quality sequences and adapters were trimmed from the raw sequences using the program Trimmomatic v. 0.32 (Bolger et al., 2014) with the default settings noted in the program Trinity v. 2.6.5 (Grabherr et al., 2011). I used two methods to assemble the new RNA-seq data, a genome-guided approach and a de novo approach. For the genome-guided approach, the cleaned raw sequences from the sea stars with available genomes (*Acanthaster planci* assembly OKI-Apl\_1.0, *Asterias rubens* assembly eAstRub1.3, *Patiria miniata* assembly Pmin\_1.0, and *Pisaster ochraceus* assembly ASM1099431v1) were first aligned back to their respective genomes and prepared for the genome-guided assembly using the program GSNAP (Wu and Watanabe, 2005). The genome-guided assembly was then built with the genome-guided option of Trinity v. 2.6.5 with the default

settings. The rest of the new RNA-seq libraries were directly assembled with the Trinity v. 2.6.5 denovo option after the sequences were cleaned with Trimmomatic v. 0.32. Previously assembled transcriptomes without a genome were downloaded from the Transcriptome Shotgun Assembly database (TSA) (Table 1). The new samples collected for this thesis mainly came from sea stars of the northeastern Pacific, which I analyzed along with data for other sea stars acquired from previous studies including some from outside of this region.

Order	Species	Mode of Spawning	Tissue type	Individual	ORF-single + CD-Hit
Velatida	<i>Pteraster tessellatus</i>	P	T	Male1_PteTes	15,386
			O	Female1_PteTes	16,697
Forcipulatida	<i>Asterias amurensis</i>	P	O	Female1_AstAra *	18,194
Forcipulatida		P	T	Male1_AstAra *	18,163
Forcipulatida	<i>Asterias forbesi</i>	P	O	Female1_AstFor *	18,768
Forcipulatida	<i>Asterias rubens</i>	P	O	Female1_AstRub *	21,334
Forcipulatida	<i>Evasterias troschelii</i>	P	O	Female1_EvaTro	18,093
Forcipulatida		P	T	Male1_EvaTro	16,771
Forcipulatida	<i>Leptasterias spp</i>	B	O	Female1_LepSp *	22,587
Forcipulatida		B	T	Male1_LepHex	28,805
Forcipulatida		B	O	Female1_LepHex	23,576
Forcipulatida		B	O	Female2_LepHex	22,453
Forcipulatida		B	O	Female3_LepHex	18,926
Forcipulatida		B	O	Female4_LepHex	23,250
Forcipulatida		B	T	Male2_LepHex	27,188
Forcipulatida		B	T	Male3_LepHex	25,329
Forcipulatida		B	O	Female5_LepHex	18,711
Forcipulatida	<i>Marthasterias glacialis</i>	P	O	Female1_MarGla *	24,594
Forcipulatida	<i>Pisaster brevispinus</i>	P	O	Female1_PisBre	19,957
Forcipulatida		P	T	Male1_PisBre	20,897
Forcipulatida	<i>Pisaster ochraceus</i>	P	O	Female1_Pis_Och *	2,520
Forcipulatida		P	O	Female2_Pis_Och *	9,810
Forcipulatida		P		Female3_Pis_Och	23,046
Forcipulatida	<i>Pisaster giganteus</i>	P	O	Female1_Pis_Gig *	10,436
Forcipulatida	<i>Pycnopodia helianthoides</i>	P	T	Male1_PycHel	18,688
Spinulosida	<i>Echinaster spinulosus</i>	P	O	Female1_EchSpi *	21,949
Spinulosida	<i>Henricia spp</i>	P	O	Female1_HenSpp *	24,749
Spinulosida	<i>Henricia leviuscula</i>	P	O	Female1_HenLev	19,312
Spinulosida		P	T	Male1_HenLev	22,541
Spinulosida	<i>Henricia pumila</i>	B	O	Female1_HenPum	20,638
Spinulosida		B	T	Male1_HenPum	19,515
Spinulosida	<i>Henricia sanguinolenta</i>	B	O	Female1_HenSan	22,522
Spinulosida	<i>Henricia-gray-pink</i>	P	O	Female1_HenGP	23,215
Spinulosida	<i>Henricia gray-arpits</i>	P	T	Male1_HenG	20,524
Spinulosida		P	O	Female_HenG	20,287
Valvatida	<i>Acanthaster cf. solaris</i>	P	O	Female1_AcaSol *	7,274
Valvatida		P	T	Male1_AcaSol *	10,589
Valvatida		P	T	Male2_AcaSol *	16,119
Valvatida		P	O	Female2_AcaSol *	8,045
Valvatida		P	O	Female3_AcaSol*	24,198

Order	Species	Mode of Spawning	Tissue type	Individual	ORF-single + CD-Hit
Valvatida		P	T	Male3_AcaSol	22,735
Valvatida		P	T	Male4_AcaSol	17,844
Valvatida	<i>Crossaster papposus</i>	P	O	Female1_CroPap	19,321
Valvatida	<i>Cryptasterina hystera</i>	B	H	Hermaphrodite1_Cr yHis *	20,077
Valvatida		B	H	Hermaphrodite2_Cr yHis *	20,415
Valvatida		B	H	Hermaphrodite3_Cr yHis *	19,819
Valvatida		B	H	Hermaphrodite4_Cr yHis *	22,124
Valvatida	<i>Cryptasterina pentagona</i>	P	O	Female1_CryPen *	20,840
Valvatida		P	T	Male1_CryPen *	19,943
Valvatida		P	T	Male2_CryPen *	17,274
Valvatida		P	O	Female2_CryPen	19,341
Valvatida		P	O	Female3_CryPen	18,268
Valvatida	<i>Dermasterias imbricata</i>	P	O	Female1_Derlmb	18,728
Valvatida		P	T	Male1_Derlmb	19,017
Valvatida	<i>Patiria miniata</i>	P	O	Female1_PatMin *	36,638
Valvatida		P	O	Female2_PatMin *	30,756
Valvatida		P	O	Female3_PatMin	31,932
Valvatida		P	O	Female4_PatMin	34,781
Valvatida		P	O	Female5_PatMin	39,197
Valvatida		P	O	Female6_PatMin	39,805
Valvatida		P	O	Female7_PatMin	35,852
Valvatida		P	O	Female8_PatMin	39,269
Valvatida		P	O	Female9_PatMin	38,889
Valvatida		P	T	Male1_PatMin	37,056
Valvatida		P	O	Female10_PatMin	17,117
Valvatida	<i>Solaster dawsoni</i>	P	O	Female1_SolDaw	17,842
Valvatida	<i>Solaster endeca</i>	P	O	Female1_SolEnd	18,032
Valvatida	<i>Solaster stimpsoni</i>	P	O	Female1_SolSti	17,168
Valvatida		P	T	Male1_SolSti	18,407
Paxillosida	<i>Luidia clathrata</i>	P	O	Female1_LuiCla *	20,492
Paxillosida	<i>Astropecten aranciicus</i>	P	O	Female1_AstAra *	15,551
Paxillosida		P	O	Female2_AstAra *	15,721
Paxillosida		P	O	Female3_AstAra *	16,358



**Table 4.1** List of transcriptomes and transcript counts. The new RNA-seq libraries collected from this study are deposited in the unpublished NCBI BioProject no. PRJNA667548. An asterisk indicates the RNA-seq libraries or the transcriptome shotgun assembly sequences downloaded from NCBI projects: Reich et al., 2015 (NCBI BioProject no. PRJNA236087), Musacchia et al., 2017 (NCBI BioProject no. PRJEB20544), Hall et al., 2017 (NCBI BioProject no. PRJDB3175), PRJNA612126, Unpublished (NCBI BioProject no PRJNA612126), Guerra et al., 2020 (NCBI BioProject no PRJNA412251), Hart et al., 2020 in review (NCBI BioProject no PRJNA544828), Bates et al. 2019 (NCBI BioProject no PRJNA398668), and Hart et al., 2013 (NCBI BioProject no PRJNA175319). F = ovary, M = testis, H = ovotestis, P = planktonic, B = benthic

### 4.2.3. Orthologous gene identification

The transcriptome libraries were grouped into male or female gene sets to identify orthologous gene alignments for selection analysis. Each of the gene sets included libraries made from either the male or the female gonads, plus the libraries made from the ovotestis of *Cryptasterina hystera*. The male gene set was composed of orthologs from 20 testis and 4 ovotestis transcriptomes that included the following species: Velatida: *Pteraster tessellatus*; Forcipulatida: *Asterias amurensis*, *Evasterias troschelii*, *Leptasterias hexactis* (three transcriptomes), *Pisaster brevispinus*, and *Pycnopodia helianthoides*; Spinulosida: *Henricia leviuscula*, *Henricia pumila*, and *Henricia gray-arpits*; Valvatida: *Acanthaster* cf. *solaris* (four transcriptomes), *Cryptasterina pentagona* (two transcriptomes), *Cryptasterina hystera* (four transcriptomes), *Dermasterias imbricata*, *Patiria miniata*, and *Solaster stimpsoni*. The female gene set was composed of 53 transcriptomes: (Velatida) *Pteraster tessellatus*; (Forcipulatida) *Asterias amurensis*, *Asterias forbesi*, *Asterias rubens*, *Cryptasterina hystera* (four transcriptomes), *Cryptasterina pentagona* (three transcriptomes), *Evasterias troschelii*, *Leptasterias hexactis* (six transcriptomes), *Marthasterias glacialis*, *Pisaster brevispinus*, *Pisaster giganteus*, *Pisaster ochraceus* (three transcriptomes); (Spinulosida) *Echinaster spinulosus*, *Henricia leviuscula*, *Henricia pumila*, *Henricia sanguinolenta*, three unidentified *Henricia* spp. (including two cryptic species from the northeastern Pacific that are similar to *H. leviuscula* but have distinctive gray or pink body colouration); (Paxillosoida) *Astropecten aranciacus* (three transcriptomes) and *Luidia clathrata*; (Valvatida) *Acanthaster* cf. *solaris* (three transcriptomes), *Crossaster papposus*, *Dermasterias imbricata*, *Patiria miniata* (ten transcriptomes), *Solaster*

*dawsoni*, *Solaster endeca*, and *Solaster stimpsoni*. Both gene sets included multiple species with planktonic and with benthic fertilization.

To prevent the erroneous identification of paralogs or other similarities as orthologous genes (e.g., due to the presence of different isoform variants in different assemblies), non-orthologous similarities between libraries were filtered out using the single ORF per gene option in Transdecoder (<http://transdecoder.github.io>; Haas, 2013), and by reducing the redundancy of the libraries with the program CD-Hit (Li & Godzik, 2006) with an identity setting of 92. An identity setting greater than 92 in CD-Hit was not successful at removing similar isoforms previously labeled by the program Trinity v. 2.6.5 (Grabherr et al., 2011). An orthology analysis was then performed with the program OrthoFinder (Emms & Kelly, 2015) using the multiple sequence alignment option and with a modified Diamond dependency command. The identity percentage filter for the pairwise analysis of OrthoFinder with Diamond was changed to 50% to further prevent the erroneous inclusion of isoform differences.

Because de novo transcriptome assemblies from multiple samples of a single species (e.g., *Leptasterias* sp., for which we assembled contigs from six ovary libraries) do not always include all of the same isoforms and transcripts (see Chapter 3), the OrthoFinder results for all samples in each gene set returned relatively few orthogroups for analysis of selection associated with life-history differences among species. To increase the number of orthogroups, a second run of OrthoFinder was performed using only the largest single transcriptome (with the highest number of transcripts) for each species in each gene set. Only new orthogroups from that second run using single representative assemblies (not present in the first OrthoFinder analysis using all assemblies) were added to each of the gene sets. For the selection analyses, we retained all orthogroups with no more than two missing species (for which that gene could not be positively identified), as a compromise between the desire to include a large proportion of expressed genes in the selection analyses, and the need to avoid comparisons across analyses of large numbers of genes with few species in common.

#### **4.2.4. Annotation of gamete-recognition genes**

The assembly of GRGs from RNAseq data is often problematic for assemblers due to the highly repetitive nature of genes such as *bindin*. To maximize the number of genes that we could identify, I manually searched for each of the GRGs in all of the

transcriptome assemblies. First, the open reading frames (ORF) were predicted from each transcriptome using the program Transdecoder version 3.0.1 (<http://transdecoder.github.io>; Haas, 2013) with the default settings. A pairwise analysis was then performed on the sequences with an ORF from each of the transcriptomes to find orthologs for gamete-recognition genes. Each ORF was queried against a reference database of previously published GRGs from sea stars and other echinoderms (Appendix L; see Ch. 2 and Guerra et al., 2020, for references). The reference database for either the GRGs or the mitochondrial genes was searched with BLAST+ (Altschul et al., 1990) using a starting cutoff value for expectation scores of  $e = 1 \times 10^{-35}$  or lower. The protein domains of the hits were then predicted with SMART and TMHMM (Schultz et al., 1998, Krogh et al., 2001) to confirm domain similarities. Each of the alignments of putative GRGs was manually curated using the program Geneious Prime version 2020.0.5 (<https://www.geneious.com>).

#### **4.2.5. Selection analyses**

Each single-copy orthogroup from the OrthoFinder analyses was then assessed for evidence of selection. The orthogroups were populated with the predicted ORF nucleotide sequences (to replace the protein alignments used in OrthoFinder) from Transdecoder. I used a single nucleotide sequence from each individual that represented a consensus of the SNP variants for each gene generated by Trinity v. 2.6.5 (Grabherr et al., 2011). The orthogroups were then aligned using the MUSCLE, the gaps and stop codons were trimmed using the program PAL2NAL (Suyama et al., 2006), and a neighbor-joining gene tree was appended to the alignment using the program NINJA (Wheeler, 2009).

The program aBSREL was then used to identify branches under selection in each orthogroup and in each of the data partitions of the GRGs (Smith et al. 2015). For the orthogroups with evidence of at least one lineage or branch under selection in aBSREL, I then analyzed the same alignment for evidence of codon sites under selection using the program MEME (only the alignments with at least 1 branch under selection in aBSREL were considered, Murrell et al. 2012). In order to reduce the total number of analyses and p values generated, and to reduce the potential for false positives. The results of these complementary selection analyses were visualized using

the program R version 1.3.959 (<https://www.r-bloggers.com/2018/06/its-easy-to-cite-and-reference-r/>, Team & DC, 2013)

These two branch site codon models provide complementary insight into episodic diversifying selection (or positive selection), including episodes of selection acting at specific times in the history of the organisms (branches in the aBSREL model with high rates of  $w$  at some codons), and episodes of selection acting on specific parts of the protein (codons in the MEME model with high rates of  $w$  along some branches). I used the selection analyses to ask whether the data partitions of the GRGs in the female gene set (expressed in ovaries) show more evidence of a response to selection (more lineages under selection in aBSREL, more sites under selection in MEME) in comparison to other genes in the same transcriptomes. The analyses of the male gene set included both of these codon models, but those analyses are ongoing and not included in this thesis. Both gene sets included multiple species from genera (*Cryptasterina*, *Henricia*, *Leptasterias*) in which benthic fertilization has evolved. In these species, the strength of sexual selection is expected to be reduced (due to limited access by multiple males to each clutch of eggs, or due to self-fertilization) in comparison to species and lineages with broadcast spawning, planktonic fertilization, and potential for strong sperm competition among multiple males and high rates of sperm contact with eggs (potentially leading to strong sperm competition, polyspermy, and sexual conflict).

Several gamete-recognition genes appeared to show evidence of more branches under selection among species or lineages with planktonic fertilization. Because I sampled more species with that life history (which is more common among sea stars), each gene tree includes more branches in which that ancestral mode of reproduction is expected (and fewer branches on which the derived mode of benthic fertilization has evolved). Consequently, a simple post-hoc count of episodes of positive selection (branches) in aBSREL results is not an adequate test of the hypothesis that this life history difference could cause a difference in the apparent response to selection across each of the gene trees. For this second hypothesis test, I used the BUSTED method (Murrell et al., 2015) to test for gene-wide evidence of positive selection on the specific class of foreground branches represented by all species (terminal leaves) or ancestral lineages (internal branches) with the same mode of spawning, and asked whether those specific hypothesis tests indicated a better fit of the codon model to the data when those

foreground branches (e.g., all lineages with planktonic fertilization) were allowed to evolve with a high rate of dN/dS at some sites in the coding sequence alignment.

To provide a better comparison of non-GRGs (hundreds) to GRGs (five, including *EBR1*, *OBi1*, *ARIS1*, *ARIS2*, *ARIS3*), I picked sets of five nonGRGs that were longer than 1000 nucleotides (five sets of five genes each, 25 nonGRGs total) to the five GRGs. Shorter sequences were not used here because the short length of most nonGRGs (relative to the GRGs I identified) can reduce the sensitivity of codon models to detect sites or branches under selection. For these comparisons, each of the 30 alignments was searched for evidence of recombination using the genetic algorithm for recombination detection (GARD) (Kosakovsky et al. 2006). I used the potential breakpoints identified by GARD to divide each of the alignments into partitions that represented blocks of nonrecombining codons. I then used the programs BUSTED, aBSREL, and MEME, as noted above, to analyze each of the partitions in each of the 30 alignments.

## 4.3. Results

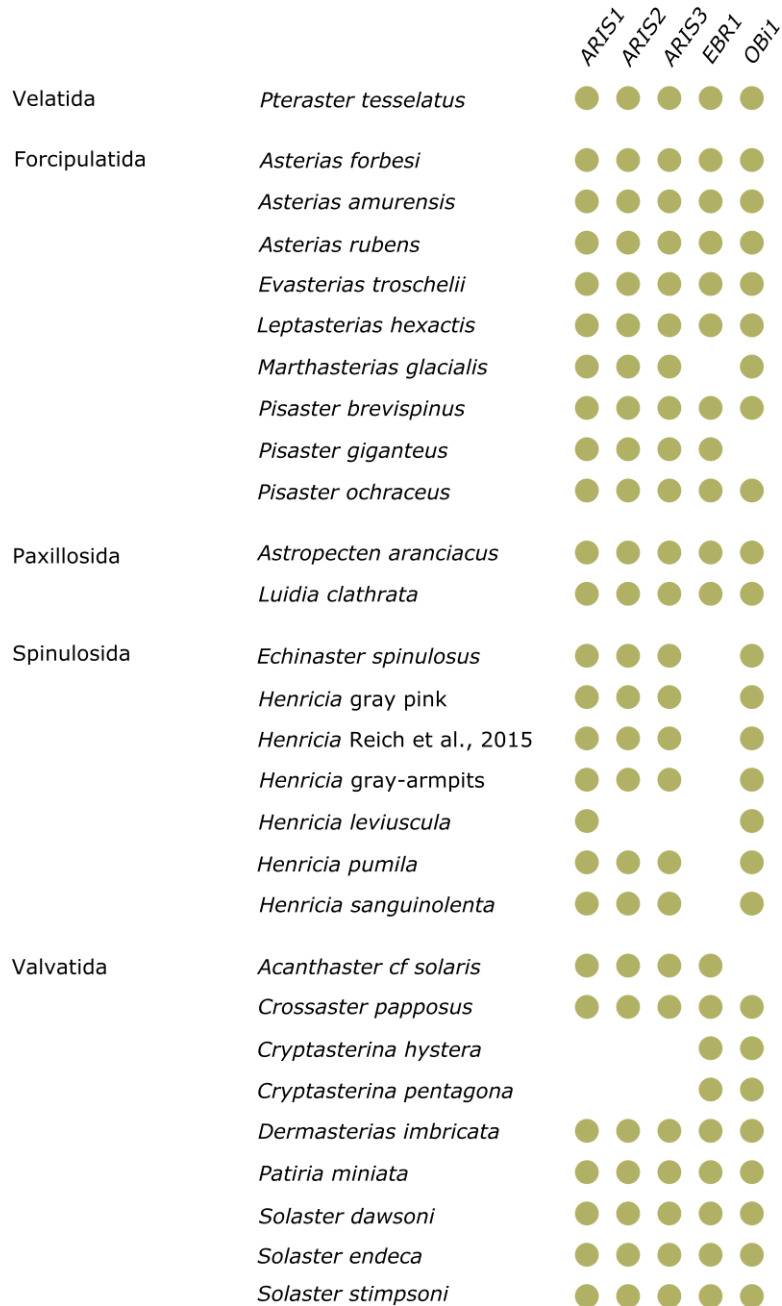
### 4.3.1. Transcriptome assemblies

A total of 73 transcriptomes representing 26 species were assessed in this study. The size of individual transcriptomes ranged from 2,551 transcripts with predicted ORF up to 78,921 transcripts with ORF (counts include contigs with multiple ORFs). The average number of transcripts per transcriptome was about 50,000 (Table 1). The smallest transcriptomes came from a small, previously published dataset for the sea star *Pisaster ochraceus*. The second smallest came from the sea star *Acanthaster cf. solaris*, and this assembly was built from a raw sequence library composed of only ~5 million sequences that produced a transcriptome with predicted ORF in 7,799 transcripts. The largest assemblies came from the genome-guided *Patiria miniata* transcriptome (78,921 ORF) and from a *Leptasterias* spp. individual with a de novo transcriptome containing 71,052 ORF.

### 4.3.2. Gamete recognition genes

Five female gamete-recognition genes (*ARIS1*, *ARIS2*, *ARIS3*, *EBR1* and *OBi1*) were found in most species (Figure1). Annotation of a sixth gene (encoding the sperm chemoattractant peptide called asterosap) was limited to a few species and those data are not analyzed here.

**Figure 4.1 List of gamete-recognition genes assembled in each species**



## **EBR1**

Complete *EBR1* coding sequences were found in all of the female transcriptomes with the exception of *Marthasterias glacialis*, *Cryptasterina hystera*, and the sea stars in the order Spinulosida. A truncated *EBR1* sequence was found in the hermaphroditic *Cryptasterina hystera*. Partial sequences with some of the *EBR1* domains were found in *M. glacialis*, *P. giganteus*, *P. ochraceus*, *Henricia* spp., and *E. spinulosus*, but because other genes in sea star genomes are known to have some similar domains, it was not possible to confidently identify *EBR1* in most of these cases.

The final alignment consisted of 10,320 nucleotides. The domains of *EBR1* were conserved among most of the sequences and in the gene assembled from the *Patiria miniata* reference genome, including a signal peptide, M12B propeptide, zinc-dependent metalloprotease domain (ZnMc), epidermal growth factor-like domain, Thrombospondin type 1 repeats (TSP1) and CUB domain repeats (bone morphogenetic protein). The prediction of the signal peptide was not consistent across all of the sequences. The composition of TSP1 repeats had some variations among sea stars: *A. cf. solaris* had a missing TSP1 domain, *Dermasterias imbricata* had an insertion of 62 codons near the first TSP1 repeat, *Solaster dawsoni* had a missing region of 125 codons, and *Luidia clathrata* had an insertion of 28 amino acids near the 3' end of the alignment. The length of the first TSP1 was also relatively short in all three *Asterias* spp. and in *Luidia clathrata*. The nucleotide sequences of the last CUB domain and TSP1 repeat all varied among sequences. The last CUB domain was absent in most species in the order Valvatida with the exception of *A. cf. solaris*. Instead, the *EBR1* of Valvatida ended with two TSP1 repeats. A complete copy of *EBR1* was also found in the male transcriptome of *Pisaster brevispinus*. Both of the expressed *EBR1* in the male *P. brevispinus* transcriptome had a sequence insertion of a size of 21 amino acids.

## **OBi1**

The other egg bindin receptor *OBi1* was found in almost all of the female sea stars. *OBi1* was missing from assemblies for *A. cf. solaris* and *Pisaster giganteus*.

The complete alignment of *OBi1* was composed of 2913 nucleotides. The 3' end of the alignment had missing regions or sequence alignments with gaps of an average of 12 amino acids in length. The alignment gaps were created as an alignment artefact as a result of the *Solaster dawsoni* and *Solaster stimpsoni* sequences. The length of *OBi1* sequences (2691 nucleotides) was similar to that of *OBi1* assembled from the *Patiria*

*miniata* reference genome (2691 nucleotides). All of the sequences had a large HSP70 domain; in some species the HSP70 domain was split into two domains (*Asterias amurensis*, *Astropecten aranciacus*, *Crossaster papposus*, *Dermasterias imbricata*, *Echinaster spinulosus*, *Henricia* spp, *Leptasterias hexactis*, *Marthasterias glacialis*, *Patiria miniata*, and *Solaster* spp.), and in some sea stars there is a gap in the predicted second domain.

### **ARIS1**

An alignment of 3,474 nucleotides was built for the gene *ARIS1*. With the exception of the *Cryptasterina* sea stars, the acrosome inducing *ARIS1* gene was present in all of the female sea stars in this analysis. The ARIS complex duplication predates echinoderms (Swalla and Smith, 2008). Similar to *EBR1*, *ARIS1* in the sea star *Dermasterias imbricata* had an insertion region (90 codons). The two paxilloids *Luidia clathrata* and *Astropecten aranciacus* had a large gap of 86 codons missing in *ARIS1* near the insertion region of *D. imbricata*.

The predicted FA58C and kringle domains were present in almost all of the sequences aligned with the exception of the paxilloids. A duplication of the kringle domain was present in *D. imbricata*. Amino acid motifs corresponding to the ARIS C-terminus domain and ARIS N-terminus domain were not consistently identified across most species (and across all three members of the *ARIS* gene family), but the nucleotide sequences aligned well with the sequences from *Asterias amurensis* (in which these two ARIS domains were previously characterized), indicating a limitation of the annotation programs to predict the ARIS domains rather than a true absence of those domains.

### **ARIS2**

The alignment of *ARIS2* was 2,406 nucleotides long. *ARIS2* was missing from *Henricia leviuscula* and the *Cryptasterina* spp. The sequences of *ARIS2* were truncated in *Pteraster tesselatus* and *Luidia clathrata* by 232 codons missing from the 3' end. As in *ARIS1*, the characteristic ARIS domains were not predicted with the annotation methods used.

### **ARIS3**

*ARIS3* was found in most sea stars with the exception of the *Cryptasterina* spp. and *Henricia leviuscula*. The alignment of *ARIS3* was of 2493 nucleotides length. *ARIS3* was shorter in *Marthasterias glacialis* (5' end), *Luidia clathrata* (3' end), and *Henricia*



*pumila* (5' end and 3' end). Similar to *ARIS1* and *ARIS2*, the ARIS domains were not detected with the annotation programs used in this study.

### **4.3.3. Episodic diversifying selection on female gamete-recognition genes**

I found more evidence of selection on *EBR1* than on any other gene, including other GRGs, and all orthogroups in the female gene set. The aBSREL analysis of *EBR1* found evidence of 11 episodes of diversifying selection, including two terminal branches (*Asterias amurensis* and *Luidia clathrate*) leading to species with planktonic fertilization, and nine internal lineages that each gave rise to at least one species with planktonic fertilization (Table 4-2). That pattern suggests that all of those episodes of selection in the history of *EBR1* evolution occurred in lineages with the ancestral mode of planktonic fertilization. The MEME analysis found 72 episodes of diversifying selection on individual codons that were broadly distributed across both repetitive and nonrepetitive domains of the predicted protein. That was the largest number of codons found under selection in any orthogroup, and was consistent with the large number of lineages under selection (also larger than any other gene in the female gene set).

The selection analysis on partitioned GRGs found additional branches and codons under selection. In particular, aBSREL analysis of the partitions of *EBR1* found 8 planktonic lineages (including 7 internal branches and the terminal branch leading to *Acanthaster cf. solaris* male 3) under selection, and MEME found 147 episodes of diversifying selection on individual codons.

Gamete-recognition genes	Branches under selection in aBSREL	Codons under selection in MEME
<i>ARIS1</i>	3	18
<i>ARIS2</i>	2	10
<i>ARIS3</i>	0	8
<i>OBi1</i>	0	1
<i>EBR1</i>	11	72

**Table 4.2 Summary of evidence of selection in the female gamete-recognition genes**

GRG	Partition number	Partition codon range	aBSREL Single	aBSREL All	aBSREL branches Planktonic	aBSREL branches Benthic	MEME sites All
<i>OBi1</i>	1	1-435	No Evidence	No Evidence			9
	2	436-826	Found Evidence	Found Evidence	1		12
	3	827-913	Found Evidence	Found Evidence	4		3
<i>EBR1</i>	1	1-282	Found Evidence	Found Evidence	1		8
	2	283-619	No Evidence	No Evidence			9
	3	620-1147	Found Evidence	Found Evidence	2		28
	4	1148-2033	Found Evidence	Found Evidence	1		36
	5	2034-2442	Found Evidence	Found Evidence	1		12
	6	2443-3240	Found Evidence	Found Evidence	3		42
	7	3241-3494	Found Evidence	No Evidence			12
<i>ARIS1</i>	1	1-781	No Evidence	Found Evidence	1		27
	2	782-1085	Found Evidence	No Evidence			9

GRG	Partition number	Partition codon range	aBSREL Single	aBSREL All	aBSREL branches Planktonic	aBSREL branches Benthic	MEME sites All
	3	1086-1158	Found Evidence	Found Evidence	3	1	12
<i>ARIS2</i>	1	1-84	No Evidence	No Evidence			3
	2	85-646	Found Evidence	Found Evidence	3		23
	3	647-808	Found Evidence	Found Evidence	3		10
<i>ARIS3</i>	1	1-108	Found Evidence	Found Evidence	2	1	7
	2	109-662	Found Evidence	Found Evidence	1		22
	3	663-845	Found Evidence	Found Evidence	1		14

**Table 4.3. Summary of evidence of selection in the female gamete-recognition genes divided into partitions between recombination breakpoints identified by GARD**

The selection analysis of *ARIS1* partitions found in 18 codons and 3 internal branches under selection. The sites under selection were distributed throughout the alignment. Descendants of all three lineages under selection included species with planktonic fertilization, and those were inferred to be episodes of selection acting on broadcast spawners. The selection analysis on the partitions of *ARIS1* found 5 branches under selection (4 branches leading to planktonic species, including an internal branch and three terminal branches leading to *Henricia* spp., *Solaster endeca*, and *Pisaster brevispinus*; and 1 benthic lineage leading to the terminal branch for *Leptasterias hexactis* 16AF), and 48 codons under selection. Similar to *ARIS1*, the *ARIS2* alignment included 10 codon sites (broadly distributed across the coding sequence) and two internal branches under selection, including one with planktonic fertilization and one with benthic fertilization. The analysis of selection on the partitions of *ARIS2* found 6 branches under selection (all planktonic lineages, including 4 internal branches plus terminal branches leading to *Evasterias troschelii* and the unidentified *Henricia* sp.), and 36 codon sites under selection. The alignment of *ARIS3* (which included a large proportion of gap sites, and only 297 codons without gaps) showed no branches under

selection in the gene tree. The selection analysis on the partitions of *ARIS3* found 5 branches under selection (4 planktonic lineages including 3 internal nodes and a terminal branch leading to *Dermasterias imbricata*; and 1 benthic lineage leading *Henricia sanguinolenta*), and 43 codon sites under selection. Although I did not use MEME to search for codons under selection among non-GRGs in which aBSREL showed no branches under selection for this section of the analysis, when I analyzed the *ARIS3* alignment using MEME I also found fewer (8) sites under selection for that GRG.

By contrast, I found little evidence of selection on *OBi1*. No branches were found under selection in the gene tree, and (in a separate analysis) a single codon site (near the codon site 312, outside of the binding site and in the middle of the first section of the HSP70 domain) was under selection in MEME. The analysis of the *OBi1* partitions provided more evidence of selection, including 5 branches (all planktonic lineages, of which 3 were internal lineages, and two were terminal branches leading to *Solaster dawsoni* and *Pteraster tessellatus*), and 24 codon sites under selection.

#### **4.3.4. Episodic diversifying selection on other genes in the female gene set**

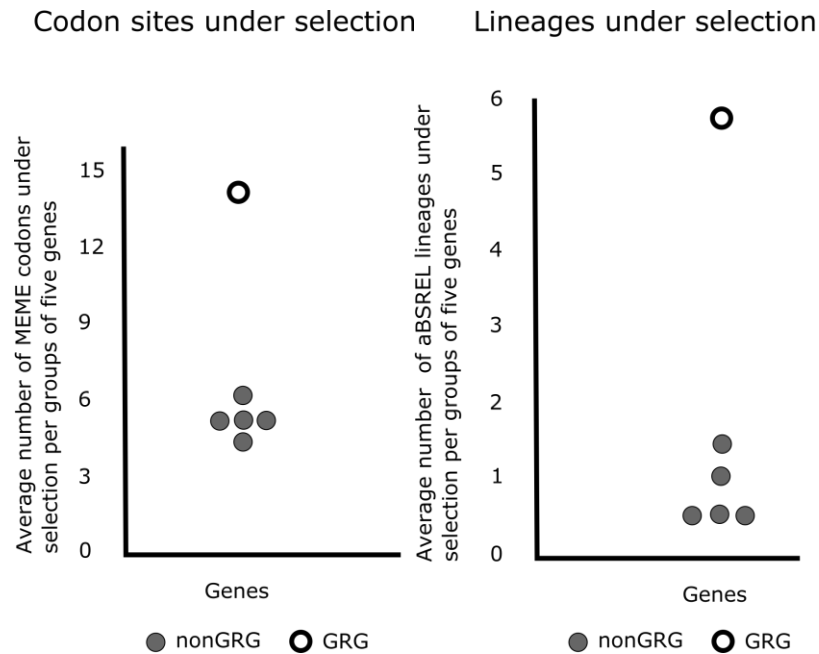
I analyzed 1150 single-copy orthogroups and found at least one lineage under selection in 69 of them (Figure 4-2). The highest number of lineages under selection in any orthogroup was 4 (compared to 11 lineages in *EBR1*). Among those 69 orthogroups with lineages under selection, 51 showed episodes of selection on individual codons. The highest number of sites under selection in an orthogroup was six (compared to 8-72 codons under selection in *EBR1* and *ARIS* genes).

**Figure 4.2.** Bubble plot of total number of episodes of diversifying selection across orthogroups in the female gene set (orange, cyan) and gamete-recognition genes (red, blue). Pairs of symbols for some GRGs show the number of positively selected branches with planktonic (red) or benthic (blue) fertilization. Symbols for single genes in different categories were jittered to make both symbols visible.



After screening for recombination and partitioning the 5 GRGs and the 25 longest nonGRGs into blocks of nonrecombining sites, I found the average numbers of codon sites under selection or lineages under selection was about three-fold larger in GRGs than in any of the five groups of non-GRGs (Figure 4-3).

**Figure 4.3. Plot of average number of MEME codons (left) and aBSREL lineages (right) under selection in GRG (white circles) and nonGRG (gray circles).**



#### **4.3.5. Tests of two hypotheses: more episodes of diversifying selection on GRGs? More episodes of diversifying selection among broadcast spawners?**

I used those results to ask whether these data indicate more episodes of positive or diversifying selection acting on GRGs compared to other orthogroups from the female gene set. First, I compared both the aBSREL results and the MEME results from analyses without assessing recombination and without partitioning individual alignments, and counted episodes of selection (associated with times in the history of the organisms, or with sites or functions in the coding sequence). The proportion of GRGs with lineages under selection in aBSREL models was about an order of magnitude greater (3 out of 5) than for other orthogroups (69 out of 1150), and the mean number of lineages under selection was greater in those three GRGs (5.3) than in those 69 other orthogroups (1.4). However, because of the unbalanced sampled of GRGs compared to other orthogroups, a Welch's test of that difference returned a non-significant result ( $t=1.4$ ,  $p=0.30$ ).

Similarly, I found more GRGs with codons under selection in MEME models (3 out of 3, including only those GRGs with at least 1 branch under selection in aBSREL)

compared to other orthogroups (51 out of 69). The mean number of codons under selection was about an order of magnitude greater in those GRGs (33) than in other orthogroups (2.3) and the range of those values did not overlap between those two classes of genes (8-72 episodes of selection in GRGs, 0-6 in other orthogroups). However, that difference was not significant ( $t=1.6$ ,  $p=0.25$ ), again due to the unbalanced sample sizes.

In general, those results are consistent with the expected pattern for this type of genome-scale comparison, with more episodes of positive selection on GRGs, probably due to their sensitivity to sexual selection and sexual conflicts of interest. However, the interpretation of that pattern is limited by the small number of GRGs that can be sampled and analyzed relative to the size of sea star genomes and the large number of genes expressed in their gonad transcriptomes.

I also used those results to ask whether there are more episodes of positive selection among GRGs from many species or lineages with broadcast spawning (and stronger sexual selection) compared to GRGs from four species with benthic fertilization (expected to have weaker sexual selection). Because the MEME results (episodes of selection on specific codons) are not associated with a particular species or lineage in the gene tree, this hypothesis cannot be tested using the MEME results. In the aBSREL results, I found a slightly larger proportion of positively selected branches among planktonic lineages (of the 16 positively selected branches for the three GRGs, 15 out of the 16 were in planktonic lineages) in gene trees for three GRGs (*EBR1*, *ARIS1*, *ARIS2*) compared to positively selected branches in 69 other orthogroups (84 positively selected branches among planktonic lineages out of 95 positively selected branches in total) (Table 4-4). That comparison does not indicate a large difference in the response to selection on GRGs associated with species differences in the mode of fertilization; it supports the overall conclusion (above) that there are more episodes of diversifying selection in parts of the genome that encode GRGs, but does not point specifically to stronger sexual selection on broadcast spawners as the cause of that difference between the two gene classes.

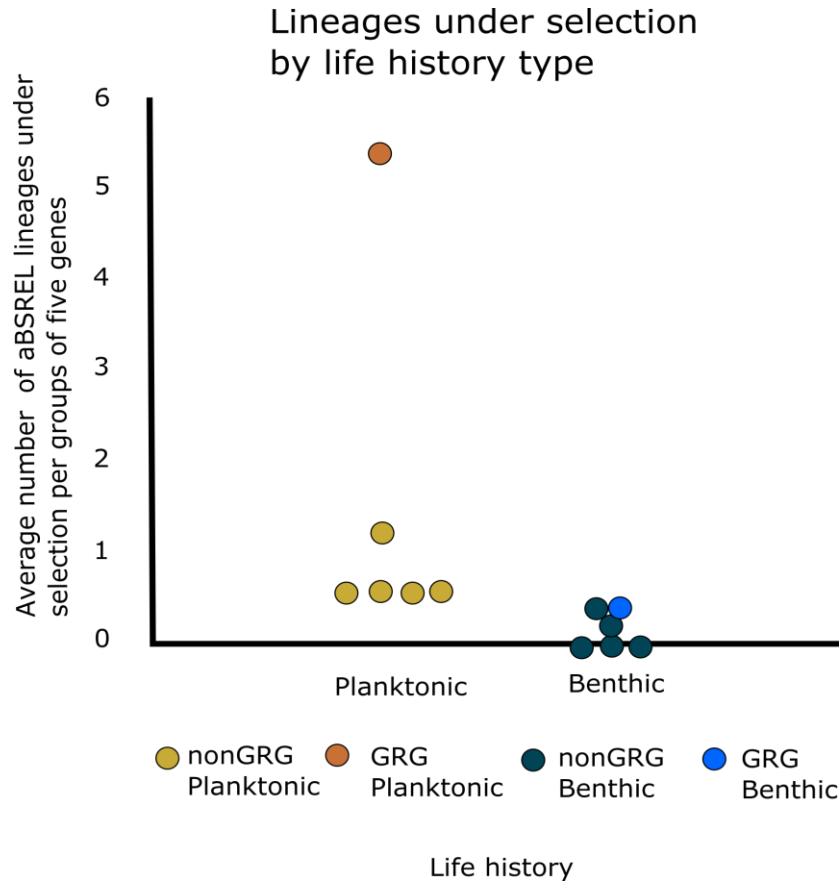
	Total number of aBSREL branches under selection in planktonic group	Total number of aBSREL branches under selection in benthic group
<b>GRG</b>	15 (93.8%)	1 (6.3%)
<b>Non-GRG</b>	84 (88.4%)	11 (11.6%)

**Table 4.4. Table of total branches under selection in aBSREL.**

Second, I carried out a more fair comparison between five groups of non-GRGs and the single group of GRGs, based on aBSREL analyses of partitions of nonrecombining blocks of codons (identified by GARD), to ask whether there is a difference in the response to selection between lineages with planktonic and benthic fertilization (Figure 4-4). Among planktonic lineages under selection in aBSREL, the mean number of lineages under selection was about three-fold higher among GRGs than in all five groups of nonGRGs. The same large difference was not present among benthic lineages under selection in aBSREL. These results support the expectation that broadcast spawners are under stronger selection linked to life history differences (in comparison to species with benthic fertilization), and that those differences act specifically on gamete-recognition genes but not other genes in the same transcriptomes.



**Figure 4.4. Plot of average aBSREL lineages under selection in planktonic (yellow = non GRG and orange = GRG) and benthic (dark blue = nonGRG and light blue = GRG) fertilizers**



An alternative approach to asking whether lineages with planktonic fertilization show more evidence of diversifying selection uses the BUSTED method. When all lineages with planktonic fertilization (including internal branches leading to at least one species of broadcast spawners) were placed together in the foreground class of branches and allowed to evolve with a high dN at some codons in the alignment, at least one of the partitions of the five GRGs (*EBR1*, *ARIS1*, *ARIS2*) were found to have a better model fit to the data when the model included that third class of positively selected codons for foreground branches (and with the benthic sea stars set as background; Table 4-5). Those results are consistent with the aBSREL and MEME results (which fit selection models to the coding sequence data without regard for the phenotypic traits of the sampled lineages), and they support the hypothesis that sexual selection acts relatively strongly on the gamete properties of broadcast spawners and generates a signal of positive selection on GRGs specifically associated with those lineages in the gene tree.

Female GRG	Partition	Episodic selection in BUSTED	P-value
<i>OBi1</i>	1-435	No	0.209
	436-826	Yes	0.048
	827-913	No	0.249
<i>EBR1</i>	1-282	No	0.403
	No	No	0.199
	620-1147	Yes	0.000
	1148-2033	Yes	0.001
	2034-2442	Yes	0.006
	2443-3240	Yes	0.020
	3241-3494	Yes	0.000
<i>ARIS1</i>	1-781	Yes	0.001
	782-1085	No	0.500
	1086-1158	Yes	0.000
<i>ARIS1</i>	1 - 84	No	0.500
	85 - 646	No	0.142
	647 - 808	Yes	0.000
<i>ARIS3</i>	1-108	Yes	0.055
	109-662	No	0.317
	663-845	Yes	0.001

**Table 4.5. Summary of the number of partitions of GRGs based on recombination breakpoints found by GARD. The partitions with significant evidence of episodic diversifying selection of sites or branches identified with BUSTED were presented as yes or no results. The corresponding p-values were provided for the BUSTED results.**

#### 4.4. Discussion

In this study I found evidence of high rates of codon evolution of gamete-recognition genes in comparison to the rest of the transcriptome, and I found evidence that the response to selection among GRGs depends on the mode of fertilization of the adult sea stars.

#### 4.4.1. Selection on gamete-recognition genes

GREGs seem to have a stronger response to selection than non-GREGs, and their high rates of codon evolution. The number of codons under selection (100 codons in *EBR1*, *ARIS1*, *ARIS2*) was similar to the total number of codon sites under selection (116) among all other orthogroups tested in the female gene set (69 genes). A similar pattern was observed in analyses of the partitions data for five GREGs and five groups of non-GREGs. The average number of codons under selection in GREGs was three-fold larger than the average number of codons under selection in the non-GREGs. Additional assessment of genes without evidence of lineages under selection may strengthen the results of this analysis, including a comparison of male genes. GREGs have previously been found to be under strong selection leading to high rates of codon evolution, and these results are consistent with this finding (Palumbi, 2009).

The egg bindin receptor *EBR1* had highly conserved protein domains across species, with the exception of a missing TSP1 domain in *A. cf. solaris*. The gene was not detected among the transcripts of the spinulosids and several other sea stars (*P. giganteus*, *P. ochraceus*, *M. glacialis*). The absence of this gene in some of the sea stars could be a result of the poor assembly of the transcript, but this seems unlikely to account for the absence of *EBR1* expression among all Spinulosida. An alternative explanation is the replacement of *EBR1* by a different sperm-binding protein in the egg coat of spinulosids. Similarly, the truncation of *EBR1* in *C. hystera* may be the result of a species-specific response to relaxation of selection associated with the evolution of internal self-fertilization. The broad distribution of sites under selection across the *EBR1* coding sequence indicates that this gene may be under several different types of selection pressures. Selection in sites outside of the regions that are predicted to interact with bindin could represent ongoing changes in secondary interactions of *EBR1* with other genes not yet described.

The conservation of the domain structure of the ARIS genes was difficult to assess as the methods used for identifying predicted protein domain structures could not identify the ARIS domains in any of the genes present including the reference ARIS genes. Unlike *ARIS2* and *ARIS3*, *ARIS1* has two additional conserved domains: FA58C and a kringle domain. Both of the additional domains of *ARIS1* were present in all of the species, with the exception of the paxillosids *A. aranciacus* and *L. clathrata*. The function of the kringle domain in *ARIS1* is unclear, but it is suspected to be involved in binding

and polymerization with other ARIS proteins (Hoshi et al. 2012). The absence of the kringle domain in *ARIS1* of the paxillosids could indicate modification of the structure and organization of the ARIS complex. It could also reflect instead a complication in the assembly process or in the identification of *ARIS1*. Selection on the coding sequence domain organization of *ARIS1* is also indicated by the duplicated kringle domain in *ARIS1* of *D. imbricata*. Of all of the species in this study, *D. imbricata* had the largest number of domain differences in combination with insertions, including 1) absence of an *OBi1* transcript, 2) a large insertion in *EBR1*, and 3) the kringle domain duplication in *ARIS1*. The functional significance of these changes in the GRGs of *D. imbricata* is not clear, but they suggest that the fertilization ecology of this large and abundant species might be a rewarding area of study.

#### **4.4.2. Evolution of mating systems**

There was some evidence of a stronger response to selection (as measured by the proportion of lineages under selection) in the GRGs from lineages with planktonic fertilization (the mode of reproduction with expected stronger sexual selection) in comparison to species with benthic fertilization. The evidence came from BUSTED analyses that showed higher values of  $w$  at some codons in GRGs of species with broadcast spawning. My comparisons of groups of non-GRGs (with relatively long coding sequences) to GRGs provided further support for the conclusion that stronger divergence of GRGs occurs among lineages with planktonic fertilization and stronger sexual selection (due to sperm to sperm competition and to sexual conflicts), but not among nonGRGs.

A comparison of male GRGs could provide additional resolution needed to further assess the expected association between rates of molecular evolution of GRGs and the ecology of spawning and fertilization. Because the current analysis is based on female GRGs, it is hard to assess whether the current pattern is unique to genes expressed in eggs. My predictions are based in part on the assumption that genes expressed in the egg coat coevolve with cognate molecules expressed in sperm, and that an evolutionary response to sexual selection on males via sperm competition will affect the evolution of egg-expressed molecules that interact with sperm molecules under selection. If most sexual selection acts directly on males and sperm traits, and if the epistatic interactions between sperm- and egg-expressed genes are not sufficiently

strong, then the evidence for selection on traits of females and eggs (and the signal of diversifying selection acting on egg-expressed genes) may be weaker than the signal of selection acting on male-expressed genes. On the other hand, similar patterns of episodic diversifying selection on male GRGs and the male gene set could indicate that fertilization ecology (and expected sexual selection associated with broadcast spawning) alone may not explain the diversification of GRGs.

#### 4.4.3. Hermaphroditism

The expression of male- or female-specific GRGs in the other gonad type could indicate the unexpected presence of both gametes in an individual. I found all of the gamete-recognition genes of female *Pisaster brevispinus* expressed in the testis transcriptome of a male individual of *Pisaster brevispinus*. That expression pattern could indicate unexpected cryptic hermaphroditism. Hermaphrodites in 'gonochoric' sea star species are rarely known to occur. Recent work in transcriptomes of *Acanthaster cf. solaris* found a similar pattern in the gonads that was confirmed to be a state of hermaphroditism with histological work (see Chapter 2; Guerra et al. 2020). Hermaphrodites have not previously been reported among *Pisaster* species, in spite of decades of research focused on their influence on community structure in the northeastern Pacific intertidal zone and susceptibility to outbreaks of sea star wasting disease, and their important role in the history of experimental ecology.

#### 4.5. References

- Altschul, S. F., Gish, W., Miller, W., Myers, E. W., & Lipman, D. J. (1990). Basic local alignment search tool. *Journal of Molecular Biology*, 215(3), 403–410.  
[https://doi.org/10.1016/S0022-2836\(05\)80360-2](https://doi.org/10.1016/S0022-2836(05)80360-2)
- Bolger, A. M., Lohse, M., & Usadel, B. (2014). Trimmomatic: A flexible trimmer for Illumina sequence data. *Bioinformatics*, 30(15), 2114–2120.  
<https://doi.org/10.1093/bioinformatics/btu170>
- Byrne, M., Hart, M. W., Cerra, A., & Cisternas, P. (2003). Reproduction and larval morphology of broadcasting and viviparous species in the *Cryptasterina* species complex. *The Biological Bulletin*, 205(3), 285-294
- Charlesworth, D., & Guttman, D. S. (1997). Plant genetics: Seeing selection in S allele sequences. *Current Biology*, 7(1), R34-R37

- Charlesworth, D., & Awadalla, P. (1998). Flowering plant self-incompatibility: the molecular population genetics of *Brassica* S-loci. *Heredity*, *81*(1), 1-
- Chia, F. S. (1966). Brooding behavior of a six-rayed starfish, *Leptasterias hexactis*. *The Biological Bulletin*, *130*(3), 304-315
- Davidson, N. M., Hawkins, A. D., & Oshlack, A. (2017). SuperTranscripts: a data driven reference for analysis and visualisation of transcriptomes. *Genome Biology*, *18*(1), 1-10
- Freedman, A. H., Clamp, M., & Sackton, T. B. (2021). Error, noise and bias in de novo transcriptome assemblies. *Molecular Ecology Resources*, *21*, 18-29
- Galindo, B. E., Vacquier, V. D., & Swanson, W. J. (2003). Positive selection in the egg receptor for abalone sperm lysin. *Proceedings of the National Academy of Sciences*, *100*(8), 4639-4643
- Grabherr, M. G., Haas, B. J., Yassour, M., Levin, J. Z., Thompson, D. A., Amit, I., Adiconis, X., Fan, L., Raychowdhury, R., Zeng, Q., Chen, Z., Mauceli, E., Hacohen, N., Gnirke, A., Rhind, N., di Palma, F., Birren, B. W., Nusbaum, C., Lindblad-Toh, K., ... Regev, A. (2011). Full-length transcriptome assembly from RNA-Seq data without a reference genome. *Nature Biotechnology*, *29*(7), 644–652. <https://doi.org/10.1038/nbt.1883>
- Guerra, V., Haynes, G., Byrne, M., Yasuda, N., Adachi, S., Nakamura, M., Nakachi, S. and Hart, M.W., (2020). Nonspecific expression of fertilization genes in the crown-of-thorns *Acanthaster* cf. *solaris*: Unexpected evidence of hermaphroditism in a coral reef predator. *Molecular Ecology*, *29*(2), 363–379. <https://doi.org/10.1111/mec.15332>
- Haas, B. J., Papanicolaou, A., Yassour, M., Grabherr, M., Blood, P. D., Bowden, J., ... & MacManes, M. D. (2013). *De novo* transcript sequence reconstruction from RNA-seq using the Trinity platform for reference generation and analysis. *Nature Protocols*, *8*(8), 1494-1512
- Hall, M. R., Kocot, K. M., Baughman, K. W., Fernandez-Valverde, S. L., Gauthier, M. E., Hatleberg, W. L., ... & Wang, T. (2017). The crown-of-thorns starfish genome as a guide for biocontrol of this coral reef pest. *Nature*, *544*(7649), 231-234
- Hart, M. W., Byrne, M., & Smith, M. J. (1997). Molecular phylogenetic analysis of life-history evolution in asterinid starfish. *Evolution*, *51*(6), 1848-1861.
- Hart, M. W. (2012). Next-generation studies of mating system evolution. *Evolution: International Journal of Organic Evolution*, *66*(6), 1675-1680
- Hart, M. W. (2013). Structure and evolution of the sea star egg receptor for sperm bindin. *Molecular Ecology*, *22*(8), 2143-2156

- Hart, M. W., Sunday, J. M., Popovic, I., Learning, K. J., & Konrad, C. M. (2014). Incipient speciation of sea star populations by adaptive gamete-recognition coevolution. *Evolution*, *68*(5), 1294-1305.
- Henshaw, J. M., Kahn, A. T., & Fritzsche, K. (2016). A rigorous comparison of sexual selection indexes via simulations of diverse mating systems. *Proceedings of the National Academy of Sciences*, *113*(3), E300-E308
- Hoshi, M., Moriyama, H., & Matsumoto, M. (2012). Structure of acrosome reaction-inducing substance in the jelly coat of starfish eggs: A mini review. *Biochemical and Biophysical Research Communications*, *425*(3), 595-598
- Kosakovsky Pond, S. L., Posada, D., Gravenor, M. B., Woelk, C. H., & Frost, S. D. (2006). Automated phylogenetic detection of recombination using a genetic algorithm. *Molecular Biology and Evolution*, *23*(10), 1891-1901
- Kosakovsky Pond, S. L., Posada, D., Gravenor, M. B., Woelk, C. H., & Frost, S. D. (2006). GARD: a genetic algorithm for recombination detection. *Bioinformatics*, *22*(24), 3096-3098
- Krogh, A., Larsson, B., Von Heijne, G., & Sonnhammer, E. L. (2001). Predicting transmembrane protein topology with a hidden Markov model: application to complete genomes. *Journal of Molecular Biology*, *305*(3), 567-580
- Li, W., & Godzik, A. (2006). Cd-hit: a fast program for clustering and comparing large sets of protein or nucleotide sequences. *Bioinformatics*, *22*(13), 1658-1659.
- Mercier, A., & Hamel, J. F. (2008). Depth-related shift in life history strategies of a brooding and broadcasting deep-sea asteroid. *Marine Biology*, *156*(2), 205-223
- Murrell, B., Weaver, S., Smith, M. D., Wertheim, J. O., Murrell, S., Aylward, A., Eren, K., Pollner, T., Martin, D. P., Smith, D. M., Scheffler, K., & Kosakovsky Pond, S. L. (2015). Gene-wide identification of episodic selection. *Molecular biology and evolution*, *32*(5), 1365–1371. <https://doi.org/10.1093/molbev/msv035>
- Musacchia, F., Vasilev, F., Borra, M., Biffali, E., Sanges, R., Santella, L., & Chun, J. T. (2017). De novo assembly of a transcriptome from the eggs and early embryos of *Astropecten aranciacus*. *PLoS One*, *12*(9), e0184090
- Pujolar, J. M., & Pogson, G. H. (2011). Positive Darwinian selection in gamete-recognition proteins of *Strongylocentrotus* sea urchins. *Molecular Ecology*, *20*(23), 4968-4982
- Palumbi, S. R. (2009). Speciation and the evolution of gamete-recognition genes: pattern and process. *Heredity*, *102*(1), 66-76.

- Reich, A., Dunn, C., Akasaka, K., & Wessel, G. (2015). Phylogenomic analyses of Echinodermata support the sister groups of Asterozoa and Echinozoa. *PLoS one*, 10(3), e0119627
- Schultz, J., Milpetz, F., Bork, P., & Ponting, C. P. (1998). SMART, a simple modular architecture research tool: identification of signaling domains. *Proceedings of the National Academy of Sciences*, 95(11), 5857-5864
- Smith, M. D., Wertheim, J. O., Weaver, S., Murrell, B., Scheffler, K., & Kosakovsky Pond, S. L. (2015). Less is more: an adaptive branch-site random effects model for efficient detection of episodic diversifying selection. *Molecular Biology and Evolution*, 32(5), 1342-1353
- Sunday, J. M., & Hart, M. W. (2013). Sea star populations diverge by positive selection at a sperm-egg compatibility locus. *Ecology and Evolution*, 3(3), 640-654
- Suyama, M., Torrents, D., & Bork, P. (2006). PAL2NAL: Robust conversion of protein sequence alignments into the corresponding codon alignments. *Nucleic Acids Research*, 34(suppl\_2), w609-612. <https://doi.org/10.1093/nar/gkl315>
- Team, R. C., & DC, R. (2019). A language and environment for statistical computing. Vienna, Austria: R Foundation for Statistical Computing; 2012. URL <https://www.R-project.org>
- Vacquier, V. D., & Swanson, W. J. (2011). Selection in the rapid evolution of gamete-recognition proteins in marine invertebrates. *Cold Spring Harbor Perspectives in Biology*, 3(11), a002931
- Wheeler, T. J. (2009). Large-scale neighbor-joining with NINJA. In *International Workshop on Algorithms in Bioinformatics* (pp. 375-389). Springer, Berlin, Heidelberg. [https://doi.org/10.1007/978-3-642-04241-6\\_31](https://doi.org/10.1007/978-3-642-04241-6_31)
- Wu, T. D., Reeder, J., Lawrence, M., Becker, G., & Brauer, M. J. (2016). GMAP and GSNAP for genomic sequence alignment: enhancements to speed, accuracy, and functionality. In *Statistical Genomics* (pp. 283-334). Humana Press, New York, NY

See Appendix AD for references to Supplemental citations.



## Chapter 5.

### Synthesis

#### Introduction

In this thesis, I studied the characteristics of gamete-recognition genes and the evidence for selection acting on them to better understand the process of reproductive isolation and speciation. Here, I summarize the findings of these studies and their broader significance.

#### **Non-sex specific expression of gamete-recognition genes**

In chapter 2, my collaborators and I found evidence of non-sex specific gamete-recognition gene (GRG) expression in the sea star *Acanthaster cf. solaris* or the crown-of-thorns sea stars (COTS). COTS are keystone predators of corals with high fecundity (Babcock et al., 2016 and Uthicke et al., 2009). Population outbreaks of COTS have resulted in the decimation of corals in the Indo-Pacific (Birkeland, 1982; Caballes, 2014; Colgan, 1987; Pratchett & Mellin et al., 2019), and the causes of the outbreaks are still not well understood. In this chapter, I studied the characteristics and expression of GRGs in COTS using new and previously published transcriptomic data, and found evidence of non-sex specific expression in two samples. The first case was a female COTS collected from the shores of Japan for this study; this female had the expression of the male GRGs *bindin* and *guanylate cyclase*. The second case was a pooled sample of males collected from the shores of Australia for a study of the testes transcriptomes of COTS (Stewart et al., 2015); this pooled sample included at least one individual with the expression of the female GRGs *ARIS1*, *ARIS2*, *ARIS3*, and *EBR1*. These findings suggested a facultative hermaphroditic state, because GRGs are sex specific and the evidence of hermaphroditism was only found in some of the individuals (Hirohashi et al. 2008). That interpretation was further corroborated by colleagues in Japan who provided histological data from three individuals that included male and female gametes in the same individual and in the same cross sections of the male or female gonads, showing the production of both sperm and eggs (Figures 2-4, 2-5).

In chapter 4, I also found some evidence of non-sex-specific expression of GRGs in the giant pink sea star *Pisaster brevispinus*. The giant pink sea star was until recently a common sea star found in temperate marine ecosystems of the Pacific coast of the U.S.A and Canada, but their populations declined after a series of sea star wasting disease events (Montecino-Latorre et al., 2016). In chapter 4, I found four female GRGs in one male *P. brevispinus*. As I prepare the manuscript for publication, I will search for male GRGs in the female *P. brevispinus* to assess whether the hermaphroditic state is evident in both sexes. If facultative hermaphroditism is rare then this state may be hard to detect as evidence is likely to be dismissed as an error or an abnormality, therefore it is likely that the frequency of facultative hermaphroditism in echinoderms is greater than is currently known. As high-throughput sequencing data become more affordable and commonly used in ecological and evolutionary analysis, the study of expression of sex-specific genes such as GRGs could be used to identify rare reproductive modes such as facultative hermaphroditism or parthenogenesis. Rare forms of facultative hermaphroditism are suspected in various marine invertebrates (Ghiselin, 1969; Marin et al., 2005).

## **Gamete-recognition genes, reproductive isolation, and speciation**

Rapid evolution of gamete compatibility genes is expected to result in reproductive isolation and speciation (Palumbi, 2009), but GRG divergence may not occur before speciation if selection on other traits (not gamete compatibility) is the process leading to reproductive isolation. In chapter 3 I compared the divergence of gamete-recognition genes in two recently diverged sea stars (<10,000 years ago; Hart & Puritz, 2020; Puritz et al., 2012) with similar morphology but with contrasting mating systems (Dartnall et al., 2003). I found little evidence of a stronger response to sexual selection in the GRGs of *C. pentagona* (in which only one lineage in the GRG *REJ1* was found to be under selection) compared to *C. hystera*. Furthermore, I found some evidence that was consistent with relaxed selection against deleterious mutations in one of the GRGs (truncation of the coding sequence in the *EBR1* gene) in the self-fertilizing *C. hystera*. My results indicated that the GRGs analyzed did not play a strong role in the divergence of *C. hystera* from *C. pentagona*. Instead, I found evidence of selection on several other genes, including *HIP1* that is predicted to be involved in spawning or in

delay of egg release and may have facilitated the evolution of internal fertilization (Parker et al., 2007; Parker, 2001). I also found other adaptations to the slow block to polyspermy, ion channels, metabolic adaptations to oxidative stress, and chromosomal regulation.

## **Mating system and gamete-recognition gene evolution**

Differences in the strength of sexual selection among species with different modes of spawning and fertilization are expected to result in a difference in the response to selection among their GRGs, and this study provided some evidence to support this expectation. In chapter 4, I compared selection on female GRGs from 26 species with broadcast spawning or with benthic fertilization. These groups are expected to differ in the strength of sexual selection because sperm competition is expected to be reduced in benthic fertilization. I found evidence of differences in response to selection on GRGs compared to non-GRGs in the form of differences in the number of lineages under selection in analyses (using BUSTED) that specifically tested the difference between the two sets of lineages with different life history traits. Past work has also found evidence of strong responses to sexual selection in male-expressed genes in comparisons between species with different mating systems (Weber et al., 2017; Pujolar and Pogson, 2011; Sunday and Hart, 2013; Hart et al., 2013), so it is possible that a stronger difference in response to sexual selection among lineages can be found in male GRGs, or among other GRGs that I was not able to identify and analyze due to limitations on the quality of annotation information or due to the evolution of new gene functions in some species.

## References

- Babcock, R. C., Milton, D. A., & Pratchett, M. S. (2016). Relationships between size and reproductive output in the crown-of-thorns starfish. *Marine Biology*, 163(11), 234. <https://doi.org/10.1007/s00227-016-3009-5>
- Birkeland, C. (1982). Terrestrial runoff as a cause of outbreaks of *Acanthaster planci* (Echinodermata: Asteroidea). *Marine Biology*, 69, 175–185. <https://doi.org/10.1007/BF00396897>
- Chapman, D. D., Shivji, M. S., Louis, E., Sommer, J., Fletcher, H., & Prodöhl, P. A. (2007). Virgin birth in a hammerhead shark. *Biology Letters*, 3(4), 425–427
- Colgan, M. W. (1987). Coral reef recovery on Guam (Micronesia) after catastrophic predation by *Acanthaster planci*. *Ecology*, 68, 1592–1605. <https://doi.org/10.2307/1939851>
- Frank, S. A. (2000). Sperm competition and female avoidance of polyspermy mediated by sperm-egg biochemistry. *Evolutionary Ecology Research*, 2(5), 613–625.
- Ghiselin, M. T. (1969). The evolution of hermaphroditism among animals. *The Quarterly Review of Biology*, 44(2), 189–208
- Hart, M. W., Sunday, J. M., Popovic, I., Learning, K. J., & Konrad, C. M. (2014). Incipient speciation of sea star populations by adaptive gamete-recognition coevolution. *Evolution*, 68(5), 1294–1305. <https://doi.org/10.1111/evo.12352>
- Hart, M. W. (2013). Structure and evolution of the sea star egg receptor for sperm bindin. *Molecular Ecology*, 22(8), 2143–2156. <https://doi.org/10.1111/mec.12251>
- Hart, M. W., & Foster, A. (2013). Highly expressed genes in gonads of the bat star *Patiria miniata*: Gene ontology, expression differences, and gamete-recognition loci. *Invertebrate Biology*, 132(3), 241–250. <https://doi.org/10.1111/ivb.12029>
- Hart, M. W., & Puritz, J. B. (2020). Correction to 'Extraordinarily rapid life-history divergence between *Cryptasterina* sea star species'. *Proceedings of the Royal Society B*, 287(1930), 20201325
- Marin IN, Anker A, Britayev TA, Palmer AR (2005) Symbiosis between the Alpheid Shrimp, *Athanas ornithorhynchus* Banner and Banner, 1973 (Crustacea: Decapoda), and the Brittle Star, *Macrophiothrix longipeda* (Lamarck, 1816) (Echinodermata: Ophiuroidea). *Zoological Studies*, 44(2) 234–241
- Mellin C, Matthews S, Anthony KR, Brown SC, Caley MJ, Johns KA, Osborne K, Puotinen M, Thompson A, Wolff NH (2019) Spatial resilience of the Great Barrier Reef under cumulative disturbance impacts. *Global Change Biology*, 25(7), 2431–2445

- Montecino-Latorre, D., Eisenlord, M. E., Turner, M., Yoshioka, R., Harvell, C. D., Pattengill-Semmens, C. V., ... & Gaydos, J. K. (2016). Devastating transboundary impacts of sea star wasting disease on subtidal asteroids. *PLoS ONE*, *11*(10), e0163190
- Palumbi, S. R. (1999). All males are not created equal: fertility differences depend on gamete-recognition polymorphisms in sea urchins. *Proceedings of the National Academy of Sciences*, *96*(22), 12632–12637. <https://doi.org/10.1073/pnas.96.22.12632>
- Palumbi, S. R. (2009). Speciation and the evolution of gamete-recognition genes: pattern and process. *Heredity*, *102*(1), 66-76.
- Parker, J. A. (2001). *The Caenorhabditis elegans homologue of huntingtin interacting protein 1 has multiple roles in development* (Doctoral dissertation, University of British Columbia).
- Parker, J. A., Metzler, M., Georgiou, J., Mage, M., Roder, J. C., Rose, A. M., Hayden, M. R., & Néri, C. (2007). Huntingtin-interacting protein 1 influences worm and mouse presynaptic function and protects *Caenorhabditis elegans* neurons against mutant polyglutamine toxicity. *Journal of Neuroscience*, *27*(41), 11056–11064. <https://doi.org/10.1523/JNEUROSCI.1941-07.2007>
- Pratchett, M. S., & Caballes, C. F. (2014). Limits to understanding and managing outbreaks of crown-of-thorns starfish (*Acanthaster* spp.). *Oceanography and Marine Biology Annual Review*, *52*, 133–200. <https://doi.org/10.1201/b17143-4>
- Pujolar, J. M., & Pogson, G. H. (2011). Positive Darwinian selection in gamete-recognition proteins of *Strongylocentrotus* sea urchins. *Molecular Ecology*, *20*(23), 4968-4982
- Puritz, J. B., Keever, C. C., Addison, J. A., Byrne, M., Hart, M. W., Grosberg, R. K., & Toonen, R. J. (2012). Extraordinarily rapid life-history divergence between *Cryptasterina* sea star species. *Proceedings of the Royal Society B: Biological Sciences*, *279*(1744), 3914–3922. <https://doi.org/10.1098/rspb.2012.1343>
- Stewart, M. J., Stewart, P., & Rivera-Posada, J. (2015). De novo assembly of the transcriptome of *Acanthaster planci* testes. *Molecular Ecology Resources*, *15*, 953–966. <https://doi.org/10.1111/1755-0998.12360>
- Sunday, J. M., & Hart, M. W. (2013). Sea star populations diverge by positive selection at a sperm-egg compatibility locus. *Ecology and Evolution*, *3*(3), 640-654
- Swalla, B. J., & Smith, A. B. (2008). Deciphering deuterostome phylogeny: molecular, morphological and palaeontological perspectives. *Philosophical Transactions of the Royal Society B: Biological Sciences*, *363*(1496), 1557-1568

Uthicke, S., Schaffelke, B., & Byrne, M. (2009). A boom–bust phylum? Ecological and evolutionary consequences of density variations in echinoderms. *Ecological Monographs*, 79, 3–24. <https://doi.org/10.1890/07-2136.1>

Weber, A. A. T., Abi-Rached, L., Galtier, N., Bernard, A., Montoya- Burgos, J. I., & Chenuil, A. (2017). Positive selection on sperm ion channels in a brooding brittle star: Consequence of life-history traits evolution. *Molecular Ecology*, 27, 3744–3759. <https://doi.org/10.1111/mec.14024>

## **Appendices**

**Appendix A. Frequency distribution of coverage. Numbers of transcripts and percent coverage in BLAST comparisons to the UniProt database, *Acanthaster planci* protein reference database, and the *Strongylocentrotus purpuratus* database**

(A)

Hit percentage cover in bin	Count in bin	> Bin below
100	3,276	3,276
90	1,287	4,563
80	878	5,441
70	782	6,223
60	749	6,972
50	778	7,750
40	838	8,588
30	740	9,328
20	673	10,001
10	216	10,217

(B)

Hit percentage cover in bin	Count in bin	> Bin below
100	3,288	3,288
90	346	3,634
80	277	3,911
70	343	4,254
60	414	4,668
50	324	4,992
40	375	5,367
30	370	5,737
20	404	6,141
10	222	6,363



(C)

Hit percentage cover in bin	Count in bin	> Bin below
100	2,862	2,862
90	915	3,777
80	667	4,444
70	593	5,037
60	617	5,654
50	597	6,251
40	619	6,870
30	494	7,364
20	420	7,784
10	172	7,956

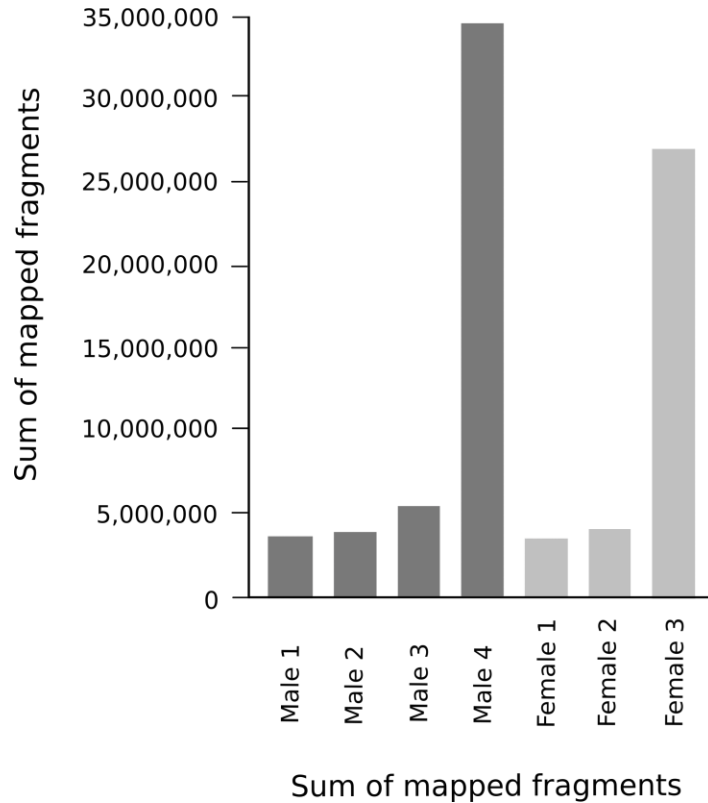
## Appendix B. List of gamete-recognition genes used as a reference database for pairwise analysis

Gene	Species	GenBank or Bioproject number	Publication
<b>Asterosap</b>	<i>Asterias amurensis</i>	NA	Nakachi 2008
<b>ARIS1</b>	<i>Asterias amurensis</i>	AB602892	Naruse et al. 2011
	<i>Acanthaster planci</i>	AB602901	
<b>ARIS2</b>	<i>Asterias amurensis</i>	AB602893	Naruse et al. 2011
	<i>Acanthaster planci</i>	AB602902	
<b>ARIS3</b>	<i>Asterias amurensis</i>	AB602894	Naruse et al. 2011
	<i>Acanthaster planci</i>	AB602903	
<b>Bindin</b>	<i>Patiria miniata</i>	FJ439659	Sunday and Hart (2013)
	<i>Evasterias troschelii</i>	KT318446	Patino et al. (2016)
	<i>Dermasterias imbricata</i>	KT318447	
	<i>Meridiastra calcar</i>	KT318448	
	<i>Patiria pectinifera</i>	KT318449	
	<i>Cryptasterina hystera</i>	KT318450	
	<i>Cryptasterina pentagona</i>	KT318451	
	<i>Parvulastra exigua</i>	KT318454	
	<i>Parvulastra parvivipara</i>	KT318452	
	<i>Parvulastra vivipara</i>	KT318453	
	<i>Pisaster ochraceus</i>	KJ481933	Popovic et al. (2014)
	<i>Pisaster giganteus</i>	KJ481934	
	<i>Pisaster brevispinus</i>	KJ481935	
<b>EBR1</b>	<i>Patiria miniata</i>	PRJNA175319	Hart 2013
<b>Guanylate cyclase</b>	<i>Asterias amurensis</i>	AB070354.1	Matsumoto et al. 2003
<b>OBI1</b>	<i>Patiria miniata</i>	PRJNA52335	Hart and Foster 2013
<b>REJ1</b>	<i>Strongylocentrotus purpuratus</i>	NM_214608.1	Moy et al. 1996
<b>REJ3</b>	<i>Strongylocentrotus purpuratus</i>	NM_214636.1	Mengerink et al. 2002

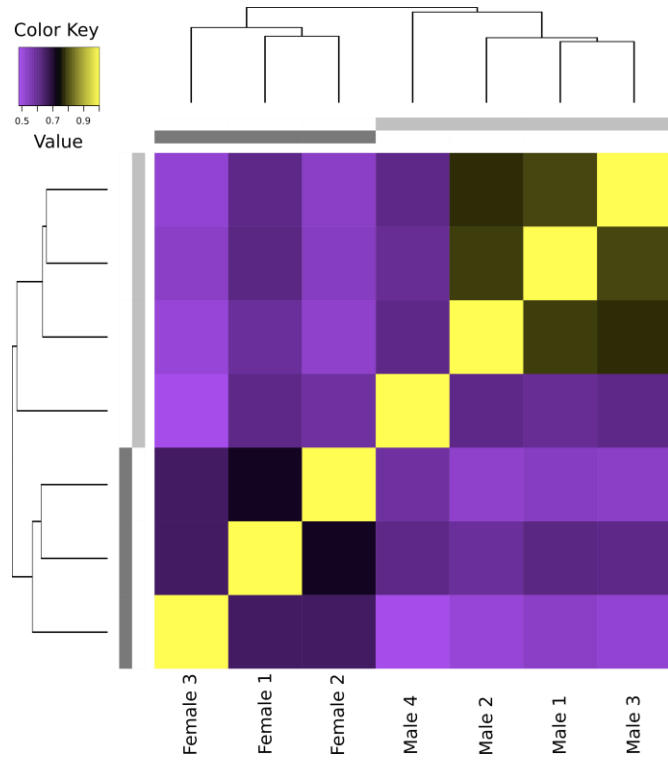
Includes sequence or BioProject accessions, and references

**Appendix C. Quality check step for samples and biological replicates. (A) Sum of mapped fragments for individual male and female samples. (B) Correlation matrix of the four samples. (C) Principal component analysis (PCA) with percent variation for each of the male and female samples.**

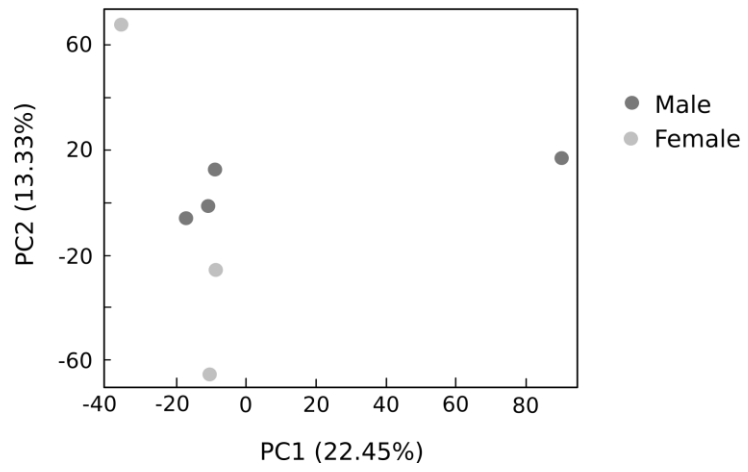
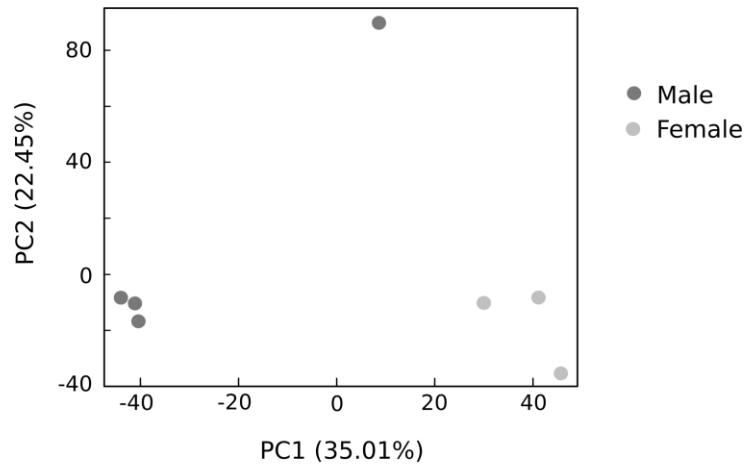
A)



B)



c)









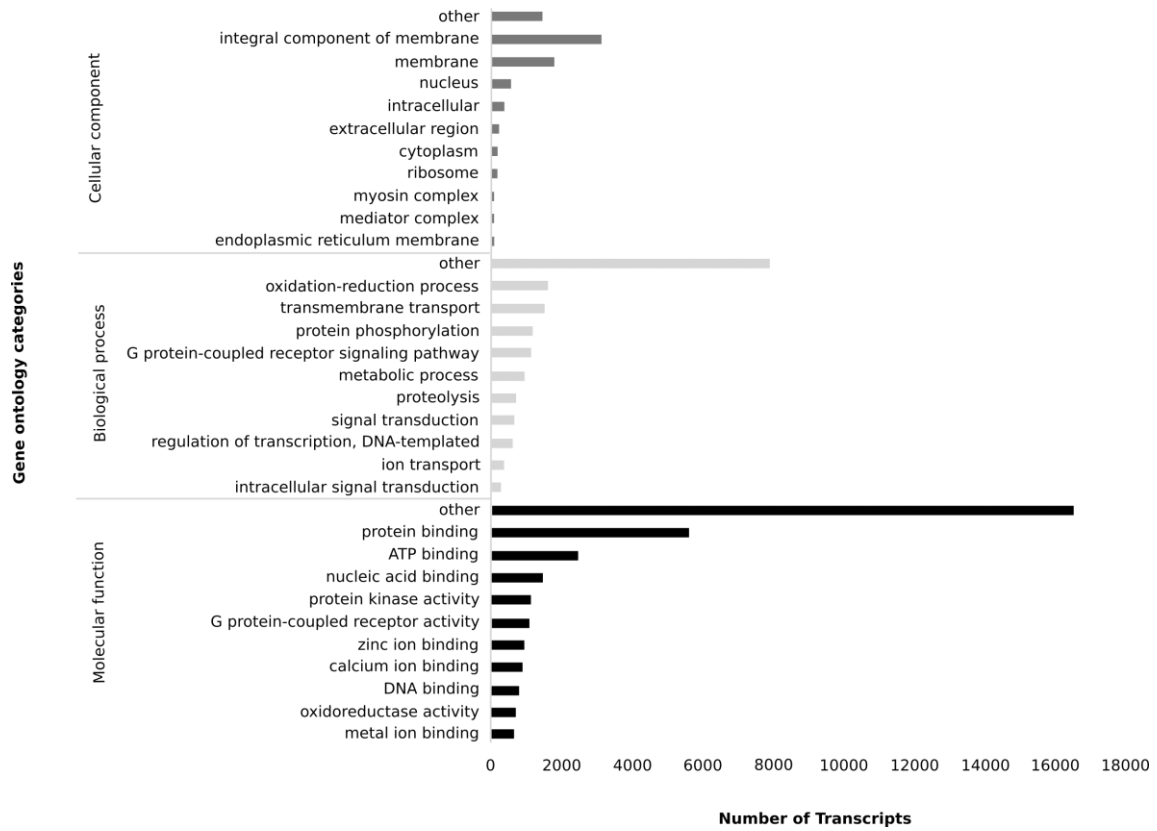




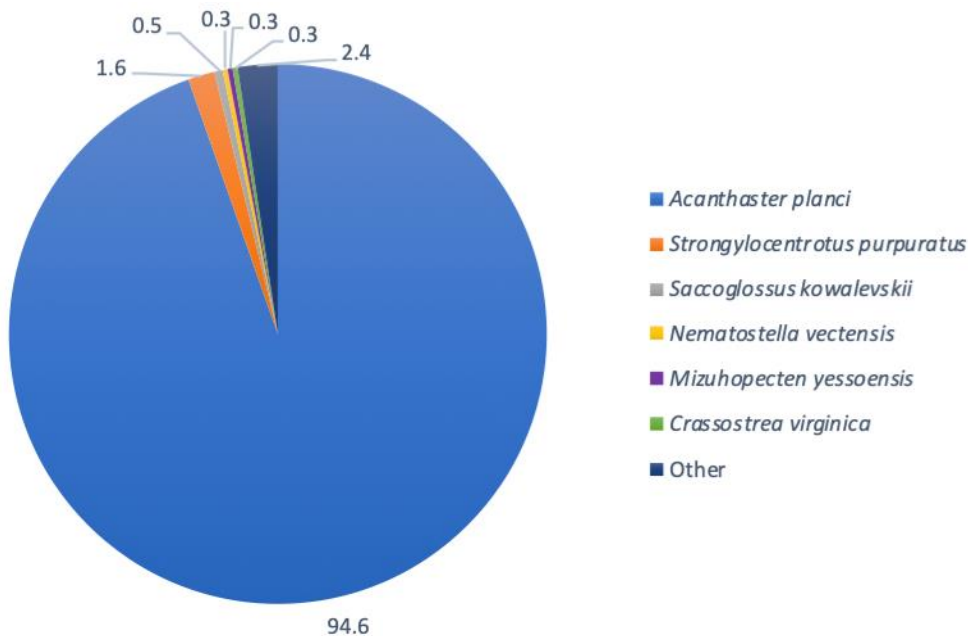
## **Appendix E. Annotations and gene ontology results. Summary of GO, annotation terms for genes expressed in COTS gonads and percentage distribution of the top annotations with the NCBI invertebrate database**

The large majority of Pfam GO annotations identified molecular function categories (56%); few of those annotations identified biological process (29%) or cellular component (15%). The most common molecular function categories were protein binding (5618), ATP binding (2461), nucleic acid binding (1470); common biological process categories included oxidation-reduction process (1625), transmembrane transport (1503), protein phosphorylation (1181); and the most common cellular component were integral component of membrane (3147), membrane (1800), nucleus (560). (B) Transcripts that were annotated with the NCBI invertebrate database were heavily populated by hits to the *Acanthaster planci* database. Other hits at a percentage of 2 or lower included the sea urchin *Strongylocentrotus purpuratus* (1.6%), the acorn worm *Saccoglossus kowalevskii* (0.5%), the sea anemone *Nematostella vectensis* (0.3%), the scallop *Mizuhopecten yessoensis* (0.3%), the oyster *Crassostrea virginica* (0.3%), and other invertebrates (2.4%) (B)

**A. Number of transcripts per Pfam Gene Ontology subcategories in the categories Molecular Function, Biological Process, and Cellular Component.**



**B. Top annotations of transcripts with the NCBI invertebrate database.**



# Appendix F. *Guanylate cyclase* alignment of *Acanthaster* cf. *solaris* and *Asterias amurensis*. The alignment shows amino acid sequence differences for the sperm receptor for asterosap

```

Asterias_amurensis_Guanylate_cyclase 1 MRCLMLSVLVAGYVWVALGTNFKIGLLVPLTDPQTGNASGFGDPVAGAFVAVDDINLNPAILPGHTVSWVEWVDTKCDINTGLTAVSDWVKRGFVGVIGPGSCDYEARLAGSINPFMF 120
Acanthaster_cf_solaris_Guanylate_cyclase 1 MRRLLLAAILVAS-AWVSHGTFDKIALLVPPFTDPQNGNIQAIGDPIAGAFFLAVEDINNSPSILPGHTLTWEWVDSQCDINVGMEAIADFWKRGFVGVIGPGSCDYEARLAGSVNFPLF 120

Asterias_amurensis_Guanylate_cyclase 121 DYGCDEGAVSNKLLYPTIYRTPPSTRIVDALVTLQKFDWDOVTVVYRNHSIWNILNAMKEEFEVHDITVGHQEVFQTGFVFNDSINPFPEIFTRKETTIRIYVFLGEMIELRSFA 240
Acanthaster_cf_solaris_Guanylate_cyclase 121 DYGCDEAAVSDKLLYPTIYRTPPSTRIVADALVITMQMFNWDOVTVVLRNHSIWHQVYVVSQAQKFNNTVQHEEIFESGFIPYNDSTPDPFPDIIRTKETTIRIYVFLGVEYELRSFA 240

Asterias_amurensis_Guanylate_cyclase 241 MAALDEGLNNGDYAILGMAIDHKIRRSQNWHSLDLFLHMGTYLDEKAAKAMESVLIAPKAPKFTFVYKSNVVKRDSVOGAPFFQTGREFHFTSAFLYDATALFAKALEETLAAGEDPFD 360
Acanthaster_cf_solaris_Guanylate_cyclase 241 IDAYDQGLTNGEYVIVGTSVDHKMRTTONWHSMSYIGWGTFEDEKAIAKFAVLIVTPKGPCKTWVYREWMMWVKATVRLSPFFGTGRYHFTFAFLYDATALFAQALQATLDAGEDPYD 360

Asterias_amurensis_Guanylate_cyclase 361 GEAVSHAMGVQYQISMLONGIDESGDGSRVMLMDMNELEADSWLTAGYGVIGVGEFIRNSGRWTFNATDDYNTPIKWPNADAGPPLDMPVCGYFEFPCPKYGLYGLGVPIVLLI 480
Acanthaster_cf_solaris_Guanylate_cyclase 361 GQIVSHIFNTPYQISMLNNOIDHTGDGVSFRVLLDMNRLOKADDYIAGFPGMVGVGEYRTIDGKWTFRNTDDYDLIHWPNMDGPPDMPVCGYFGELECPRYGLYFGVPIVLLI 480

Asterias_amurensis_Guanylate_cyclase 481 VGCAYGYFYRKKIYEGELDSLWVKINFDDVQAKGKDTNKSGISMKSMVMTLSVMTNQEQIFARIGTYRGNCAIKA/VNKHSDLTRTRVROELKAMHDVVRHNDVCOFGASVSDSPHY 600
Acanthaster_cf_solaris_Guanylate_cyclase 481 FGLTAAYYIRKRYESELDSLWVKIDFEVQAKGQTNKSGVSMKSMVMTSIVMTNQEQIFARIGTYRGNVCAIKAVHKNHIDITREVRKELKAMRDRHNDVCOFGACIDRPHI 600

Asterias_amurensis_Guanylate_cyclase 601 CILMTYCAKGLQDILENDDIKLDMFLASMIADLVKGMIIYHTSMIESHGKLSNVCVDRNRFVLOITDYGLHEFKGQGEDPDLDDVRYRNLWRAPPELLRMGKMPPLAGTPKGDVY 720
Acanthaster_cf_solaris_Guanylate_cyclase 601 CILMTYCAKGLQDILENDDIKLDMFLASLIADLVKGMIIYHTSLIESHGKLSNVCVDRNRVWLQITDYGLEQFKKAQAEEDPDMDDVRYRNLWKAPPELLRMGAKMPARGTRKGDVY 720

Asterias_amurensis_Guanylate_cyclase 721 SFAIVLTEMYSRAEYLNNDDEPEEIEKVMAGSIPPYRPLNDVNEKAPECVLKAIRSCWGEDPVERPDDFFKARTMLAPLQKGLKPNIMDNMITIMERYTNLEELVDETELQKEKA 840
Acanthaster_cf_solaris_Guanylate_cyclase 721 SFAILLTEMYSRAQPYHLNDEEPEEIIKRLKAGSIPPYRPLNDVNESAPECVLKAIRQWEEEDPEDRPFDFGARTILAPLQKGLKPNIMDNMITIMERYTNLEELVDETELQREKA 840

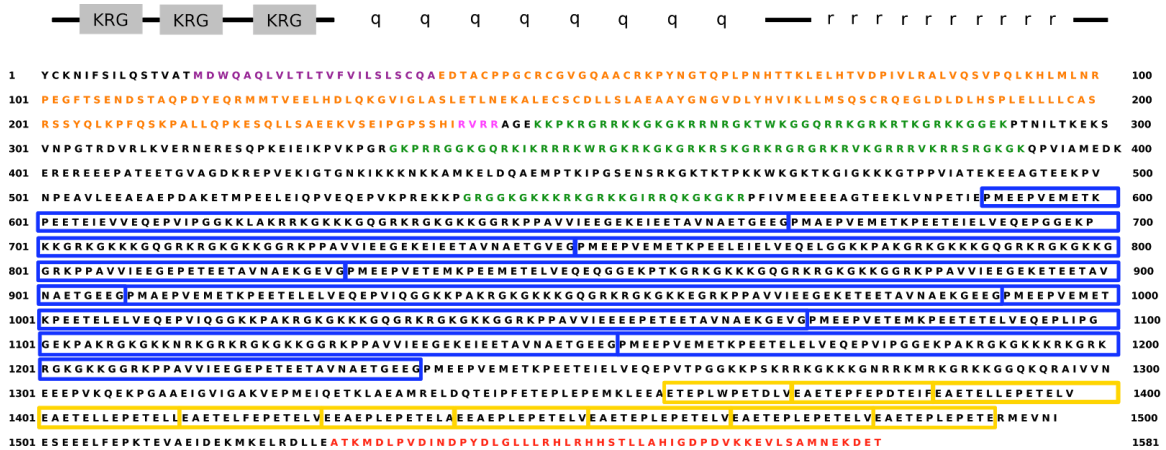
Asterias_amurensis_Guanylate_cyclase 841 KTEQLLHRMLPPSIASQLIKGISVAPEAFDMVITIFFSDIVGFTLSAASSTPIQV/VNLLNLYTTFDATISNYDVKYVETIGDAYMLV/SGLPLRNGNRHAGMIASAAWHLLEEVTFV/PH 960
Acanthaster_cf_solaris_Guanylate_cyclase 841 KTEQLLHRMLPPSIASQLIKGISVAPEAFDMVSIFFSDIVGFTLSAASSTPIQV/VNLLNLYTTFDAISNYDVKYVETIGDAYMLV/SGLPIRNGNRHAGMIASAAWHLLEDVSTFV/PH 960

Asterias_amurensis_Guanylate_cyclase 961 KRDEKLRIGIHSKGVAGVGLTMRPYCLFGDVTNTASRMESNGLALKIHWSPCEQVQLQELGGYNLVERGLVAMKKGGEILTYWLEGDQPSYKVERNKPKQDL 1068
Acanthaster_cf_solaris_Guanylate_cyclase 961 KPEEKLRIGIHSKGVAGVGLTMRPYCLFGDVTNTASRMESNGLALKIHWSPCEQVLEIEGGYELVERGLVAMKKGGEILTYWLVGDQPSYKIERVPPKQNL 1068

```

## Appendix G. Characteristics of bindin of *Acanthaster cf. solaris*. Includes a schematic diagram of repetitive domains and a translated bindin sequence with domains highlighted

Schematic diagram of repetitive domains (only) of bindin. Collagen-like domains (KRG), tandem repeat motif q (8 copies), and tandem repeat motif r (10 copies). Translated bindin sequence with domains highlighted: signal sequence (purple), preprobindin (orange), furin-type cleavage site (pink), collagen-like (green), q repeats (blue boxes), r repeats (yellow boxes), highly conserved 3' bindin core domain (red).





# Appendix I. ARIS alignments. (A) ARIS1 from Asterias amurensis and Acanthaster cf. solaris, (B) ARIS2 from Asterias amurensis and Acanthaster cf. solaris, (C) ARIS3 from Asterias amurensis and Acanthaster cf. solaris.

## (A)

Asterias amurensis ARIS1 1 -----MLVTSLCCCLVVLGLATPGARAAFGDNMDHGRDDLFEKMGKATVDVFDVGGVQLDVALEDITGQDEWILD 120  
Acanthaster of solaris ARIS1 1 FPSLQLVSSHFSVTPPIRKSRRGQHPVLACENYRVGLLNLHLGLREMLTGLCC-LLVGLATPGARAAFGDVGTHGRDDLFEKMGQARVEEFVNVGQVSLDVLDETEGQDEWILD 120

Asterias amurensis ARIS1 121 FOPFQIHNKSNRPVIEQNGSLVAENTGTCNSVFTLTPFDSSTGFYKDSYTPNPGTKSLFSYETGESEIQGDMRIRREDHITFMGSMOITLNCXDSDETVWEKEVTADIAQFNATL 240  
Acanthaster of solaris ARIS1 121 FQDFDIHQNKSRQPIVTKDGGKVAEHTGTCSSVFPYHSVTGYKYDTPAPAPGNKTLFNQNGTGVQKGDVIRVREDHLQFDGVIDMTECKTSDGANVWHKEVTPETIQFNATL 240

Asterias amurensis ARIS1 241 YMTNVRPQSGSTNPEPAYVQSFAIYWRLLRVALSRFLVSSTERLQPIFEFAIVEAVYLNDDDEEYGFDRSRAEVIQAFRTVTDNTNGELISVYKINTLYVDPADSVI-SEISHVKRTPSS 360  
Acanthaster of solaris ARIS1 241 FMTNVRPQSSSNPDPAVYQSYAVLWRLLRVALARFLSSTEQLKPIFEYALVRPVYLNDDDEEYGFDEDRAEVLEAFRTLTAHPNGSLISVYRVNSLEYDPADLLVGNLGHKIMPIR 360

Asterias amurensis ARIS1 361 GCCKPLGVEDSNIIGDGLTASSYVLEGNLSYSPDKGRNNAKAVETISAGMVMAGST-VDQWQIWEIPSDNLRVSGVMTQGFNGEDINMMVREFYVYQVGV-GTFNPNVLSAGATHI- 480  
Acanthaster of solaris ARIS1 361 GCHLPLGVENGT-ISDSQLSSSSVWL--NSAEYSAPKARLNQAQIDAVSAGAWLAGTIDANQWQIQLDQT-TVWVSGVLTQGYIYQDVTMMVTKYVSHSAEAGSLSPVFNESGVNAVP 480

Asterias amurensis ARIS1 481 --FTGNYDSHTIIVTNYLDAVSTDAIRIYPTDFENMMALRELLVCEGHEPCFDANGTDYRGTVHQTVSGTTCQRWSSQEPHMHSHFSEWENDRNDIGDHNFCRNPDGOTQWVYCYTLDPL 600  
Acanthaster of solaris ARIS1 481 VVFAGNYDSEITVKNYFDDPILTRIRILPQEWNSGIAMRIELLDGTHTECYTDSNGEDYRGTVSVTESGETCQRWVSAQEPHSHFSPENYAHRGIDGHNFCRSLDNATRPWCYTLDPS 600

Asterias amurensis ARIS1 601 SPMEFCDVGAASVSCAPITAPEADPELVYVYAPYCNFTEWEQSCQSWLFWVLEVDTTAAVNRMPIDATGEFTFEFETVTCPNDRSACSKVDVNPAINSHITLQTTVEIVDDVDKDS 720  
Acanthaster of solaris ARIS1 601 MPIGFCDVGVQAVSCTPNVTRDAPNSFYANY-APYCNFTEWENYVQTRVWVFLVLEVDSSGATNRMPIDATGEFTFEFETVTCPNDRSVCRRLDIPEAVINSHEITLQTTVEIVDDDAKDS 720

Asterias amurensis ARIS1 721 PRYLVKVKHGSDPTVDIRGVPYRPGVSHLETVTVDTHFFPEFLRNLQLELTFMVCIGREFRDPDGLGAPVEQSYTAYVPEFLYRLSTDNLSLTP--DSIATSPOSLESHDIYHSE 840  
Acanthaster of solaris ARIS1 721 PRVYLVKVKHGSDPTVDIRGVPYRPGVSHLEAVTVETHFFPLFLRDELEMLTLFMCVIGSEF-NSGDGCLTSPENSYTAAYVSPNFYRLYTAPEAFDADDIATSTQLDISHYIHAS 840

Asterias amurensis ARIS1 841 EIHRVFLVNLKALSAMSREYITINVRFLVERTDRKRIQRDRVQDKINDPIAVHQAIVFKGCPNPNSTHVAKYVACVCDNKGEMSETNFKCERSTKGVYEEGV-PSDDAENPDQGGDSK 960  
Acanthaster of solaris ARIS1 841 EMHRTVFTNKALSARSQEYITISVFRVLERAGRRRRRAILKRDQDKVDEPLVHQITLFRGCPNPNSHVDVQKQACVCESEDKGVYSRDTFECVKLSPSLDSEKQSPVDSAKTPGESNDPG 960

Asterias amurensis ARIS1 961 EGRKGGKGVVLTAVLSTLSSVGLAVLLAVAL-- 995  
Acanthaster of solaris ARIS1 961 NDSSQGHENNSATLNTSMLVPLICITLVAASLM 995

## (B)

Asterias amurensis ARIS2 1 MAVOLET-----YFFLT-----LLTF-AILPGESEAAFQGTIDDKVDFRKNMGAEYIPEFEIVDSKANFEVLEDTLNEAEYVWDFEPYNNMKNATVADPYTDINP 120  
Acanthaster of solaris ARIS2 1 KLVEDRTVCNPDHLRGLHTLVTHATMLLPRLTVLLAFLGALFGQSAARFGDAIEDKVSDFRNMGQAYISQFEIVDSSTTKFQVLEDTLNEPEYVWDFQYQYGAEGLTADTQTGSIHP 120

Asterias amurensis ARIS2 121 DNTGECSSVMFDAPYNQDVAAGYFSDVGNFISRNVSILDDQSGNDSVHKRLFTSYVRQGSFTDIDSQVNIQRDRYLSFNQNFQFFNCTNTMGENIWSFANTTDTIEFRSTIYFTN 240  
Acanthaster of solaris ARIS2 121 ENTGECSSVIFSAPEYQENVTGVYFSDQGNFVSRNVSILDDQSGANKRLFTSYVRQGSFTDIDSQVNIQRDRYLSFNQNFQFFNCTNTMGENIWSFANTTDTIEFRSTIYFTN 240

Asterias amurensis ARIS2 241 VRPVPADPAGTKGMSWVTSNVDLIYRLNRVAIVNFVSSALVKPVLDFVIEPFDQAQGD--PEPNRASIEIQFOTTIESAGGELLALNATSLQYIARDQVAGENSSNLDDLIYIPDG 360  
Acanthaster of solaris ARIS2 241 VRPVPADPAGTKGMSWVTSNVDLIYRLNRVAIVNFVSSALVKPVLDFVIEPFDQAQGD--PEPNRASIEIQFOTTIESAGGELLALNATSLQYIARDQVAGENSSNLDDLIYIPDG 360

Asterias amurensis ARIS2 361 SQCCQYVETDKCRQTLWLFKVIDLNVGIVENDLPIDATGTFKFRFAKHQCVDATEANPSCVDLGLDPTFISLEVTIQTVVQVVDATKDSPTVILVMSGANGEDLRGGVDPPTRGVNLH 480  
Acanthaster of solaris ARIS2 361 TOCCQYVGTARCRQIWNFNFLVLELDDVVTDDMPIDATGTFKFLFAKYQCNPDTEKPIDCIEMNVDPILTISLEVTIQTVVQVVDSTSDPTIQLVSLTNGNEDLRSG--GRRGVNLH 480

Asterias amurensis ARIS2 481 EDVNIIVKYTEFLRSDFDLTLFMVCKEDKTNSPGGCLDVEISNRVYAYQSEFFRYAYAVEGGEVNT--SYNTDLDNDNTVQSLTNNAYDSANEVYNGFTNTALSQERLSYITITTV 600  
Acanthaster of solaris ARIS2 481 EPVSIQVYFPEFLRRDFDLTLFMVCKSNLSSDAGCLSAQAQRYVAYSANAFQVAVETDNGDSTTVYDSSSLTNDNKVQKLTNAYDSTNEVYNGFTNTALSQERLSYITITTV 600

Asterias amurensis ARIS2 601 FRLIEKPGRRRR--ANQPQQMSTRFSGMGGA-GLVYPPRRHRRRGGIMSAALPQGHVEMTFNGCPENSTFSPASYHCECNRVGETYSKETFQCGSKSLAPDQEIINRDKV- 720  
Acanthaster of solaris ARIS2 601 FRLVQKPSARRRRAIARTQLITLSSLDGVERMARGLMAYGLPRARTRRDIMEAVADPQGHYITLTFNGCPANSTFNAGTYHCQCDRESERYSTESFTQCGPKSLPPGLAVPVDVEDLQ 720

Asterias amurensis ARIS2 721 EPDSGRMPSSGISTAPDSALFYAVLTVWFTGFLCLL-- 758  
Acanthaster of solaris ARIS2 721 -PDSSGAP----SIVANNALFVCFIV--SILIMYVK 758

## (C)

Asterias amurensis ARIS3 1 -----MFFYGGMARLFFG---LVLVLLVRMSRA--GFGDDISQDNEEDNRFANMGQVTKDSFDVESGVVTLQNLVQDTEGIEKIWIILDFQYPRNIDAMPVNELDGQLMMDQ 120  
Acanthaster of solaris ARIS3 1 RRLRLVRLTFTVRLGWHCRCGPMSPFNGMWCILTLVLAQLSRALGAFGDDISQDNEEDNRFANMGQVTKDIFDVQSGNVTLQNLVQDTEGIEKIWIILDFQYPRNIDAMPVNELDGQLMMDQ 120

Asterias amurensis ARIS3 121 TSECSVYETASWNDYFNDYFTDKDSTGLASKKLTQFTRGSLNGDGF-RDNKIFTGDMGLFFTKDSINEDFIWQMTDITDDEIEYRKLTYTNRPKDPLVSTGGISFVQSHIELI 240  
Acanthaster of solaris ARIS3 121 TSACSNVYEDADWDTFFNDSYIQDKGSSLTSKNLFITIKRGDIDTIGIMRNDKIIFQGDMAITFANCKDSNEEYVWEMTAITSDEIYRKLTYATNIRPKDPEPTGGVSVFQSHIELI 240

Asterias amurensis ARIS3 241 WRLSRVLTKFLSSTALIRPLEFARVAVYDALDRAVPTQSALHIFRFTVVDSDTQMLSYNTDLSLVYDPDNTNHNAINADYQDPDGLDAAPDCEFKLDEGTQTLQCCQQTWFEKLVLD 360  
Acanthaster of solaris ARIS3 241 WRISRSVLAKFLSSTALIKPVEFARVAVYDEQNRVPTQSALHIFRFTVVDSDTQMLSYNTDLSLVYDPDNTNHNAINADYQDPDGLDAAPDCEFKLDEGTQTLQCCQQTWFEKLVLD 360

Asterias amurensis ARIS3 361 VDTSGQVQDNRPVDAAGTFEFLYLYGCEKTNNEFDKATCQVGTDPKASALITQTTVFIQDMEDDQVITLQSLTGAENEDPSYGTGSRGVAHKETYDLKVKFSPALLRKDYDLDLL 480  
Acanthaster of solaris ARIS3 361 IDTSTQVQDNRPVDAAGTFEFLYLYGCEKTNNEFDKATCQVGTDPKASALITQTTVFIQDMEDDQVITLQSLTGAENEDPSYGTGSRGVAHKETYDLKVKFSPALLRKDYDLDLL 480

Asterias amurensis ARIS3 481 LFMVCKGEEYASDQYAGQCEAPSSDRYVAHRDGSFSPFVSNENGT-TLLDEYNSSHVAEDTYQPLESQEYLREDESQALAVPVHOSKFNVALSGESAVYITTYVRLVERLQVPL 600  
Acanthaster of solaris ARIS3 481 LFMVCKGQYASDQYAGQCEAPSEDYVAHYDATFNPIRITDDNGTVILNAYNTHTVENDVQQLHLQEYLR-ESGETLAIPVHRSTFYNLALSAESDYITTYVRLVRIID--TQG 600

Asterias amurensis ARIS3 601 RKRATLPHKMHVILSKSVMGRTRTKGKSTGTHIERSRDEVEDSARDTHGHAVPFTMGCPEDSEHIEQLDCRCVKEYSKLTFCLEPGEVDEEETNEVQETNDEDDLLKPKGSK 720  
Acanthaster of solaris ARIS3 601 RKRRAALPHMQDILAKSVVGRAGVGRGTGTHIERSRDEVEDSARDTHGHAVPFTMGCPEDSEHIEQLDCRCVKEYSKLTFCLEPGEVDEEETNEVQETNDEDDLLKPKGSK 720

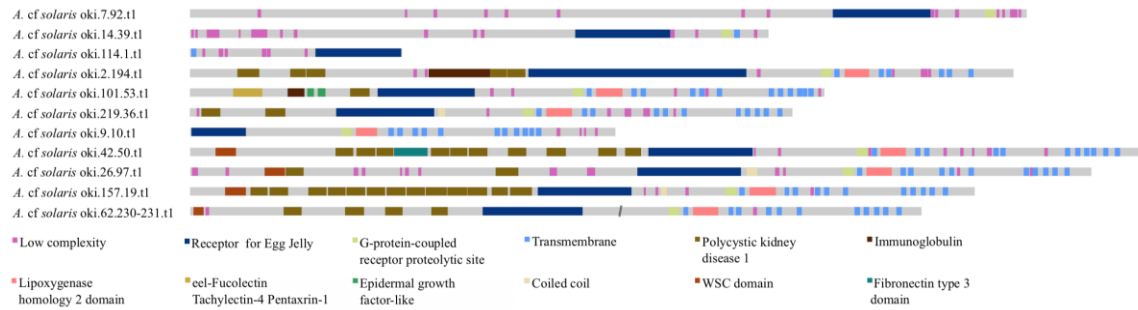
Asterias amurensis ARIS3 721 TGMAPATSCVTLVITANAIIVLM-RMH 749  
Acanthaster of solaris ARIS3 721 TAHAQCIACPSILLANSLFLKLDY 749







**Appendix K. Domain architecture comparison among eleven predicted receptor for egg jelly (REJ) genes from the *Acanthaster cf. solaris* genome. Domains of each predicted gene were acquired from the programs SMART and Pfam. Predicted genes oki.62.230 and oki.62.231 were concatenated together for the diagram**























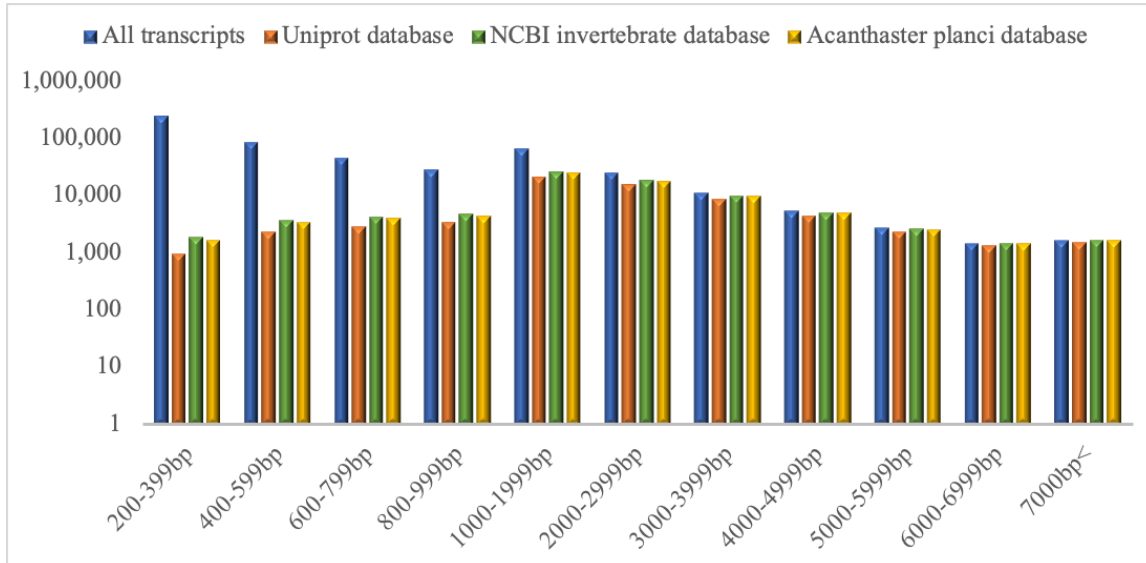


## Appendix M. Summary statistics for the reference transcriptome assembled from all *Cryptasterina hystera* and *C. pentagona* individuals

Summary statistics	Species	Tissue	Individual	Value
Cleaned Illumina reads				593,663,412
Total transcripts in reference				525,005
Total genes				286,387
Total ORF transcripts				102,511
GC content (%)				42.93
Median transcript length (nt)				424
Average transcript length (nt)				818
Transcript contig N50 (nt)				1,432
BLASTX - SwissProt				78,332
BLASTP - SwissProt				65,901
BLASTP - NCBI invertebrate database				81,651
BLASTP - <i>A. planci</i> database				79,049
eggNOG				63,116
HMMER - Pfam				66,796
TMHMM				20,058
Unique transcripts from all BLAST searches				95,355
Total <i>C. hystera</i> transcripts				279,634
Total <i>C. hystera</i> ORF				67,574
Total <i>C. pentagona</i> transcripts				371,846
Total <i>C. pentagona</i> ORF				78,751
	<i>Cryptasterina hystera</i>	ovotestis	hermaphrodite 1	61,310,066
			hermaphrodite 2	68,655,552
			hermaphrodite 3	56,712,146
			hermaphrodite 4	69,824,173
	<i>Cryptasterina pentagona</i>	ovary	female 1	69,438,433
			female 2	72,168,663
			female 3	67,472,449
		testis	male 1	63,631,112
			male 2	64,450,818

A reference transcriptome was built from nine RNA-seq libraries (four *C. hystera* and five *C. pentagona*) with a minimum phred score of 33 and a total of 593 million trimmed reads. The reference transcriptome was composed of 525,005 transcripts from which Trinity reported 286,387 genes and Transdecoder found 102,511 transcripts with open reading frames (ORFs). At the species level, the assembly of *C. hystera* had 279,634 transcripts from which 67,574 had ORFs. The *C. pentagona* assembly had 371,846 genes from which 78,751 had ORFs. A blast search of the transcripts with ORFs with a minimum expectation score of  $e = 1 \times 10^{-20}$  had 24,743 (31% of total ORFs) of *C. pentagona* transcripts as a match to 53,736 (79% of total ORFs) of *C. hystera* transcripts. The larger number of transcripts assembled in *C. pentagona* than in *C. hystera* may be due to the higher expected heterozygosity in *C. pentagona*, in which the additional transcripts may reflect a second allele with differing SNPs.

**Appendix N. Transcript length of reference transcriptome and annotated transcripts (y-axis = number of transcripts, x-axis = length of transcripts)**



The reference transcriptome, or the predicted peptide candidates of the reference transcriptome acquired with Transdecoder (Haas et al., 2013), were searched for homologous hits using a custom Uniprot database which included Kyoto Encyclopedia of Genes and Genomes (KEGG) (Ogata et al., 1999) and Gene Ontology (GO) annotations, the NCBI *Acanthaster planci* protein database, and the NCBI invertebrate reference database. The translated sequences were also annotated with the protein domains predicted by HMMER (Finn et al., 2011) and the transmembrane helices predicted by TMHMM (Krogh et al., 2001).

**Appendix O. Counts of sequence length coverage (“count in bin”) and counts of transcripts that have at least the sequence percentage length coverage at each level (“> bin below”; e.g. 11,446 transcripts have a hit percentage cover of 90% or higher) for the reference transcriptome with the *Acanthaster planci* reference database and the UniProt reference database**

Reference	Hit percentage cover in bin	Count in bin	> Bin below
<i>Acanthaster</i>	100	10095	10095
	90	1351	11446
	80	1017	12463
	70	925	13388
	60	1019	14407
	50	875	15282
	40	796	16078
	30	715	16793
	20	608	17401
	10	389	17790
Uniprot	100	3874	3874
	90	1679	5553
	80	1204	6757
	70	1077	7834
	60	979	8813
	50	1112	9925
	40	1080	11005
	30	1074	12079
	20	867	12946
	10	317	13263



## Appendix P. List of the most expressed annotated DE transcripts from each comparison

Differential Expression comparison	Ontology	Trinity gene name	Full name	Potential isoform	NCBI reference match	Average TPM Herm	Average TPM Female	Average TPM Male
Female vs Male	Female	TRINITY_DN52374_c1_g1_i1	H2BL4-like	Late histone H2B.L4	487.6705	9049.796	2.1565	
Female vs Male	Female	TRINITY_DN60856_c4_g4_i1	H2B7	Histone H2B 7	966.28	4606.251	1.5755	
Female vs Male	Female	TRINITY_DN54712_c4_g1_i1	H2A	Histone H2A	22108863	0	2880.168	0.2465
Female vs Male	Female	TRINITY_DN60995_c3_g3_i2	LVN1	Development-specific protein LVN1.2	22080400	259.3858	1558.954	0.3095
Female vs Male	Female	TRINITY_DN41918_c7_g1_i1	H1FV	histone_H1.0-like	22101248	151.5648	1419.127	0.463
Female vs Male	Female	TRINITY_DN64153_c1_g3_i1	PTPRK	receptor-type_tyrosine-protein_phosphatase_kappa	13415647	70.7425	1223.345	0.5945
Female vs Male	Female	TRINITY_DN48178_c2_g1_i2	H4	Histone H4	22110516	86.749	1166.145	0.3215
Female vs Male	Female	TRINITY_DN56872_c2_g2_i1	CALD1	caldesmon-like_isoform_X4	22109039	0.03125	993.693	0.1755
Female vs Male	Female	TRINITY_DN54946_c0_g1_i13	BHMT1	Betaine--homocysteine S-methyltransferase 1	22108462	85.2015	960.3173	0.2885
Female vs Male	Female	TRINITY_DN62347_c1_g1_i8	H3	Histone H3, embryonic	22082253	36.75525	728.542	0
Female vs Male	Female	TRINITY_DN64720_c3_g1_i1	EBR1	Egg receptor for bindin	22084205	10.63475	498.5953	1.703
Female vs Male	Female	TRINITY_DN64410_c2_g1_i4	SC6A5	Sodium- and chloride-dependent glycine transporter 2	22099145	73.19775	281.1847	0
Female vs Male	Female	TRINITY_DN65193_c3_g1_i4	HYAL	Hyalin	22088734	1.56675	50.06467	1.361
Female vs Male	Female	TRINITY_DN42075_c5_g2_i1	UNIV	Univin	22089149	0.747	38.03367	0.0145
Female vs Male	Female	TRINITY_DN64428_c0_g2_i5	FBP1	Fibropellin-1	22081480	1.19225	10.79667	0
Female vs Male	Male	TRINITY_DN51054_c1_g1_i4	Bindin			6854.114	4.202333	22958.83
Female vs Male	Male	TRINITY_DN63978_c1_g1_i4	NCKX3	Sodium/potassium/calcium exchanger 3	22105073	100.3945	1.378333	1192.771
Female vs Male	Male	TRINITY_DN64348_c1_g1_i2	GCY	guanylate cyclase	22107162	308.5743	1.443667	1089.988
Female vs Male	Male	TRINITY_DN47852_c2_g1_i7	SP63	63 kDa sperm flagellar membrane protein	22090393	0.1055	0.062	907.0715
Female vs Male	Male	TRINITY_DN61421_c0_g3_i5	HCN4	Potassium/sodium hyperpolarization-activated cyclic nucleotide-gated channel 4	22109179	71.043	0.016667	357.9895
Female vs Male	Male	TRINITY_DN61351_c3_g1_i4	CTSR1	Cation channel sperm-associated protein 1	22081596	44.93325	0.343333	258.1955

Differential Expression comparison	Ontology	Trinity gene name	Full name	Potential isoform	NCBI reference match	Average TPM Herm	Average TPM Female	Average TPM Male
Female vs Male	Male	TRINITY_DN54466_c2_g1_i3	HCN1	Potassium/sodium hyperpolarization-activated cyclic nucleotide-gated channel 1	22100809	31.87625	0.064667	242.379
Female vs Male	Male	TRINITY_DN54018_c2_g2_i6	CTSR3	Cation channel sperm-associated protein 3	22107721	20.882	0.795667	209.13
Female vs Male	Male	TRINITY_DN62496_c2_g1_i9	SL9C1	Sodium/hydrogen exchanger 10	22089278	0.03475	0.549667	133.417
Female vs Male	Male	TRINITY_DN61780_c4_g1_i2	REJ1		22098115	12.0485	0.271667	86.698
Female vs Male	Male	TRINITY_DN61917_c0_g1_i4	PDE10	cAMP and cAMP-inhibited cGMP 3',5'-cyclic phosphodiesterase 10A	22081884	10.36225	0.250667	82.2745
Female vs Male	Male	TRINITY_DN59859_c4_g1_i4	ZBP1/sp38	Zona pellucida-binding protein 1	22082164	61.39575	0.109	81.1285
Female vs Male	Male	TRINITY_DN60562_c8_g1_i1	EFCB9	EF-hand calcium-binding domain-containing protein 9	22094445	0	0.032667	78.1645
Female vs Male	Male	TRINITY_DN63488_c1_g2_i6	EFCB5	EF-hand calcium-binding domain-containing protein 5	22089636	28.75425	0.011	75.1935
Female vs Male	Male	TRINITY_DN50149_c0_g1_i11	HCN2	Potassium/sodium hyperpolarization-activated cyclic nucleotide-gated channel 2	22080165	1.10725	0.040333	21.17
Female vs Male	Male	TRINITY_DN63337_c1_g2_i9	REJ3		22107069	4.73775	0.013	1.1535
Hermaphrodite vs Female	Female	TRINITY_DN54712_c4_g1_i1	H2A	Histone H2A	22108863	0	2880.168	0.2465
Hermaphrodite vs Female	Female	TRINITY_DN63842_c1_g1_i1	VIT6	Vitellogenin-6	22087199	0	1199.405	396.744
Hermaphrodite vs Female	Female	TRINITY_DN56577_c1_g3_i4	RL21	60S ribosomal protein L21	22079484	0.0205	734.2237	236.5215
Hermaphrodite vs Female	Female	TRINITY_DN47674_c2_g1_i3	RL22	60S ribosomal protein L22	22100623	0.04875	712.336	1432.355
Hermaphrodite vs Female	Female	TRINITY_DN45088_c10_g1_i1	RS14B	40S ribosomal protein S14b {ECO:0000305}	22102036	0.0675	628.8693	423.657
Hermaphrodite vs Female	Female	TRINITY_DN42547_c4_g2_i2	RS12	40S ribosomal protein S12	22093230	0.052	500.358	611.9935
Hermaphrodite vs Female	Female	TRINITY_DN64720_c3_g1_i1	EBR1 short	Egg receptor for bindin	22084205	10.63475	498.5953	1.703

Differential Expression comparison	Ontology	Trinity gene name	Full name	Potential isoform	NCBI reference match	Average TPM Herm	Average TPM Female	Average TPM Male
<b>Hermaphrodite vs Female</b>	Female	TRINITY_DN40387_c2_g1_i11	NOTCH1	neurogenic_locus_notch_homolog_protein_1-like	22098497	0	452.579	0.162
<b>Hermaphrodite vs Female</b>	Female	TRINITY_DN57175_c6_g1_i3	FUCL5	Fucolectin-5	22098497	0.0125	341.7633	0.0865
<b>Hermaphrodite vs Female</b>	Female	TRINITY_DN54726_c6_g1_i8	RL36A	Ribosomal protein rpl-36.A {ECO:0000305}	20606136	0.0185	296.4837	164.5075
<b>Hermaphrodite vs Female</b>	Female	TRINITY_DN42496_c2_g1_i3	PPIA	Peptidyl-prolyl cis-trans isomerase	26276386	0.1275	294.687	406.084
<b>Hermaphrodite vs Female</b>	Female	TRINITY_DN64198_c2_g1_i4	RL10	60S ribosomal protein L10 {ECO:0000305}	22092450	0.015	274.774	59.273
<b>Hermaphrodite vs Female</b>	Female	TRINITY_DN53609_c1_g1_i10	NOTC3	Neurogenic locus notch homolog protein 3	22098544	0	244.9077	0.1725
<b>Hermaphrodite vs Female</b>	Female	TRINITY_DN52003_c4_g3_i6	SUSD2	Sushi domain-containing protein 2	22089467	0.034	237.622	132.892
<b>Hermaphrodite vs Female</b>	Female	TRINITY_DN54726_c6_g1_i2	RL44	60S ribosomal protein L44	0.0285	225.262	183.4595	
<b>Hermaphrodite vs Female</b>	Female	TRINITY_DN64542_c1_g2_i2	GLOL	Highly reducing polyketide synthase gloL {ECO:0000303 PubMed:23688303}	22090459	0	224.6253	0.5215
<b>Hermaphrodite vs Female</b>	Female	TRINITY_DN56951_c5_g1_i2	VIT1	Vitellogenin-1	22105422	0.00525	194.4887	65.6165
<b>Hermaphrodite vs Female</b>	Female	TRINITY_DN41776_c7_g3_i2	TCTP	Translationally-controlled tumor protein homolog	22095198	0.2975	180.0323	217.24
<b>Hermaphrodite vs Female</b>	Female	TRINITY_DN57654_c2_g1_i1	RIR2	Ribonucleoside-diphosphate reductase subunit M2	22090701	0.011	179.336	42.436
<b>Hermaphrodite vs Female</b>	Female	TRINITY_DN47418_c0_g1_i1	PSA1	Proteasome subunit alpha type-1	22108919	0	166.7177	34.816
<b>Hermaphrodite vs Female</b>	Female	TRINITY_DN46639_c4_g1_i3	SODC	Superoxide dismutase [Cu-Zn]	22094823	0	165.3217	14.6545
<b>Hermaphrodite vs Female</b>	Female	TRINITY_DN54865_c0_g1_i15	FCGBP	IgGfc-binding protein	22089467	0	118.0777	0.444

Differential Expression comparison	Ontology	Trinity gene name	Full name	Potential isoform	NCBI reference match	Average TPM Herm	Average TPM Female	Average TPM Male
<b>Hermaphrodite vs Female</b>	Hermaphrodite	TRINITY_DN64324_c1_g1_i1	BIND	Bindin	22099883	2955.055	0.034	276.6985
<b>Hermaphrodite vs Female</b>	Hermaphrodite	TRINITY_DN63842_c1_g1_i10	VIT6	Vitellogenin-6	22087199	1683.643	0	0
<b>Hermaphrodite vs Female</b>	Hermaphrodite	TRINITY_DN51457_c7_g1_i13	.	ly6/PLAUR_domain-containing_protein_2-like	22100632	704.574	0	0
<b>Hermaphrodite vs Female</b>	Hermaphrodite	TRINITY_DN52108_c5_g1_i4	TYB12	Thymosin beta-12	423.0395	0.024	0.149	
<b>Hermaphrodite vs Female</b>	Hermaphrodite	TRINITY_DN43452_c10_g1_i3	RPS6	40S ribosomal protein S6	22108234	223.0313	0	7.652
<b>Hermaphrodite vs Female</b>	Hermaphrodite	TRINITY_DN60366_c4_g2_i12	G3P   GAPDH	Glyceraldehyde-3-phosphate dehydrogenase	22101615	105.6035	0	0
<b>Hermaphrodite vs Female</b>	Hermaphrodite	TRINITY_DN49178_c4_g1_i4	RPS11	40S ribosomal protein S11	22096415	81.96825	0	8.943
<b>Hermaphrodite vs Female</b>	Hermaphrodite	TRINITY_DN62660_c4_g1_i11	GGNBP2	Gametogenetin-binding protein 2	22102167	70.46125	0.003333	0
<b>Hermaphrodite vs Female</b>	Hermaphrodite	TRINITY_DN41235_c6_g1_i1	MSMO1	Methylsterol monooxygenase 1	22087102	69.2975	0	0.039
<b>Hermaphrodite vs Female</b>	Hermaphrodite	TRINITY_DN55784_c2_g1_i3	GGT3	Glutathione hydrolase 3	22091163	48.6665	0	7.7065
<b>Hermaphrodite vs Female</b>	Hermaphrodite	TRINITY_DN64754_c2_g1_i4	DYSF	Dysferlin	22096607	20.6055	0	0
<b>Hermaphrodite vs Male</b>	Male	TRINITY_DN64324_c1_g1_i4	BIND	Bindin	22099883	0.00825	1.983667	6798.144
<b>Hermaphrodite vs Male</b>	Male	TRINITY_DN47674_c2_g1_i3	RL22	60S ribosomal protein L22	22100623	0.04875	712.336	1432.355
<b>Hermaphrodite vs Male</b>	Male	TRINITY_DN44171_c0_g1_i2	NDUA4	Cytochrome c oxidase subunit NDUFA4	0.01725	69.42533	805.833	
<b>Hermaphrodite vs Male</b>	Male	TRINITY_DN42547_c4_g2_i2	RS12	40S ribosomal protein S12	22093230	0.052	500.358	611.9935

Differential Expression comparison	Ontology	Trinity gene name	Full name	Potential isoform	NCBI reference match	Average TPM Herm	Average TPM Female	Average TPM Male
<b>Hermaphrodite vs Male</b>	Male	TRINITY_DN52454_c8_g1_i1	EFHD1	EF-hand domain-containing protein D1	22090015	0	0.517667	509.706
<b>Hermaphrodite vs Male</b>	Male	TRINITY_DN59775_c3_g2_i11	SYCP3	Synaptonemal complex protein 3	22082719	0	3.133667	437.1525
<b>Hermaphrodite vs Male</b>	Male	TRINITY_DN42496_c2_g1_i3	PPIA	Peptidyl-prolyl cis-trans isomerase	26276386	0.1275	294.687	406.084
<b>Hermaphrodite vs Male</b>	Male	TRINITY_DN63842_c1_g1_i1	VIT6	Vitellogenin-6	22087199	0	1199.405	396.744
<b>Hermaphrodite vs Male</b>	Male	TRINITY_DN61807_c3_g2_i4	RL17	60S ribosomal protein L17	22104718	0.56475	147.3943	306.4545
<b>Hermaphrodite vs Male</b>	Male	TRINITY_DN47290_c5_g2_i15	FRIS	Soma ferritin	22088322	0	154.6387	277.302
<b>Hermaphrodite vs Male</b>	Male	TRINITY_DN62750_c5_g1_i3	ROP1L	Ropporin-1-like protein	22083804	0.01575	13.22667	262.52
<b>Hermaphrodite vs Male</b>	Male	TRINITY_DN59199_c1_g1_i4	GBLP	Guanine nucleotide-binding protein subunit beta-2-like 1	22087508	0	40.433	229.2845
<b>Hermaphrodite vs Male</b>	Hermaphrodite	TRINITY_DN63948_c1_g2_i1	COX1	Cytochrome c oxidase subunit 1	5087.015	16.71633	22.925	
<b>Hermaphrodite vs Male</b>	Hermaphrodite	TRINITY_DN63842_c1_g1_i10	VIT-like	Vitellogenin like	22087199	1683.643	0	0
<b>Hermaphrodite vs Male</b>	Hermaphrodite	TRINITY_DN60856_c4_g4_i1	H2B7	Histone H2B 7	966.28	4606.251	1.5755	
<b>Hermaphrodite vs Male</b>	Hermaphrodite	TRINITY_DN52374_c1_g1_i1	H2BL4	Late histone H2B.L4	487.6705	9049.796	2.1565	
<b>Hermaphrodite vs Male</b>	Hermaphrodite	TRINITY_DN61703_c0_g1_i8	TBB	Tubulin beta chain	22082185	450.208	7.081667	3.008
<b>Hermaphrodite vs Male</b>	Hermaphrodite	TRINITY_DN52108_c5_g1_i4	TYB12	Thymosin beta-12	423.0395	0.024	0.149	
<b>Hermaphrodite vs Male</b>	Hermaphrodite	TRINITY_DN42547_c4_g2_i3	RS12	40S ribosomal protein S12	22093230	378.6335	159.966	1.1825

Differential Expression comparison	Ontology	Trinity gene name	Full name	Potential isoform	NCBI reference match	Average TPM Herm	Average TPM Female	Average TPM Male
<b>Hermaphrodite vs Male</b>	Hermaphrodite	TRINITY_DN40467_c8_g1_i2	RS23	40S ribosomal protein S23	11679331	375.421	6.277667	1.1555
<b>Hermaphrodite vs Male</b>	Hermaphrodite	TRINITY_DN54712_c4_g1_i7	H2A	Histone H2A	22108863	262.1318	761.3043	0.564
<b>Hermaphrodite vs Male</b>	Hermaphrodite	TRINITY_DN60995_c3_g3_i2	LVN1	Development-specific protein LVN1.2	22080400	259.3858	1558.954	0.3095
<b>Hermaphrodite vs Male</b>	Hermaphrodite	TRINITY_DN57371_c1_g5_i4	H1D	Histone H1-delta	22092438	234.2978	0	0

The female individuals of *C. pentagona* had 942 transcripts DE with *C. hystera* and 209 transcripts DE within the top 1000 most expressed transcripts. In the comparison of *C. pentagona* females with *C. hystera*, the top most expressed genes were located in the nucleus (histone H2A, 133 aa; superoxide dismutase [Cu-Zn], 152 aa), cytoplasm (60S ribosomal protein L21, L22, and L44 with 153, 139 and 38 amino acids; 40S ribosomal protein S14b and S12 with 152 and 142 aa; ribosomal protein rpl-36, 133 aa; peptidyl-prolyl cis-trans isomerase, 165 aa; highly reducing polyketide synthase gloL, 486 aa; translationally-controlled tumor protein homolog, 116 aa; proteasome subunit alpha type-1, 283 aa), extracellular region (Fucolectin-5, 202 aa; vitellogenin-1, 1594; vitellogenin-6, 1463 aa; IgGFc-binding protein, 258 aa), cell membrane (neurogenic locus notch homolog protein 1 like, 126 aa; neurogenic locus notch homolog protein 3, 235 aa; sushi domain-containing protein 2, 154 aa), and endoplasmic reticulum (ribonucleoside-diphosphate reductase subunit M2, 405 aa). Vitellogenin-6 was also DE in *C. hystera*, but both of these isoforms were not the same and the differences were not within the ORF. In addition, some of these transcripts were not as long as the reference transcripts from the NCBI marine invertebrate reference database. The functions of the DE genes included DNA replication, housekeeping, sperm recognition, oocyte development, immunity, antifungal (Xu & Gridley, 2012). EBR1 was also DE, but it was not among the top 1000 most DE. Parts of a fibropellin-like transcript were DE in female *C. pentagona* and *C. hystera*, but the gene was too short to identify. The differential expression analysis of *C. pentagona* female and males was populated with

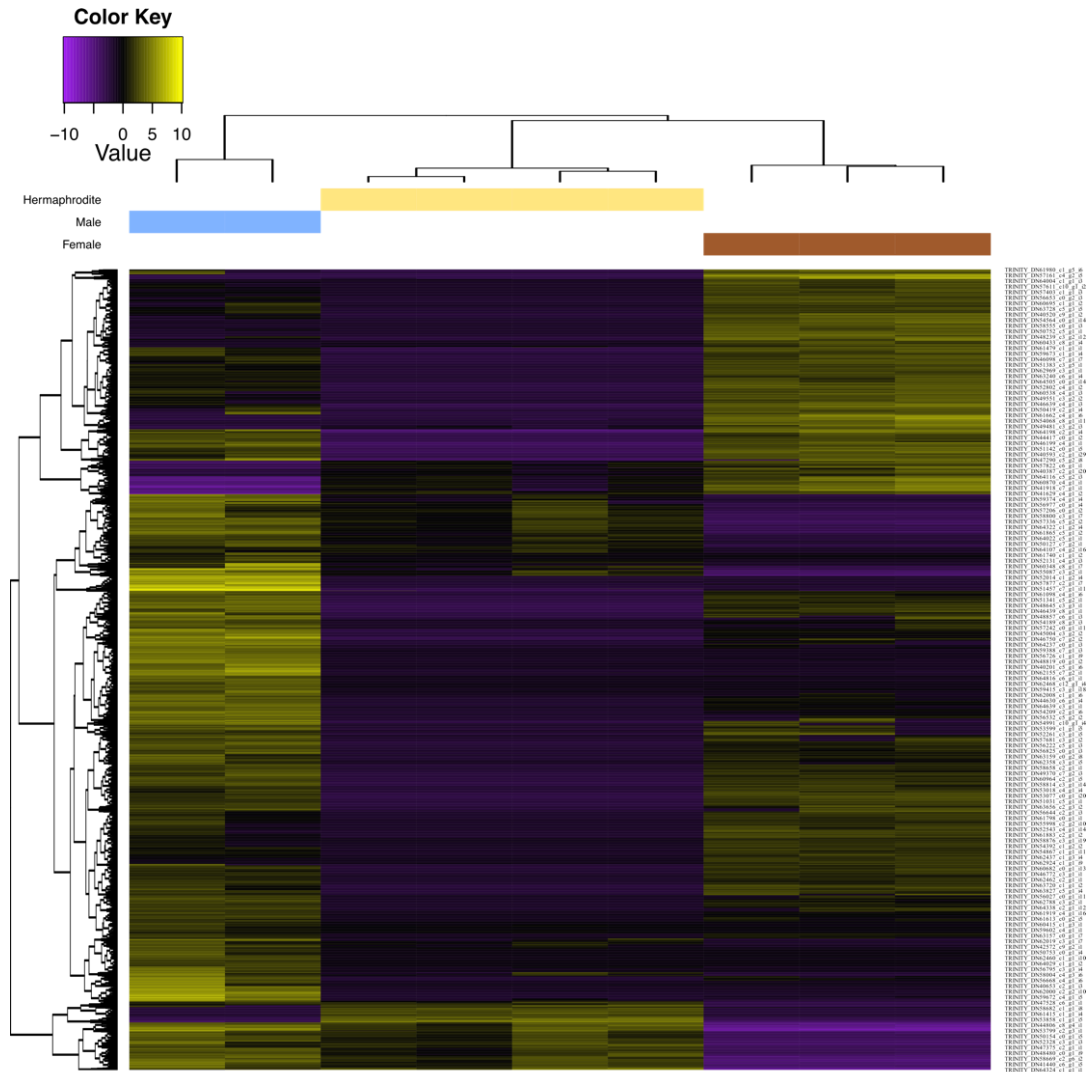
unknown genes and incomplete genes. For example, only the metazoan conserved histone genes, the development-specific protein (LVN1, 238 aa), and the receptor-4type tyrosine protein phosphate kappa (PTPRK, 135 aa) were annotated from the 20 most expressed genes outside the histone genes. Other genes including hyalin-like genes and fucoselectin-like genes were too short to discern if these genes belonged to other type of genes. The top annotated DE genes included genes linked to functions in the nucleus (histone H1, H3, H4, H2BL4, H2a, H2B7 with 276, 137, 104, 620, 133, and 93 aa respectively), extracellular region (univin, 386 aa; EBR1, 3310 aa), cytoplasm (betaine-homocysteine S-methyltransferase, 361 aa), cytoskeleton (caldesmon-like, 158 aa), and cell membrane (receptor type tyrosine protein phosphatase kappa, 135 aa; sodium and chloride dependent glycine transporter 2, 663 aa). The functions of these genes included housekeeping, sperm recognition, larval development, and oocyte maturation (Gao et al., 2017).

The male *C. pentagona* had all 1000 DE genes with *C. hystera*, and it had 791 DE genes with the female *C. pentagona*. The most expressed transcripts of the male *C. pentagona* in the *C. pentagona* female comparison were located in the membrane (sodium/potassium/calcium exchanger 3, 632 aa; guanylate cyclase, 1014 aa; and 63 kDa sperm flagellar membrane protein, 255 aa), plasma membrane (potassium/sodium hyperpolarization-activated cyclic nucleotide-gated channel 4, 547 aa; cation channel sperm-associated protein 1, 478 aa; potassium/sodium hyperpolarization-activated cyclic nucleotide-gated channel 1, 789 aa; cation channel sperm-associated protein 3, 396aa; cation channel sperm-associated protein 3, 1268 aa; REJ1, 1876; potassium/sodium hyperpolarization-activated cyclic nucleotide-gated channel 2, 269), cytoplasm (cAMP and cAMP-inhibited cGMP 3',5'-cyclic phosphodiesterase 10A, 814 aa; EF-hand calcium-binding domain-containing protein 9, 1436 aa; EF-hand calcium-binding domain-containing protein 9, 154 aa), and extracellular (Zona pellucida-binding protein 1, 1236 aa). These genes were linked to gamete-recognition, calcium transfer, fertilization, and sperm motility. The comparison of *C. pentagona* males with *C. hystera* had all of the 1000 most expressed genes. These transcripts were linked to the extracellular region (bindin, 190 aa; peptidyl-prolyl cis-trans isomerase, 165 aa; and vitellogenin-6, 1463 aa), cytoplasm (60S ribosomal protein L22, 139 aa; 40S ribosomal protein S12, 142; 40S ribosomal protein S12, 185 aa; and Soma ferritin, 174 aa), mitochondrion (EF-hand domain-containing protein D1, 210 aa;

cytochrome c oxidase subunit NDUFA4, 2087 bp), nucleus (synaptonemal complex protein 3, 209 aa; and synaptonemal complex protein 3, 320 aa), and flagellum (ropporin-1-like protein, 224 aa). These transcripts were linked to gamete interaction, oocyte development, electron transport, iron homeostasis, protein synthesis.



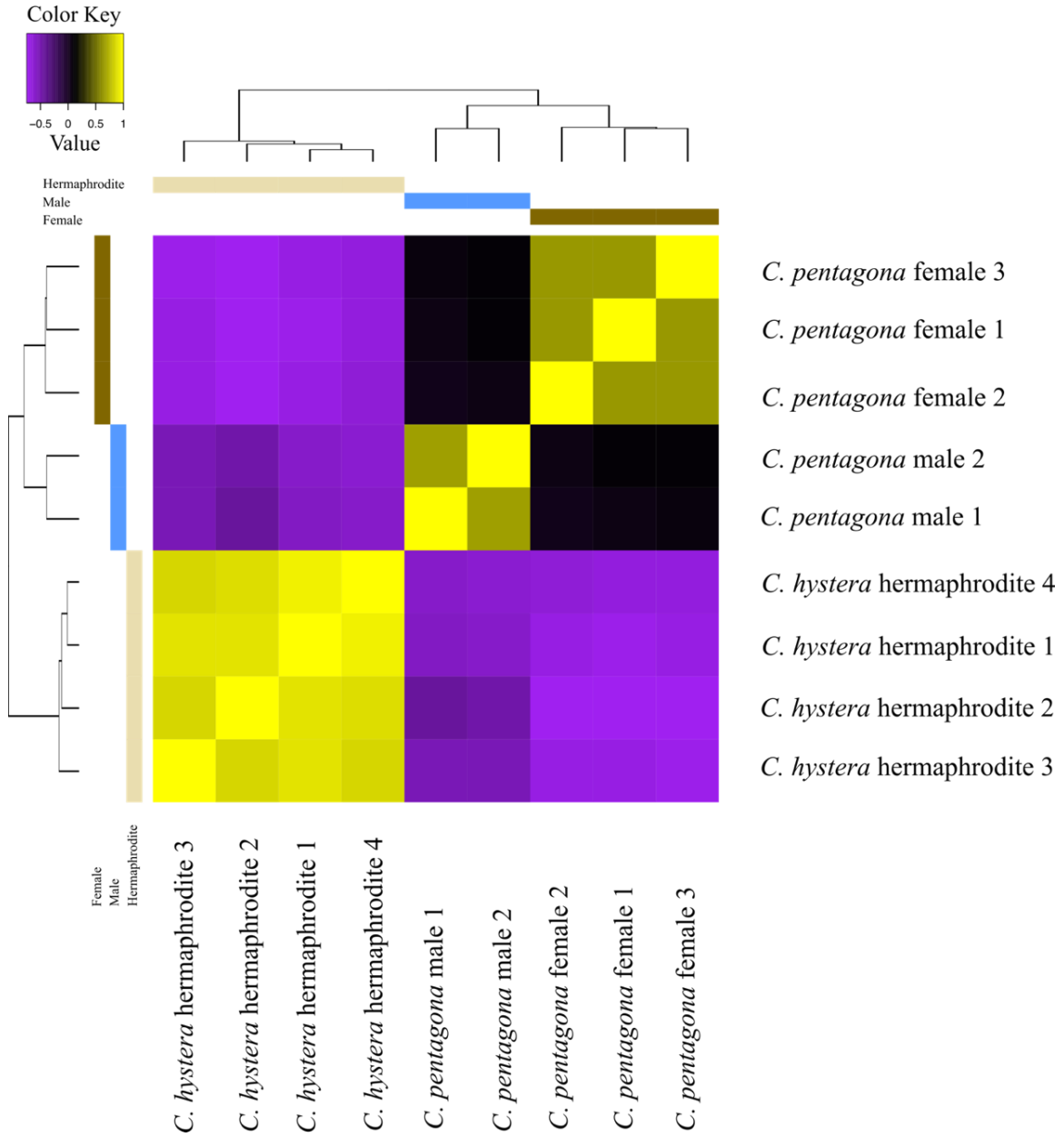
**Appendix Q. Heatmap of the top 1000 most expressed genes (from left to right: male (blue), hermaphrodite (yellow), female (brown))**



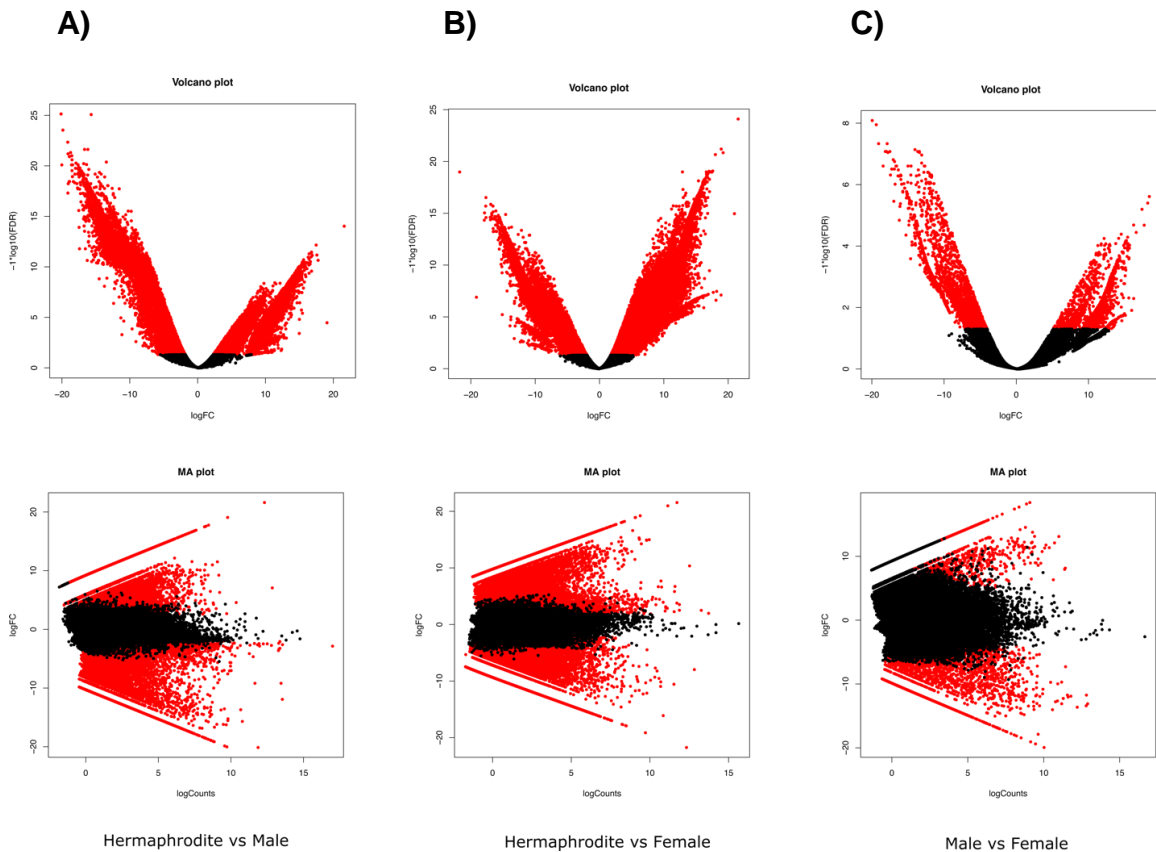
Gene expression differences among transcriptomes of the three types of tissues were assessed with DE analysis pipeline of Trinity (Grabherr et al., 2011). All nine libraries were used for the DE analysis as all nine libraries either grouped together or showed high similarity in the PCA analysis and heatmap. The grouping of each of the libraries with their corresponding tissues confirmed their closer biological similarity to their biological group rather than to other biological groups.

The number of up-regulated differential expressed genes was higher between species than between the male and female individuals of *C. pentagona*. The hermaphroditic *C. hystera* had 17,393 and 16,145 genes up-regulated compared to *C. pentagona* females and males respectively. A similarly high number of differentially expressed (DE) genes were found up-regulated in *C. pentagona* females (24,188 genes) and males (12,192 genes) compared to *C. hystera*. The DE transcript differences between the sexes of *C. pentagona* sexes were smaller, with males having 1,611 genes up-regulated and females having 675 upregulated genes.

**Appendix R. Sample correlation matrix heatmap of all nine *Cryptasterina* individuals (from left to right: hermaphrodite (light brown), male (blue), female (brown))**



**Appendix S. Volcano and MA plots of transcriptome comparisons. A) *C. hystera* vs male individuals of *C. pentagona*, B) *C. hystera* vs female individuals of *C. pentagona*, and C) male vs female individuals of *C. pentagona*. Volcano plot display the fold change (FC) and false discovery change (FDR). MA plot displays the fold change ( $\log_2$  in y-axis) of each comparison vs the average expression (log counts). Red dots are differentially expressed transcripts and black dots are transcripts that did not meet the threshold**



Significance of expression among libraries was assessed using a p-value cutoff of  $p = 0.1$  and false discovery rate (FDR) of eight-fold. A volcano plot showed the significant differential expressed genes of the comparison of each of the biological groups: A) hermaphrodite vs male, male vs female, and hermaphrodite vs female. The male comparisons in the volcano plot had the most down-regulated transcripts. The

comparison of the female and hermaphrodite transcriptomes had the most differentially expressed and up-regulated transcripts. MA plots of the biological groups showed a higher similarity between the transcriptomes of *C. pentagona* male and female individuals than the similarities found between *C. pentagona* groups and *C. hystera*.

## Appendix T. Top 1000 most expressed genes.

DE comparison	UP regulated	Number of transcripts
Hermaphrodite vs Female	Female UP	942
	Hermaphrodite UP	58
Hermaphrodite vs Male	Male UP	1000
	Hermaphrodite UP	0
Male vs Female	Male UP	791
	Female UP	209

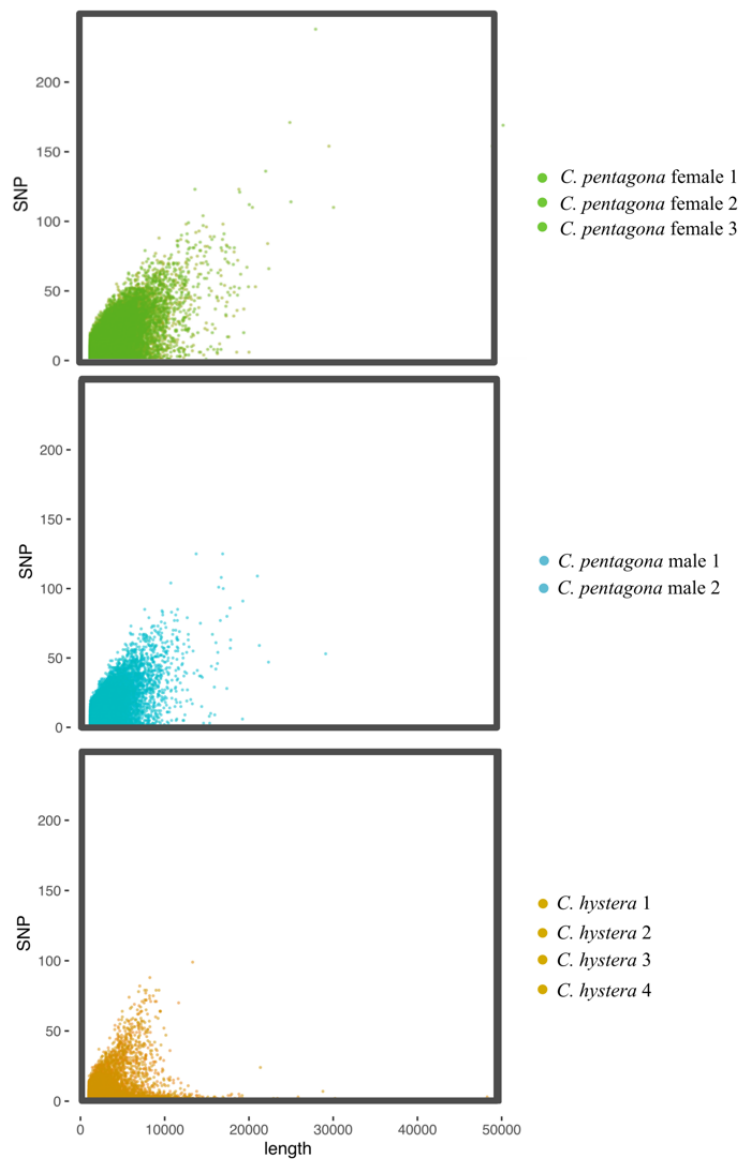
The 1000 most expressed genes per biological group had a strong representation of male transcripts in *C. pentagona*. *C. hystera* had only 58 genes differentially expressed with the female individuals of *C. pentagona* and 0 genes with the male *C. pentagona* when we looked at the top 1000 most expressed genes in the DE analysis. One third of the transcripts (17 transcripts) in the comparison between *C. hystera* and female *C. pentagona* were unknown.

The top three most expressed genes with annotations, among the 1000 most expressed gene per comparison, were *bindin*, *vitellogenin-6* and a *ly6/PLAUR* containing domain protein. Isoforms of these three genes were also expressed in either female or male individuals of *C. pentagona*. The remaining transcripts had functions in the cytoskeleton (*thymosin beta-12*, 115 amino acids (aa)), cytoplasm (*40S ribosomal protein S6* and *S11*, 247 aa and 154 aa respectively; *glyceraldehyde-3-phosphate dehydrogenase*, 333 aa; *gametogenetin-binding protein 2*, 551 aa; and *piwi-like protein 1*, 883 aa), endoplasmic reticulum (*methylsterol monooxygenase 1*, 285 aa), vacuole membrane (*glutathione hydrolase 3*, 619 aa), and plasma membrane (*dysferlin*, 2084 aa). These genes are linked to the immunity response, brood size reduction, oxidative protection caused by anoxia, sperm development, testicular development controlled by steroid, glutathione breakdown, germ cell development and movement, and skeletal muscle structure. *C. hystera* did not have any DE genes in the top 1000 most expressed genes in the DE analysis with male *C. pentagona*. Outside of the top 1000 DE genes, *C. hystera* had DE transcripts in the following categories: extracellular region (*vitellogenin-6*, 1468 aa; and a short section of *bindin*, 190 aa), plasma membrane (*ly6/PLAUR*

domain containing protein, 185 aa; dysferlin, 2085 aa), cytoskeleton (thymosin-beta 12, 116 aa), cytosol (40S ribosomal protein S6, S11 with 248 aa and 155 aa respectively; glyceraldehyde-3-phosphate dehydrogenase, 334 aa), cytoplasmic vesicle (gametogenetin-binding protein 2, 217 aa), endoplasmic reticulum membrane (methylsterol monooxygenase 1, 286 aa); and membrane (gluthanione hydrolase 3, 620 aa). The most expressed transcript was the *C. hystera* section of bindin.

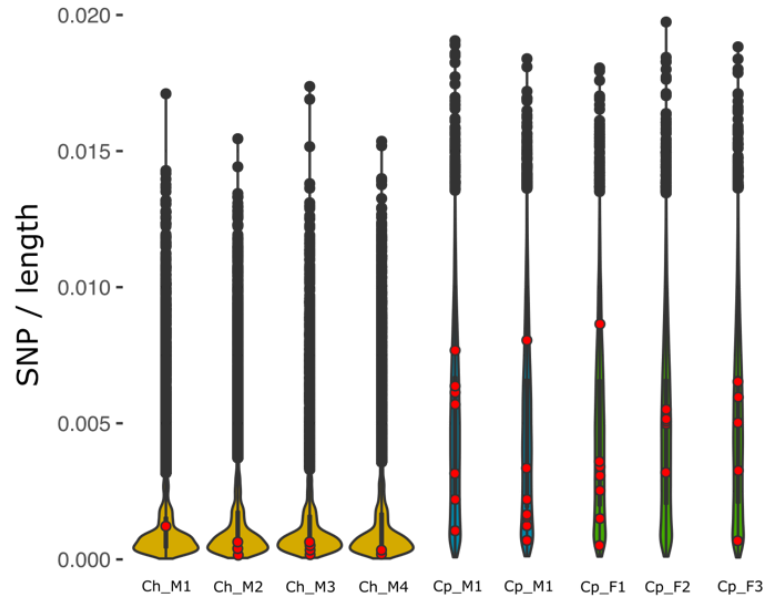
**Appendix U. SNPs of individual *C. pentagona* females, *C. pentagona* males, and *C. hystera*. A) Scatter plots of SNPs of each *Cryptasterina* spp. individual for transcripts longer than 1000 bp. Green = *C. pentagona* female, Blue = *C. pentagona* male, Orange = *C. hystera*; B) Violin plot of the ratio of SNPs of each transcript divided by the length of the transcript. Orange = *C. hystera*, Green = *C. pentagona* female, Blue = *C. pentagona* male, Red dots = Gamete recognition genes**

A)





B)



The transcriptomes of *C. pentagona* had more SNPs than *C. hystera*. The gonochoric *C. pentagona* transcriptomes had median values of 0.004 SNPs per base pair within each transcript of 1000 bp length or longer, a value that was four times higher than the median value of 0.001 SNPs per base pair in *C. hystera* (Figure S6). The number of SNPs increased with the length of the transcript in *C. pentagona*, whereas the number of SNPs was low in both longer and shorter transcripts in *C. hystera*.



























































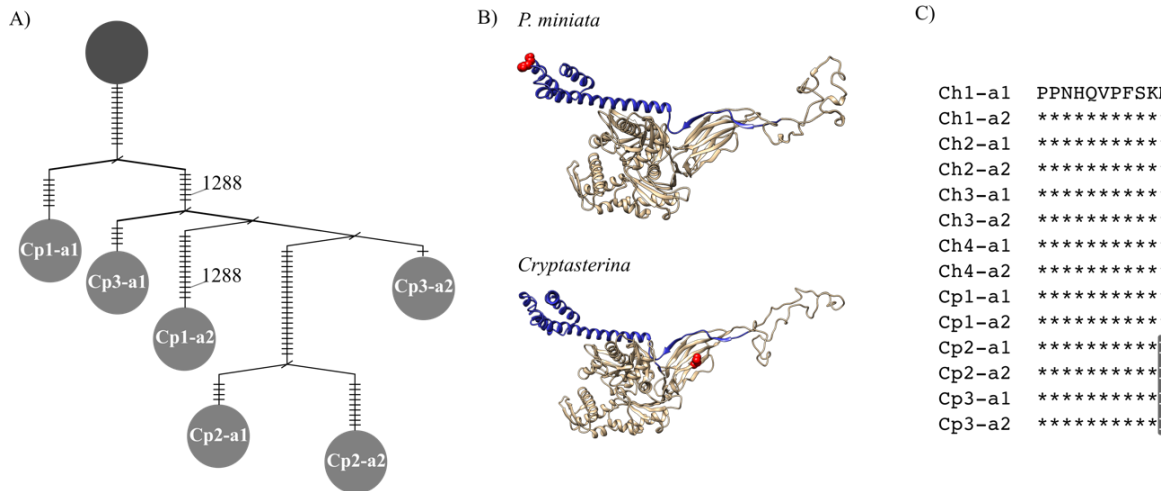






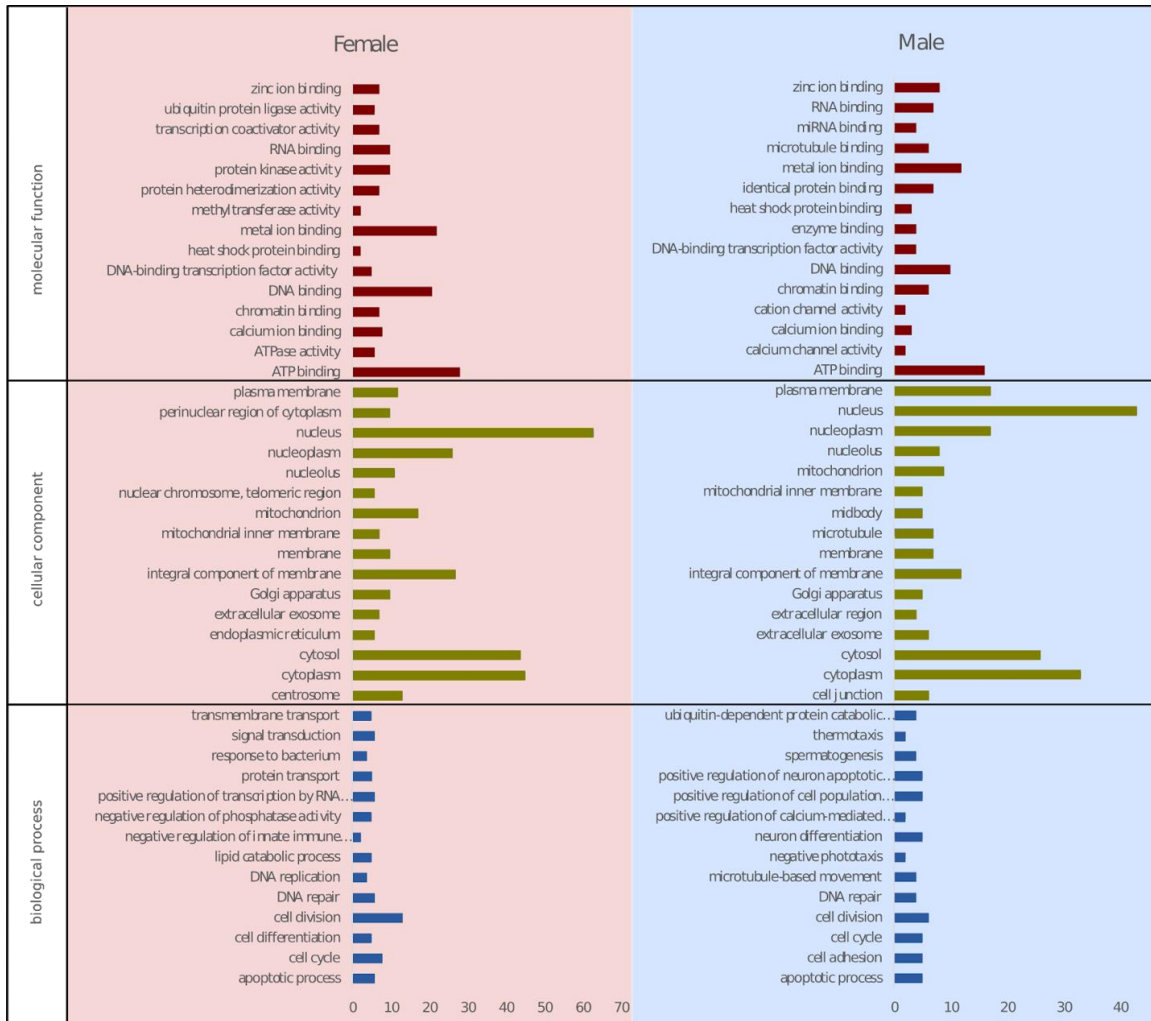
motif (VTEAP**E**PVVTEAPEPVTTKPPE**S**AETETPV in *C. pentagona* and VTEAP**K**PVVTEAPEPVTTKPPE**P**AETETPV in *C. hystera*). The *E/K* polymorphism represented a difference between the pair of alleles in one heterozygous *C. hystera* individual relative to all other gene copies, and it was not observed in previously characterized *bindin* sequences (Patiño et al., 2016). The *S/P* polymorphism was a fixed difference between the two species, and was also previously observed (Patiño et al., 2016).

**Appendix X. *OBI1* A) TCS of alleles of *C. pentagona* females, B) protein structure of *OBI1 Cryptasterina* reference protein and of *Patiria miniata* from (Hart et al., 2014). Red sections represent the codon regions under selection. Blue sections are the substrate-binding region, C) Amino acid alignment of region under selection in *Cryptasterina* individuals (Ch = *C. hystera*, Cp = *C. pentagona*)**





**Appendix Y. Gene ontology of genes with evidence of episodic diversifying selection in aBSREL. Left = female comparison (*C. pentagona* female vs *C. hystera*), right = male comparison (*C. pentagona* male vs *C. hystera*)**



For the genes with evidence of episodic diversifying selection, we looked at the GO categories of the transcripts that were only under selection in the female gene set or in the male gene set. The GO categories were diverse in both gene sets, but some of the over-represented GO functions in the female gene set were also the over-represented GO functions in the male gene set. Unique molecular function categories in the male gene set included calcium channel activity, hemi-methylated DNA-binding, and signaling receptor binding; cellular components included cation ion channel, microtubule,

and synaptic vesicle; biological processes included cell adhesion, microtubule-based movement, and pre-miRNA processing. Unique molecular function categories in the female gene set included 5-oxoprolinase (ATP-hydrolyzing) activity, alkylglycerophosphoethanolamine phosphodiesterase activity, and ATPase activity; cellular components included anaphase-promoting complex, centriole, and nuclear body; biological processes included apical protein localization, endocytosis, and response to cAMP. The over-represented categories of each gene set shared similarities between groups. The over-represented categories for molecular function were zinc ion binding, metal ion binding, DNA binding, and ATP binding. The over-represented cellular components included nucleus, cytoplasm, and cytosol. And the over-represented biological processes included cell division, cell cycle, and DNA repair.

## Appendix Z. Selection results of group comparison C. *hystera* vs C. *pentagona* A) male comparison and B) female comparison

A)

Male comparison	Gene name	MEME	aBSREL branch
OG0000295	ACBG2 Long-chain-fatty-acid--CoA ligase ACSBG2		Internal C. <i>pentagona</i>
OG0000229	ACRC Acidic repeat-containing protein	1	Internal C. <i>pentagona</i>
OG0000445	AIFM1 Apoptosis-inducing factor 1, mitochondrial	1	Internal C. <i>pentagona</i>
OG0000289	APEH Acylamino-acid-releasing enzyme	2	Internal C. <i>pentagona</i> and C. <i>hystera</i>
OG0000852	ARP10 Actin-related protein 10	1	C. <i>pentagona</i>
OG0000118	ASB8 Ankyrin repeat and SOCS box protein 8	NA	C. <i>hystera</i>
OG0000848	ATS6 A disintegrin and metalloproteinase with thrombospondin motifs 6	1	C. <i>pentagona</i>
OG0000587	AVT3B Amino acid transporter AVT3B	1	C. <i>pentagona</i>
OG0000603	BACE1 Beta-secretase 1	NA	C. <i>pentagona</i>
OG0000963	BBS2 Bardet-Biedl syndrome 2 protein homolog	NA	Internal C. <i>pentagona</i>
OG0000273	BIRC3 Baculoviral IAP repeat-containing protein 3	3	Internal C. <i>pentagona</i>
OG0000372	BMBL Protein brambleberry	1	C. <i>pentagona</i>
OG0000232	BOP1 Ribosome biogenesis protein bop1	1	Internal C. <i>pentagona</i>
OG0000696	BPI Bactericidal permeability-increasing protein	1	Internal C. <i>pentagona</i>
OG0001140	CATB Cathepsin B	1	Internal C. <i>hystera</i>
OG0000622	CCD15 Coiled-coil domain-containing protein 15	2	Internal C. <i>hystera</i>
OG0000183	CPAS1 Circularly permuted Ras protein 1	1	C. <i>pentagona</i>
OG0000540	CPNE8 Copine-8	NA	Internal C. <i>hystera</i>
OG0000111	DCAF6 DDB1- and CUL4-associated factor 6	1	Internal C. <i>pentagona</i>
OG0000538	DL Neurogenic locus protein delta	2	Internal C. <i>pentagona</i>
OG0000417	DSRAD Double-stranded RNA-specific adenosine deaminase	NA	Internal C. <i>pentagona</i>
OG0000342	ENL Protein ENL	1	C. <i>pentagona</i>
OG0000467	FBP1L Formin-binding protein 1-like	NA	C. <i>hystera</i>
OG0000599	FBX42 F-box only protein 42		Internal C. <i>pentagona</i>
OG0000113	FBX46 F-box only protein 46		Internal C. <i>pentagona</i>
OG0000128	FER Tyrosine-protein kinase Fer	2	C. <i>hystera</i>
OG0001494	FKBP2 FK506-binding protein 2	1	C. <i>pentagona</i>
OG0000730	FKBP4 Peptidyl-prolyl cis-trans isomerase FKBP4	1	Internal C. <i>pentagona</i>
OG0000768	FXJ1B Forkhead box protein J1-B	NA	C. <i>pentagona</i>
OG0000778	GABPA GA-binding protein alpha chain	1	Internal C. <i>hystera</i>
OG0000023	GANP Germinal-center associated nuclear protein	2	Internal C. <i>pentagona</i>
OG0001593	GMFB Glia maturation factor beta	NA	Internal C. <i>hystera</i>
OG0000150	HDGR3 Hepatoma-derived growth factor-related protein 3	1	Internal C. <i>pentagona</i>
OG0000661	HINFP Histone H4 transcription factor	NA	Internal C. <i>pentagona</i>
OG0000151	HIP1 Huntingtin-interacting protein 1	1	Internal C. <i>hystera</i>
OG0000708	HMCN2 Hemicentin-2	NA	C. <i>pentagona</i>
OG0001265	IER5 Immediate early response gene 5 protein	1	Internal C. <i>pentagona</i>
OG0000089	INCE Inner centromere protein	1	Internal C. <i>pentagona</i> , Internal C. <i>hystera</i>

Male comparison	Gene name		MEME	aBSREL branch
OG0001371	KCTD6	BTB/POZ domain-containing protein KCTD6	3	Internal <i>C. pentagona</i> and <i>C. hystera</i>
OG0000114	KIF19	Kinesin-like protein KIF19	NA	Internal <i>C. pentagona</i>
OG0000353	KIF25	Kinesin-like protein KIF25	3	Internal <i>C. hystera</i>
OG0000777	KIRR2	Kin of IRRE-like protein 2	NA	Internal <i>C. pentagona</i>
OG0000416	LKHA4	Leukotriene A-4 hydrolase	1	Internal <i>C. pentagona</i>
OG0000468	LNx2	Ligand of Numb protein X 2		Internal <i>C. pentagona</i>
OG0000340	LRC45	Leucine-rich repeat-containing protein 45	2	Internal <i>C. pentagona</i>
OG0000282	MIC60	MICOS complex subunit Mic60	2	Internal <i>C. hystera</i>
OG0000157	MSH2	DNA mismatch repair protein Msh2	1	<i>C. pentagona</i>
OG0000186	MSH5	MutS protein homolog 5	NA	Internal <i>C. pentagona</i>
OG0000132	NAA25	N-alpha-acetyltransferase 25, NatB auxiliary subunit	NA	<i>C. hystera</i>
OG0000254	NBN	Nibrin	1	Internal <i>C. pentagona</i>
OG0000190	NOM1	Nucleolar MIF4G domain-containing protein 1	2	Internal <i>C. pentagona</i> and <i>C. hystera</i>
OG0000453	NUB1	NEDD8 ultimate buster 1	1	<i>C. pentagona</i>
OG0000137	ODO1	2-oxoglutarate dehydrogenase, mitochondrial	NA	Internal <i>C. hystera</i>
OG0000154	OGA	Protein O-GlcNAcase	NA	Internal <i>C. hystera</i>
OG0000616	P3A2	DNA-binding protein P3A2	NA	Internal <i>C. hystera</i>
OG0000204	PDE8B	High affinity cAMP-specific and IBMX-insensitive 3',5'-cyclic phosphodiesterase 8B	1	Internal <i>C. pentagona</i>
OG0000605	PPIL2	RING-type E3 ubiquitin-protein ligase PPIL2	1	<i>C. hystera</i>
OG0000377	PRC1	Protein regulator of cytokinesis 1	2	Internal <i>C. hystera</i>
OG0000141	PSMD1	26S proteasome non-ATPase regulatory subunit 1	2	<i>C. pentagona</i>
OG0001106	RDH12	Retinol dehydrogenase 12	NA	Internal <i>C. pentagona</i>
OG0001025	RFC2	Replication factor C subunit 2	NA	Internal <i>C. pentagona</i> and <i>C. hystera</i>
OG0000826	RFFL	E3 ubiquitin-protein ligase rifflylin	NA	Internal <i>C. hystera</i>
OG0000019	RHG21	Rho GTPase-activating protein 21	2	Internal <i>C. pentagona</i> and <i>C. hystera</i>
OG0000942	RL1D1	Ribosomal L1 domain-containing protein 1	1	Internal <i>C. pentagona</i>
OG0001052	RM01	39S ribosomal protein L1, mitochondrial	2	Internal <i>C. pentagona</i> and <i>C. hystera</i>
OG0000426	RNF8	E3 ubiquitin-protein ligase RNF8	2	<i>C. hystera</i>
OG0000964	RNFT2	RING finger and transmembrane domain-containing protein 2		Internal <i>C. pentagona</i>
OG0001124	S2543	Solute carrier family 25 member 43	NA	<i>C. pentagona</i> , <i>C. pentagona</i>
OG0000376	SDHA	Succinate dehydrogenase [ubiquinone] flavoprotein subunit, mitochondrial	1	Internal <i>C. pentagona</i>
OG0000203	SENp3	Sentrin-specific protease 3	1	<i>C. hystera</i>
OG0000030	SETB1	Histone-lysine N-methyltransferase SETDB1	4	<i>C. pentagona</i>
OG0001244	SNAA	Alpha-soluble NSF attachment protein	NA	<i>C. hystera</i>
OG0001412	SNG3	Synaptogyrin-3	NA	Internal <i>C. pentagona</i>
OG0000534	STIP1	Stress-induced-phosphoprotein 1	1	<i>C. pentagona</i>
OG0000302	SYTC	Threonine--tRNA ligase, cytoplasmic	NA	Internal <i>C. pentagona</i> and <i>C. hystera</i>
OG0000907	TADH	Tauropine dehydrogenase	1	Internal <i>C. pentagona</i>
OG0000120	TERB1	Telomere repeats-binding bouquet formation protein 1	1	Internal <i>C. pentagona</i>
OG0000545	TF2H1	General transcription factor IIH subunit 1	1	<i>C. hystera</i>
OG0000403	TM9S4	Transmembrane 9 superfamily member 4	2	Internal <i>C. pentagona</i>
OG0001013	TPGS2	Tubulin polyglutamylase complex subunit 2	1	Internal <i>C. pentagona</i>
OG0000058	TRD7A	Tudor domain-containing protein 7A	2	Internal <i>C. pentagona</i>

Male comparison	Gene name		MEME	aBSREL branch
OG0000039	TUT4	Terminal uridylyltransferase 4	1	C. pentagona
OG0001081	UHRF1	E3 ubiquitin-protein ligase UHRF1	1	Internal C. pentagona
OG0000444	VATA	V-type proton ATPase catalytic subunit A	1	C. pentagona
OG0001064	WDR38	WD repeat-containing protein 38	1	C. pentagona
OG0000870	WDR89	WD repeat-containing protein 89	NA	C. pentagona
OG0000145	ZC12A	Endoribonuclease ZC3H12A	2	Internal <i>C. pentagona</i> , Internal <i>C. hystera</i>
OG0000469	ZN665	Zinc finger protein 665	NA	<i>C. hystera</i>
OG0000062		Unknown	9	<i>C. hystera</i>
OG0000084		Unknown	2	Internal C. pentagona
OG0000124		Unknown	2	Internal C. pentagona
OG0000167		Unknown	NA	Internal C. pentagona
OG0000202		Unknown	1	C. pentagona
OG0000267		Unknown	2	Internal C. pentagona
OG0000313		Unknown	2	C. pentagona, Internal C. pentagona
OG0000355		Unknown	7	Internal C. pentagona, C. pentagona
OG0000370		Unknown	NA	Internal C. pentagona
OG0000755		Unknown	NA	Internal C. pentagona
OG0001188		Unknown	NA	Internal C. pentagona
OG0001385		Unknown	NA	<i>C. hystera</i>
OG0001402		Unknown	NA	C. pentagona
OG0001520		Unknown	NA	C. pentagona

**B)**

Female comparison	Gene name		MEME	aBSREL branch	aBSREL p-value
OG0000144	4ET	Eukaryotic translation initiation factor 4E transporter	2	<i>C. pentagona</i> , Internal <i>C. pentagona</i>	0.02718, 0.02888
OG0000417	A16A1	Aldehyde dehydrogenase family 16 member A1	2	Internal <i>C. pentagona</i>	0.01109
OG0000814	AAPK2	5'-AMP-activated protein kinase catalytic subunit alpha-2	1	Internal <i>C. hystera</i>	0.00112
OG0000517	ABCB7	ATP-binding cassette sub-family B member 7, mitochondrial	1	<i>C. pentagona</i>	0.03194
OG0000444	ACRC	Acidic repeat-containing protein	1	Internal <i>C. pentagona</i>	0.0121, 0.01969
OG0000701	AIFM1	Apoptosis-inducing factor 1, mitochondrial	2	Internal <i>C. pentagona</i>	0.0027
OG0000855	AL7A1	Alpha-aminoadipic semialdehyde dehydrogenase	1	<i>C. pentagona</i>	0.00581
OG0001366	ANM6	Protein arginine N-methyltransferase 6	1	<i>C. pentagona</i>	0
OG0000108	ATAD2	ATPase family AAA domain-containing protein 2	6	<i>C. hystera</i>	0
OG0000064	ATAD5	ATPase family AAA domain-containing protein 5	6	Internal <i>C. pentagona</i>	0.00342
OG0000187	BAIP3	BAI1-associated protein 3	2	Internal <i>C. pentagona</i>	0.00181
OG0001560	BCAL2	Branched-chain-amino-acid aminotransferase-like protein 2	NA	Internal <i>C. pentagona</i>	0.04844
OG0000504	BIRC3	Baculoviral IAP repeat-containing protein 3	1	Internal <i>C. pentagona</i>	0.03363
OG0001184	CAB45	45 kDa calcium-binding protein	NA	Internal <i>C. pentagona</i>	0.00867
OG0001472	CATB	Cathepsin B	1	Internal <i>C. hystera</i>	0.04467
OG0001756	CATR	Caltractin	NA	<i>C. pentagona</i>	0
OG0000885	CCD77	Coiled-coil domain-containing protein 77	1	Internal <i>C. pentagona</i>	0.03056
OG0001228	CCR4A	Carbon catabolite repressor protein 4 homolog 1	NA	<i>C. hystera</i>	0
OG0000774	CDC16	Cell division cycle protein 16 homolog	1	Internal <i>C. pentagona</i>	0
OG0000026	CE192	Centrosomal protein of 192 kDa	4	Internal <i>C. pentagona</i>	0.0118
OG0000024	CELR1	Cadherin EGF LAG seven-pass G-type receptor 1	NA	Internal <i>C. pentagona</i> and <i>C. hystera</i> , Internal <i>C. pentagona</i>	0, 0, 0.0414
OG0001552	CF163	Uncharacterized protein C6orf163 homolog	NA	Internal <i>C. pentagona</i> and <i>C. hystera</i>	0
OG0000411	CLCN4	H(+)/Cl(-) exchange transporter 4	NA	<i>C. pentagona</i>	0.00446
OG0000104	CND1	Condensin complex subunit 1	2	<i>C. pentagona</i>	0.03181
OG0000653	COG8	Conserved oligomeric Golgi complex subunit 8	1	Internal <i>C. pentagona</i>	0.01374
OG0000817	CPNE8	Copine-8	NA	Internal <i>C. hystera</i>	0
OG0000611	CPT2	Carnitine O-palmitoyltransferase 2, mitochondrial	NA	<i>C. pentagona</i>	0.02141
OG0000374	DDX54	ATP-dependent RNA helicase DDX54	2	<i>C. hystera</i>	0
OG0000772	DELE1	DAP3-binding cell death enhancer 1	NA	Internal <i>C. pentagona</i>	0.04901

Female comparison	Gene name	MEME	aBSREL branch	aBSREL p-value	
OG0001354	DHDH	Trans-1,2-dihydrobenzene-1,2-diol dehydrogenase	1	Internal <i>C. pentagona</i>	0
OG0000042	DLG5	Disks large homolog 5	2	<i>C. pentagona</i>	0.01037,
OG0000088	DUOX1	Dual oxidase 1	3	Internal <i>C. pentagona</i>	0.02102,
OG0000580	ENL	Protein ENL	NA	Internal <i>C. pentagona</i>	0.02505
OG0000311	EPS8	Epidermal growth factor receptor kinase substrate 8	1	Internal <i>C. pentagona</i>	1.00E-05
OG0000274	ERAP1	Endoplasmic reticulum aminopeptidase 1	1	<i>C. pentagona</i> , Internal <i>C. pentagona</i> , 0.00688	0
OG0000082	EST1A	Telomerase-binding protein EST1A	1	<i>C. pentagona</i>	8.00E-05
OG0001666	F167A	Protein FAM167A	1	<i>C. pentagona</i>	1.40E-04
OG0000732	FBP1L	Formin-binding protein 1-like	NA	<i>C. hystera</i>	0.01521
OG0000878	FBX42	F-box only protein 42	1	Internal <i>C. pentagona</i>	0.04927
OG0000271	FER	Tyrosine-protein kinase Fer	NA	<i>C. hystera</i>	7.60E-04
OG0001011	FRRS1	Putative ferric-chelate reductase 1	NA	Internal <i>C. pentagona</i>	7.00E-05
OG0001071	FXJ1B	Forkhead box protein J1-B	1	<i>C. pentagona</i>	0
OG0001080	GABPA	GA-binding protein alpha chain	1	Internal <i>C. hystera</i>	0.0483
OG0001426	GDPD1	Lysophospholipase D GDPD1	1	Internal <i>C. pentagona</i> and <i>C. hystera</i>	0.04098
OG0000033	GLOL	Highly reducing polyketide synthase gloL	8	Internal <i>C. pentagona</i> and <i>C. hystera</i>	5.30E-04
OG0001931	GMFB	Glia maturation factor beta	NA	Internal <i>C. hystera</i>	0
OG0000038	GON4L	GON-4-like protein	1	<i>C. hystera</i>	0.00124
OG0000175	GSLG1	Golgi apparatus protein 1	1	Internal <i>C. pentagona</i>	0.03665
OG0001767	HEBP2	Heme-binding protein 2	NA	Internal <i>C. pentagona</i>	2.70E-04
OG0001085	HES1	Transcription factor HES-1	1	Internal <i>C. pentagona</i>	0.03352
OG0000123	HIL	Hillarlin	6	<i>C. hystera</i> , <i>C. pentagona</i>	0.00437
OG0000947	HINFP	Histone H4 transcription factor	NA	<i>C. pentagona</i>	0, 0
OG0000321	HIP1	Huntingtin-interacting protein 1	1	Internal <i>C. hystera</i>	2.00E-04
OG0000197	HLTF	Helicase-like transcription factor	2	<i>C. pentagona</i>	0
OG0001724	IAH1	Isoamyl acetate-hydrolyzing esterase 1 homolog	1	Internal <i>C. pentagona</i>	0
OG0000111	IQEC1	IQ motif and SEC7 domain-containing protein 1	1	<i>C. pentagona</i>	0.00292
OG0001717	KCTD6	BTB/POZ domain-containing protein KCTD6	NA	Internal <i>C. pentagona</i> and <i>C. hystera</i>	0.02482
OG0000597	KIF25	Kinesin-like protein KIF25	2	Internal <i>C. hystera</i>	5.00E-05
OG0000262	KIZ	Centrosomal protein kizuna	2	<i>C. pentagona</i> , Internal <i>C. hystera</i>	0.01528
OG0000423	KLH29	Kelch-like protein 29	NA	<i>C. pentagona</i>	0.00065,
OG0000129	KS6C1	Ribosomal protein S6 kinase delta-1	2	Internal <i>C. pentagona</i>	0.01223
OG0000935	KTNA1	Katanin p60 ATPase-containing subunit A1	NA	Internal <i>C. hystera</i>	0
OG0000096	LBN	Limbin	8	<i>C. hystera</i>	0.00675
OG0000733	LNX2	Ligand of Numb protein X 2	1	Internal <i>C. pentagona</i>	0.00172
OG0000293	LPIN2	Phosphatidate phosphatase LPIN2	1	Internal <i>C. pentagona</i>	0

Female comparison	Gene name	MEME	aBSREL branch	aBSREL p-value	
OG0000541	LRC43	Leucine-rich repeat-containing protein 43	NA	Internal <i>C. pentagona</i>	0
OG0001468	LUCI	Coelenterazine h 2-monooxygenase	NA	Internal <i>C. pentagona</i> , <i>C. pentagona</i>	0.00384, 0.04142
OG0000725	MAK	Serine/threonine-protein kinase MAK	1	Internal <i>C. pentagona</i>	0.04366
OG0000031	MCAF1	Activating transcription factor 7-interacting protein 1	3	Internal <i>C. pentagona</i>	0
OG0000813	MCCB	Methylcrotonoyl-CoA carboxylase beta chain, mitochondrial	1	Internal <i>C. pentagona</i>	0.00646
OG0000661	MED17	Mediator of RNA polymerase II transcription subunit 17	1	Internal <i>C. pentagona</i>	0.02143
OG0000621	MET16	RNA N6-adenosine-methyltransferase METTL16	2	Internal <i>C. pentagona</i>	0.03428
OG0000514	MIC60	MICOS complex subunit Mic60	4	Internal <i>C. hystera</i>	0
OG0000872	MIGA	Mitoguardin	NA	Internal <i>C. pentagona</i>	0.01295
OG0001087	MINY1	Ubiquitin carboxyl-terminal hydrolase MINDY-1	1	Internal <i>C. pentagona</i>	0.01618
OG0000097	MRP1	Multidrug resistance-associated protein 1	NA	Internal <i>C. pentagona</i>	0, 0
OG0000052	MYCP P	C-myc promoter-binding protein	2	<i>C. pentagona</i>	0
OG0000283	NAA25	N-alpha-acetyltransferase 25, NatB auxiliary subunit	NA	<i>C. hystera</i>	0
OG0000895	NAA30	N-alpha-acetyltransferase 30	2	Internal <i>C. pentagona</i>	0
OG0000479	NBN	Nibrin	2	Internal <i>C. pentagona</i>	9.00E-05
OG0000287	NOA1	Nitric oxide-associated protein 1	NA	<i>C. pentagona</i> , Internal <i>C. hystera</i>	0.00004, 0.00347, 0.02162
OG0000386	NOM1	Nucleolar MIF4G domain-containing protein 1	4	<i>C. hystera</i>	0
OG0001258	NUP43	Nucleoporin Nup43	2	Internal <i>C. pentagona</i>	5.70E-04
OG0001063	ODBA	2-oxoisovalerate dehydrogenase subunit alpha, mitochondrial	NA	Internal <i>C. pentagona</i>	0
OG0000414	ODFP2	Outer dense fiber protein 2	1	<i>C. pentagona</i>	0.00182
OG0000288	ODO1	2-oxoglutarate dehydrogenase, mitochondrial	NA	Internal <i>C. hystera</i>	0
OG0001187	OFUT1	GDP-fucose protein O-fucosyltransferase 1	1	Internal <i>C. hystera</i>	0
OG0000326	OGA	Protein O-GlcNAcase	NA	Internal <i>C. hystera</i>	0.01078
OG0000149	OPLA	5-oxoprolinase	1	<i>C. pentagona</i>	0.00363
OG0000461	OPTN	Optineurin	NA	<i>C. pentagona</i>	0.04413
OG0001811	PA216	HRAS-like suppressor 3	4	Internal <i>C. pentagona</i>	0
OG0000160	PALB2	Partner and localizer of BRCA2	3	Internal <i>C. pentagona</i>	1.00E-05
OG0001672	PAQR A	Monocyte to macrophage differentiation factor 2	1	Internal <i>C. pentagona</i>	0.00221
OG0000107	PEX1	Peroxisome biogenesis factor 1	4	Internal <i>C. pentagona</i> , <i>C. pentagona</i>	0.00101, 0.00558
OG0001055	PLB1	Phospholipase B1, membrane-associated	2	Internal <i>C. hystera</i>	1.40E-04
OG0000388	PYGB	Glycogen phosphorylase, brain form	2	Internal <i>C. pentagona</i>	0.04584
OG0001355	RFC2	Replication factor C subunit 2	1	Internal <i>C. pentagona</i> and <i>C. hystera</i>	4.70E-04



Female comparison	Gene name	MEME	aBSREL branch	aBSREL p-value
OG0000449	RHG12 Rho GTPase-activating protein 12	2	Internal <i>C. hystera</i>	1.00E-05
OG0000067	RHG20 Rho GTPase-activating protein 20	1	Internal <i>C. pentagona</i>	0.02915
OG0001261	RL1D1 Ribosomal L1 domain-containing protein 1	NA	Internal <i>C. pentagona</i>	0.00569
OG0000456	RMI1 RecQ-mediated genome instability protein 1	2	Internal <i>C. pentagona</i>	0.00104
OG0001152	RNF13 E3 ubiquitin-protein ligase RNF13	2	Internal <i>C. pentagona</i> and <i>C. hystera</i>	0
OG0000717	RNF37 RING finger protein 37	4	<i>C. pentagona</i>	1.00E-05
OG0000685	RNF8 E3 ubiquitin-protein ligase RNF8	1	<i>C. hystera</i>	0
OG0000404	RRP1B Ribosomal RNA processing protein 1 homolog B	2	Internal <i>C. pentagona</i>	9.90E-04
OG0000314	S12A9 Solute carrier family 12 member 9	10	Internal <i>C. hystera</i>	0, 0, 7.00E-05
OG0000978	S18B1 MFS-type transporter SLC18B1	6	Internal <i>C. pentagona</i>	1.30E-04
OG0000629	SDHA Succinate dehydrogenase [ubiquinone] flavoprotein subunit, mitochondrial	1	Internal <i>C. pentagona</i>	0.00132
OG0000566	SEM2A Semaphorin-2A	7	Internal <i>C. pentagona</i>	0
OG0000401	SENP3 Sentrin-specific protease 3	1	<i>C. hystera</i>	0.01948
OG0000068	SETB1 Histone-lysine N-methyltransferase SETDB1	NA	<i>C. pentagona</i> , Internal <i>C. hystera</i>	0, 0.02869, 0.04228, 0.02869, 0.04228
OG0000100	SFI1 Protein SFI1 homolog	3	<i>C. pentagona</i>	0.01031
OG0001575	SNAA Alpha-soluble NSF attachment protein	NA	Internal <i>C. pentagona</i> and <i>C. hystera</i>	0
OG0000773	SOAT1 Sterol O-acyltransferase 1	NA	<i>C. pentagona</i>	0.02469
OG0000130	SOS2 Son of sevenless homolog 2	1	<i>C. hystera</i>	0
OG0000807	STIP1 Stress-induced-phosphoprotein 1	NA	Internal <i>C. pentagona</i>	0.00814
OG0000544	SYTC Threonine--tRNA ligase, cytoplasmic	NA	Internal <i>C. pentagona</i> and <i>C. hystera</i>	0
OG0000241	SYVC Valine--tRNA ligase	5	Internal <i>C. pentagona</i>	0
OG0001624	TAF11 Transcription initiation factor TFIID subunit 11	NA	<i>C. pentagona</i>	0
OG0000822	TAPT1 Transmembrane anterior posterior transformation protein 1 homolog	1	Internal <i>C. pentagona</i>	4.00E-05
OG0000230	TDRKH Tudor and KH domain-containing protein	3	Internal <i>C. pentagona</i>	0.00995
OG0000248	TERB1 Telomere repeats-binding bouquet formation protein 1	2	Internal <i>C. pentagona</i>	0.00439
OG0000823	TF2H1 General transcription factor IIH subunit 1	NA	<i>C. hystera</i>	0
OG0000040	TF3C1 General transcription factor 3C polypeptide 1	2	<i>C. hystera</i>	3.00E-05
OG0000406	TFP11 Tuftelin-interacting protein 11	1	<i>C. pentagona</i>	0.00149
OG0000599	THOP1 Thimet oligopeptidase	3	Internal <i>C. pentagona</i> and <i>C. hystera</i>	0
OG0000995	TM10C tRNA methyltransferase 10 homolog C	1	Internal <i>C. pentagona</i>	0.02794
OG0000090	TOP2A DNA topoisomerase 2-alpha	1	<i>C. pentagona</i>	0.0441

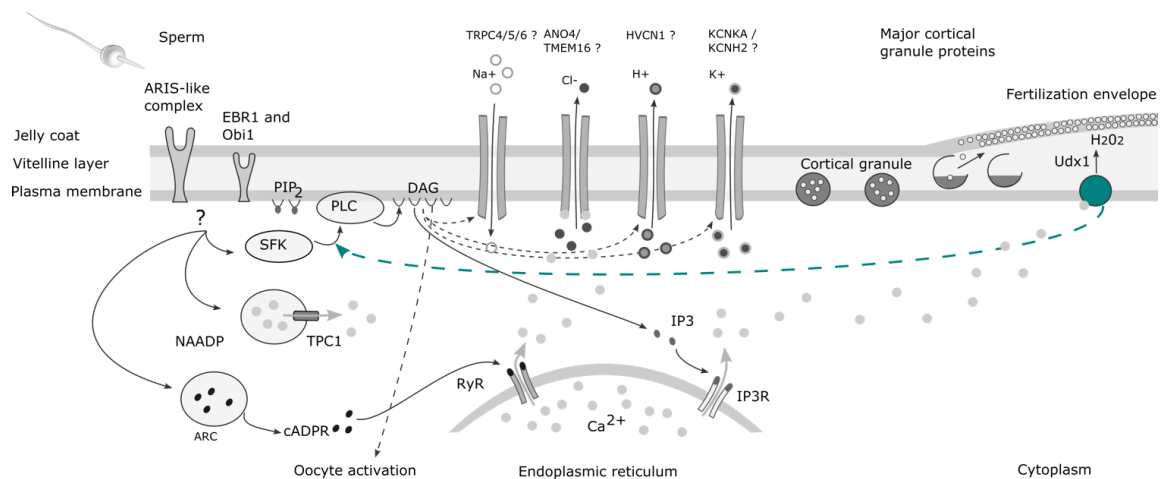
Female comparison	Gene name		MEME	aBSREL branch	aBSREL p-value
OG0000437	TRAD1	TRAF-type zinc finger domain-containing protein 1	2	Internal <i>C. pentagona</i>	0.01539, 0.02293
OG0001663	TSN7	Tetraspanin-7	NA	Internal <i>C. pentagona</i>	0.00614
OG0001089	UBE3D	E3 ubiquitin-protein ligase E3D	1	<i>C. pentagona</i>	0.04804
OG0000125	UBP47	Ubiquitin carboxyl-terminal hydrolase 47	2	Internal <i>C. hystera</i>	0
OG0000443	UBP5	Ubiquitin carboxyl-terminal hydrolase 5	1	<i>C. pentagona</i>	0.00511
OG0000464	UN5BA	Netrin receptor UNC5B-a	2	<i>C. pentagona</i>	0.0042
OG0000138	unc-89	muscle M-line assembly protein unc-89-like	3	Internal <i>C. pentagona</i>	0
OG0000493	VKGC	Vitamin K-dependent gamma-carboxylase	1	Internal <i>C. pentagona</i>	3.20E-04
OG0000299	VPS18	Vacuolar protein sorting-associated protein 18 homolog	NA	Internal <i>C. pentagona</i> and <i>C. hystera</i>	0
OG0001174	WDR89	WD repeat-containing protein 89	1	Internal <i>C. pentagona</i>	0.0289
OG0000297	ZC12A	Endoribonuclease ZC3H12A	8	Internal <i>C. pentagona</i> and <i>C. hystera</i> , Internal <i>C. pentagona</i> , <i>C. pentagona</i>	0, 0, 0
OG0000341	ZN112	Zinc finger protein 112	NA	<i>C. pentagona</i>	0.0108, 0.04137
OG0000734	ZN665	Zinc finger protein 665	1	Internal <i>C. pentagona</i> and <i>C. hystera</i>	0
OG0001327		uncharacterized	NA	<i>C. pentagona</i>	0
OG0001451		uncharacterized	1	Internal <i>C. pentagona</i>	0.04962
OG0000501		uncharacterized	NA	Internal <i>C. pentagona</i>	0
OG0000850		uncharacterized	1	Internal <i>C. pentagona</i>	0.00433
OG0000399		uncharacterized	1	Internal <i>C. pentagona</i>	0.00641
OG0000282		uncharacterized	1	Internal <i>C. pentagona</i>	0
OG0001023		uncharacterized	NA	Internal <i>C. pentagona</i>	0.01288
OG0001058		uncharacterized	NA	Internal <i>C. pentagona</i>	0.01978
OG0000463		uncharacterized	10	<i>C. pentagona</i> , Internal <i>C. pentagona</i>	0, 0
OG0000882		uncharacterized	1	<i>C. pentagona</i>	0.00196
OG0000152		myosin-11-like	4	<i>C. hystera</i> , <i>C. pentagona</i>	0, 0, 0

**Appendix AA. Orthogroups with evidence of selection in both branch site models (aBSREL) and in alignment-wide tests (MK) in the female and the male gene set. Gene acronyms and annotation from Blast with reference databases. The best hit to a reference gene in the NCBI *Acanthaster planci* database is also shown. Type of selection detected in the McDonald & Kreitman test. Branches under selection in aBSREL. Four orthogroups did not show evidence of individual codons under selection in MEME**

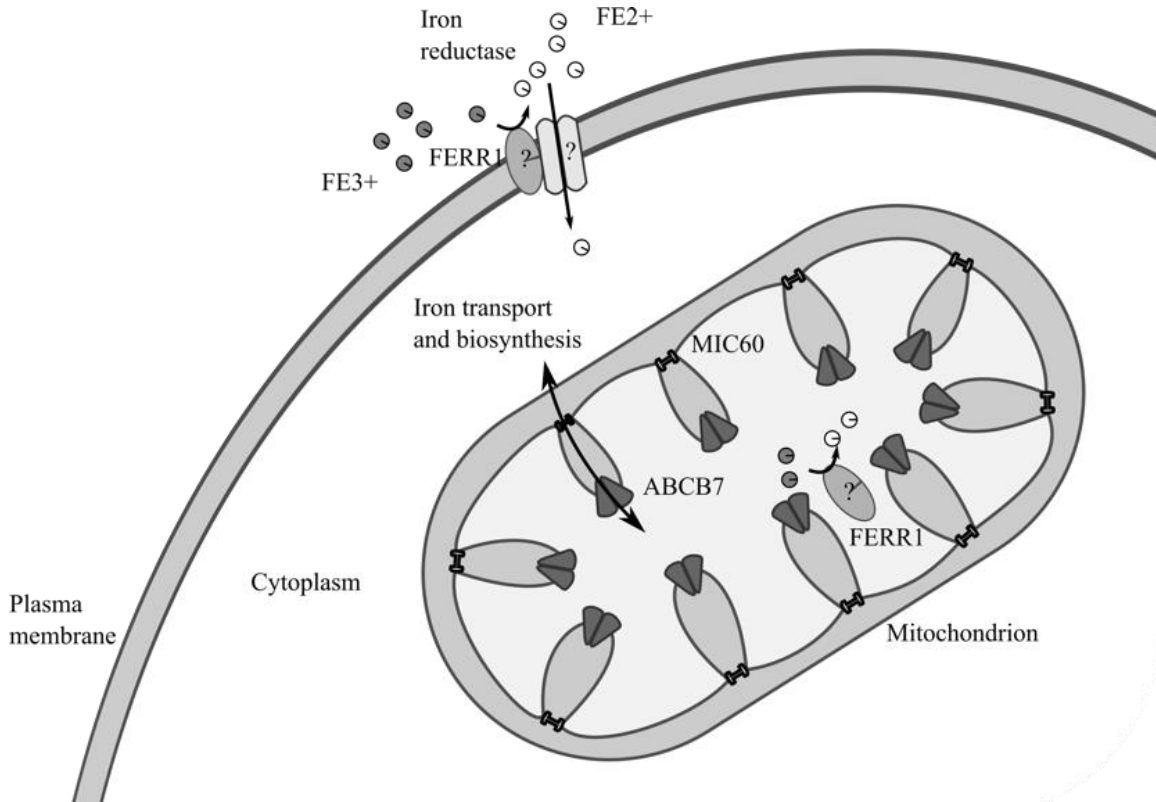
Female and male gene set	Gene	Function	McDonald & Kreitman	aBSREL branch	MEME codon
F-OG0000517	ABCB7	ATP-binding cassette sub-family B member 7	Balancing	Terminal <i>C. pentagona</i>	366
F-OG0000514	MIC60	MICOS complex subunit Mic60	Positive	Internal <i>C. hystera</i>	2, 3, 82, 168
F-OG0001085	HES1-4	transcription factor HES 1-4	Balancing	Terminal and internal <i>C. pentagona</i>	149
F-OG0000104	CND1	condensin complex subunit 1	Balancing	Terminal <i>C. pentagona</i>	1482, 519
F-OG0000935	KTNA1	katanin p60 ATPase-containing subunit A1	Positive	Internal <i>C. hystera</i>	
F-OG0001011	FRRS1	putative ferric-chelate reductase 1	Positive	Internal <i>C. pentagona</i>	
F-OG0000187	UNC13D or BAIP3	protein unc-13 homolog D-like	Positive	Internal <i>C. pentagona</i>	5, 48
F-OG0000282	Unknown	uncharacterized LOC110977921	Positive	Internal <i>C. pentagona</i>	1002
M-OG0000229	ACRC	acidic repeat-containing protein-like	Balancing	Internal <i>C. pentagona</i>	276
M-OG0000353	KIF25	kinesin-like protein	Balancing	Internal <i>C. hystera</i>	21, 628, 647

Female and male gene set	Gene	Function	McDonald & Kreitman	aBSREL branch	MEME codon
M-OG0001402	Unknown	uncharacterized LOC110973096	Balancing	Terminal C. <i>pentagona</i>	
M-OG0000313	Unknown	uncharacterized LOC110975594	Balancing	Terminal and internal C. <i>pentagona</i>	401, 559
F-OG0000321, M-OG0000151	HIP1	huntingtin-interacting protein 1-like	Positive	Internal C. <i>hystera</i>	949   949
F-OG0000817, M-OG0000540	CPNE8	copine 8-like	Balancing	Internal C. <i>hystera</i>	

**Appendix AB. Schematics of potential role of *Udx1* as an intracellular calcium influx extender in the egg. Successful contact between sperm and egg (mediated by gamete-recognition genes) initiates three intracellular calcium influx pathways activated by cyclic ADP ribose (*cADPR*), nicotinic acid adenine dinucleotide-phosphate (*NAADP*), and the 1,4,5-triphosphate (*IP3*) production in sea stars. *cADPR* and *IP3* binds to receptor (*RyR*) and *IP3* receptor respectively to release calcium from the endoplasmic reticulum. And *NAADP* induces the release of calcium through the two-pore channel (*TPC1*). *IP3* is released from DAG through the H<sub>2</sub>O<sub>2</sub> sensitive Src family tyrosine kinase (*SFK*) and phospholipase C (*PLC*) activity. The H<sub>2</sub>O<sub>2</sub> product from the calcium sensitive *Udx1* interacts with cortical granules during the formation of the fertilization envelope after fertilization and it could also be acting as a secondary activator for the *SFK* and *PLC* activity. Other annotated signal molecules found in the reference transcriptome of *Cryptasterina* noted in this figure (*TRPC4/5/6/7*, *ANO4/TMEM16*, *HVCN1* and *KCNKA / KCNH2*) could be activated through plasma membrane deactivation or *DAG* activation (Ramos et al., 2014; Wong et al., 2004; Wozniak & Carlson, 2020)**



**Appendix AC. Potential localization of expression of three genes under selection (*FERR1*, *MIC60*, and *ABCB7*) likely linked to oxidative stress and iron metabolism. The iron reductase ( $Fe^{3+}$  to  $Fe^{2+}$ ) *FERR1* gene could either be expressed internally in the mitochondrion or in the plasma membrane of the cell along with an ion transporter. *MIC60* is likely expressed in the cristae junctions of the mitochondrion along with other interacting MICO molecules to provide structure. The mitochondrial transmembrane protein *ABCB7* is likely expressed in the crista of the mitochondrion.**



## Appendix AD. Reference for Supplemental Material of Chapter 3

- Finn, R. D., Clements, J., & Eddy, S. R. (2011). HMMER web server: Interactive sequence similarity searching. *Nucleic Acids Research*, 39(suppl\_2), W29-37. <https://doi.org/10.1093/nar/gkr367>
- Gao, L. L., Zhou, C. X., Zhang, X. L., Liu, P., Jin, Z., Zhu, G. Y., Ma, Y., Li, J., Yang, Z. X., & Zhang, D. (2017). ZP3 is Required for Germinal Vesicle Breakdown in Mouse Oocyte Meiosis. *Scientific Reports*, 7, 1–10. <https://doi.org/10.1038/srep41272>
- Grabherr, M. G., Haas, B. J., Yassour, M., Levin, J. Z., Thompson, D. A., Amit, I., Adiconis, X., Fan, L., Raychowdhury, R., Zeng, Q., Chen, Z., Mauceli, E., Hacohen, N., Gnirke, A., Rhind, N., di Palma, F., Birren, B. W., Nusbaum, C., Lindblad-Toh, K., ... Regev, A. (2011). Full-length transcriptome assembly from RNA-Seq data without a reference genome. *Nature Biotechnology*, 29(7), 644–652. <https://doi.org/10.1038/nbt.1883>
- Guerra, V., Haynes, G., Byrne, M., Yasuda, N., Adachi, S., Nakamura, M., Nakachi, S., & Hart, M. W. (2020). Nonspecific expression of fertilization genes in the crown-of-thorns *Acanthaster cf. solaris*: Unexpected evidence of hermaphroditism in a coral reef predator. *Molecular Ecology*, 29(2), 363–379. <https://doi.org/10.1111/mec.15332>
- Haas, B. J., Papanicolaou, A., Yassour, M., Grabherr, M., Blood, P. D., Bowden, J., Couger, M. B., Eccles, D., Li, B., Lieber, M., Macmanes, M. D., Ott, M., Orvis, J., Pochet, N., Strozzi, F., Weeks, N., Westerman, R., William, T., Dewey, C. N., ... Regev, A. (2013). De novo transcript sequence reconstruction from RNA-seq using the Trinity platform for reference generation and analysis. *Nature Protocols*, 8(8), 1494–1512. <https://doi.org/10.1038/nprot.2013.084>
- Hart, M. W., & Foster, A. (2013). Highly expressed genes in gonads of the bat star *Patiria miniata*: Gene ontology, expression differences, and gamete-recognition loci. *Invertebrate Biology*, 132(3), 241–250. <https://doi.org/10.1111/ivb.12029>
- Hart, M. W., Sunday, J. M., Popovic, I., Learning, K. J., & Konrad, C. M. (2014). Incipient speciation of sea star populations by adaptive gamete-recognition coevolution. *Evolution*, 68(5), 1294–1305. <https://doi.org/10.1111/evo.12352>
- Krogh, A., Larsson, B., Von Heijne, G., & Sonnhammer, E. L. L. (2001). Predicting transmembrane protein topology with a hidden Markov model: Application to complete genomes. *Journal of Molecular Biology*, 305(3), 567–580. <https://doi.org/10.1006/jmbi.2000.4315>

- Matsumoto, M., Solzin, J., Helbig, A., Hagen, V., Ueno, S. ichi, Kawase, O., Maruyama, Y., Ogiso, M., Godde, M., Minakata, H., Kaupp, U. B., Hoshi, M., & Weyand, I. (2003). A sperm-activating peptide controls a cGMP-signaling pathway in starfish sperm. *Developmental Biology*, 260(2), 314–324. [https://doi.org/10.1016/S0012-1606\(03\)00236-7](https://doi.org/10.1016/S0012-1606(03)00236-7)
- Mengerink, K. J., Moy, G. W., & Vacquier, V. D. (2002). suREJ3, a polycystin-1 protein, is cleaved at the GPS domain and localizes to the acrosomal region of sea urchin sperm. *Journal of Biological Chemistry*, 277(2), 943–948. <https://doi.org/10.1074/jbc.M109673200>
- Moy, G. W., Mendoza, L. M., Schulz, J. R., Swanson, W. J., Glabe, C. G., & Vacquier, V. D. (1996). The sea urchin sperm receptor for egg jelly is a modular protein with extensive homology to the human polycystic kidney disease protein, PKD1. *Journal of Cell Biology*, 133(4), 809–817. <https://doi.org/10.1083/jcb.133.4.809>
- Nakachi, M., Hoshi, M., Matsumoto, M., & Moriyama, H. (2008). Conserved sequences of sperm-activating peptide and its receptor throughout evolution, despite speciation in the sea star *Asterias amurensis* and closely related species. *Zygote (Cambridge, England)*, 16(3), 229–237. <https://doi.org/10.1017/S0967199408004759>
- Ogata, H., Goto, S., Sato, K., Fujibuchi, W., Bono, H., & Kanehisa, M. (1999). KEGG: Kyoto encyclopedia of genes and genomes. In *Nucleic Acids Research* (Vol. 27, Issue 1, pp. 29–34). <https://doi.org/10.1093/nar/27.1.29>
- Patiño, S., Keever, C. C., Sunday, J. M., Popovic, I., Byrne, M., & Hart, M. W. (2016). Sperm Bindin Divergence under Sexual Selection and Concerted Evolution in Sea Stars. *Molecular Biology and Evolution*, 33(8), 1988–2001. <https://doi.org/10.1093/molbev/msw081>
- Popovic, I., Marko, P. B., Wares, J. P., & Hart, M. W. (2014). Selection and demographic history shape the molecular evolution of the gamete compatibility protein bindin in *Pisaster* sea stars. *Ecology and Evolution*, 4(9), 1567–1588. <https://doi.org/10.1002/ece3.1042>
- Ramos, I., Reich, A., & Wessel, G. M. (2014). Two-pore channels function in calcium regulation in sea star oocytes and embryos. *Development (Cambridge)*, 141(23), 4598–4609. <https://doi.org/10.1242/dev.113563>
- Wong, J. L., Créton, R., & Wessel, G. M. (2004). The oxidative burst at fertilization is dependent upon activation of the dual oxidase *udx1*. *Developmental Cell*, 7(6), 801–814. <https://doi.org/10.1016/j.devcel.2004.10.014>
- Wozniak, K. L., & Carlson, A. E. (2020). Ion channels and signaling pathways used in the fast polyspermy block. *Molecular Reproduction and Development*, 87(3), 350–357. <https://doi.org/10.1002/mrd.23168>



Xu, J., & Gridley, T. (2012). Notch Signaling during Oogenesis in *Drosophila melanogaster*. *Genetics Research International*, 2012(Type 1), 1–10. <https://doi.org/10.1155/2012/648207>